

Annex 11.- Publications Screenshots



Human aquaporin 4 gating dynamics under axially oriented electric-field impulses: A non-equilibrium molecular-dynamics study

Mario Bernardi,¹ Paolo Marracino,^{1,a)} Mohammad Reza Ghaani,² Micaela Liberti,^{1,a)} Federico Del Signore,¹ Christian J. Burnham,² José-Antonio Gárate,³ Francesca Apollonio,^{1,a)} and Niall J. English^{2,a)}

¹Department of Information Engineering, Electronics and Telecommunications, La Sapienza University, 00184 Rome, Italy

²School of Chemical and Bioprocess Engineering, University College Dublin, Belfield, Dublin, D4, Ireland

³Centro Interdisciplinario de neurociencia de Valparaíso, CINV, Universidad de Valparaíso, 05101 Valparaíso, Chile

(Received 14 June 2018; accepted 30 November 2018; published online 31 December 2018)

Human aquaporin 4 has been studied using non-equilibrium molecular dynamics simulations in the absence and presence of pulses of external electric fields. The pulses were 100 ns in duration and 0.005–0.015 V/Å in intensity acting along the pores' axes. Water diffusivity and the dipolar response of various residues of interest within the pores have been studied. Results show relatively little change in levels of water permeability *per se* within aquaporin channels during axially oriented field impulses, although care must be taken with regard to statistical certainty. However, the spatial variation of water permeability vis-à-vis electric-field intensity within the milieu of the channels, as revealed by heterogeneity in diffusivity-map gradients, indicates the possibility of somewhat enhanced diffusivity, owing to several residues being affected substantially by external fields, particularly for HIS 201 and 95 and ILE 93. This has the effect of increasing slightly intra-pore water diffusivity in the “pore-mouths” locale, albeit rendering it more spatially uniform overall vis-à-vis zero-field conditions (via manipulation of the selectivity filter). *Published by AIP Publishing.*
<https://doi.org/10.1063/1.5044665>

I. INTRODUCTION

Aquaporins (AQPs) are a wide-ranging suite of trans-membrane proteins, forming channels with elective water-conductance properties. This selective permeation arises from osmotic-pressure differentials between either sides of the membrane, disallowing strictly ions' and protons' passage therethrough.^{1,2} AQPs exist in all known life forms, and form the bedrock of regulating precisely cellular water content. In man, defective AQP function is implicated in a deal of pathological conditions, e.g., congenital cataracts.³ Since discovered by Agre *et al.*,⁴ several hundred have been characterized.^{3,5}

A more extensive elucidation of AQP-based water transport would help advance progress in medicine, gauging more clearly their function and possible implication in medical conditions. Although such water fluxes are estimated relatively routinely via reconstitution of AQP channels in liposomes and tracking volume changes due to impermeable-solute concentrations, isotope labeling offers another intriguing possibility.^{1,2,4,6–8} To assess single-channel permeability, knowledge of AQP density is *sine qua non*—clearly, accurate measurement of lipid-to-protein composition in a liposome represents

a formidable, typically intractable undertaking. Even armed with such pore-density information, arriving at any reliable and plausible atomistic-level elucidation of underlying water-permeation mechanisms through AQPs is not feasible by experiment, arising from inability to probe the exceedingly brief, sub-nanosecond water-passage time scales.^{9,10} Bearing in mind these reasonably rapid kinetics, classical molecular dynamics (MD) has become a very valuable tool for gaining theoretical insights into the underlying mechanisms,^{11,12,21,13–20} owing, naturally, to increasing availability of atomic-resolution structures for AQPs.^{22–24} Indeed, “two-stage filter” mechanisms have been proposed, wherein the pore serves as a “selectivity filter” (SF) at its narrowest point in the aromatic/arginine region at the extracellular end as one stage, whilst the histidine 95 and cysteine 178 residues act as another stage at the cytoplasmic end. Moreover, a well-conserved pair of asparagine-proline-alanine (NPA) motifs with opposite orientations features well-defined water rotation upon water passage; this is a key feature of all aquaporins, with the aforementioned residues being conserved in all AQP families.²⁵ MD has examined AQPs' proton-blocking capacity,^{26–31} permeation of solutes other than water,^{32–35} and gating behavior,^{36–38} together with facilitation of cell adhesion.³⁹

The atomic structure of h-AQP4 has been resolved by x-ray crystallography at a resolution of 1.8 Å [Protein Data Bank (PDB) entry code 3GD8].⁴⁰ In common with all AQPs, h-AQP4 forms homo-tetramers in cell membranes; each

^{a)}Authors to whom correspondence should be addressed: marracino@diet.uniroma1.it, Tel.: +39-06-4458-5457; liberti@diet.uniroma1.it, Tel.: +39-06-4458-5353; apollonio@diet.uniroma1.it, Tel.: +39-06-4458-5374; and niall.english@ucd.ie, Tel.: +353-1-716-1646, Fax: +353-1-716-1177.

phospholipid-bilayer boundary on either side of the membrane, to lead to enhanced water diffusivity through the pores themselves.

SUPPLEMENTARY MATERIAL

See [supplementary material](#) for sample mean-squared displacement graphs and further details on computation of MSD and water-density profiles.

ACKNOWLEDGMENTS

Niall J. English and Christian J. Burnham thank Science Foundation Ireland (Grant No. 15/ERC/I3142) and also the Irish Centre for High-End Computing for the provision of High-Performance Computing facilities. M.R.G. thanks Science Foundation Ireland for an Academia-to-Industry Fellowship (17/IFB/5406). José-Antonio Gárate acknowledges financial support from ICM-ECONOMIA P09-022-F. Francesca Apollonio acknowledges financial support from the Sapienza University of Rome, Research Projects, 2015 (Grant No. C26A15T3T2). Paolo Marracino thanks the COST Action TD1104—European network for development of EP-based technologies and treatments (EP4Bio2Med). Micaela Liberti acknowledges the support received within the framework of the Joint IIT-Sapienza LAB on Life-NanoScience Project (81/13 16 April 2013).

- ¹S. Hohmann, S. Nielsen, and P. Agre, *Aquaporins: Volume 51* (Elsevier Science Publishing Co., Inc., San Diego, USA, 2001).
- ²M. Borgnia, S. Nielsen, A. Engel, and P. Agre, *Annu. Rev. Biochem.* **68**, 425 (1999).
- ³L. S. King, D. Kozono, and P. Agre, *Nat. Rev. Mol. Cell Biol.* **5**, 687 (2004).
- ⁴G. M. Preston, T. P. Carroll, W. B. Guggino, and P. Agre, *Science* **256**, 385 (1992).
- ⁵A. Engel and H. Stahlberg, *Int. Rev. Cytol.* **215**, 75 (2002).
- ⁶P. H. Baylis, *Cell Biochem. Funct.* **6**, 223 (1988).
- ⁷G. Calamita, *Mol. Microbiol.* **37**, 254 (2000).
- ⁸M. J. Borgnia, D. Kozono, G. Calamita, P. C. Maloney, and P. Agre, *J. Mol. Biol.* **291**, 1169 (1999).
- ⁹Y. Fujiyoshi, K. Mitsuoka, B. L. de Groot, A. Philippsen, H. Grubmüller, P. Agre, and A. Engel, *Curr. Opin. Struct. Biol.* **12**, 509 (2002).
- ¹⁰R. M. Stroud, D. Savage, L. J. W. Miercke, J. K. Lee, S. Khademi, and W. Harries, *FEBS Lett.* **555**, 79 (2003).
- ¹¹B. L. de Groot and H. Grubmüller, *Science* **294**, 2353 (2001).
- ¹²E. Tajkhorshid, P. Nollert, M. Ø. Jensen, L. J. W. Miercke, J. O'Connell, R. M. Stroud, and K. Schulten, *Science* **296**, 525 (2002).
- ¹³F. Zhu, E. Tajkhorshid, and K. Schulten, *FEBS Lett.* **504**, 212 (2001).
- ¹⁴F. Zhu, E. Tajkhorshid, and K. Schulten, *Biophys. J.* **83**, 154 (2002).
- ¹⁵F. Zhu, E. Tajkhorshid, and K. Schulten, *Biophys. J.* **86**, 50 (2004).
- ¹⁶M. Hashido, M. Ikeguchi, and A. Kidera, *FEBS Lett.* **579**, 5549 (2005).
- ¹⁷M. Hashido, A. Kidera, and M. Ikeguchi, *Biophys. J.* **93**, 373 (2007).
- ¹⁸M. Ø. Jensen and O. G. Mouritsen, *Biophys. J.* **90**, 2270 (2006).
- ¹⁹B.-G. Han, A. B. Guliaev, P. J. Walian, and B. K. Jap, *J. Mol. Biol.* **360**, 285 (2006).
- ²⁰G. F. Mangiatordi, D. Alberga, D. Trisciuzzi, G. Lattanzi, and O. Nicolotti, *Int. J. Mol. Sci.* **17**, 1119 (2016).
- ²¹M. Ø. Jensen, E. Tajkhorshid, and K. Schulten, *Biophys. J.* **85**, 2884 (2003).
- ²²B. L. de Groot, A. Engel, and H. Grubmüller, *FEBS Lett.* **504**, 206 (2001).
- ²³H. Sui, B.-G. Han, J. K. Lee, P. Walian, and B. K. Jap, *Nature* **414**, 872 (2001).
- ²⁴D. Fu, A. Libson, L. J. Miercke, C. Weitzman, P. Nollert, J. Krucinski, and R. M. Stroud, *Science* **290**, 481 (2000).
- ²⁵J. S. Hub, C. Aponte-Santamaría, H. Grubmüller, and B. L. de Groot, *Biophys. J.* **99**, L97 (2010).

- ²⁶B. L. de Groot, T. Frigato, V. Helms, and H. Grubmüller, *J. Mol. Biol.* **333**, 279 (2003).
- ²⁷N. Chakrabarti, E. Tajkhorshid, B. Roux, and R. Pomès, *Structure* **12**, 65 (2004).
- ²⁸N. Chakrabarti, B. Roux, and R. Pomès, *J. Mol. Biol.* **343**, 493 (2004).
- ²⁹B. Ilan, E. Tajkhorshid, K. Schulten, and G. A. Voth, *Proteins: Struct., Funct., Bioinf.* **55**, 223 (2004).
- ³⁰H. Chen, Y. Wu, and G. A. Voth, *Biophys. J.* **90**, L73 (2006).
- ³¹B. L. de Groot and H. Grubmüller, *Curr. Opin. Struct. Biol.* **15**, 176 (2005).
- ³²M. O. Jensen, E. Tajkhorshid, and K. Schulten, *Structure* **9**, 1083 (2001).
- ³³M. Ø. Jensen, S. Park, E. Tajkhorshid, and K. Schulten, *Proc. Natl. Acad. Sci. U. S. A.* **99**, 6731 (2002).
- ³⁴J. S. Hub and B. L. de Groot, *Biophys. J.* **91**, 842 (2006).
- ³⁵J. Hénin, E. Tajkhorshid, K. Schulten, and C. Chipot, *Biophys. J.* **94**, 832 (2008).
- ³⁶H. Khandelia, M. Ø. Jensen, and O. G. Mouritsen, *J. Phys. Chem. B* **113**, 5239 (2009).
- ³⁷N. Smolin, B. Li, D. A. C. Beck, and V. Daggett, *Biophys. J.* **95**, 1089 (2008).
- ³⁸D. Alberga, O. Nicolotti, G. Lattanzi, G. P. Nicchia, A. Frigeri, F. Pisani, V. Benfenati, and G. F. Mangiatordi, *Biochim. Biophys. Acta, Biomembr.* **1838**, 3052 (2014).
- ³⁹M. Ø. Jensen, R. O. Dror, H. Xu, D. W. Borhani, I. T. Arkin, M. P. Eastwood, and D. E. Shaw, *Proc. Natl. Acad. Sci. U. S. A.* **105**, 14430 (2008).
- ⁴⁰J. D. Ho, R. Yeh, A. Sandstrom, I. Chorny, W. E. C. Harries, R. A. Robbins, L. J. W. Miercke, and R. M. Stroud, *Proc. Natl. Acad. Sci. U. S. A.* **106**, 7437 (2009).
- ⁴¹S. Kaptan, M. Assentoft, H. P. Schneider, R. A. Fenton, J. W. Deitmer, N. MacAulay, and B. L. de Groot, *Structure* **23**, 2309 (2015).
- ⁴²T. O. Wambo, R. A. Rodriguez, and L. Y. Chen, *Biochim. Biophys. Acta, Biomembr.* **1859**, 1310 (2017).
- ⁴³J. Tong, Z. Wu, M. M. Briggs, K. Schulten, and T. J. McIntosh, *Biophys. J.* **111**, 90 (2016).
- ⁴⁴N. J. English and D. A. Mooney, *J. Chem. Phys.* **126**, 091105 (2007).
- ⁴⁵N. J. English, G. Y. Solomentssev, and P. O'Brien, *J. Chem. Phys.* **131**, 035106 (2009).
- ⁴⁶G. Y. Solomentssev, N. J. English, and D. A. Mooney, *J. Chem. Phys.* **133**, 235102 (2010).
- ⁴⁷N. J. English and C. J. Waldron, *Phys. Chem. Chem. Phys.* **17**, 12407 (2015).
- ⁴⁸N. Todorova, A. Bentvelzen, N. J. English, and I. Yarovsky, *J. Chem. Phys.* **144**, 085101 (2016).
- ⁴⁹F. Apollonio, M. Liberti, A. Paffi, C. Merla, P. Marracino, A. Denzi, C. Marino, and G. d'Inzeo, *IEEE Trans. Microwave Theory Tech.* **61**, 2031 (2013).
- ⁵⁰P. Marracino, M. Liberti, G. d'Inzeo, and F. Apollonio, *Bioelectromagnetics* **36**, 377 (2015).
- ⁵¹P. Marracino, F. Apollonio, M. Liberti, G. d'Inzeo, and A. Amadei, *J. Phys. Chem. B* **117**, 2273 (2013).
- ⁵²F. Apollonio, M. Liberti, A. Amadei, M. Aschi, M. Pellegrino, M. D'Alessandro, M. D'Abramo, A. Di Nola, and G. d'Inzeo, *IEEE Trans. Microwave Theory Tech.* **56**, 2511 (2008).
- ⁵³A. Amadei and P. Marracino, *RSC Adv.* **5**, 96551 (2015).
- ⁵⁴P. Marracino, A. Amadei, F. Apollonio, G. d'Inzeo, M. Liberti, A. di Crescenzo, A. Fontana, R. Zappacosta, and M. Aschi, *J. Phys. Chem. B* **115**, 8102 (2011).
- ⁵⁵R. Mulero, A. S. Prabhu, K. J. Freedman, and M. J. Kim, *J. Assoc. Lab. Autom.* **15**, 243 (2010).
- ⁵⁶J.-A. Garate, N. J. English, and J. M. D. MacElroy, *J. Chem. Phys.* **134**, 055110 (2011).
- ⁵⁷R. Reale, N. J. English, J.-A. Garate, P. Marracino, M. Liberti, and F. Apollonio, *J. Chem. Phys.* **139**, 205101 (2013).
- ⁵⁸P. Marracino, M. Liberti, E. Trapani, C. Burnham, M. Avena, J.-A. Garate, F. Apollonio, and N. English, *Int. J. Mol. Sci.* **17**, 1133 (2016).
- ⁵⁹J.-A. Garate, N. J. English, and J. M. D. MacElroy, *Mol. Simul.* **35**, 3 (2009).
- ⁶⁰J.-A. Garate, N. J. English, and J. M. D. MacElroy, *J. Chem. Phys.* **131**, 114508 (2009).
- ⁶¹N. J. English, J.-A. Garate, and J. M. D. MacElroy, *Carbon Nanotubes: Growth Application* (InTech, 2011).
- ⁶²F. C. Bernstein, T. F. Koetzle, G. J. Williams, E. F. Meyer, M. D. Brice, J. R. Rodgers, O. Kennard, T. Shimanouchi, and M. Tasumi, *J. Mol. Biol.* **112**, 535 (1977).
- ⁶³A. D. MacKerell, D. Bashford, M. Bellott, R. L. Dunbrack, J. D. Evanseck, M. J. Field, S. Fischer, J. Gao, H. Guo, S. Ha, D. Joseph-McCarthy, L. Kuchnir, K. Kucera, F. T. K. Lau, C. Mattos, S. Michnick, T. Ngo, D. T. Nguyen,



ARTICLE

Behavioral and synaptic alterations relevant to obsessive-compulsive disorder in mice with increased EAAT3 expression

Claudia Delgado-Acevedo^{1,2,3}, Sebastián F. Estay^{2,3,4}, Anna R. Radke^{5,6}, Ayesha Sengupta⁵, Angélica P. Escobar^{1,3}, Francisca Henríquez-Belmar^{1,2}, Cristopher A. Reyes^{1,2}, Valentina Haro-Acuña^{1,2}, Elías Utreras^{7,8}, Ramón Sotomayor-Zárate^{1,9}, Andrew Cho⁷, Jens R. Wendland^{10,11}, Ashok B. Kulkarni⁷, Andrew Holmes⁵, Dennis L. Murphy¹⁰, Andrés E. Chávez^{2,3,4} and Pablo R. Moya^{1,2,3,10}

Obsessive-compulsive disorder (OCD) is a severe, chronic neuropsychiatric disorder with a strong genetic component. The *SLC1A1* gene encoding the neuronal glutamate transporter EAAT3 has been proposed as a candidate gene for this disorder. Gene variants affecting *SLC1A1* expression in human brain tissue have been associated with OCD. Several mouse models fully or partially lacking EAAT3 have shown no alterations in baseline anxiety-like or repetitive behaviors. We generated a transgenic mouse model (EAAT3^{9lo}) to achieve conditional, Cre-dependent EAAT3 overexpression and evaluated the overall impact of increased EAAT3 expression at behavioral and synaptic levels. Mice with EAAT3 overexpression driven by CaMKII α -promoter (EAAT3^{9lo}/CMKII) displayed increased anxiety-like and repetitive behaviors that were both restored by chronic, but not acute, treatment with fluoxetine or clomipramine. EAAT3^{9lo}/CMKII mice also displayed greater spontaneous recovery of conditioned fear. Electrophysiological and biochemical analyses at corticostriatal synapses of EAAT3^{9lo}/CMKII mice revealed changes in NMDA receptor subunit composition and altered NMDA-dependent synaptic plasticity. By recapitulating relevant behavioral, neurophysiological, and psychopharmacological aspects, our results provide support for the glutamatergic hypothesis of OCD, particularly for the increased EAAT3 function, and provide a valuable animal model that may open novel therapeutic approaches to treat this devastating disorder.

Neuropsychopharmacology (2019) 0:1–11; <https://doi.org/10.1038/s41386-018-0302-7>

INTRODUCTION

Obsessive-compulsive disorder (OCD) is a neuropsychiatric disorder characterized by intrusive thoughts (obsessions), repetitive ritualistic behaviors (compulsions), and anxiety, with a worldwide prevalence of 2–3% [1]. The only approved pharmacotherapy for OCD is (selective) serotonin reuptake inhibitors; however, 40–50% of affected individuals fail to respond to medication [2, 3]. Thus, there is a critical need to understand the neurobiological underpinnings of OCD.

The glutamatergic hypothesis of OCD has accumulated support over the last decades [4, 5]. Neuroimaging studies indicate alterations in the cortical–striatal–thalamic–cortical (CSTC) circuitry, which includes glutamatergic corticostriatal projections synapsing onto striatal spiny projection neurons and/or interneurons [4, 6–10]. Altered glutamate levels from cerebrospinal fluid studies have been reported in OCD [11, 12]. Beneficial effects

of anti-glutamatergic agents including memantine, N-acetylcysteine, riluzole, ketamine, and rapastinel have been reported in treatment-resistant OCD individuals [5, 13–17]. In addition, some genetic animal models with altered glutamatergic neurotransmission at the CSTC circuitry exhibit OCD relevant behaviors [10, 18–20].

Family-based linkage and case-control association studies have suggested *SLC1A1* (Solute Carrier, Family 1, member 1) as a candidate gene in OCD [21–28], although no variants within the *SLC1A1* locus have reached significance in genome-wide association studies [29, 30], likely due to limited statistical power. *SLC1A1* encodes for the neuronal excitatory amino acid transporter EAAT3, highly expressed in brain regions proposed to be affected in OCD [31]. EAAT3 is located postsynaptically, with roles on regulating glutamate spillover, NMDAR function and synaptic plasticity [32–

¹Instituto de Fisiología, Facultad de Ciencias, Universidad de Valparaíso, Valparaíso, Chile; ²Núcleo Milenio NUMIND Biology of Neuropsychiatric Disorders, Facultad de Ciencias, Universidad de Valparaíso, Valparaíso, Chile; ³Centro Interdisciplinario de Neurociencias de Valparaíso CINV, Facultad de Ciencias, Universidad de Valparaíso, Valparaíso, Chile; ⁴Instituto de Neurociencias, Facultad de Ciencias, Universidad de Valparaíso, Valparaíso, Chile; ⁵Laboratory of Behavioral and Genomic Neuroscience, National Institute on Alcohol Abuse and Alcoholism, Rockville, MD, USA; ⁶Department of Psychology and Center for Neuroscience and Behavior, Miami University, Oxford, OH, USA; ⁷Functional Genomics Section and Gene Transfer Core, National Institute of Dental and Craniofacial Research, Bethesda, MD, USA; ⁸Department of Biology, Faculty of Sciences, Universidad de Chile, Santiago, Chile; ⁹Centro de Neurobiología y Fisiopatología Integrativa, Facultad de Ciencias, Universidad de Valparaíso, Valparaíso, Chile and ¹⁰Laboratory of Clinical Science, National Institute of Mental Health, Bethesda, MD, USA

Correspondence: Pablo R. Moya (pablo.moya@uv.cl) or Andrés E. Chávez (andres.chavez@uv.cl)

¹¹Present address: Takeda Pharmaceutical Company Limited, 35 Landsdowne Street, Cambridge, MA 02139, USA

These authors contributed equally: Claudia Delgado-Acevedo, Sebastián F. Estay.

Dr. Dennis L. Murphy passed away on September 23, 2017.

Received: 2 August 2018 Revised: 1 December 2018 Accepted: 15 December 2018

Published online: 26 December 2018

10

validity for our animal model and recapitulate the human psychopharmacology of OCD.

In summary, our data support the notion that EAAT3 has a role in the pathogenesis of OCD relevant behaviors as EAAT3^{9/0}/CMKII mice exhibit increased anxiety, increased repetitive behaviors, and greater spontaneous recovery of fear, many of which are core symptoms of OCD. In addition, increased EAAT3 expression impairs corticostriatal synapses which could contribute, at least in part, to the neuronal basis involved in OCD. We believe this new model will allow gaining deeper insight on the role of EAAT3 in the pathogenesis of OCD and perhaps shedding light on novel therapeutic avenues for this devastating disorder.

FUNDING AND DISCLOSURE

This work was supported by Millennium Nucleus NuMIND (ICM MINECOM NC130011) and Millennium Institute CINV (ICM MINECOM P09-022F), both grants from the Millennium Scientific Initiative of the Ministry of Economy, Development and Tourism (Chile) (PRM and AEC); Fondecyt Grant #1141272 (Chile) (PRM); NIMH Intramural Research Program (USA) (DLM); NICDR Intramural Research Program (USA) (ABK); NIAAA Intramural Research Program (USA) (AH). Partially supported by Fondecyt Grants # 1151091 (AEC) and 1160398 (RSZ). JRW is a current employee and stockholder of Takeda Pharmaceuticals and a former employee and stockholder of Nestlé Health Science, Pfizer, and F. Hoffmann-La Roche. PRM has received research funds from F. Hoffmann-La Roche. All other authors declare no competing interests.

ACKNOWLEDGEMENTS

The authors especially thank Dr. Carla Alvarez and Pedro Espinosa for their work that forms the basis for Figures 4 and 5.

ADDITIONAL INFORMATION

Supplementary Information accompanies this paper at (<https://doi.org/10.1038/s41386-018-0302-7>).

Publisher's note: Springer Nature remains neutral with regard to jurisdictional claims in published maps and institutional affiliations.

REFERENCES

- Murphy DL, Moya PR, Wendland JR, Timpano KR. Genetic contributions to obsessive-compulsive disorder (OCD) and OCD-related disorders. In: Berrettini JNW, (ed). Principles of psychiatric genetics. Cambridge, UK: Cambridge University Press; 2012. p. 121–33.
- DSM-5. Diagnostic and statistical manual of mental disorders (DSM-5). 5th ed. Arlington, VA: American Psychiatric Association; 2013.
- Koran LM, Hanna GL, Hollander E, Nestadt G, Simpson HB, American Psychiatric Association. Practice guideline for the treatment of patients with obsessive-compulsive disorder. *Am J Psychiatry*. 2007;164:5–53.
- Ahmari SE, Dougherty DD. Dissecting OCD circuits: from animal models to targeted treatments. *Depress Anxiety*. 2015;32:550–62.
- Pittenger C. Glutamatergic agents for OCD and related disorders. *Curr Treat Options Psychiatry*. 2015;2:271–83.
- Menzies L, Chamberlain SR, Laird AR, Thelen SM, Sahakian BJ, Bullmore ET. Integrating evidence from neuroimaging and neuropsychological studies of obsessive-compulsive disorder: the orbitofronto-striatal model revisited. *Neurosci Biobehav Rev*. 2008;32:525–49.
- Rosenberg DR, Hanna GL. Genetic and imaging strategies in obsessive-compulsive disorder: potential implications for treatment development. *Biol Psychiatry*. 2000;48:1210–22.
- Tian L, Meng C, Jiang Y, Tang Q, Wang S, Xie X, et al. Abnormal functional connectivity of brain network hubs associated with symptom severity in treatment-naïve patients with obsessive-compulsive disorder: a resting-state functional MRI study. *Prog Neuropsychopharmacol Biol Psychiatry*. 2016;66:104–11.
- Vaghi MM, Vertes PE, Kitzbichler MG, Apergis-Schoute AM, van der Flier FE, Fineberg NA, et al. Specific frontostriatal circuits for impaired cognitive flexibility and goal-directed planning in obsessive-compulsive disorder: evidence from resting-state functional connectivity. *Biol Psychiatry*. 2017;81:708–17.
- Zike I, Xu T, Hong N, Veenstra-VanderWeele J. Rodent models of obsessive compulsive disorder: evaluating validity to interpret emerging neurobiology. *Neuroscience*. 2017;345:256–73.
- Bhattacharyya S, Khanna S, Chakrabarty K, Mahadevan A, Christopher R, Shankar SK. Anti-brain autoantibodies and altered excitatory neurotransmitters in obsessive-compulsive disorder. *Neuropsychopharmacology*. 2009;34:2489–96.
- Chakrabarty K, Bhattacharyya S, Christopher R, Khanna S. Glutamatergic dysfunction in OCD. *Neuropsychopharmacology*. 2005;30:1735–40.
- Coric V, Taskiran S, Pittenger C, Wasyluk S, Mathalon DH, Valentine G, et al. Riluzole augmentation in treatment-resistant obsessive-compulsive disorder: an open-label trial. *Biol Psychiatry*. 2005;58:424–8.
- Grant P, Lougee L, Hirschtritt M, Swedo SE. An open-label trial of riluzole, a glutamate antagonist, in children with treatment-resistant obsessive-compulsive disorder. *J Child Adolesc Psychopharmacol*. 2007;17:761–7.
- Pittenger C, Krystal JH, Coric V. Glutamate-modulating drugs as novel pharmacotherapeutic agents in the treatment of obsessive-compulsive disorder. *NeuroRx*. 2006;3:69–81.
- Rodriguez CI, Kegeles LS, Levinson A, Feng T, Marcus SM, Vermes D, et al. Randomized controlled crossover trial of ketamine in obsessive-compulsive disorder: proof-of-concept. *Neuropsychopharmacology*. 2013;38:2475–83.
- Rodriguez CI, Zwerling J, Kalanthroff E, Shen H, Filippou M, Jo B, et al. Effect of a novel NMDA receptor modulator, rapastinel (Formerly GLYX-13), in OCD: proof of concept. *Am J Psychiatry*. 2016;173:1239–41.
- Nordstrom EJ, Burton FH. A transgenic model of comorbid Tourette's syndrome and obsessive-compulsive disorder circuitry. *Mol Psychiatry*. 2002;7:617–25.
- Shmelkov SV, Hormigo A, Jing D, Proenca CC, Bath KG, Milde T, et al. Slitrk5 deficiency impairs corticostriatal circuitry and leads to obsessive-compulsive-like behaviors in mice. *Nat Med*. 2010;16:598–602.
- Welch JM, Lu J, Rodriguez RM, Trotta NC, Peca J, Ding JD, et al. Cortico-striatal synaptic defects and OCD-like behaviours in Sapap3-mutant mice. *Nature*. 2007;448:894–900.
- Dickel DE, Veenstra-VanderWeele J, Cox NJ, Wu X, Fischer DJ, Van Etten-Lee M, et al. Association testing of the positional and functional candidate gene SLC1A1/EAAC1 in early-onset obsessive-compulsive disorder. *Arch Gen Psychiatry*. 2006;63:778–85.
- Hanna GL, Veenstra-VanderWeele J, Cox NJ, Boehnke M, Himle JA, Curtis GC, et al. Genome-wide linkage analysis of families with obsessive-compulsive disorder ascertained through pediatric probands. *Am J Med Genet*. 2002;114:541–52.
- Arnold PD, Sicard T, Burroughs E, Richter MA, Kennedy JL. Glutamate transporter gene SLC1A1 associated with obsessive-compulsive disorder. *Arch Gen Psychiatry*. 2006;63:769–76.
- Shugart YY, Wang Y, Samuels JF, Grados MA, Greenberg BD, Knowles JA, et al. A family-based association study of the glutamate transporter gene SLC1A1 in obsessive-compulsive disorder in 378 families. *Am J Med Genet B Neuropsychiatr Genet*. 2009;150B:886–92.
- Stewart SE, Fagerness JA, Platto J, Smoller JW, Scharf JM, Illmann C, et al. Association of the SLC1A1 glutamate transporter gene and obsessive-compulsive disorder. *Am J Med Genet B Neuropsychiatr Genet*. 2007;144B:1027–33.
- Veenstra-VanderWeele J, Kim SJ, Gonen D, Hanna GL, Leventhal BL, Cook EH, et al. Genomic organization of the SLC1A1/EAAC1 gene and mutation screening in early-onset obsessive-compulsive disorder. *Mol Psychiatry*. 2001;6:160–7.
- Wendland JR, Moya PR, Timpano KR, Anavitate AP, Kruse MR, Wheaton MG, et al. A haplotype containing quantitative trait loci for SLC1A1 gene expression and its association with obsessive-compulsive disorder. *Arch Gen Psychiatry*. 2009;66:408–16.
- Willour VL, Yao Shugart Y, Samuels J, Grados M, Cullen B, Bienvenu OJ 3rd, et al. Replication study supports evidence for linkage to 9p24 in obsessive-compulsive disorder. *Am J Hum Genet*. 2004;75:508–13.
- Mattheisen M, Samuels JF, Wang Y, Greenberg BD, Fyer AJ, McCracken JT, et al. Genome-wide association study in obsessive-compulsive disorder: results from the OCGAS. *Mol Psychiatry*. 2015;20:337–44.
- Stewart SE, Yu D, Scharf JM, Neale BM, Fagerness JA, Mathews CA, et al. Genome-wide association study of obsessive-compulsive disorder. *Mol Psychiatry*. 2013;18:788–98.
- Kanai Y, Hediger MA. The glutamate/neutral amino acid transporter family SLC1: molecular, physiological and pharmacological aspects. *Pflug Arch*. 2004;447:469–79.
- Diamond JS. Neuronal glutamate transporters limit activation of NMDA receptors by neurotransmitter spillover on CA1 pyramidal cells. *J Neurosci*. 2001;21:8328–38.
- Li MH, Underhill SM, Reed C, Phillips TJ, Amara SG, Ingram SL. Amphetamine and methamphetamine increase NMDAR-GluN2B synaptic currents in midbrain dopamine neurons. *Neuropsychopharmacology*. 2017;42:1539–47.



RIP-MD: a tool to study residue interaction networks in protein molecular dynamics

Sebastián Contreras-Riquelme^{1,2,3}, Jose-Antonio Garate⁴,
Tomas Perez-Acle^{1,4} and Alberto J.M. Martin³

¹ Computational Biology Laboratory (DLab), Fundacion Ciencia & Vida, Santiago, Chile

² Facultad de Ciencias de la Vida, Universidad Andrés Bello, Santiago, Chile

³ Network Biology Laboratory, Centro de Genómica y Bioinformática, Facultad de Ciencias, Universidad Mayor, Santiago, Chile

⁴ Centro Interdisciplinario de Neurociencia de Valparaíso, Valparaíso, Chile

ABSTRACT

Protein structure is not static; residues undergo conformational rearrangements and, in doing so, create, stabilize or break non-covalent interactions. Molecular dynamics (MD) is a technique used to simulate these movements with atomic resolution. However, given the data-intensive nature of the technique, gathering relevant information from MD simulations is a complex and time consuming process requiring several computational tools to perform these analyses. Among different approaches, the study of residue interaction networks (RINs) has proven to facilitate the study of protein structures. In a RIN, nodes represent amino-acid residues and the connections between them depict non-covalent interactions. Here, we describe residue interaction networks in protein molecular dynamics (RIP-MD), a visual molecular dynamics (VMD) plugin to facilitate the study of RINs using trajectories obtained from MD simulations of proteins. Our software generates RINs from MD trajectory files. The non-covalent interactions defined by RIP-MD include H-bonds, salt bridges, VdWs, cation- π , π - π , Arginine-Arginine, and Coulomb interactions. In addition, RIP-MD also computes interactions based on distances between C α s and disulfide bridges. The results of the analysis are shown in an user friendly interface. Moreover, the user can take advantage of the VMD visualization capacities, whereby through some effortless steps, it is possible to select and visualize interactions described for a single, several or all residues in a MD trajectory. Network and descriptive table files are also generated, allowing their further study in other specialized platforms. Our method was written in python in a parallelized fashion. This characteristic allows the analysis of large systems impossible to handle otherwise. RIP-MD is available at <http://www.dlab.cl/ripmd>.

Subjects Bioinformatics, Biophysics, Computational Biology

Keywords Residue interaction networks, Molecular dynamics, VMD plugin, Trajectory analysis

INTRODUCTION

The function of proteins is determined by both their 3D structure and their behavior. Therefore, the traditional dogma *sequence* \rightarrow *structure* \rightarrow *function* is currently restated as

Submitted 25 March 2018
Accepted 25 October 2018
Published 7 December 2018

Corresponding authors
Tomas Perez-Acle, tomas@dlab.cl
Alberto J.M. Martin,
alberto.martin@umayor.cl

Academic editor
Rüdiger Ettrich

Additional Information and
Declarations can be found on
page 14

DOI 10.7717/peerj.5998

© Copyright
2018 Contreras-Riquelme et al.

Distributed under
Creative Commons CC-BY 4.0

OPEN ACCESS

How to cite this article Contreras-Riquelme S, Garate J-A, Perez-Acle T, Martin AJM. 2018. RIP-MD: a tool to study residue interaction networks in protein molecular dynamics. *PeerJ* 6:e5998 DOI 10.7717/peerj.5998

protein, revealing an initial concerted action at the beginning of the closing process, with an overall reduction of correlations for the closed state. In the case study of GJC, a comparison of the initial structure and a short MD simulation revealed that inter-chain interfaces are stabilized mainly by HBs and SBs, and that Arg-Arg and Cation- π interactions tend to disappear over the trajectory.

Residue interaction networks in protein molecular dynamics is freely available for the academic community, and it is distributed in three forms: a webserver, where users can analyze a single PDB; an standalone version that can take advantage of multi-core systems to generate these RINs; and a VMD plugin that executes the standalone version of the software and at the same time benefits from the graphical viewer of VMD. All these distributions, together with manuals and help files can be accessed from <http://dlab.cl/ripmd>.

ACKNOWLEDGEMENTS

The authors would like to acknowledge F. Villanelo and other DLab members for their useful comments, suggestions and discussions of the work presented here.

ADDITIONAL INFORMATION AND DECLARATIONS

Funding

This work was partially supported by Programa de Apoyo a Centros con Financiamiento Basal AFB 17004 to Fundación Ciencia Vida; ICM-Economía project to Instituto Milenio Centro Interdisciplinario de Neurociencias de Valparaíso (CINV) [P09-022-F]; FONDECYT projects [1160574, 11140342, 1181089]; from the US Air Force Office of Scientific Research [FA9550-16-1-0384]; and Beca de Asistencia Académica from Universidad Nacional Andrés Bello to Sebastián Contreras-Riquelme. This research was also supported by the supercomputing infrastructure of the Chilean National Laboratory for High Performance Computing (NLHPC) [ECM-02]. There was no additional external funding received for this study. The funders had no role in study design, data collection and analysis, decision to publish, or preparation of the manuscript.

Grant Disclosures

The following grant information was disclosed by the authors:

Programa de Apoyo a Centros con Financiamiento Basal AFB 17004 to Fundación Ciencia Vida.

ICM-Economía project to Instituto Milenio Centro Interdisciplinario de Neurociencias de Valparaíso (CINV): P09-022-F.

FONDECYT projects: 1160574, 11140342, 1181089.

US Air Force Office of Scientific Research: FA9550-16-1-0384.

Beca de Asistencia Académica from Universidad Nacional Andrés Bello to Sebastián Contreras-Riquelme.

Chilean National Laboratory for High-Performance Computing (NLHPC): ECM-02.

RESEARCH ARTICLE

The connexin26 human mutation N14K disrupts cytosolic intersubunit interactions and promotes channel opening

Juan M. Valdez Capuccino¹, Payal Chatterjee², Isaac E. García^{3,4} , Wesley M. Botello-Smith², Han Zhang², Andrew L. Harris¹ , Yun Luo² , and Jorge E. Contreras^{1,5} 

A group of human mutations within the N-terminal (NT) domain of connexin 26 (Cx26) hemichannels produce aberrant channel activity, which gives rise to deafness and skin disorders, including keratitis-ichthyosis-deafness (KID) syndrome. Structural and functional studies indicate that the NT of connexin hemichannels is folded into the pore, where it plays important roles in permeability and gating. In this study, we explore the molecular basis by which N14K, an NT KID mutant, promotes gain of function. In macroscopic and single-channel recordings, we find that the N14K mutant favors the open conformation of hemichannels, shifts calcium and voltage sensitivity, and slows deactivation kinetics. Multiple copies of MD simulations of WT and N14K hemichannels, followed by the Kolmogorov–Smirnov significance test (KS test) of the distributions of interaction energies, reveal that the N14K mutation significantly disrupts pairwise interactions that occur in WT hemichannels between residue K15 of one subunit and residue E101 of the adjacent subunit (E101 being located at the transition between transmembrane segment 2 [TM2] and the cytoplasmic loop [CL]). Double mutant cycle analysis supports coupling between the NT and the TM2/CL transition in WT hemichannels, which is disrupted in N14K mutant hemichannels. KS tests of the α carbon correlation coefficients calculated over MD trajectories suggest that the effects of the N14K mutation are not confined to the K15–E101 pairs but extend to essentially all pairwise residue correlations between the NT and TM2/CL interface. Together, our data indicate that the N14K mutation increases hemichannel open probability by disrupting interactions between the NT and the TM2/CL region of the adjacent connexin subunit. This suggests that NT–TM2/CL interactions facilitate Cx26 hemichannel closure.

Introduction

Connexins are a family of transmembrane proteins encoded by 21 human genes, found in almost every human tissue, which play key roles in physiology and pathology (Söhl and Willecke, 2003). At the structural level, the basic topology of a connexin protein consists of four transmembrane segments (TM1–4), two extracellular loops (E1 and E2), and one cytoplasmic loop (CL), with both the N- and C-terminal domains facing the cytosol. The assembly of six connexin proteins forms a hemichannel that is trafficked to the plasma membrane, where it can dock with another hemichannel of an adjacent cell to form a gap junction channel (GJC; Goodenough et al., 1996; Gaietta et al., 2002; Sosinsky and Nicholson, 2005). Both unpaired he-

michannels and GJCs are permeable to atomic ions and small molecules (Harris, 2001). Hemichannels at the plasma membrane are mostly closed when they are not part of GJCs. This is achieved by negative membrane potential and normal extracellular Ca^{2+} concentrations that together significantly reduce hemichannel open probability (Ebihara et al., 2003; Bukauskas and Verselis, 2004; Fasciani et al., 2013; Verselis and Srinivas, 2013; Bargiello et al., 2018).

The mechanisms by which extracellular Ca^{2+} controls gating in connexin hemichannels is related to interactions of Ca^{2+} ions with negatively charged residues lining the extracellular entrance of the channel pore (near the border of the TM1 and

¹Department of Pharmacology, Physiology & Neuroscience, New Jersey Medical School, Rutgers University, Newark, NJ; ²Department of Pharmaceutical Sciences, College of Pharmacy, Western University of Health Sciences, Pomona, CA; ³Laboratory of Molecular Physiology and Biophysics, Facultad de Odontología, Universidad de Valparaíso, Valparaíso, Chile; ⁴Centro Interdisciplinario de Neurociencias de Valparaíso, Universidad de Valparaíso, Valparaíso, Chile; ⁵Rutgers School of Graduate Studies, Newark, NJ.

Correspondence to Jorge E. Contreras: contrero@njms.rutgers.edu; Yun Luo: luoy@westernu.edu.

This work is part of the special collection entitled "Molecular Physiology of the Cell Membrane: An Integrative Perspective from Experiment and Computation."

© 2018 Valdez Capuccino et al. This article is distributed under the terms of an Attribution–Noncommercial–Share Alike–No Mirror Sites license for the first six months after the publication date (see <http://www.rupress.org/terms/>). After six months it is available under a Creative Commons License (Attribution–Noncommercial–Share Alike 4.0 International license, as described at <https://creativecommons.org/licenses/by-nc-sa/4.0/>).

pathology caused by N14K mutation, because severe skin lesions are thought to be caused by the increase of connexin hemichannel activity that disrupts the normal homeostasis necessary for skin proliferation and differentiation (Djalilian et al., 2006). Our work suggests that the molecular basis of the pathology is the disruption of pairwise interactions between the NT and TM2/CL regions, which leads to favoring of the open conformation of the Cx26 hemichannel.

Acknowledgments

We thank Yu Liu for technical support.

The research reported in this publication was supported by the National Institutes of Health/National Institute of General Medical Sciences (grants RO1-GM099490 to J.E. Contreras and RO1-GM101950 to A.L. Harris and J.E. Contreras); Fondo Nacional de Desarrollo Científico y Tecnológico grant 3150634 and Programa de Atracción e Inserción de Capital Humano Avanzado a la Academia PAI 79170081 to I.E. García. The computational work was supported by National Science Foundation XSE DE research allocation MCB160119. J.E. Contreras is supported by the Health Resources and Services Administration through grant D34HP26020 to New Jersey Medical School Hispanic Center of Excellence.

The authors declare no competing financial interests.

Author contributions: J.M. Valdez Capuccino and J.E. Contreras designed research; Y. Luo designed the MD simulations; J.M. Valdez Capuccino, I.E. García, and J.E. Contreras performed research; P. Chatterjee, W.M. Botello-Smith, H. Zhang and Y. Luo performed the MD simulations; A.L. Harris provided guidance for molecular dynamics design and interpretations; J.M. Valdez Capuccino, I.E. García, and J.E. Contreras analyzed experimental data; and J.M. Valdez Capuccino, I.E. García, A.L. Harris, Y. Luo, and J.E. Contreras wrote the paper.

José D. Faraldo-Gómez served as editor.

Submitted: 18 August 2018

Revised: 21 October 2018

Accepted: 17 November 2018

References

- Bargiello, T.A., S. Oh, Q. Tang, N.K. Bargiello, T.L. Dowd, and T. Kwon. 2018. Gating of Connexin Channels by transjunctional-voltage: Conformations and models of open and closed states. *Biochim Biophys Acta Biomembr.* 1860:22–39. <https://doi.org/10.1016/j.bbmem.2017.04.028>
- Bennett, B.C., M.D. Purdy, K.A. Baker, C. Acharya, W.E. McIntire, R.C. Stevens, Q. Zhang, A.L. Harris, R. Abagyan, and M. Yeager. 2016. An electrostatic mechanism for Ca(2+)-mediated regulation of gap junction channels. *Nat. Commun.* 7:1–12. <https://doi.org/10.1038/ncomms9770>
- Bukauskas, F.F., and V.K. Verselis. 2004. Gap junction channel gating. *Biochim. Biophys. Acta.* 1662:42–60. <https://doi.org/10.1016/j.bbmem.2004.01.008>
- Case, D.A., R.M. Betz, D.S. Cerutti, T.E. Cheatham, T.A. Darden III, R.E. Duke, T.J. Giese, H. Gohlke, A.W. Goetz, N. Homeyer, et al. 2016. AMBER 2016 Reference Manual, University of California, San Francisco. 923 pp.
- Djalilian, A.R., D. McGaughey, S. Patel, E.Y. Seo, C. Yang, J. Cheng, M. Tomic, S. Sinha, A. Ishida-Yamamoto, and J.A. Segre. 2006. Connexin 26 regulates epidermal barrier and wound remodeling and promotes psoriasisiform response. *J. Clin. Invest.* 116:1243–1253. <https://doi.org/10.1172/JCI27186>
- Ebihara, L. 1996. Xenopus connexin38 forms hemi-gap-junctional channels in the nonjunctional plasma membrane of Xenopus oocytes. *Biophys. J.* 71:742–748. [https://doi.org/10.1016/S0006-3495\(96\)79273-1](https://doi.org/10.1016/S0006-3495(96)79273-1)
- Ebihara, L., X. Liu, and J.D. Pal. 2003. Effect of external magnesium and calcium on human connexin46 hemichannels. *Biophys. J.* 84:277–286. [https://doi.org/10.1016/S0006-3495\(03\)74848-6](https://doi.org/10.1016/S0006-3495(03)74848-6)
- Ek Vitorin, J.F., T.K. Pontifex, and J.M. Burt. 2016. Determinants of Cx43 Channel Gating and Permeation: The Amino Terminus. *Biophys. J.* 110:127–140. <https://doi.org/10.1016/j.bpj.2015.10.054>
- Fasciani, I., A. Temperán, L.F. Pérez-Atencio, A. Escudero, P. Martínez-Montero, J. Molano, J.M. Gómez-Hernández, C.L. Paino, D. González-Nieto, and L.C. Barrio. 2013. Regulation of connexin hemichannel activity by membrane potential and the extracellular calcium in health and disease. *Neuropharmacology.* 75:479–490. <https://doi.org/10.1016/j.neuropharm.2013.03.040>
- Gaietta, G., T.J. Deerinck, S.R. Adams, J. Bouwer, O. Tour, D.W. Laird, G.E. Sosinsky, R.Y. Tsien, and M.H. Ellisman. 2002. Multicolor and electron microscopic imaging of connexin trafficking. *Science.* 296:503–507. <https://doi.org/10.1126/science.1068793>
- García, I.E., F. Villanelo, G.F. Contreras, A. Pupo, B.I. Pinto, J.E. Contreras, T. Pérez-Acle, O. Alvarez, R. Latorre, A.D. Martínez, and C. González. 2018. The syndromic deafness mutation G12R impairs fast and slow gating in Cx26 hemichannels. *J. Gen. Physiol.* 150:697–711. <https://doi.org/10.1085/jgp.201711782>
- Gerido, D.A., A.M. DeRosa, G. Richard, and T.W. White. 2007. Aberrant hemichannel properties of Cx26 mutations causing skin disease and deafness. *Am. J. Physiol. Cell Physiol.* 293:C337–C345. <https://doi.org/10.1152/ajpcell.00626.2006>
- Gleitsman, K.R., S.M. Kedrowski, H.A. Lester, and D.A. Dougherty. 2008. An intersubunit hydrogen bond in the nicotinic acetylcholine receptor that contributes to channel gating. *J. Biol. Chem.* 283:35638–35643. <https://doi.org/10.1074/jbc.M807226200>
- Glykos, N.M. 2006. Software news and updates. Carma: a molecular dynamics analysis program. *J. Comput. Chem.* 27:1765–1768. <https://doi.org/10.1002/jcc.20482>
- Goodenough, D.A., J.A. Goliger, and D.L. Paul. 1996. Connexins, connexons, and intercellular communication. *Annu. Rev. Biochem.* 65:475–502. <https://doi.org/10.1146/annurev.bi.65.070196.002355>
- Harris, A.L. 2001. Emerging issues of connexin channels: biophysics fills the gap. *Q. Rev. Biophys.* 34:325–472. <https://doi.org/10.1017/S0033583501003705>
- Jo, S., T. Kim, V.G. Iyer, and W. Im. 2008. CHARMM-GUI: a web-based graphical user interface for CHARMM. *J. Comput. Chem.* 29:1859–1865. <https://doi.org/10.1002/jcc.20945>
- Jorgensen, W.L., J. Chandrasekhar, J.D. Madura, R.W. Impey, and M.L. Klein. 1983. Comparison of simple potential functions for simulating liquid water. *J. Chem. Phys.* 79:926–935. <https://doi.org/10.1063/1.445869>
- Kash, T.L., A. Jenkins, J.C. Kelley, J.R. Trudell, and N.L. Harrison. 2003. Coupling of agonist binding to channel gating in the GABA(A) receptor. *Nature.* 421:272–275. <https://doi.org/10.1038/nature01280>
- Klauda, J.B., R.M. Venable, J.A. Freites, J.W. O'Connor, D.J. Tobias, C. Mondragon-Ramirez, I. Vorobyov, A.D. MacKerell Jr., and R.W. Pastor. 2010. Update of the CHARMM all-atom additive force field for lipids: validation on six lipid types. *J. Phys. Chem. B.* 114:7830–7843. <https://doi.org/10.1021/jp101759q>
- Kwon, T., B. Roux, S. Jo, J.B. Klauda, A.L. Harris, and T.A. Bargiello. 2012. Molecular dynamics simulations of the Cx26 hemichannel: insights into voltage-dependent loop-gating. *Biophys. J.* 102:1341–1351. <https://doi.org/10.1016/j.bpj.2012.02.009>
- Kwon, T., Q. Tang, and T.A. Bargiello. 2013. Voltage-dependent gating of the Cx32*43E1 hemichannel: conformational changes at the channel entrances. *J. Gen. Physiol.* 141:243–259. <https://doi.org/10.1085/jgp.201210839>
- Laha, K.T., and D.A. Wagner. 2011. A state-dependent salt-bridge interaction exists across the β/α intersubunit interface of the GABAA receptor. *Mol. Pharmacol.* 79:662–671. <https://doi.org/10.1124/mol.110.068619>
- Lee, J.R., A.M. Derosa, and T.W. White. 2009. Connexin mutations causing skin disease and deafness increase hemichannel activity and cell death when expressed in Xenopus oocytes. *J. Invest. Dermatol.* 129:870–878. <https://doi.org/10.1038/jid.2008.335>
- Levit, N.A., G. Mese, M.G. Basaly, and T.W. White. 2012. Pathological hemichannels associated with human Cx26 mutations causing Keratitis-Ichthyosis-Deafness syndrome. *Biochim. Biophys. Acta.* 1818:2014–2019. <https://doi.org/10.1016/j.bbmem.2011.09.003>



Characterization of Retinal Functionality at Different Eccentricities in a Diurnal Rodent

María-José Escobar^{1*}, César Reyes¹, Rubén Herzog², Joaquín Araya^{2,3}, Mónica Otero¹, Cristóbal Ibaceta² and Adrián G. Palacios²

¹ Departamento de Electrónica, Universidad Técnica Federico Santa María, Valparaíso, Chile, ² Centro Interdisciplinario de Neurociencia de Valparaíso, Universidad de Valparaíso, Valparaíso, Chile, ³ Programa de Doctorado en Neurociencia, Universidad de Santiago de Chile, Santiago, Chile

OPEN ACCESS

Edited by:

Lisa Mapelli,
University of Pavia, Italy

Reviewed by:

Günther Zeck,
Natural and Medical Sciences
Institute, Germany
Evelyn Semagor,
Newcastle University, United Kingdom

*Correspondence:

María-José Escobar
mariajose.escobar@usm.cl

Received: 27 February 2018

Accepted: 05 November 2018

Published: 03 December 2018

Citation:

Escobar M-J, Reyes C, Herzog R, Araya J, Otero M, Ibaceta C and Palacios AG (2018) Characterization of Retinal Functionality at Different Eccentricities in a Diurnal Rodent. *Front. Cell. Neurosci.* 12:444. doi: 10.3389/fncel.2018.00444

Although the properties of the neurons of the visual system that process central and peripheral regions of the visual field have been widely researched in the visual cortex and the LGN, they have scarcely been documented for the retina. The retina is the first step in integrating optical signals, and despite considerable efforts to functionally characterize the different types of retinal ganglion cells (RGCs), a clear account of the particular functionality of cells with central vs. peripheral fields is still wanting. Here, we use electrophysiological recordings, gathered from retinas of the diurnal rodent *Octodon degus*, to show that RGCs with peripheral receptive fields (RF) are larger, faster, and have shorter transient responses. This translates into higher sensitivity at high temporal frequencies and a full frequency bandwidth when compared to RGCs with more central RF. We also observed that imbalances between ON and OFF cell populations are preserved with eccentricity. Finally, the high diversity of functional types of RGCs highlights the complexity of the computational strategies implemented in the early stages of visual processing, which could inspire the development of bio-inspired artificial systems.

Keywords: retina, MEA, central vs. periphery, RGCs, spatiotemporal analysis, receptive field properties

1. INTRODUCTION

The visual system integrates optical signals to create specific features of the images such as movement, contrast, and color (Van Essen et al., 1992; Masland, 2012). Although some studies suggest that there exists within the visual cortex a functional and modular segregation of regions that attend to the central vs. peripheral visual field (Stone, 1983; Orban et al., 1986; Loschky et al., 2017), the existence of such segregation at the level of the retina remains hardly studied. On the other hand, studies have described that any point of a visual scene is anatomically covered through a variety of different RGC types (for example, parasol and midget RGCs in primates or alpha cell RGCs in rodents) that form potential visual channels (e.g., ON / OFF) acting as functional filters for the physical world (Field and Chichilnisky, 2007). Moreover, Polyak (1957) raised what is still an unresolved problem how the diversity of RGCs contributes to forming a variety of visual channels as a function of retinal eccentricity, which is vital for many species (Boycott and Wässle, 1974; Golisch and Meister, 2010).

strategies for understanding the visual world (Nasr et al., 2011; Loschky et al., 2017). Interestingly, using a deep neural network the authors in Wang and Cottrell (2017) have shown that information coming from peripheral vision is as crucial for scene recognition as central vision.

A diversity of visual strategies can be created through the articulation of a variety of functional RGCs types located in the retina. Predictive coding theory hypothesizes that the role of neural encoding is to remove predictable information from the environment and to leave only the information that cannot be predicted. The work of Nirenberg et al. (2010) goes in this direction, suggesting that heterogeneity in RGC types is needed for predictive coding in different kinds of environments. Moreover, Gjorgjieva et al. (2014) recently reported that optimal coding in the retina is reached not by isolated ON or OFF neuronal populations, but by a mixture of ON/OFF neurons, suggesting a combined coding strategy.

AUTHOR CONTRIBUTIONS

MJ-E designed the experiments, analyzed data and wrote the paper. CR, MO, and RH analyzed data. JA and CI performed the retinal experiments. AP edited the paper.

REFERENCES

- Anishchenko, A., Greschner, M., Elstrott, J., Sher, A., Litke, A. M., Feller, M. B., et al. (2010). Receptive field mosaics of retinal ganglion cells are established without visual experience. *J. Neurophysiol.* 103, 1856–1864. doi: 10.1152/jn.00896.2009
- Arcaro, M. J., McMains, S. A., Singer, B. D., and Kastner, S. (2009). Retinotopic organization of human ventral visual cortex. *J. Neurosci.* 29, 10638–10652. doi: 10.1523/JNEUROSCI.2807-09.2009
- Armañanzas, R., and Ascoli, G. A. (2015). Towards the automatic classification of neurons. *Trends Neurosci.* 38, 307–318. doi: 10.1016/j.tins.2015.02.004
- Baden, T., Berens, P., Franke, K., Román Rosón, M., Bethge, M., and Euler, T. (2016). The functional diversity of retinal ganglion cells in the mouse. *Nature* 529, 345–350. doi: 10.1038/nature16468
- Ben-Simon, A., Ben-Shahar, O., Vasserman, G., Ben-Tov, M., and Segev, R. (2012). Visual acuity in the archerfish: behavior, anatomy, and neurophysiology. *J. Vision* 12:18. doi: 10.1167/12.12.18
- Bobu, C., Lahmam, M., Vuillez, P., Ouarour, A., and Hicks, D. (2008). Photoreceptor organisation and phenotypic characterization in retinas of two diurnal rodent species: potential use as experimental animal models for human vision research. *Vision Res.* 48, 424–432. doi: 10.1016/j.visres.2007.08.011
- Boycott, B. B., and Wässle, H. (1974). The morphological types of ganglion cells of the domestic cat's retina. *J. Physiol.* 240, 397–419. doi: 10.1113/jphysiol.1974.sp010616
- Campi, K. L., and Krubitzer, L. (2010). Comparative studies of diurnal and nocturnal rodents: differences in lifestyle result in alterations in cortical field size and number. *J. Compar. Neurol.* 518, 4491–4512. doi: 10.1002/cne.22466
- Chávez, A. E., Bozinovic, F., Peichl, L., and Palacios, A. G. (2003). Retinal spectral sensitivity, fur coloration, and urine reflectance in the genus *Octodon* (Rodentia): implications for visual ecology. *Invest. Ophthalmol. Vis. Sci.* 44, 2290. doi: 10.1167/jovs.02-0670
- Chichilnisky, E. J. (2001). A simple white noise analysis of neuronal light response. *Netw. Comput. Neural Syst.* 12, 199–213. doi: 10.1080/713663221
- Chichilnisky, E. J., and Kalmar, R. S. (2002). Functional asymmetries in ON and OFF ganglion cells of primate retina. *J. Neurosci.* 22, 2737–2747. doi: 10.1523/JNEUROSCI.22-07-02737.2002

FUNDING

FONDECYT 1140403 and 1150638, CONICYT-Basal Project FB0008; Grant ICM-P09-022-F supported by the Millenium Scientific Initiative of the Ministerio de Economía, Desarrollo y Turismo (Chile); ONR Research Grant # N62909-14-1-N121.

ACKNOWLEDGMENTS

We would also like to thank to Dr. Ronny Vallejos and Dr. Felipe Osorio for their valuable comments about the statistical analysis of the results and Dr. John Ewer for English suggestions.

SUPPLEMENTARY MATERIAL

The Supplementary Material for this article can be found online at: <https://www.frontiersin.org/articles/10.3389/fncel.2018.00444/full#supplementary-material>

Supplementary Figure 1 | Comparison between all the spatiotemporal parameters studied in this article. The relation between two parameters is represented as scatter-plots for the upper triangular matrix, and as level curves for the lower triangular matrix. The color code used is the same for all the article: the two centers are shown in red and orange; while the two peripheries are represented in green and blue.

- Croner, L. J., and Kaplan, E. (1995). Receptive fields of P and M ganglion cells across the primate retina. *Vision Res.* 35, 7–24.
- Curcio, C. A., and Allen, K. A. (1990). Topography of ganglion cells in human retina. *J. Compar. Neurol.* 300, 5–25.
- Dacey, D. M. (2000). Parallel pathways for spectral coding in primate retina. *Ann. Rev. Neurosci.* 23, 743–775. doi: 10.1146/annurev.neuro.23.1.743
- Dacey, D. M., and Petersen, M. R. (1992). Dendritic field size and morphology of midgenet and parasol ganglion cells of the human retina. *Proc. Natl. Acad. Sci. U.S.A.* 89(20):9666–9670.
- Demb, J. B., and Singer, J. H. (2015). Functional circuitry of the retina. *Ann. Rev. Vis. Sci.* 1, 263–289. doi: 10.1146/annurev-vision-082114-035334
- Demb, J. B., Zaghlool, K., and Sterling, P. (2001). Cellular basis for the response to second-order motion cues in Y retinal ganglion cells. *Neuron* 32, 711–721. doi: 10.1016/S0896-6273(01)00484-6
- Deny, S., Ferrari, U., Macé, E., Yger, P., Caplette, R., Picaud, S., et al. (2017). Multiplexed computations in retinal ganglion cells of a single type. *Nat. Commun.* 8, 1–17. doi: 10.1038/s41467-017-02159-y
- Devries, S. H. (2000). Bipolar cells use kainate and AMPA receptors to filter visual information into separate channels. *Neuron* 28, 847–856. doi: 10.1016/S0896-6273(00)00158-6
- Devries, S. H., and Baylor, D. A. (1997). Mosaic arrangement of ganglion cell receptive fields in rabbit retina. *J. Neurophysiol.* 78, 2048–2060.
- Dräger, U. C., and Olsen, J. F. (1981). Ganglion cell distribution in the retina of the mouse. *Invest. Ophthalmol. Vis. Sci.* 20, 285–293.
- Enroth-Cugell, C., and Robson, J. (1966). The contrast sensitivity of retinal ganglion cells of the cat. *J. Physiol.* 187, 517–552.
- Field, G. D., and Chichilnisky, E. J. (2007). Information processing in the primate retina: circuitry and coding. *Annu. Rev. Neurosci.* 30, 1–30. doi: 10.1146/annurev.neuro.30.051606.094252
- Gaillard, F., Bonfield, S., Gilmour, G. S., Kuny, S., Mema, S. C., Martin, B. T., et al. (2008). Retinal anatomy and visual performance in a diurnal cone-rich laboratory rodent, the Nile grass rat (*Arvicanthus niloticus*). *J. Compar. Neurol.* 510, 525–538. doi: 10.1002/cne.21798
- Gauthier, J. L., Field, G. D., Sher, A., Shlens, J., Greschner, M., Litke, A. M., et al. (2009). Uniform signal redundancy of parasol and



Transprotein-Electropore Characterization: A Molecular Dynamics Investigation on Human AQP4

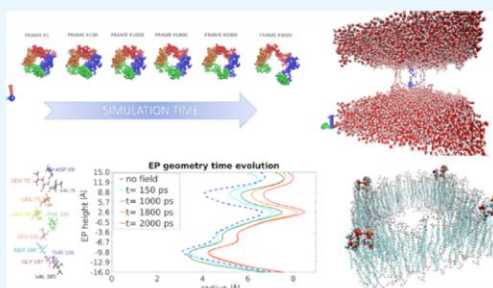
Paolo Marracino,^{*,†} Mario Bernardi,[†] Micaela Liberti,^{*,†} Federico Del Signore,[†] Erika Trapani,^{†,||} José-Antonio Gárate,[‡] Christian J. Burnham,[§] Francesca Apollonio,^{*,†} and Niall J. English^{*,§}

[†]Department of Information Engineering, Electronics and Telecommunications, La Sapienza University, 00184 Rome, Italy

[‡]Centro Interdisciplinario de neurociencia de Valparaíso, Universidad de Valparaíso, 05101 Valparaíso, Chile

[§]School of Chemical and Bioprocess Engineering, University College Dublin, Belfield, D4 Dublin, Ireland

ABSTRACT: Electroporation characterization is a topic of intensive interest probed by extensive ongoing research efforts. Usually, these studies are carried out on lipid-bilayer electroporation. Surprisingly, the possibility of water-channel electropore formation across transmembrane proteins themselves, particularly in view of such a promising application, has not yet been elucidated. The present work examines the geometrical and kinetic aspects of electropores and their stability in such a protein milieu (as opposed through the phospholipid membranes) in depth, by means of scrutiny of such a process in human-AQP4 as a well-representative prototype. The residues forming the electropore's walls, organized in loops, reveal the formation mechanism by their dipole alignment and translational response in response to applied axial electric fields in nonequilibrium molecular dynamics simulation. The magnitude of sustaining electric fields (keeping a stable electropore open) were determined. This suggests that transmembrane proteins could play a central role in electroporation applications, e.g., in medicine and biotechnology.



INTRODUCTION

The membrane phospholipid bilayer can be studied as a thin isolating sheet dividing two electrolyte solutions and enveloping intracellular components and organelles.¹ If this structure is exposed to an electric field pulse able to induce a transmembrane potential above a certain threshold value, the cell membrane will be permeabilized.² Depending on the duration of the pulse and the field intensity, the two systems on either side of the bilayer will no longer be isolated if electroporation through the membrane occurs, and molecules that could not flow through the transport-selective endogenous channels in bilayer-embedded proteins are then allowed to permeate through the electroporated membrane.³ The transiently reversible opening of the cell enables drugs and oligonucleotides to be transported, in addition to, inter alia, antibodies, permitting the initiation of biological events by changing the inside of the cell.⁴

The mechanistic detail of how pores form under the action of applied electric fields is inherently challenging to be elucidated by experiments; conversely, this is entirely possible to explore using carefully conducted molecular dynamics (MD) simulation due to the very short time scales of the pore-formation process and also the small space scale of lipid pores (a few nanometers).⁵ According to MD simulations of lipid bilayers, nanometer-sized aqueous pores are formed inside the lipid bilayers during the pulse application⁶ and the kinetics of

the opening and closure of these pores appear to be on the order of nanoseconds.⁷ However, this description is not completely satisfactory, since it does not take into consideration, for instance, that ultrashort pulses with a very high amplitude (tens of kV/cm) and duration of a few nanoseconds, called nanopulses, have displayed long-term effects on membrane permeability and conductivity of cells and tissues, most probably due to oxidation of the membrane phospholipids induced by the field.⁸

Even if not yet fully demonstrated, another option of long-lasting (electropore) permeability due to nanopulses could be related to the involvement of transmembrane proteins when cells are exposed to such short and intense electric fields. Recent *in vitro* studies have considered the possibility that nanopulses could influence specific ion channel behavior as voltage-gated ion channels in bovine chromaffin cells,⁹ whereas in a separate study, it has been proven that the calcium increase induced by ultrashort pulsed electric fields was mediated by voltage-gated calcium channels.¹⁰ Further evidence of specific involvement of voltage-sensitive ion channels has been presented in ref 11, whereas activation of

Received: August 30, 2018

Accepted: October 22, 2018

Published: November 13, 2018



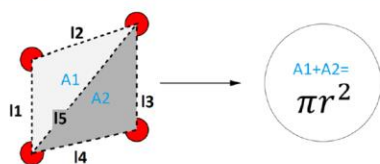


Figure 9. Pores are made of 11 loops, each one consisting of a repetition of four identical residues. The centers of mass of the residues for a single loop are depicted in red here. Summing the areas of the two triangles, obtained by Heron's formula, it is possible to estimate the radius of the pore corresponding to a given loop.

internal coordinates,^{48,49} to be consistent with pH 7.5. This tetramer is then embedded in a palmitoylphosphatidylethanolamine lipid bilayer, which is solvated and equilibrated. The membrane's overlapping lipids were removed and a solvation shell of 20 Å is added on the $\pm z$ axes. This entire system is made electrically neutral by the presence of Na^+ and Cl^- ions, the resulting concentration being 55 mM. The resulting periodic cell volume is $101 \times 101 \times 80 \text{ Å}^3$.

Molecular Dynamics Simulation. CHARMM27⁴⁹ and TIP3P⁵⁰ potential models were used. CHARMM27 is a nonpolarizable potential, in contrast to previous work of English et al.,^{51–53} but returns qualitative acceptable outcomes.⁵⁴ Long-range electrostatic interactions were handled by the particle mesh Ewald method, making use of r-RESPA decomposition.¹⁷ Each simulation relies on an NPT reservoir for coupling. The reservoir pressure and temperature point were set respectively to 1 atm and 298 K. Temperature was controlled through a Langevin thermostat with a damping coefficient of 1 ps^{-1} .^{55–57} The applied electric field was static, and acted in the direction of the positive z -axis; as reported above, a strength of 0.05 V/Å led to electroporation. The static-field force was applied to atomic partial charges, using $f = qE_0$. This kind of system response of water to electric fields in nanoscale geometries embedded in phospholipid bilayers has been studied extensively by Garate and co-workers.^{17,58,59,60}

Pore Profile. To obtain the cross-sectional area of the electropore, an equivalent-area method was implemented, keeping in mind that each of the 11 residues is at a slightly different "height" along the z -axes. Here, we consider a square as composed of two triangles, whose areas are computed through Heron's formula

$$A_{\text{tr1}} = \sqrt{p(p-l_1)(p-l_2)(p-l_3)}$$

$$A_{\text{tr2}} = \sqrt{p(p-l_3)(p-l_4)(p-l_5)}$$

$$A = A_{\text{tr1}} + A_{\text{tr2}} = \pi r^2$$

where A is the cross-sectional area, l_1 , l_2 , and l_3 are the side lengths, and p is the semiperimeter, i.e., $1/2(l_1 + l_2 + l_3)$. The radius of the circle inscribed in the square, as shown in Figure 9, provides a rough estimate of the electropore radius within a given residue loop.

AUTHOR INFORMATION

Corresponding Authors

*E-mail: marracino@diet.uniroma1.it. Tel: +39-06-4458-5457 (P.M.).

*E-mail: micaela.liberti@uniroma1.it. Tel: +39-06-4458-5353 (M.L.).

*E-mail: francesca.apollonio@uniroma1.it. Tel: +39-06-4458-5374 (F.A.).

*E-mail: niall.english@ucd.ie. Tel: +353-1-716-1646. Fax: +353-1-716-1177 (N.J.E.).

ORCID

Niall J. English: 0000-0002-8460-3540

Present Address

[†]Accenture Consulting, Piazzale dell'industria, 40, 00144 Rome, Italy (E.T.).

Notes

The authors declare no competing financial interest.

ACKNOWLEDGMENTS

The authors thank Zdenek Futera, Mohammad Reza Ghaani, and Massimiliano Avena for interesting discussions and technical assistance. J.A.G. acknowledges financial support from CM-Economía grant P09-022-F CINV and Universidad de Valparaíso, FONDECYT grant No. 1180987 and PAI grant No. 77170045. M.L. acknowledges financial support from grant No. RM11715C7DCB8473, University Sapienza of Rome and F.A. acknowledges financial support from grant No. RM116154E273BDD4 University Sapienza of Rome.

REFERENCES

- (1) Van Meer, G.; Voelker, D. R.; Feigenson, G. W. Membrane lipids: where they are and how they behave. *Nat. Rev. Mol. Cell Biol.* **2008**, *9*, 112–124.
- (2) (a) Schwan, H. P. *Biological Effects and Dosimetry of Nonionizing Radiation*; Springer: Boston, MA, 1983. (b) Kotnik, T.; Pucihar, G.; Miklavcic, D. Induced transmembrane voltage and its correlation with electroporation-mediated molecular transport. *J. Membr. Biol.* **2010**, *236*, 3–13.
- (3) Weaver, J. C.; Chizmadzhev, Y. A. Theory of electroporation: a review. *Bioelectrochem. Bioenergy* **1996**, *41*, 135–160.
- (4) Mir, L. M. Bases and rationale of the electrochemotherapy. *EJC Suppl.* **2006**, *4*, 38–44.
- (5) Tarek, M. Membrane Electroporation: A Molecular Dynamics Simulation. *Biophys. J.* **2005**, *88*, 4045–4053.
- (6) Tieleman, D. P. The molecular basis of electroporation. *BMC Biochem.* **2004**, *5*, No. 10.
- (7) Vernier, P. T.; Levine, Z. A.; Wu, Y.-H. H.; Joubert, V.; Ziegler, M. J.; Mir, L. M.; Tieleman, D. P.; et al. Electroporating fields target oxidatively damaged areas in the cell membrane. *PLoS One* **2009**, *4*, No. e7966, DOI: 10.1371/journal.pone.0007966.
- (8) Breton, M.; Mir, L. M. Investigation of the chemical mechanisms involved in the electropulsation of membranes at the molecular level. *Bioelectrochemistry* **2018**, *119*, 76–83.
- (9) Craviso, G. L.; Choe, S.; Chatterjee, P.; Chatterjee, I.; Vernier, P. T. Nanosecond electric pulses: A novel stimulus for triggering Ca^{2+} influx into chromaffin cells via voltage-gated Ca^{2+} channels. *Cell. Mol. Neurobiol.* **2010**, *30*, 1259–1265.
- (10) Semenov, I.; Xiao, S.; Kang, D.; Schoenbach, K. H.; Pakhomov, A. G. Cell stimulation and calcium mobilization by picosecond electric pulses. *Bioelectrochemistry* **2015**, *105*, 65–71.
- (11) Burke, R. C.; Bardet, S. M.; Carr, L.; Romanenko, S.; Arnaud-Cormos, D.; Leveque, P.; O'Connor, R. P. Nanosecond pulsed electric fields depolarize transmembrane potential via voltage-gated K^+ , Ca^{2+} and TRPM8 channels in U87 glioblastoma cells. *Biochim. Biophys. Acta* **2017**, *1859*, 2040–2050.
- (12) Muratori, C.; Pakhomov, A. iG.; Gianulis, E.; Meads, J.; Casciola, M.; Mollica, P. A.; Pakhomova, O. N. Activation of the phospholipid scramblase TMEM16F by nanosecond pulsed electric fields (nsPEF) facilitates its diverse cytophysiological effects. *J. Biol. Chem.* **2017**, *292*, 19381–19391.
- (13) Hohmann, S.; Nielsen, S.; Agre, P. *Aquaporins*; Academic Press: San Diego, CA, 2001.

Please cite this article in press as: Horng et al., Continuum Gating Current Models Computed with Consistent Interactions, Biophysical Journal (2019), <https://doi.org/10.1016/j.bpj.2018.11.3140>

Biophysical Journal
Article



Continuum Gating Current Models Computed with Consistent Interactions

Tzzy-Leng Horng,¹ Robert S. Eisenberg,^{2,3} Chun Liu,² and Francisco Bezanilla^{4,5,*}

¹Department of Applied Mathematics, Feng Chia University, Taichung, Taiwan; ²Department of Applied Mathematics, Illinois Institute of Technology, Chicago, Illinois; ³Department of Physiology and Biophysics, Rush University, Chicago, Illinois; ⁴Department of Biochemistry and Molecular Biology and Institute for Biophysical Dynamics, University of Chicago, Chicago, Illinois; and ⁵Centro Interdisciplinario de Neurociencia de Valparaíso, Facultad de Ciencias, Universidad de Valparaíso, Valparaíso, Chile

ABSTRACT The action potential of nerve and muscle is produced by voltage-sensitive channels that include a specialized device to sense voltage. The voltage sensor depends on the movement of charges in the changing electric field as suggested by Hodgkin and Huxley. Gating currents of the voltage sensor are now known to depend on the movements of positively charged arginines through the hydrophobic plug of a voltage sensor domain. Transient movements of these permanently charged arginines, caused by the change of transmembrane potential V , further drag the S4 segment and induce opening/closing of the ion conduction pore by moving the S4-S5 linker. This moving permanent charge induces capacitive current flow everywhere. Everything interacts with everything else in the voltage sensor and protein, and so it must also happen in its mathematical model. A Poisson-Nernst-Planck (PNP)-steric model of arginines and a mechanical model for the S4 segment are combined using energy variational methods in which all densities and movements of charge satisfy conservation laws, which are expressed as partial differential equations in space and time. The model computes gating current flowing in the baths produced by arginines moving in the voltage sensor. The model also captures the capacitive pile up of ions in the vestibules that link the bulk solution to the hydrophobic plug. Our model reproduces the signature properties of gating current: 1) equality of ON and OFF charge Q in integrals of gating current, 2) saturating voltage dependence in the $Q(\text{charge})$ -voltage curve, and 3) many (but not all) details of the shape of gating current as a function of voltage. Our results agree qualitatively with experiments and can be improved by adding more details of the structure and its correlated movements. The proposed continuum model is a promising tool to explore the dynamics and mechanism of the voltage sensor.

INTRODUCTION

Much of biology depends on the voltage across cell membranes. The voltage across the membrane must be sensed before it can be used by proteins. Permanent charges move in the strong electric fields within membranes, so carriers of sensing charge were proposed as voltage sensors even before membrane proteins were known to span lipid membranes (1). The movement of permanent charges of the voltage sensor is gating current, and the movement is the voltage-sensing mechanism. Permanent charge is our name for a charge or charge density independent of the local electric field (for example, the charge and charge distribution of Na^+ but not the charge in a highly polarizable anion like Br^- or the nonuniform charge distribution of

H_2O in the liquid state with its complex time dependent (and perhaps nonlinear) polarization response to the local electric field).

Knowledge of membrane protein structure has allowed us to identify and look at the atoms that make up the voltage sensor. Protein structures do not include the membrane potentials and macroscopic concentrations that power gating currents, and therefore, simulations are needed. Atomic-level simulations like molecular dynamics (MD) do not provide an easy extension from the atomic timescale $\sim 10^{-15}$ s to the biological timescale of gating currents that starts at $\sim 10^{-6}$ s and reaches $\sim 10^{-2}$ s. Calculations of gating currents from simulations must average the trajectories (lasting $\sim 10^{-1}$ s sampled every 10^{-15} s) of $\sim 10^6$ atoms, all of which interact through the electric field to conserve charge and current while conserving mass. It is difficult to enforce continuity of current flow in simulations of atomic dynamics because simulations compute only local behavior, whereas continuity

Submitted October 11, 2018, and accepted for publication November 28, 2018.

*Correspondence: fbezanilla@uchicago.edu

Editor: Michael Grabe.

<https://doi.org/10.1016/j.bpj.2018.11.3140>

© 2018 Biophysical Society.

This is an open access article under the CC BY-NC-ND license (<http://creativecommons.org/licenses/by-nc-nd/4.0/>).

Please cite this article in press as: Horng et al., Continuum Gating Current Models Computed with Consistent Interactions, *Biophysical Journal* (2019), <https://doi.org/10.1016/j.bpj.2018.11.3140>

well represented by the simulations. The good agreement of our numerical results with salient features of gating current measured experimentally would be impossible by simply tuning of parameters if our model had not captured the essence of physics for the voltage sensor. The continuum approach seems to be a good model of voltage sensors, provided that it 1) takes into account all interactions crucial to the movement of gating charges and S4; 2) computes their correlations consistently, so all variables satisfy all equations under all conditions with one set of parameters; and 3) satisfies conservation of current. This last point gave us a new insight: what is measured experimentally does not correspond to the transfer of the arginines because the total current, containing a displacement current, is smaller than the arginine current. It should be noted, however, that the total energy provided by the voltage clamp is qV , where q is the time integral of the measured gating current and V is the applied voltage. This is the total energy that explains the correspondence of charge per channel with the charge estimated by the limiting slope method (33–35).

We have simplified the profile of the energy barrier in the hydrophobic plug because the PMF in that region, and its variation with potential and conditions, is unknown. There is plenty of detailed information on the amino acid side chains in the plug and how each one of them changes the kinetics and steady-state properties of gating charge movement (6). Therefore, the next step is to model the details of interactions of the moving arginines with the wall of the hydrophobic plug and the contributions from other surrounding charged protein components. Some of the effects to be included are as follows:

- 1) Steric and dielectric interactions of the arginines that this model does not include. These include the interaction of arginines with negative charges of the S2 and S3 segments and the negative phospholipids as well as the hydrophobic residues in the plug. These interactions may be responsible for the simultaneous movement of two to three arginines across the plug, which is an experimental result that this model does not reproduce (36,37).
- 2) Time dependence of the plug energy barrier V_b . Once the first arginine enters the hydrophobic plug by carrying some water with it, this partial wetting of the hydrophobic plug will lower V_b , chiefly consisting of solvation energy, and enable the next arginine to enter the plug with less difficulty. This might explain the cooperativity of movement among arginines when they jump through the plug. The addition of details in the plug may also produce intermediate states that have been measured experimentally. In this situation, arginines may transiently dwell within the plug.
- 3) A very strong electric field might affect the hydration equilibrium of the hydrophobic plug and would lower its hydration energy barrier as well (38). This cooperativity of movement may help explain the quick saturation

in the upper right branch of the QV curve (and smaller τ_2). It may also explain the experimentally observed translocation of two to three arginines simultaneously (36,37).

The power of this mathematical modeling is precisely the implementation of interactions and the various effects in a consistent manner. Implementing the various effects listed above is likely to lead to a better prediction of the currents and to the design of experiments to further test and extend the model.

Further work must address the mechanism of coupling between the voltage sensor movements and the conduction pore. For example, the spring constant of the two sides of S4 have been made equal, which does not take into account the structural reality that one side has a linker to S3, whereas the other links to the pore opening. It seems likely that the classical mechanical models of coupling will need to be extended to include coupling through the electrical field. The charges involved are large. The distances are small, so the changes in electric forces that accompany movements of charged mass (and flows of displacement current) are likely to be large and important. It is possible that the voltage sensor modifies the stability of a fundamentally stochastically unstable, nearly bistable, conduction current (of single channels) by triggering sudden transitions from closed to open state in a controlled process reminiscent of Coulomb blockade in a noisy environment (39).

SUPPORTING MATERIAL

Supporting Materials and Methods, one figure, and one data file are available at [http://www.biophysj.org/biophysj/supplemental/S0006-3495\(18\)34501-6](http://www.biophysj.org/biophysj/supplemental/S0006-3495(18)34501-6).

AUTHOR CONTRIBUTIONS

All authors conceived the research, T.-L. H. wrote the code and carried out the computations, and all authors contributed to the interpretation and writing of the manuscript.

ACKNOWLEDGMENTS

Dr. Horng thanks the support of National Center for Theoretical Sciences Mathematical Division of Taiwan and Dr. Ren-Shiang Chen for the long-term helpful discussions.

This research was sponsored in part by the National Institutes of Health grant R01GM030376 (F.B.), National Science Foundation Division of Mathematical Sciences grant 1759535 (C.L.), National Science Foundation Division of Mathematical Sciences grant 1759536 (C.L.), and Ministry of Science and Technology grant 106-2115-M-035-001-MY2 (T.-L.H.).

SUPPORTING CITATIONS

References (40–51) appear in the [Supporting Material](#).



Astroglial Ca^{2+} -Dependent Hyperexcitability Requires P2Y_1 Purinergic Receptors and Pannexin-1 Channel Activation in a Chronic Model of Epilepsy

Mario Wellmann^{1,2}, Carla Álvarez-Ferradas^{1,3}, Carola J. Maturana^{4,5}, Juan C. Sáez^{4,5} and Christian Bonansco^{1*}

¹Centro de Neurobiología y Plasticidad Cerebral CNPC, Instituto de Fisiología, Facultad de Ciencias, Universidad de Valparaíso, Valparaíso, Chile, ²Escuela de Fonoaudiología, Facultad de Medicina, Universidad de Valparaíso, Valparaíso, Chile, ³Escuela de Ciencias de la Salud, Universidad Viña del Mar, Valparaíso, Chile, ⁴Departamento de Ciencias Fisiológicas, Facultad Ciencias Biológicas, Pontificia Universidad Católica de Chile, Santiago, Chile, ⁵Instituto de Neurociencias, Centro Interdisciplinario de Neurociencias de Valparaíso, Universidad de Valparaíso, Valparaíso, Chile

OPEN ACCESS

Edited by:

Christian Lohr,
Universität Hamburg, Germany

Reviewed by:

Rheinallt Parri,
Aston University, United Kingdom
Frank Kirchhoff,
Saarland University, Germany

*Correspondence:

Christian Bonansco
christian.bonansco@uv.cl

Received: 03 July 2018

Accepted: 06 November 2018

Published: 23 November 2018

Citation:

Wellmann M, Álvarez-Ferradas C, Maturana CJ, Sáez JC and Bonansco C (2018) Astroglial Ca^{2+} -Dependent Hyperexcitability Requires P2Y_1 Purinergic Receptors and Pannexin-1 Channel Activation in a Chronic Model of Epilepsy. *Front. Cell. Neurosci.* 12:446. doi: 10.3389/fncel.2018.00446

Astrocytes from the hippocampus of chronic epileptic rats exhibit an abnormal pattern of intracellular calcium oscillations, characterized by an augmented frequency of long lasting spontaneous Ca^{2+} transients, which are sensitive to purinergic receptor antagonists but resistant to tetrodotoxin. The above suggests that alterations in astroglial Ca^{2+} -dependent excitability observed in the epileptic tissue could arise from changes in astrocyte-to-astrocyte signaling, which is mainly mediated by purines in physiological and pathological conditions. In spite of that, how purinergic signaling contributes to astrocyte dysfunction in epilepsy remains unclear. Here, we assessed the possible contribution of $\text{P2Y}_1\text{R}$ as well as pannexin1 and connexin43 hemichannels—both candidates for non-vesicular ATP-release—by performing astroglial Ca^{2+} imaging and dye uptake experiments in hippocampal slices from control and fully kindled rats. $\text{P2Y}_1\text{R}$ blockade with MRS2179 decreased the mean duration of astroglial Ca^{2+} oscillations by reducing the frequency of slow Ca^{2+} transients, and thereby restoring the balance between slow (ST) and fast transients (FT) in the kindled group. The potential contribution of astroglial pannexin1 and connexin43 hemichannels as pathways for purine release (e.g., ATP) was assessed through dye uptake experiments. Astrocytes from kindled hippocampi exhibit three-fold more EtBr uptake than controls, whereby pannexin1 hemichannels (Panx1 HCs) accounts for almost all dye uptake with only a slight contribution from connexin43 hemichannels (Cx43 HCs). Confirming its functional involvement, Panx1 HCs inhibition decreased the mean duration of astroglial Ca^{2+} transients and the frequency of slow oscillations in kindled slices, but had no noticeable effects on the control group. As expected, Cx43 HCs blockade did not have any effects over the mean duration of astroglial Ca^{2+} oscillations. These findings suggest that $\text{P2Y}_1\text{R}$ and Panx1 HCs play a pivotal role in astroglial pathophysiology, which

the data and wrote the manuscript. C  F performed the experiments. CM performed EtBr dye uptake experiments and analyzed the data. JS contributed in experimental design of the EtBr uptake experiments and in the edition of the article.

FUNDING

This work was supported by grants 1130491 from FONDECYT and CID 1/2006 to CB, scholarship 22120213 from CONICYT-Chile to MW and ICM-Econom   P09-022-F Centro Interdisciplinario de Neurociencias de Valpara  so to JS.

REFERENCES

- Aguado, F., Espinosa-Parrilla, J. F., Carmona, M. A., and Soriano, E. (2002). Neuronal activity regulates correlated network properties of spontaneous calcium transients in astrocytes *in situ*. *J. Neurosci.* 22, 9430–9444. doi: 10.1523/jneurosci.22-21-09430.2002
-   lvarez-Ferradas, C., Morales, J. C., Wellmann, M., Nualart, F., Roncagliolo, M., Fuenzalida, M., et al. (2015). Enhanced astroglial Ca^{2+} signaling increases excitatory synaptic strength in the epileptic brain. *Glia* 63, 1507–1521. doi: 10.1002/glia.22817
- Alves, M., Gomez-Villafuertes, R., Delanty, N., Farrell, M. A., O'Brien, D. F., Miras-Portugal, M. T., et al. (2017). Expression and function of the metabotropic purinergic P2Y receptor family in experimental seizure models and patients with drug-refractory epilepsy. *Epilepsia* 58, 1603–1614. doi: 10.1111/epi.13850
- Anderson, C. M., Bergher, J. P., and Swanson, R. A. (2004). ATP-induced ATP release from astrocytes. *J. Neurochem.* 88, 246–256. doi: 10.1111/j.1471-4159.2004.02204.x
- Araque, A., Carmignoto, G., Haydon, P. G., Oliet, S. H. R., Robitaille, R., and Volterra, A. (2014). Gliotransmitters travel in time and space. *Neuron* 81, 728–739. doi: 10.1016/j.neuron.2014.02.007
- Aronica, E., Zurolo, E., Iyer, A., de Groot, M., Anink, J., Carbonell, C., et al. (2011). Upregulation of adenosine kinase in astrocytes in experimental and human temporal lobe epilepsy. *Epilepsia* 52, 1645–1655. doi: 10.1111/j.1528-1167.2011.03115.x
- Barros-Barbosa, A. R., Ferreirinha, F., Oliveira,   ., Mendes, M., Lobo, M. G., Santos, A., et al. (2016). Adenosine $\text{A}_{2\text{A}}$ receptor and ecto-5'-nucleotidase/CD73 are upregulated in hippocampal astrocytes of human patients with mesial temporal lobe epilepsy (MTLE). *Purinergic Signal.* 12, 719–734. doi: 10.1007/s11302-016-9535-2
- Beckel, J. M., Argall, A. J., Lim, J. C., Xia, J., Lu, W., Coffey, E. E., et al. (2014). Mechanosensitive release of ATP through pannexin channels and mechanosensitive upregulation of pannexin channels in optic nerve head astrocytes: a mechanism for purinergic involvement in chronic strain. *Glia* 62, 1486–1501. doi: 10.1002/glia.22695
- Bennett, M. R., Buljan, V., Farnell, L., and Gibson, W. G. (2006). Purinergic junctional transmission and propagation of calcium waves in spinal cord astrocyte networks. *Biophys. J.* 91, 3560–3571. doi: 10.1529/biophysj.106.082073
- Bonan, C. D., Amaral, O. B., Rockenbach, I. C., Walz, R., Battastini, A. M., Izquierdo, I., et al. (2000a). Altered ATP hydrolysis induced by pentylentetrazol kindling in rat brain synaptosomes. *Neurochem. Res.* 25, 775–779. doi: 10.1023/A:1007557205523
- Bonan, C. D., Walz, R., Pereira, G. S., Worm, P. V., Battastini, A. M., Cavalheiro, E. A., et al. (2000b). Changes in synaptosomal ectonucleotidase activities in two rat models of temporal lobe epilepsy. *Epilepsy Res.* 39, 229–238. doi: 10.1016/s0920-1211(00)00095-4
- Bonansco, C., Couve, A., Perea, G., Ferradas, C.   ., Roncagliolo, M., and Fuenzalida, M. (2011). Glutamate released spontaneously from astrocytes sets the threshold for synaptic plasticity. *Eur. J. Neurosci.* 33, 1483–1492. doi: 10.1111/j.1460-9568.2011.07631.x
- Bonansco, C., Gonz  lez De La Vega, A., Gonz  lez Alegre, P., Borde, M., Garc   Segura, L. M., and Bu  o, W. (2002). Tetanic stimulation of schaffer collaterals induces rhythmic bursts via NMDA receptor activation in rat CA1 pyramidal neurons. *Hippocampus* 12, 434–446. doi: 10.1002/hipo.10023
- Bowser, D. N., and Khakh, B. S. (2007). Vesicular ATP is the predominant cause of intercellular calcium waves in astrocytes. *J. Gen. Physiol.* 129, 485–491. doi: 10.1085/jgp.200709780
- Buckmaster, P. S., Abrams, E., and Wen, X. (2017). Seizure frequency correlates with loss of dentate gyrus GABAergic neurons in a mouse model of temporal lobe epilepsy. *J. Comp. Neurol.* 525, 2592–2610. doi: 10.1002/cne.24226
- Burda, J. E., and Sofroniew, M. V. (2014). Reactive gliosis and the multicellular response to CNS damage and disease. *Neuron* 81, 229–248. doi: 10.1016/j.neuron.2013.12.034
- Cheung, G., Chever, O., and Rouach, N. (2014). Connexons and pannexons: newcomers in neurophysiology. *Front. Cell. Neurosci.* 8:348. doi: 10.3389/fncel.2014.00348
- Chever, O., Lee, C.-Y., and Rouach, N. (2014). Astroglial connexin43 hemichannels tune basal excitatory synaptic transmission. *J. Neurosci.* 34, 11228–11232. doi: 10.1523/jneurosci.0015-14.2014
- Cie  slak, M., Wojtczak, A., and Komosi  y  ski, M. (2017). Role of the purinergic signaling in epilepsy. *Pharmacol. Rep.* 69, 130–138. doi: 10.1016/j.pharep.2016.09.018
- Corcoran, M. E., Kroes, R. A., Burgdorf, J. S., and Moskal, J. R. (2011). Regional changes in gene expression after limbic kindling. *Cell. Mol. Neurobiol.* 31, 819–834. doi: 10.1007/s10571-011-9672-7
- Cotrina, M. L., Lin, J. H., Alves-Rodrigues, A., Liu, S., Li, J., Azmi-Ghadimi, H., et al. (1998). Connexins regulate calcium signaling by controlling ATP release. *Proc. Natl. Acad. Sci. U S A* 95, 15735–15740. doi: 10.1073/pnas.95.26.15735
- Dahl, G. (2015). ATP release through pannexon channels. *Philos. Trans. R. Soc. Lond. B Biol. Sci.* 370:20140191. doi: 10.1098/rstb.2014.0191
- Delekat, A., F  chtemeier, M., Schumacher, T., Ulbrich, C., Foddis, M., and Petzold, G. C. (2014). Metabotropic P2Y1 receptor signalling mediates astrocytic hyperactivity *in vivo* in an Alzheimer's disease mouse model. *Nat. Commun.* 5:5422. doi: 10.1038/ncomms6422
- Di Castro, M. A., Chuquet, J., Liaudet, N., Bhaukaurally, K., Santello, M., Bouvier, D., et al. (2011). Local Ca^{2+} detection and modulation of synaptic release by astrocytes. *Nat. Neurosci.* 14, 1276–1284. doi: 10.1038/nn.2929
- Ding, S., Fellin, T., Zhu, Y., Lee, S. Y., Auberson, Y. P., Meaney, D. F., et al. (2007). Enhanced astrocytic Ca^{2+} signals contribute to neuronal excitotoxicity after status epilepticus. *J. Neurosci.* 27, 10674–10684. doi: 10.1523/jneurosci.2001-07.2007
- Dubyak, G. R. (2009). Both sides now: multiple interactions of ATP with pannexin-1 hemichannels. Focus on “a permeant regulating its permeation pore: inhibition of pannexin 1 channels by ATP”. *Am. J. Physiol. Cell Physiol.* 296, C235–C241. doi: 10.1152/ajpcell.00639.2008
- Engel, T., Alves, M., Sheedy, C., and Henshall, D. C. (2016). ATPergic signalling during seizures and epilepsy. *Neuropharmacology* 104, 140–153. doi: 10.1016/j.neuropharm.2015.11.001
- Engel, T., Gomez-Villafuertes, R., Tanaka, K., Mesuret, G., Sanz-Rodr  guez, A., Garc  a-Huerta, P., et al. (2012). Seizure suppression and neuroprotection by

ACKNOWLEDGMENTS

We thank Guillermo Rodriguez, Tania Cerda and Carlina Tapia for their excellent technical assistance, Dr. Gertrudis Perea for her critical comments, helpful discussions and suggestions for the present manuscript and Dr. Marco Fuenzalida for critically reading the previous versions.

SUPPLEMENTARY MATERIAL

The Supplementary Material for this article can be found online at: <https://www.frontiersin.org/articles/10.3389/fncel.2018.00446/full#supplementary-material>



Chapter 1

Rule-Based Models and Applications in Biology

Álvaro Bustos, Ignacio Fuenzalida, Rodrigo Santibáñez,
Tomás Pérez-Acle, and Alberto J. M. Martín

Abstract

Complex systems are governed by dynamic processes whose underlying causal rules are difficult to unravel. However, chemical reactions, molecular interactions, and many other complex systems can be usually represented as concentrations or quantities that vary over time, which provides a framework to study these dynamic relationships. An increasing number of tools use these quantifications to simulate dynamically complex systems to better understand their underlying processes. The application of such methods covers several research areas from biology and chemistry to ecology and even social sciences.

In the following chapter, we introduce the concept of rule-based simulations based on the Stochastic Simulation Algorithm (SSA) as well as other mathematical methods such as Ordinary Differential Equations (ODE) models to describe agent-based systems. Besides, we describe the mathematical framework behind *Kappa* (κ), a rule-based language for the modeling of complex systems, and some extensions for spatial models implemented in PISKaS (Parallel Implementation of a Spatial Kappa Simulator). To facilitate the understanding of these methods, we include examples of how these models can be used to describe population dynamics in a simple predator–prey ecosystem or to simulate circadian rhythm changes.

Key words Stochastic simulation, Rule-based modeling, κ language

1 The Stochastic Simulation Algorithm (SSA)

The SSA, also known as Gillespie’s algorithm [10], is the basis of most stochastic simulation tools available. This algorithm and the tools based on it assume there is a homogeneous and “well-stirred” system of particles named **agents**. Agents can represent any type of entity within a system, i.e., molecules or individuals, and the interactions between agents are determined by a set of **rules** or equations taking place at certain rates. These rules are ordered and divided into agents to which the rule applies and products (outcome agents). For instance, in a system of chemical reactions described by an equation or rule (*reactants* \rightarrow *products*), every set of particles matching the left side of the equation (or reactant agents) has an equal probability of being

Nomenclature

Term	Definition
Agent	Abstract representations of entities on a system. An agent can bind each other's agents through its <i>sites</i> . Optionally, each <i>site</i> could harbor a <i>state</i> , a label that recapitulates a feature of the mentioned <i>site</i> , or a numeric property of the agent.
Bond	A representation of binding between two <i>sites</i> of two different agents.
Compartment	Declaration that represents a physical or logical space or volume which is part of a system.
Rule	Chemical equations that represent elemental reactions where reactants are <i>agents</i> with a set of features necessary and sufficient for a transformation to occur (<i>Left-Hand Side</i>) and the resulting pattern for each participating <i>agent</i> (<i>Right-Hand Side</i>). κ <i>rules</i> declare reactions that change the value of a <i>site</i> , create or destroy <i>bonds</i> between <i>agents</i> , and create or remove <i>agents</i> on the modeled system.
Site	Abstract representation of a physical or logical interface where an <i>agent</i> binds another <i>agent</i> or where different <i>states</i> are declared.
Specie	Each of the individual instances of an <i>agent</i> .
State	Abstract representation of a qualitative or quantitative characteristic that recapitulates a feature of the declared <i>site</i> .
Transport	Declaration that states the <i>link</i> that uses an <i>agent</i> to travel from one compartment to another. Additionally, it may declare the frequency and time employed to move the agent between compartments.

Acknowledgements

The authors would like to kindly acknowledge the financial support received from FONDECYT Inicio 11140342 and award numbers FA9550-16-1-0111 and FA9550-16-1-0384 of the USA Air Force Office of Scientific Research. This research was partially supported by the supercomputing infrastructure of the Chilean NLHPC [ECM-02]. Basal Funding Program from CONICYT PFB-16 to Fundacion Ciencia & Vida and Instituto Milenio Centro Interdisciplinario de Neurociencia de Valparaiso CINV ICM-Economia [P09-022-F].

Disaccharide-Based Anionic Amphiphiles as Potent Inhibitors of Lipopolysaccharide-Induced Inflammation

Alessio Borio^{+, [a]} Aurora Holgado^{+, [b]} Jose Antonio Garate,^[c] Rudi Beyaert,^[b] Holger Heine,^[d] and Alla Zamyatina^{*, [a]}

Despite significant advances made in the last decade in the understanding of molecular mechanisms of sepsis and in the development of clinically relevant therapies, sepsis remains the leading cause of mortality in intensive care units with increasing incidence worldwide. Toll-like receptor 4 (TLR4)—a transmembrane pattern-recognition receptor responsible for propagating the immediate immune response to Gram-negative bacterial infection—plays a central role in the pathogenesis of sepsis and chronic inflammation-related disorders. TLR4 is complexed with the lipopolysaccharide (LPS)-sensing protein myeloid differentiation-2 (MD-2) which represents a preferred target for establishing new anti-inflammatory treatment strategies. Herein we report the development, facile synthesis, and biological evaluation of novel disaccharide-based TLR4-MD-2

antagonists with potent anti-endotoxic activity at micromolar concentrations. A series of synthetic anionic glycolipids entailing amide-linked β -ketoacyl lipid residues was prepared in a straightforward manner by using a single orthogonally protected nonreducing diglucosamine scaffold. Suppression of the LPS-induced release of interleukin-6 and tumor necrosis factor was monitored and confirmed in human immune cells (MNC and THP1) and mouse macrophages. Structure–activity relationship studies and molecular dynamics simulations revealed the structural basis for the high-affinity interaction between anionic glycolipids and MD-2, and highlighted two compounds as leads for the development of potential anti-inflammatory therapeutics.

Introduction

Toll-like receptor 4 (TLR4) is a mammalian pattern recognition receptor responsible for a protective inflammatory response to Gram-negative infection. TLR4 is physically associated with a co-receptor protein myeloid differentiation factor 2 (MD-2) which can directly bind bacterial surface antigen lipopolysaccharide (LPS). The TLR4-MD-2 complex senses picomolar quantities of pathogenic LPS and initiates an intracellular pro-inflammatory signaling cascade leading to the expression of cytokines, chemokines and co-stimulatory molecules that ensure a prompt host reaction to bacterial invasion. LPS, a large 20 kDa heterogeneous glycan, entails a small (ca. 2 kDa) glyco-

lipid portion which anchors LPS in the outer leaflet of the outer bacterial membrane. This diglucosamine-based glycolipid designated as Lipid A can be recognized and bound by the MD-2-TLR4 complex and is responsible for the endotoxic action of LPS.^[1,2] The molecular basis of TLR4 activation by pathogenic *E. coli* LPS has been solved by extensive X-ray studies (Figure 1 A). It was unambiguously postulated that the hexaacetylation by (*R*)-3-acyloxyacyl- and (*R*)-3-hydroxyacyl lipid chains (C₁₂–C₁₄) in *E. coli* Lipid A is decisive for the activation of TLR4 complex.^[3,4]

The co-crystal structure of human TLR4-MD-2 complex with *Ra*-LPS (PDB ID: 3FXI) disclosed that five lipid chains of *E. coli* Lipid A are bound with high affinity by the leucine-rich hydrophobic binding cleft of the co-receptor protein MD-2, whereas the sixth lipid chain is exposed on the surface of MD-2 which eventually causes and supports the dimerization of two TLR4-MD-2-LPS-receptor complexes.^[3] The formation of hexameric [TLR4-MD-2-LPS]₂ complex results in the recruitment of adaptor proteins to the intracellular TIR domains of TLR4 which initiates the induction of the pro-inflammatory signaling cascade (Figure 1 B).^[5]

The structural basis for disruption of the TLR4-mediated signaling by TLR4 antagonists has also been extensively studied. The co-crystal structures of the TLR4-MD-2 complex with bound TLR4 antagonists of natural origin, lipid IVa^[6] (biosynthetic precursor of *E. coli* Lipid A), and synthetic antisepsis drug candidate Eritoran^[7] (Figure 2) were recently solved. Analysis of co-crystal structures suggested that the lower number



[a] A. Borio,⁺ Prof. Dr. A. Zamyatina
Department of Chemistry, University of Natural Resources and Life Sciences,
Muthgasse 18, 1190 Vienna (Austria)
E-mail: alla.zamyatina@boku.ac.at

[b] A. Holgado,⁺ Prof. Dr. R. Beyaert
Department for Biomedical Molecular Biology, Unit of Molecular Signal
Transduction in Inflammation, Ghent University, Center for Inflammation
Research, VIB, Technologiepark 927, 9052 Ghent (Belgium)

[c] Dr. J. A. Garate
Centro Interdisciplinario de Neurociencia de Valparaíso (CINV), Universidad
de Valparaíso, Valparaíso (Chile)

[d] Prof. Dr. H. Heine
Research Group Innate Immunity, Research Center Borstel—Leibniz Lung
Center, Airway Research Center North (ARCN), German Center for Lung Dis-
ease (DZL), Parkallee 22, 23845 Borstel (Germany)

[*] These authors contributed equally to this manuscript.

 Supporting information and the ORCID identification number(s) for the
author(s) of this article can be found under:
 <https://doi.org/10.1002/cmdc.201800505>.

tively charged residues of MD-2 and negatively charged phosphate groups of LAM 2 were computed with a cutoff of 0.7 nm between the phosphorous atoms and the NZ or CZ for K or R residues, respectively. Atom positional root mean square displacement (RMSD) of F126 at the end of the simulation with respect to the initial structure (PDB IDs: 3FXI for hMD-2 and 2Z64 for mMD-2) was computed after a roto-translational fit to on the C α atoms of MD-2. Free energy of binding was estimated by the LIE method: $\Delta G_{\text{bind}} = \alpha \Delta \langle E_{\text{vdw}} \rangle + \beta \Delta \langle E_{\text{el}} \rangle$, with $\langle E_{\text{vdw}} \rangle$ and $\langle E_{\text{el}} \rangle$ the average ligand-surrounding van der Waals and electrostatic interaction energies, respectively; Δ indicates the difference between the ligand-bound and unbound simulations. The unbound condition was defined as the ligand in a water-octane interface; $\alpha = 0.18$, $\beta = 0.09$, using exponential averages for each pose.^[75–76] ΔG_{bind} is related to the dissociation constant K_{d} : $\Delta G_{\text{bind}} = RT \ln K_{\text{d}}$, where T and R are the absolute temperature and gas constant.

Acknowledgements

We are grateful for financial support from the Austrian Science Fund (FWF) grants P-22116 and P-28915 (A.B. and A.Z.); CM-Economia grant P09-022-F CINV and Universidad de Valparaíso and FONDECYT grant 1180987 (J.A.G.); a grant from the VIB, the Fund for Scientific Research Flanders (FWO) and Ghent University (GOA) (A.H. and R.B.).

Conflict of interest

The authors declare no conflict of interest.

Keywords: drug discovery • antiseptics • carbohydrates • glycolipids • innate immunity

- [1] G. L. Hold, C. E. Bryant, in *Bacterial Lipopolysaccharides* (Eds.: Y. A. Kniel, M. A. Valvano), Springer, Heidelberg, 2011, pp. 371–387.
- [2] B. S. Park, J. O. Lee, *Exp. Mol. Med.* **2013**, 45, e66.
- [3] B. S. Park, D. H. Song, H. M. Kim, B. S. Choi, H. Lee, J. O. Lee, *Nature* **2009**, 458, 1191–1195.
- [4] U. Ohto, K. Fukase, K. Miyake, T. Shimizu, *Proc. Natl. Acad. Sci. USA* **2012**, 109, 7421–7426.
- [5] H. Kumar, T. Kawai, S. Akira, *Biochem. Biophys. Res. Commun.* **2009**, 388, 621–625.
- [6] U. Ohto, K. Fukase, K. Miyake, Y. Satow, *Science* **2007**, 316, 1632–1634.
- [7] H. M. Kim, B. S. Park, J.-I. Kim, S. E. Kim, J. Lee, S. C. Oh, P. Enkhbayar, N. Matsushima, H. Lee, O. J. Yoo, J.-O. Lee, *Cell* **2007**, 130, 906–917.
- [8] M. L. DeMarco, R. J. Woods, *Mol. Immunol.* **2011**, 49, 124–133.
- [9] A. Molinaro, O. Holst, F. Di Lorenzo, M. Callaghan, A. Nurisso, G. D'Errico, A. Zamyatina, F. Peri, R. Berisio, R. Jerala, J. Jiménez-Barbero, A. Siliipo, S. Martín-Santamaría, *Chem. Eur. J.* **2015**, 21, 500–519.
- [10] B. D. Needham, M. S. Trent, *Nat. Rev. Microbiol.* **2013**, 11, 467–481.
- [11] N. J. Gay, M. F. Symmons, M. Gangloff, C. E. Bryant, *Nat. Rev. Immunol.* **2014**, 14, 546–558.
- [12] S. M. Opal, *Int. J. Med. Microbiol.* **2007**, 297, 365–377.
- [13] R. S. Hotchkiss, G. Monneret, D. Payen, *Nat. Rev. Immunol.* **2013**, 13, 862–874.
- [14] X. Wang, P. J. Quinn, A. Yan, *Biol. Rev.* **2015**, 90, 408–427.
- [15] S. M. Opal, P. Laterre, B. Francois, *JAMA* **2013**, 309, 1154–1162.
- [16] S. Abdollahi-Roodsaz, L. A. B. Joosten, M. F. Roelofs, T. R. D. J. Radstake, G. Matera, C. Popa, J. W. M. Van der Meer, M. G. Netea, W. B. van den Berg, *Arthritis Rheum.* **2007**, 56, 2957–2967.
- [17] H. Hammad, M. Chieppa, F. Perros, M. A. Willart, R. N. Germain, B. N. Lambrecht, *Nat. Med.* **2009**, 15, 410–416.
- [18] J. Li, A. Csakai, J. Jin, F. Zhang, H. Yin, *ChemMedChem* **2016**, 11, 154–165.
- [19] P. Rallabhandi, R. L. Phillips, M. S. Boukhvalova, L. M. Pletneva, K. A. Shirey, T. L. Gioannini, J. P. Weiss, J. C. Chow, L. D. Hawkins, S. N. Vogel, J. C. G. Blanco, *mBio* **2012**, 3, e00218-12.
- [20] K. A. Shirey, W. Lai, A. J. Scott, M. Lipsky, P. Mistry, L. M. Pletneva, C. L. Karp, J. McAlees, T. L. Gioannini, J. Weiss, W. H. Chen, R. K. Ernst, D. P. Rossignol, F. Gusovsky, J. C. G. Blanco, S. N. Vogel, *Nature* **2013**, 497, 498–502.
- [21] T. van der Poll, S. M. Opal, *Lancet Infect. Dis.* **2008**, 8, 32–43.
- [22] A. Savva, T. Roger, *Front. Immunol.* **2013**, 4, 387.
- [23] D. Rittirsch, M. A. Flierl, P. A. Ward, *Nat. Rev. Immunol.* **2008**, 8, 776–787.
- [24] P. Jantaruk, S. Roytrakul, S. Sitthisak, D. Kunthalert, *PLoS ONE* **2017**, 12, e0183852.
- [25] W. Ishida, Y. Harada, K. Fukuda, A. Fukushima, *Invest. Ophthalmol. Visual Sci.* **2016**, 57, 30–39.
- [26] C. D. Giomei, T. Sigurdardóttir, A. Schmidchen, M. Modelsson, *Antimicrob. Agents Chemother.* **2005**, 49, 2845–2850.
- [27] J. K. Ryu, S. J. Kim, S. H. Rah, J. I. Kang, H. E. Jung, D. Lee, H. K. Lee, J. O. Lee, B. S. Park, T. Y. Yoon, H. M. Kim, *Immunity* **2017**, 46, 38–50.
- [28] I. Zanoni, R. Ostuni, L. Marek, S. Barresi, R. Barbalat, G. Barton, F. Granucci, J. Kagan, *Cell* **2011**, 147, 868–880.
- [29] R. Rajalaiah, D. J. Perkins, D. D. C. Ireland, S. N. Vogel, *Proc. Natl. Acad. Sci. USA* **2015**, 112, 8391–8396.
- [30] A. Teghanemt, R. L. Widstrom, T. L. Gioannini, J. P. Weiss, *J. Biol. Chem.* **2008**, 283, 21881–21889.
- [31] E. Monnet, G. Lapeyre, E. V. Poelgeest, P. Jacqmin, K. de Graaf, J. Reijers, M. Moerland, J. Burggraaf, C. de Min, *Clin. Pharmacol. Ther.* **2017**, 101, 200–208.
- [32] T. Roger, C. Froidevaux, D. Le Roy, M. K. Reymond, A. L. Chanson, D. Mauri, K. Burns, B. M. Riederer, S. Akira, T. Calandra, *Proc. Natl. Acad. Sci. USA* **2009**, 106, 2348–2352.
- [33] B. La Ferla, V. Spinosa, G. D'Orazio, M. Palazzo, A. Balsari, A. A. Foppoli, C. Rumio, F. Nicotra, *ChemMedChem* **2010**, 5, 1677–1680.
- [34] Y. Wang, X. Shan, G. Chen, L. Jiang, Z. Wang, Q. Fang, X. Liu, J. Wang, Y. Zhang, W. Wu, G. Liang, *Br. J. Pharmacol.* **2015**, 172, 4391–4405.
- [35] S. Kaeothip, G. Paranjape, S. E. Terrill, A. F. G. Bongat, M. L. D. Udan, T. Kamkhachorn, H. L. Johnson, M. R. Nichols, A. V. Demchenko, *RSC Adv.* **2011**, 1, 83–92.
- [36] S. Bennett, *Surgery* **2012**, 30, 673–678.
- [37] N. Kissoon, R. Daniels, T. van der Poll, S. Finfer, K. Reinhart, *Crit. Care Med.* **2016**, 44, e446.
- [38] A. Perner, A. C. Gordon, D. De Backer, G. Dimopoulos, J. A. Russell, J. Lipman, J. U. Jensen, J. Myburgh, M. Singer, R. Bellomo, T. Walsh, *Intensive Care Med.* **2016**, 42, 1958–1969.
- [39] F. B. Mayr, V. B. Talisa, V. Balakumar, C. H. Chang, M. Fine, S. Yende, *JAMA* **2017**, 317, 530–531.
- [40] D. W. Chang, C. H. Tseng, M. F. Shapiro, *Crit. Care Med.* **2015**, 43, 2085–2093.
- [41] S. H. Park, N. D. Kim, J. K. Jung, C. K. Lee, S. B. Han, Y. Kim, *Pharmacol. Ther.* **2012**, 133, 291–298.
- [42] T. Kawai, S. Akira, *Nat. Immunol.* **2010**, 11, 373–384.
- [43] C. E. Bryant, A. Ouellette, K. Lohmann, M. Vandenplas, J. N. Moore, D. J. Maskell, B. A. Farnfield, *Vet. Immunol. Immunopathol.* **2007**, 116, 182–189.
- [44] W. J. Christ, O. Asano, A. L. Robidoux, M. Perez, Y. Wang, G. R. Dubuc, W. E. Gavin, L. D. Hawkins, P. D. McGuinness, M. A. Mullarkey, et al., *Science* **1995**, 268, 80.
- [45] T. Kawata, J. R. Bristol, D. P. Rossignol, J. R. Rose, S. Kobayashi, H. Yokohama, A. Ishibashi, W. J. Christ, K. Katayama, I. Yamatsu, Y. Kishi, *Br. J. Pharmacol.* **1999**, 127, 853–862.
- [46] W. J. Christ, P. D. McGuinness, O. Asano, Y. Wang, M. A. Mullarkey, M. Perez, L. D. Hawkins, T. A. Blythe, G. R. Dubuc, A. L. Robidoux, *J. Am. Chem. Soc.* **1994**, 116, 3637–3638.
- [47] K. L. Irvine, M. Gangloff, C. M. Walsh, D. R. Spring, N. J. Gay, C. E. Bryant, *PLoS ONE* **2014**, 9, e98776.
- [48] J. R. Rose, W. J. Christ, J. R. Bristol, T. Kawata, D. P. Rossignol, *Infect. Immun.* **1995**, 63, 833–839.
- [49] E. Lien, T. K. Means, H. Heine, A. Yoshimura, S. Kusumoto, K. Fukase, M. J. Fenton, M. Oikawa, N. Qureshi, B. Monks, R. W. Finberg, R. R. Ingalls, D. T. Golenbock, *J. Clin. Invest.* **2000**, 105, 497–504.

ESSAY

Influences: The Cell Physiology Laboratory in Montemar, Chile

Francisco Bezanilla^{1,2} 



Looking back, I was really lucky. In 1967, Dr. Joaquín Luco arranged for me, a student from the Catholic University, to join the Laboratorio de Fisiología Celular in Montemar to work on my doctoral thesis under the supervision of Dr. Eduardo (Guayo) Rojas from the University of Chile. I had completed three years at medical school and three years at engineering school, but my laboratory experience basically comprised short encounters with research in Joaquín Luco's neurophysiology laboratory and with the squid giant axon (Fig. 1) in Francisco (Pancho) Huneeus' laboratory across the street. But the Montemar laboratory was very different. The approach was quantitative and dealt with a subject that had fascinated me since I was in high school, when I learned for the first time that the nerve impulse was an electrical event. Electricity had been my hobby since I was in junior high, learning by doing as I moved from crystal radios to transmitters and TV sets. I became a radio amateur, not so much to contact other hams, but as an excuse to build a more powerful transmitter that could reach farther away, learning electronics in the process. At that time, everything I built was with vacuum tubes. When I arrived in Montemar, the first assignment from Guayo was to build my own setup with parts available in the laboratory, including micromanipulators, a microscope, pieces of plexiglass, and (wow!) solid-state operational amplifiers. For me, this was like arriving in paradise. I immediately built the voltage clamp with Philbrick op-amps and vacuum tubes in voltage follower configuration as amplifiers for the internal and external electrodes, which I replaced later with operational amplifiers.

The laboratory is located in Montemar, on the coast of Chile, a few kilometers north of the city of Valparaíso. The laboratory, which had previously been a brothel and conveniently had plumbing in all rooms, was bought by the rector of the University of Chile at the request of Dr. Mario Luxoro to establish a research laboratory for scientists working on the giant axon of the Humboldt squid *Dosidicus gigas*. This large squid, which can reach almost 2 m in length, was caught offshore by fishermen using small boats launched from the marine station ~100 m from the laboratory. Guayo and Mario had previously worked at this sta-



Figure 1. Opening the mantle of a Humboldt squid in the boat. Insets show a dissected axon (scale in cm, top) and an axon being mounted in the recording chamber (bottom).

tion, where they showed that a protease injected into the axon abolished action potentials but not the resting potential, demonstrating for the first time that proteins played a fundamental role in ionic conduction underlying the nerve impulse (1). However, the rules of the station's director at that time were incompatible with the schedule of experiments and squid collection, which prompted Mario to procure the new laboratory from the rector of the University.

The Laboratorio de Fisiología Celular had two floors on which rooms had been converted into laboratories for Mario, Guayo, Dr. Mitzi Canessa, Dr. Siegmund Fischer, and Dr. Fernando Vargas. All these principal investigators used the giant axon from the Humboldt squid as their biological preparation because the axons are so large (typically 1 mm in diameter and 20 cm long), and there are several giant fibers on each side of the squid. The projects, involving electrophysiology and biochemistry, varied from the sodium-potassium pump to streaming potentials to ion

¹Department of Biochemistry and Molecular Biology, University of Chicago, Chicago, IL; ²Centro Interdisciplinario de Neurociencia de Valparaíso, Facultad de Ciencias, Universidad de Valparaíso, Valparaíso, Chile.

Correspondence to Francisco Bezanilla: fbezanilla@chicago.edu.

© 2018 Bezanilla This article is distributed under the terms of an Attribution-Noncommercial-Share Alike-No Mirror Sites license for the first six months after the publication date (see <http://www.rupress.org/terms/>). After six months it is available under a Creative Commons License (Attribution-Noncommercial-Share Alike 4.0 International license, as described at <https://creativecommons.org/licenses/by-nc-sa/4.0/>).

Rockefeller University Press

J. Gen. Physiol. 2018 Vol. 150 No. 11 1464–1468



<https://doi.org/10.1085/jgp.201812157>

1464

I would like to thank Cecilia Hidalgo and Juan Bacigalupo for some of the old pictures. A movie that tells the story of the Montemar Laboratory produced by Cabala Productions and under the auspices of CINV may be found at: <https://www.youtube.com/watch?v=KPey93HBekc>.

Lesley C. Anson served as editor.

References

1. Rojas, E., and M. Luxoro. 1963. *Nature*. 199:78–79.
2. Hidalgo, C., and R. Latorre. 1970a. *J. Physiol.* 211:193–202.
3. Hidalgo, C., and R. Latorre. 1970b. *J. Physiol.* 211:173–191.
4. Latorre, R., and M.C. Hidalgo. 1969. *Nature*. 221:962–963.
5. Atwater, I., et al. 1969. *J. Physiol.* 201:657–664.
6. Bezanilla, F., et al. 1970b. *J. Physiol.* 207:151–164.
7. Armstrong, C.M. 1971. *J. Gen. Physiol.* 58:413–437.
8. Armstrong, C.M., et al. 1973. *J. Gen. Physiol.* 62:375–391.
9. Bezanilla, F., et al. 1970a. *J. Physiol.* 211:729–751.
10. Rojas, E., et al. 1970. *Nature*. 225:747–748.
11. Atwater, I., et al. 1970. *J. Physiol.* 211:753–765.
12. Vergara, J., and F. Bezanilla. 1976. *Nature*. 259:684–686.
13. Kaiser, J. 1995. *Science*. 267:821–822.
14. Castillo, J.P., et al. 2011. *Proc. Natl. Acad. Sci. USA*. 108:20556–20561.
15. Castillo, J.P., et al. 2015. *Nat. Commun.* 6:7622.
16. Mathur, C., et al. 2018. *Sci. Rep.* 8:2207.



Chaos versus noise as drivers of multistability in neural networks

Patricio Orio,^{1,2} Marilyn Gatica,¹ Rubén Herzog,¹ Jean Paul Maidana,¹ Samy Castro,¹ and Kesheng Xu¹

¹Centro Interdisciplinario de Neurociencia de Valparaíso, Universidad de Valparaíso, Pje Harrington 287, 2360103 Valparaíso, Chile

²Instituto de Neurociencia, Facultad de Ciencias, Universidad de Valparaíso, Gran Bretaña 1111, 2360102 Valparaíso, Chile

(Received 9 June 2018; accepted 1 October 2018; published online 18 October 2018)

The multistable behavior of neural networks is actively being studied as a landmark of ongoing cerebral activity, reported in both functional Magnetic Resonance Imaging (fMRI) and electroencephalography recordings. This consists of a continuous jumping between different partially synchronized states in the absence of external stimuli. It is thought to be an important mechanism for dealing with sensory novelty and to allow for efficient coding of information in an ever-changing surrounding environment. Many advances have been made to understand how network topology, connection delays, and noise can contribute to building this dynamic. Little or no attention, however, has been paid to the difference between local chaotic and stochastic influences on the switching between different network states. Using a conductance-based neural model that can have chaotic dynamics, we showed that a network can show multistable dynamics in a certain range of global connectivity strength and under deterministic conditions. In the present work, we characterize the multistable dynamics when the networks are, in addition to chaotic, subject to ion channel stochasticity in the form of multiplicative (channel) or additive (current) noise. We calculate the Functional Connectivity Dynamics matrix by comparing the Functional Connectivity (FC) matrices that describe the pair-wise phase synchronization in a moving window fashion and performing clustering of FCs. Moderate noise can enhance the multistable behavior that is evoked by chaos, resulting in more heterogeneous synchronization patterns, while more intense noise abolishes multistability. In networks composed of nonchaotic nodes, some noise can induce multistability in an otherwise synchronized, nonchaotic network. Finally, we found the same results regardless of the multiplicative or additive nature of noise. *Published by AIP Publishing.* <https://doi.org/10.1063/1.5043447>

Over the last few years, great attention has been given to the multistable dynamics of the brain activity, evidenced in large-scale brain recordings. It is of interest to learn what are the possible origins of this dynamics and the factors that can favor or hinder it. In this article, we study the multistable synchrony patterns in an oscillatory neural network under the influence of chaotic or stochastic dynamics. To our knowledge, this is the first time that the interaction between chaos and noise is assessed in this context and using the same type of analysis that is currently being applied to functional Magnetic Resonance Imaging and magnetoencephalography or electro- recordings. Under the conditions of weak coupling, we observe that the Functional Connectivity patterns that are detected seem to have more variety when the nodes in the network are chaotic. Noise or stochasticity, on the other hand, can enhance the multistability allowing the network to show a larger variety of synchrony patterns and promoting multistability in some networks that do not show it in the deterministic condition.

I. INTRODUCTION

The brain allows organisms to respond to external and internal stimuli with appropriate behaviors. To do so, it must

cope with a vast repertoire of ever-changing stimuli from which the relevant ones are extracted and decisions are made. To accomplish this, it is necessary that brain dynamics does not settle in one single strong attractor but rather dynamically display several possible synchrony configurations. This has been evidenced over the last year as the *Functional Connectivity Dynamics* (FCD).^{1,2}

Neural systems are characterized by high dimensionality and multiple nonlinear interactions between its components, often with delays and feedbacks.³ In such systems, one may expect to find the coexistence of stable and unstable attractors, but at the same time, if the global coupling is too strong, only one fully synchronized state is found.⁴ Thus, neural systems must possess destabilizing factors that produce the itinerancy.⁵ In the study of the factors that can make a network to be constantly itinerating, most of the attention has been paid to connectivity features.^{6,7} Numerical simulations of biologically plausible excitable models have shown that synaptic delays are important for the appearance of partially synchronized subnetwork states^{3,8–10} as well as slowly fluctuating patterns of synchronization.^{11,12} It has also been shown that multiple attractors can be found only within a range of the global coupling strength.^{3,4} Another significant factor under study is the connectivity pattern or network topology. The observed structural connectivity (SC) of the human brain enables multistability, which is lost when the connections are randomized.⁹

is a chimera state^{37,56} and it can be observed in one FC of Fig. 3 and transiently in the FC matrix of Fig. 5(a). Thus, our network model not only shows different patterns of synchrony, but they are also transient in nature. It is worth to emphasize that this occurs in the absence and the presence of noise, but more prominently when the nodes are of chaotic nature.

As our base model (the node) represents a single neuron, we found it appropriate to add the noise as ion channel stochasticity, a form of multiplicative noise. This noise introduces distinctive spectral properties to the system²⁶ with consequences that have not been investigated in all scenarios. Moreover, multiplicative noise has been shown to have a distinct effect on the temporal statistics of a multistable model.^{30,31} In our case, we were not able to find a significant difference in the effect of multiplicative versus additive noise. Nevertheless, propagation of multiplicative noise in neural models can have distinctive temporal properties, as in the related Huber & Braun model⁵⁷ and others.^{58,59} We expect some differences in the temporal characteristics of switching between different FCs in our network model, but a proper assessment of this will require longer simulations and an analysis method that captures the switching behavior in a better temporal way, such as the use of Hidden Markov (or semi-Markov) Models.⁶⁰

Our findings have some issues that need to be considered when interpreting them. We are studying multistability in a medium-sized network of oscillatory neurons and trying to relate its behavior to phenomena observed at much larger scales (whole brain). Ideally, this study should be replicated using models of brain areas as nodes of the network. Many such models exist, with different degrees of complexity^{4,22,61,62} and some present chaotic oscillatory behavior at the node level. However, all of them share a common mathematical structure with our model: sigmoid-shape functions of voltage (voltage dependency of ion channel in single neuron models and of firing rate in large-scale models) and time delays reflected in first- or second-order differential equations (ion channel activation or synaptic dynamics). Therefore, we expect the overall dynamics to be very similar to the model presented here. The main difference between our model and the large-scale ones is the nature of the connection between nodes. We have used electrical synapses, a type of bidirectional synapse that has a dampening effect with a natural tendency to synchronize a network, while long-range connections in the brain are unidirectional with an excitatory nature. This type of connection generates more complex dynamics, especially when time delays are considered,³ and does not always have the tendency toward synchrony as the coupling is increased (our preliminary work). On the other hand, the use of models inspired in large-scale brain dynamics will demand the use of noise formulations that reflect correctly the variability introduced by synaptic stochasticity and the jitter of action potential transmission. Finally, network topologies other than small-world should be explored.

Compared to other works about FCD,^{1,2,13} and to our own previous work,¹⁶ we have made a subtle methodological innovation in the calculation of the FCD matrix. Typically, to compare the different FCs obtained in consecutive time

windows, a correlation between the vectorized FCs is performed,¹³ while we chose here to use the angular distance. Correlation has the disadvantage of being normalized by the variance of the vectors, and thus when the network is near or at full synchrony, the difference between FCs is exaggerated because of the uniformity of the vectors. When working in the most multistable regime, or with experimental data, this is not a problem because the network is far from being synchronous. As in this work we were doing a sweep over the coupling conductance parameter to observe all the possible network regimes, we had to change this measure and found that the angular distance was more appropriated. For this reason, there are some numerical differences between our results at the deterministic limit and the results of our previous work. Nevertheless, regarding the difference between networks composed of chaotic or nonchaotic networks, the main observations are the same.

The chaotic nature of brain dynamics, given by its high dimensionality and strong nonlinearities, must play a role in the observed multistable dynamics. How this interacts with the also existing stochastic dynamics remains to be elucidated, and here we present the first attempt to raise the question. Future work will have to be directed toward the use of models related to large-scale brain dynamics that can generate multistability without noise.

ACKNOWLEDGMENTS

We thank the funding from Fondecyt Project Nos. 1181076 (P.O.) and 3170342 (K.X.) from CONICYT, Chile. J.P.M. and M.G. are recipients of a Ph.D. FIB-UV fellowship from UV. S.C. and R.H. are recipients of a Ph.D. fellowship Grant from CONICYT (Chile). P.O. is partially funded by the Advanced Center for Electrical and Electronic Engineering (FB0008 Conicyt, Chile). The Centro Interdisciplinario de Neurociencia de Valparaíso (CINV) is a Millennium Institute supported by the Millennium Scientific Initiative of the Ministerio de Economía (ICM-MINECON, Proyecto P09-022-F, CINV, Chile).

¹J. Cabral, M. L. Kringelbach, and G. Deco, *Neuroimage* **160**, 84 (2017).

²M. G. Preti, T. A. W. Bolton, and D. Van De Ville, *Neuroimage* **160**, 41 (2017).

³G. Deco, V. Jirsa, A. R. McIntosh, O. Sporns, and R. Kötter, *Proc. Natl. Acad. Sci. U.S.A.* **106**, 10302 (2009).

⁴G. Deco and V. K. Jirsa, *J. Neurosci.* **32**, 3366 (2012).

⁵K. Friston, M. Breakspear, and G. Deco, *Front. Comput. Neurosci.* **6**, 1 (2012).

⁶G. Deco, A. Ponce-Alvarez, D. Mantini, G. L. Romani, P. Hagmann, and M. Corbetta, *J. Neurosci.* **33**, 11239 (2013).

⁷D. S. Bassett and O. Sporns, *Nat. Neurosci.* **20**, 353 (2017).

⁸A. Ghosh, Y. Rho, A. R. McIntosh, R. Kötter, and V. K. Jirsa, *PLoS Comput. Biol.* **4**, e1000196 (2008).

⁹J. Cabral, H. Luckhoo, M. Woolrich, M. Joensson, H. Mohseni, A. Baker, M. L. Kringelbach, and G. Deco, *Neuroimage* **90**, 423 (2014).

¹⁰C. A. Lea-Carnall, M. A. Montemurro, N. J. Trujillo-Barreto, L. M. Parkes, and W. El-Dereby, *PLoS Comput. Biol.* **12**, e1004740 (2016).

¹¹L. L. Gollo and M. Breakspear, *Philos. Trans. R. Soc. B Biol. Sci.* **369**, 20130532 (2014).

¹²L. L. Gollo, A. Zalesky, R. M. Hutchison, M. van den Heuvel, and M. Breakspear, *Philos. Trans. R. Soc. B Biol. Sci.* **370**, 20140165 (2015).

¹³E. C. A. Hansen, D. Battaglia, A. Spiegler, G. Deco, and V. K. Jirsa, *Neuroimage* **105**, 525 (2015).

¹⁴G. Deco, J. Cabral, M. W. Woolrich, A. B. A. Stevner, T. J. van Hartevelt, and M. L. Kringelbach, *Neuroimage* **152**, 538 (2017).



Innexins: Expression, Regulation, and Functions

Juan Güiza¹, Iván Barria¹, Juan C. Sáez^{2,3} and José L. Vega^{1*}

¹ Laboratorio de Fisiología Experimental, Instituto Antofagasta, Universidad de Antofagasta, Antofagasta, Chile,

² Departamento de Fisiología, Pontificia Universidad Católica de Chile, Santiago, Chile, ³ Instituto de Neurociencias, Centro Interdisciplinario de Neurociencias de Valparaíso, Universidad de Valparaíso, Valparaíso, Chile

The innexin (Inx) proteins form gap junction channels and non-junctional channels (named hemichannels) in invertebrates. These channels participate in cellular communication playing a relevant role in several physiological processes. Pioneer studies conducted mainly in worms and flies have shown that innexins participate in embryo development and behavior. However, recent studies have elucidated new functions of innexins in *Arthropoda*, *Nematoda*, *Annelida*, and *Cnidaria*, such as immune response, and apoptosis. This review describes emerging data of possible new roles of innexins and summarizes the data available to date.

Keywords: gap junction, pannexin, connexin, invertebrates, channels, hemichannels

OPEN ACCESS

Edited by:

Christoph Fahlke,
Forschungszentrum Jülich, Germany

Reviewed by:

Zhao-Wen Wang,
University of Connecticut School of
Medicine, United States
Francesco Zonta,
ShanghaiTech University, China

*Correspondence:

José L. Vega
joseluis.vega@uantof.cl

Specialty section:

This article was submitted to
Membrane Physiology and Membrane
Biophysics,
a section of the journal
Frontiers in Physiology

Received: 03 July 2018

Accepted: 18 September 2018

Published: 11 October 2018

Citation:

Güiza J, Barria I, Sáez JC and Vega JL
(2018) Innexins: Expression,
Regulation, and Functions.
Front. Physiol. 9:1414.
doi: 10.3389/fphys.2018.01414

INTRODUCTION

Intercellular communication plays a key role in many cell functions (Dykes and Macagno, 2006). Innexins are integral membrane proteins that participate in cellular communication, forming gap junction channels, and hemichannels (Vega et al., 2013). Gap junction channels allow the diffusion of ions, second messengers and small molecules between adjacent cells (Sáez et al., 2003), whereas hemichannels (also named innexons) allow the exchange between the cell interior with the extracellular milieu (Dahl and Muller, 2014). Krishnan and collaborators described the first innexin in 1993. They studied a mutant fly that failed to respond to a light-off stimulus and identified a gene called *Pas* (for Passover, also known as shaking-B), which encodes a protein of 361 amino acids and is expressed in giant fibers. Notably, this mutation causes synaptic dysfunction in giant fiber neurons, which are responsible for coordinating the response promoted by light-off (Krishnan et al., 1993). Subsequently, this protein was expressed in paired *Xenopus* oocytes where it forms gap junction channels (Phelan et al., 1998a). In 1993, a gene called *unc-7* was identified in *Caenorhabditis elegans* (*C. elegans*), which was required for coordinated locomotion (Starich et al., 1993). With this background, the new family of genes was first proposed as OPUS for OGRE (gene that encodes the innexin 1 protein), *Pas*, *unc-7* and Shaking-B, but subsequently, the name was changed to innexins for invertebrate homologs of connexins (Phelan et al., 1998b). Notably, studies previous to the description of the innexins reported the existence of gap junctions in invertebrates without being associated with any specific function, such as the gap junctions in semiferous epithelium of *Triatoma infestans* (Miranda and Cavicchia, 1988), intestinal tissue of *Sagitta setosa* (Duvert et al., 1980), photoreceptor cells of *Apis mellifera* (Pabst and Kral, 1989), giant axon and inner nerve of *Aglanta digitale* (Weber et al., 1982), endoderm of *Polyorchis penicillatus* (King and Spencer, 1979), and ciliated cells of *Pleurobrachia bachei* (Satterlie and Case, 1978). We currently know many functions of the innexins as cell-cell communication pathways mediated by gap junction channels and as well as hemichannels.

regeneration (Oviedo et al., 2010). Additionally, exposure to heptanol, a blocker of gap junctions, results in an anteriorization of both blastemas, generating a loss of tail development or appearance of an ectopic eye, pharynx, and complete head at the posterior in *D. japonica* (Nogi and Levin, 2005).

INNEXINS A THERAPEUTIC TARGETS OF PARASITIC DISEASES

Malaria Disease

Clinical studies find that probenecid, a blocker of hemichannels formed by innexins, has a powerful antiparasitic effect (Nzila et al., 2003; Sowunmi et al., 2004; Masseno et al., 2009). For example, probenecid increases the sensitivity of a highly resistant plasmodium strain against antifolate components (Nzila et al., 2003). The mechanism has not been elucidated, but it is not associated with sensitivity status of the parasite or with alterations of the dihydrofolate reductase or dihydropteroate synthase (Nzila and Al-Zahrani, 2013). In fact, it has been suggested that it is a transport-based mechanism linked to folate salvage (Nzila and Al-Zahrani, 2013). In clarifying whether probenecid affects the activity of gap junction channels, hemichannels or both, it has been reported that probenecid inhibits the activity of innexin- or pannexin-formed hemichannels (Wang et al., 2015). Moreover, the effect of probenecid on innexin-formed gap junction channel has not been evaluated. Also, it has been described that Cx46 or chimera Cx32E143-formed hemichannels are not affected by probenecid (Silverman et al., 2008). Moreover, in human erythrocytes, antimalarial drugs such as artemisinin and artesunate reduce the activity of channels formed by pannexin-1, a homolog of innexin in vertebrates (Dahl et al., 2013).

Chagas Disease

Suramin, a blocker of hemichannels, has a powerful trypanocidal effect (Bisaggio et al., 2006). For example, the exposure of *T. cruzi* infected-LLC-MK2 cells to suramin causes a partial or complete detachment of the flagellum from the cell body in trypomastigote forms (Bisaggio et al., 2006). Although the mechanism has not been elucidated, it has been described that suramin affects the activity of several enzymes such as kinases, phosphatases, ATPases, oxidases and phospholipases (Voogd et al., 1993). Furthermore, suramin acts as antagonist of P2X and P2Y purinoceptors (Voogd et al., 1993). In trypanosomes, a prolonged incubation (5–7 days) with suramin causes an increase in Mg²⁺-dependent ecto-ATPase activity (Bisaggio et al., 2003). Although the effect of suramin on the innexin-formed hemichannels has not been described,

it has been described that suramin blocks the permeability of Cx43 hemichannels activated by removal of extracellular Ca²⁺ without much effect on gap junctional communication (Chi et al., 2014). Currently, suramin is used for treatment of parasitic diseases caused by protozoa (Sowunmi et al., 2004).

Arthropod Vectors

Pharmacological inhibitors of gap junctions are potential insecticides (Calkins and Piermarini, 2015). For example, mefloquine and meclofenamic acids are toxic to adult female *A. aegypti* and upon topically application to the cuticle, carbenoxolone showed full efficacy (Calkins and Piermarini, 2015). The authors suggest that the mechanism would be an alteration of renal function in the mosquito (Calkins and Piermarini, 2015).

CONCLUDING REMARKS

The innexin proteins are members of the gap junction family found in invertebrates and are involved in a series of biological functions. Many studies show the importance of the formation of innexin gap junctions between neighbor cells, demonstrating the necessity of intercellular communication to coordinate different processes, such as embryonic development, which emphasizes their role in morphogenesis and neurogenesis. Additionally, gap junctions within the adult stage participate in physiological functions, behavior, and memory. Fewer reports describe the importance of the no-junctional channels formed by innexin proteins, although specifically in processes of immune response and apoptosis.

AUTHOR CONTRIBUTIONS

JG, JCS, and JLV contributed conception and design of the study. JG and JLV organized the database. JG wrote the first draft of the manuscript. IB, JCS, and JLV wrote sections of the manuscript. All authors contributed to manuscript revision, read, and approved the submitted version.

FUNDING

This work was partially supported by a MINEDUC-UA project code ANT 1755 (to JLV), Fondo Nacional de Desarrollo Científico y Tecnológico (FONDECYT) 1150291 (to JCS) and ICM-Economía P09-022-F Centro Interdisciplinario de Neurociencias de Valparaíso (to JCS). JG and IB hold a CONICYT-Ph.D. fellowship, Chile.

REFERENCES

- Altun, Z., Chen, B., Wang, Z., and Hall, D. (2009). High resolution map of *Caenorhabditis elegans* gap junction proteins. *Dev. Dyn.* 238, 1936–1950. doi: 10.1002/dvdy.22025
- Anava, S., Rand, D., Zilberstein, Y., and Ayali, A. (2009). Innexin genes and gap junction proteins in the locust frontal ganglion. *Insect Biochem. Mol. Biol.* 39, 224–233. doi: 10.1016/j.ibmb.2008.12.002
- Anava, S., Saad, Y., and Ayali, A. (2013). The role of gap junction proteins in the development of neural network functional topology. *Insect Mol. Biol.* 22, 457–472. doi: 10.1111/imb.12036
- Ashburner, M., Ball, C. A., Blake, J. A., Botstein, D., Butler, H., Cherry, J. M., et al. (2000). Gene ontology: tool for the unification of biology. *Gene Ontol. Consortium Nat. Genet.* 25, 25–29. doi: 10.1038/75556
- Ayukawa, T., Matsumoto, K., Ishikawa, H. O., Ishio, A., Yamakawa, T., Aoyama, N., et al. (2012). Rescue of Notch signaling in cells incapable of GDP-L-fucose

This Accepted Manuscript has not been copyedited and formatted. The final version may differ from this version.

JNeurosci

THE JOURNAL OF NEUROSCIENCE

Research Articles: Cellular/Molecular

Morphological and biophysical determinants of the intracellular and extracellular waveforms in nigral dopaminergic neurons: A computational study

Luciana López-Jury^{1,2}, Rodrigo C. Meza^{1,3}, Matthew T. C. Brown⁴, Pablo Henny¹ and Carmen C. Canavier²

¹Laboratorio de Neuroanatomía, Departamento de Anatomía, and Centro Interdisciplinario de Neurociencia, NeuroUC, Escuela de Medicina, Pontificia Universidad Católica de Chile, Av. Libertador Bernardo O'Higgins 340, Santiago, 8330023, Chile

²Department of Cell Biology and Anatomy and the Alcohol and Drug Abuse Center of Excellence, Louisiana State University Health Sciences Center, New Orleans, Louisiana, USA 70112

³Centro Interdisciplinario de Neurociencia de Valparaíso CINV and Millennium Nucleus of Biology of Neuropsychiatric Disorders NuMIND, Facultad de Ciencias, Universidad de Valparaíso, Valparaíso, Chile 2360102.

⁴Medical Research Council Anatomical Neuropharmacology Unit, University of Oxford, Oxford OX1 3TH, United Kingdom.

DOI: 10.1523/JNEUROSCI.0651-18.2018

Received: 8 March 2018

Revised: 12 July 2018

Accepted: 9 August 2018

Published: 13 August 2018

Author contributions: L.L.-J., R.C.M., and M.T.C.B. performed research; L.L.-J. and R.C.M. analyzed data; L.L.-J. wrote the first draft of the paper; P.H. and C.C.C. designed research; P.H. and C.C.C. wrote the paper.

Conflict of Interest: The authors declare no competing financial interests.

We thank Ted Carnevale for assistance with the NEURON code. We also thank Peter J. Magill and J. P. Bolam for training and supervision during electrophysiological and anatomical experiments reported in this study. This work was supported by Fondecyt N° 1141170 and Anillo ACT-1109 grants to P.H. and NIH R01DA041705 and a grant from the Alcohol and Drug Abuse Center of Excellence (ADACE) at the Louisiana State University Health Sciences Center to C.C. M.T.C. current address: Wellcome Trust, Gibbs Building, 215 Euston Road, London NW1 2BE, UK.

Corresponding authors: Carmen Canavier: ccanav@lsuhsc.edu; Pablo Henny: phenny@uc.cl

Cite as: J. Neurosci.; 10.1523/JNEUROSCI.0651-18.2018

Alerts: Sign up at www.jneurosci.org/cgi/alerts to receive customized email alerts when the fully formatted version of this article is published.

Accepted manuscripts are peer-reviewed but have not been through the copyediting, formatting, or proofreading process.

Copyright © 2018 the authors

27 **Number of words for Discussion:** 1490

28 **Conflict of interest:** The authors declare no competing financial interests.

29 **Acknowledgements:** We thank Ted Carnevale for assistance with the NEURON code.

30 We also thank Peter J. Magill and J. P. Bolam for training and supervision during electro-
31 physiological and anatomical experiments reported in this study. This work was supported
32 by Fondecyt N° 1141170 and Anillo ACT-1109 grants to P.H. and NIH R01DA041705 and
33 a grant from the Alcohol and Drug Abuse Center of Excellence (ADACE) at the Louisiana
34 State University Health Sciences Center to C.C. M.T.C current address: Wellcome Trust,
35 Gibbs Building, 215 Euston Road, London NW1 2BE, UK.

36
37 **Abstract:**

38 Action potentials (APs) in nigral dopaminergic neurons often exhibit two separate compo-
39 nents, the first reflecting spike initiation in the dendritically located axon initial segment
40 (AIS) and the second the subsequent dendro-somatic spike. These components are sepa-
41 rated by a *notch* in the ascending phase of the somatic extracellular waveform and in the
42 temporal derivative of the somatic intracellular waveform. Still, considerable variability ex-
43 ists in the presence and magnitude of the *notch* across neurons. To systematically ad-
44 dress the contribution of AIS, dendritic and somatic compartments to shaping the two-
45 component APs, we modeled APs of previously *in vivo* electrophysiologically characterized
46 and 3D-reconstructed male mouse and rat dopaminergic neurons. A parsimonious two-
47 domain model, with high (AIS) and lower (dendro-somatic) Na^+ conductance, reproduced
48 the notch in the temporal derivatives, but not in the extracellular APs, regardless of mor-
49 phology. The notch was only revealed when somatic active currents were reduced, con-
50 straining the model to three domains. Thus an initial AIS spike is followed by an actively-
51 generated spike by the axon-bearing dendrite (ABD), in turn followed mostly passively by
52 the soma. The transition from being a source compartment for the AIS spike to a source
53 compartment for the ABD spike satisfactorily explains the extracellular somatic notch.
54 Larger AISs and thinner ABD (but not soma-to-AIS distance), accentuate the AIS compo-
55 nent. We conclude that variability in AIS size and ABD caliber explains variability in AP
56 extracellular waveform and separation of AIS and dendro-somatic components, given the
57 presence of at least three functional domains with distinct excitability characteristics.

58
59

60 **Significance:**

61 Midbrain dopamine neurons make an important contribution to circuits mediating motiva-
62 tion and movement. Understanding the basic rules that govern the electrical activity of sin-
63 gle dopaminergic neurons is therefore essential to reveal how they ultimately contribute to



Gating charge displacement in a monomeric voltage-gated proton (H_v1) channel

Emerson M. Carmona^a, H. Peter Larsson^b, Alan Neely^a, Osvaldo Alvarez^{a,c}, Ramon Latorre^{a,1}, and Carlos Gonzalez^{a,1}

^aCentro Interdisciplinario de Neurociencia de Valparaíso, Universidad de Valparaíso, 2351319 Valparaíso, Chile; ^bDepartment of Physiology and Biophysics, University of Miami, Miami, FL 33136; and ^cDepartamento de Biología, Facultad de Ciencias, Universidad de Chile, 7800003 Santiago, Chile

Contributed by Ramon Latorre, July 18, 2018 (sent for review June 6, 2018; reviewed by Thomas E. DeCoursey and Francesco Tombola)

The voltage-gated proton (H_v1) channel, a voltage sensor and a conductive pore contained in one structural module, plays important roles in many physiological processes. Voltage sensor movements can be directly detected by measuring gating currents, and a detailed characterization of H_v1 charge displacements during channel activation can help to understand the function of this channel. We succeeded in detecting gating currents in the monomeric form of the *Ciona*-H_v1 channel. To decrease proton currents and better separate gating currents from ion currents, we used the low-conducting H_v1 mutant N264R. Isolated ON-gating currents decayed at increasing rates with increasing membrane depolarization, and the amount of gating charges displaced saturates at high voltages. These are two hallmarks of currents arising from the movement of charged elements within the boundaries of the cell membrane. The kinetic analysis of gating currents revealed a complex time course of the ON-gating current characterized by two peaks and a marked Cole-Moore effect. Both features argue that the voltage sensor undergoes several voltage-dependent conformational changes during activation. However, most of the charge is displaced in a single central transition. Upon voltage sensor activation, the charge is trapped, and only a fast component that carries a small percentage of the total charge is observed in the OFF. We hypothesize that trapping is due to the presence of the arginine side chain in position 264, which acts as a blocking ion. We conclude that the movement of the voltage sensor must proceed through at least five states to account for our experimental data satisfactorily.

Hv1 proton channel | gating currents | trapping | voltage sensor | kinetic model

Voltage-gated proton (H_v1) channels are transmembrane proteins that regulate cellular pH, producing outward proton currents in response to depolarization. Since the discovery of the *Ciona intestinalis*, mouse, and human H_v1 genes in 2006 (1, 2), the relevance of this channel in physiological and pathophysiological processes has increased continuously (3). H_v1 is a voltage-gated ion channel with a unique structure and properties. It is a homodimer (4–6) containing four transmembrane alpha helices in each subunit (S1 to S4). Both the voltage sensor and the permeation pathway of this channel originate from these four transmembrane segments. The fourth transmembrane helix (S4) contains three conserved arginine residues responsible for the channel voltage sensitivity (7, 8). The intracellular N-terminal domain is variable in both length and sequence among different species. The intracellular C-terminal domain forms a coiled-coil structure necessary for dimer formation (6). H_v1 is voltage- (7) and pH-dependent (9), is highly selective to protons (10), has a small unitary conductance (11), and displays a cooperative gating between subunits (8, 12). However, there are still many open questions regarding the mechanisms of H_v1 activation. In particular, we do not know the details regarding how the gating charges are displaced during activation and how these movements are related to channel opening.

H_v1 voltage sensor movement has been studied principally by two methods: accessibility assays and fluorescence. In the first case,

membrane-impermeable thiol-reactive methanethiosulfonate (MTS) probes were used to test the state-dependent accessibility of a cysteine residue introduced into a specific region of the voltage sensor (13). In the case of H_v1, accessibility experiments indicate that both S1 (14) and S4 (7) undergo conformational changes during activation and that there is cooperativity between the subunits of the channel (8). The second approach involves the use of voltage-clamp fluorometry (VCF) (15). In VCF, the conformational changes of the channel are monitored by a fluorescent probe bound to a cysteine introduced into a specific site using mutagenesis (16, 17). VCF experiments revealed two conformational changes during activation (18); following the S4 movement, there is a displacement of S1 associated with the opening of the channel (14). The caveat of these methodologies is that they are indirect approaches to studying the dynamics of the H_v1 voltage sensor. In contrast, gating currents directly report the movement of the voltage-sensing charges across the membrane electric field, making it possible to study the kinetics of this process in detail.

In the *Shaker* voltage-gated potassium channel, gating currents are produced by the movement of arginine residues in the S4 transmembrane segment within the voltage sensor domain (19, 20). Three of these arginine residues are conserved in S4 of H_v1 and were shown to be responsible for the voltage-dependent gating of the channel (7). Since the *Ciona*-H_v1 channels express well in oocytes, it should be possible to record gating currents induced by the activation of this channel. Indeed, preliminary studies on H_v1 gating current have been reported (21–23).

Significance

H_v1 proton channels, since their open probability increases with depolarization and low pH, are fundamental in sustaining the suitable pH gradient for cell survival. Here, we have characterized the gating current elicited by the monomeric mutant proton channel N264R with the aim of understanding the voltage-dependent processes that control channel opening. Gating currents precede ion currents, indicating that a large fraction of gating charge is displaced before H_v1 opening. The voltage sensor displacements are complex and consist of numerous well-defined states. However, most of the charge is displaced in a single transition that probably leads to channel opening. The positively charged arginine in the N264R channel promotes gating charge trapping in addition to blocking the proton currents.

Author contributions: E.M.C., H.P.L., A.N., O.A., R.L., and C.G. designed research; E.M.C. performed research; E.M.C., H.P.L., A.N., O.A., R.L., and C.G. analyzed data; and E.M.C., H.P.L., A.N., O.A., R.L., and C.G. wrote the paper.

Reviewers: T.E.D., Rush University; and F.T., University of California, Irvine.

The authors declare no conflict of interest.

Published under the PNAS license.

¹To whom correspondence may be addressed. Email: ramon.latorre@uv.cl or carlos.gonzalez@uv.cl.

This article contains supporting information online at www.pnas.org/lookup/suppl/doi:10.1073/pnas.1809705115/-DCSupplemental.

pulse decreased this energy to 17 kJ/mol, but, upon returning to -70 mV, the charge needed to surmount a 27-kJ/mol barrier height to return from B_1 to the A_3 state (Fig. 5F). This activation energy difference predicts an A_3 -to- B_1 charge movement at 150 mV to be 27 times faster than the B_1 -to- A_3 movement at -70 mV. Our results indicate that the difference between the slow kinetic component of the ON (4 ms) is 22 times faster than the slow OFF component (88 ms) (compare Fig. 2D with Fig. 4C), which is in reasonable agreement with the calculation using the five-state model.

A New H_v1 Channel Kinetic Model Is Needed. Previously, by a fluorophore attached to the S4 voltage sensor in dimeric H_v1 channels, we revealed two S4 charge movements: The first one precedes channel opening, with S4 charge movements in both subunits independently, and the second one correlates with channel opening, defined as the fluorescence hook (18). To make it compatible with our previous model, only B_2 in the present model would be correlated with an open channel. Then, the hook would be the transition from B_2 to B_1 , which is fast and closes the channel, while transition B_1 to A_3 would be the main S4 transition, which is slow. In the kinetic model of dimeric H_v1 proposed by us (18), voltage sensor movement involved three closed and one open state, where the movement of both voltage sensors within the dimer is necessary before the opening of the permeation pathway of each subunit (18). Here, we found that each independent H_v1 voltage sensor transits through different states, suggesting that the movement of charge is more complex than previously thought. The most significant fact is that more than 50% of gating charge displacement, on the monomeric H_v1 channel, occurs before opening (in 5 ms at 150 mV, when the open probability of the monomeric H_v1 channel is only 0.2, 65% of the gating charge has been displaced). Dimer formation confers cooperative gating to H_v1 channels (8). Therefore, it is possible that the displacement of dimeric voltage sensors is different from the monomeric voltage sensors movement.

Molecular Mechanism for Trapping. We envision that the rate-limiting step that keeps the charges from returning to their resting configuration involves a blocked-like phenomenon mediated by the arginine side chain, much like the documented blockade of H_v1 channels by guanidinium reagents (31–33). Moreover, as reported before using the dimeric human H_v1 mutant N214R (34, 35) and mouse mutant N210R (24), we found that the N264R mutant open channel behaves as an inward rectifier (SI Appendix, Fig. S6). Blockade by the positively charged arginine located in the internal vestibule of the channel should be relieved by hyperpolarizing voltages, and the mutant channel should behave as an inward rectifier as found experimentally (SI Appendix, Fig. S6). We should also consider that the mutation introduced at position 264 can decrease proton currents by changing the electrostatic potential in the neighborhood of the H_v1 channel internal entrance. Although our data indicate that the N264 mutant does not modify the channel voltage dependence (SI Appendix, Figs. S3 and S4), measurements of this position accessibility to thiol-modifying agents was shown to be state-dependent. However, structural models suggest that this position is outside the electric field (7, 36), but more experiments are needed to confirm this claim. Finally, the inspection of the proton current recording of the monomeric *Ciona*-N264R mutant suggests that the positively charged guanidinium stabilizes the closed state of the channel, making the channel deactivation slower in the dimeric and monomeric *Ciona*- H_v1 (SI Appendix, Figs. S3 and S6), and in the dimeric mouse and human H_v1 containing the equivalent N210R (24) and N214R (35) mutation, respectively. A possible explanation to these findings is that the gating charge is trapped when the channel is activated upon depolarization, and it recovers slowly during the repolarization process, as we showed in this study.

We conclude that trapping is a consequence of the presence of the charged arginine chain in position 264. Given the fast

deactivation rate shown by the WT monomeric H_v1 channel, the presence of a neutral asparagine in that position may have the effect of collapsing the barrier that separates states A_3 from B_1 .

Methods

Mutagenesis, Transcription, and Sequencing. The single N264R mutation was introduced with a QuikChange kit (Promega Corp.) in a pSP64T-contained *C. intestinalis* H_v1 sequence kindly provided by Yasushi Okamura, Osaka University, Osaka, Japan. The $\Delta N\Delta C$ H_v1 was constructed with a stop codon at Val270 and an initiator methionine replacing Glu129 (6). Primers were designed using the web service QuikChange Primer Design. Mutant DNA was amplified by PCR, checked by sequencing, and then linearized with NotI restriction enzyme. In vitro transcription was performed with an mMESSAGE mMACHINE kit (Ambion) using RNA polymerase SP6. RNA was quantified by absorbance at 260 nm, and its integrity was checked by electrophoresis in 1% agarose gel with ethidium bromide at 0.6 μ g/ μ L.

Oocyte Extraction and RNA Injection. *X. laevis* oocytes were obtained and injected with 50 nL of RNA at a concentration of 1 μ g/ μ L according to previously described methodologies (26).

Electrophysiology. Voltage clamp recordings were performed in inside-out giant patches of oocytes membranes (37). The internal and external solutions contained 100 mM Hepes, 2 mM $MgCl_2$, 1 mM EGTA, and 50 mM *N*-methyl-D-glucamine (NMDG)-methanesulfonate. pH was adjusted with NMDG or methanesulfonate to 7.0. Measurements were performed at room temperature (22 °C). Pipettes of borosilicate capillary glass (1B150F-4; World Precision Instruments) were pulled on a horizontal pipette puller (Sutter Instruments) and fire polished until obtaining a diameter between 15 and 24 μ m (resistances of 0.8 to 1.2 M Ω in the bath solution). Data were acquired with an Axopatch 200B amplifier (Axon Instruments). Both the voltage command and current output were filtered at 20 kHz with 8-pole Bessel low-pass filters (Frequency Devices). Analog signals were sampled with a 16-bit A/D converter (Digidata 1440A; Axon Instruments) at 250 kHz. Recordings were filtered off-line at 10 kHz by a digital 8-pole Bessel low-pass filter before analysis. Experiments were performed using Clampex 8 acquisition software (Axon Instruments). Capacitive currents were compensated by analog circuitry, and linear capacitive currents were subtracted using a P/8 protocol with a subsweep holding potential of -90 mV (38).

Gating Current Simulations. A five-state kinetic model was simulated solving the equation $dP(t)/dt = P(t)Q$, where $P(t)$ is the probability vector of the states and Q is the transition rate matrix. We solved the time dependency of $P(t)$ using the spectral expansion (39). Forward and reverse kinetic constants, $\alpha(V)$ and $\beta(V)$, respectively, were modeled as $\alpha(V) = \alpha_0 \exp(xz\delta e_0 V/kT)$ and $\beta(V) = \beta_0 \exp((x-1)z\delta e_0 V/kT)$, where α_0 and β_0 are the kinetic constants at $V = 0$ mV, $z\delta e_0$ is the charge moved in the transition, x is the fraction of the charge moved from a well to the barrier peak in each forward transition, and k and T have their usual meanings. Gating currents $I_g(t)$ were obtained with the equation $I_g(t) = NF(t)Z$, where N is the number of channels, $F(t)$ is the net occupancy flux of each transition (40), and Z is a vector containing the charge associated to each transition. Parameters used in the model are listed in SI Appendix, Table S1.

Note. While this paper was under revision, detection of gating currents in the dimeric human proton channel mutant W207A-N214R (W257A-N264R in *Ciona*- H_v1) was reported (41). The method used by the authors to measure gating currents was stepping to a depolarizing voltage from different holding potentials, which is essentially a “Cole-Moore” protocol. Surprisingly, the gating current data do not show a Cole-Moore effect like the one reported here. This is an unexpected result, considering that the data also indicate that the gating current kinetics is defined by multiple states (41). However, the lack of a well-defined Cole-Moore effect may be due to the fast activation kinetics conferred by the W207A mutation (42).

ACKNOWLEDGMENTS. We thank Dr. David Baez for carrying out some of the initial preliminary experiments. This work was supported by Comisión Nacional de Investigación Científica y Tecnológica (CONICYT)-Programa Formación de Capital Humano Avanzado (PFCHA)/Doctorado Nacional/2017-21170395 (to E.M.C.), Fondo Nacional de Desarrollo Científico y Tecnológico (Fondecyt) Grants ACT 1104, Fondecyt 1180464 (to C.G.), 1150273 (to R.L.), and the US Air Force Office of Scientific Research (AFOSR) under Award FA9550-16-1-0384 (to R.L.). The Centro Interdisciplinario de Neurociencia de Valparaíso is a Millennium Institute supported by the Millennium Scientific Initiative of the Chilean Ministry of Economy, Development, and Tourism (P029-022-F).



Schwann Cell Responses and Plasticity in Different Dental Pulp Scenarios

Eduardo Couve^{1*} and Oliver Schmachtenberg²

¹Laboratorio de Microscopía Electrónica, Instituto de Biología, Facultad de Ciencias, Universidad de Valparaíso, Valparaíso, Chile, ²Centro Interdisciplinario de Neurociencias de Valparaíso (CINV), Facultad de Ciencias, Universidad de Valparaíso, Valparaíso, Chile

Mammalian teeth have evolved as dentin units that enclose a complex system of sensory innervation to protect and preserve their structure and function. In human dental pulp (DP), mechanosensory and nociceptive fibers form a dense meshwork of nerve endings at the coronal dentin-pulp interface, which arise from myelinated and non-myelinated axons of the Raschkow plexus (RP). Schwann cells (SCs) play a crucial role in the support, maintenance and regeneration after injury of these fibers. We have recently characterized two SC phenotypes hierarchically organized within the coronal and radicular DP in human teeth. Myelinating and non-myelinating SCs (nmSCs) display a high degree of plasticity associated with nociceptive C-fiber sprouting and axonal degeneration in response to DP injuries from dentin caries or physiological root resorption (PRR). By comparative immunolabeling, confocal and electron microscopy, we have characterized short-term adaptive responses of SC phenotypes to nerve injuries, and long-term changes related to aging. An increase of SCs characterizes the early responses to caries progression in association with axonal sprouting in affected DP domains. Moreover, during PRR, the formation of bands of Büngner is observed as part of SC repair tracks functions. On the other hand, myelinated axon density is significantly reduced with tooth age, as part of a gradual decrease in DP defense and repair capacities. The remarkable plasticity and capacity of SCs to preserve DP innervation in different dental scenarios constitutes a fundamental aspect to improve clinical treatments. This review article discusses the central role of myelinating and non-mSCs in long-term tooth preservation and homeostasis.

Keywords: tooth, glia, myelin, aging, caries, dentin

OPEN ACCESS

Edited by:

Mauricio Antonio Retamal,
Universidad del Desarrollo, Chile

Reviewed by:

Ivo Lambrichts,
University of Hasselt, Belgium
Igor Adameyko,
Karolinska Institutet (KI), Sweden

*Correspondence:

Eduardo Couve
eduardo.couve@uv.cl

Received: 16 June 2018

Accepted: 17 August 2018

Published: 05 September 2018

Citation:

Couve E and Schmachtenberg O
(2018) Schwann Cell Responses
and Plasticity in Different Dental
Pulp Scenarios.
Front. Cell. Neurosci. 12:299.
doi: 10.3389/fncel.2018.00299

THE DENTIN-PULP INTERFACE IN MULTICUSP TEETH

From an evolutionary perspective, a single tooth is a dentin unit formed by odontoblasts, protected by enameloid or enamel and containing an innervated dental pulp (DP). During vertebrate evolution, the appearance of cone-shaped teeth in fish constitutes a crucial event within the adaptation of vertebrate feeding mechanisms, from sucking to predatory animals (Smith and Johanson, 2015). Moreover, the increase in tooth size and shape complexity is related with a gradual reduction of the robust mechanisms of continuous tooth replacement observed in polyphyodonts, to a non- or single-renewal mechanism in mammals (monophyodont or diphyodont dentition).

different human DP stem cell populations (hDPSCs) which can be induced to differentiate into SCs, expressing p75NTR, Sox10 and S100 (Al-Zer et al., 2015). hDPSCs also express neurotrophic factors like NGF, and are able to promote axonal outgrowth *in vitro* (Martens et al., 2014), suggesting the potential usefulness of hDPSCs for tissue engineering therapies of injured peripheral nerves (Luo et al., 2018).

THE SCHWANN CELL RESPONSE TO ROOT RESORPTION

Physiological root resorption (PRR) is an asymptomatic process which in humans forms part of the natural mechanism of tooth replacement. It is mediated by odontoclasts that progressively reduce the root and DP tissue prior to exfoliation (Moorrees et al., 1963). During the PRR process, a reduction of DP innervation has been characterized as a Wallerian-like axonal degeneration process (Monteiro et al., 2009), leading to a reduction of nerve fiber bundles and nerve endings. In parallel, myelin sheath degradation (Figure 2C) and a progressive reduction of myelinated axons is associated with an activation of autophagic activity by SCs (Suzuki et al., 2015). In fact, a chronic compression of peripheral nerves constitutes an injury that promotes demyelination and activation of repair SC phenotypes, suggesting that SCs are directly sensitive to mechanical stimuli (Belin et al., 2017). SCs display considerable phenotypic plasticity and facilitate the surprisingly fast recovery of peripheral nerves after PRR or other insults (Boerboom et al., 2017).

Demyelination of damaged axons implies the accumulation of myelin debris within the SC. Myelin debris acts as an obstacle for the regeneration of axons and is considered a major contributor to the inflammatory response after nerve injury (Gaudet et al., 2011). Indeed, there is an increase of immunocompetent cells during the PRR process, suggesting a progressive inflammatory condition (Angelova et al., 2004). However, SCs are able to activate an autophagic pathway to promote myelin clearance during Wallerian degradation (Gomez-Sanchez et al., 2015).

In injured peripheral nerves, adaptive SCs reprogram into immature phenotypes with proliferative capacity forming bands of Büngner to allow axonal regeneration (Suzuki et al., 2015). Moreover, a remarkable feature at advanced stages of root resorption in deciduous teeth is an increase of major histocompatibility complex (MHC) class II (HLA-DR) expression in SCs in association with immunocompetent cell recruitment (Suzuki et al., 2015). PRR is associated with a progressive asymptomatic chronic inflammatory process that comprises axonal degeneration of DP nerves, in which dedifferentiation of SCs, proliferation and expression of repair SC markers is observed. The immunocompetent function of SCs as antigen processing and presenting cells has been associated with immune responses and the recruitment of inflammatory cells to injured peripheral nerves; observations that remain an attractive topic for the understanding of the immunomodulatory functions of

SCs (Meyer zu Hörste et al., 2008; Meyer Zu Horste et al., 2010).

AGING OF SCHWANN CELLS

A reduced expression in SC phenotype markers (S100 and MBP) has been determined at the dentin-pulp interface in aged permanent teeth, suggesting a reduction in the sensory and regenerative capacity of the DP with age (Couve et al., 2018). Furthermore, at the dentin-pulp interface of aged teeth, a smaller number of nerve endings projects through the odontoblast layer, and terminal SCs display a reduced degree of arborization (Figures 2D–F). Age-related changes within the glial network of the DP are related to the diminished regenerative capacity observed for peripheral sensory nerves with age (Verdú et al., 2000; Painter et al., 2014). It has been suggested that the impairment of regenerative capacity associated to the aging progress derives from reduced SC plasticity related to myelin debris clearance (Painter et al., 2014; Painter, 2017). Dedifferentiation of SCs following peripheral nerve injury tends to be delayed with age in correspondence with a delayed onset of key regulatory factor signaling, like c-jun expression (Chen et al., 2017). During the reprogramming process of SCs within injured peripheral nerves, a downregulation of myelin protein expression (e.g., MBP), is accompanied by an upregulation of the transcription factor c-jun, the low affinity neurotrophin receptor (p75NTR) and GFAP (Arthur-Farraj et al., 2012). However, in the DP of teeth from aged individuals, a reduced expression of p75NTR suggests a limited defense and regenerative capacity of SCs (Couve et al., 2018).

CONCLUSION

The evolution of vertebrate teeth produced an increasingly complex neuronal and glial network within the DP to protect the longer lasting teeth. Specifically, SCs form a prominent network at the coronal dentin-pulp interface in human teeth, playing a crucial role in the support and maintenance of DP nerves. SCs, nerve endings and immune cells create a multicellular barrier at the dentin-pulp interface sensing and responding to environmental changes and threats. The characterization of terminal SC plasticity contributes to our growing understanding of the central roles of these versatile cells within the DP scenario.

AUTHOR CONTRIBUTIONS

EC wrote the manuscript with OS.

ACKNOWLEDGMENTS

This study was supported by Fondecyt Grant nos. 1141281 (EC) and 1171228 (OS). The Centro Interdisciplinario de Neurociencias de Valparaíso (CINV) is a Millennium Institute (P09-022-F) supported by the Millennium Scientific Initiative of the Ministry of Economy, Development and Tourism (Chile).



Contents lists available at ScienceDirect

BBA - Biomembranes

journal homepage: www.elsevier.com/locate/bbamem

Review

Role of astrocyte connexin hemichannels in cortical spreading depression

Maximiliano Rovegno^a, Juan C. Sáez^{b,c,*}^a Departamento de Medicina Intensiva, Facultad de Medicina, Pontificia Universidad Católica de Chile, Santiago, Chile^b Departamento de Fisiología, Facultad de Biología, Pontificia Universidad Católica de Chile, Santiago, Chile^c Instituto Milenio, Centro Interdisciplinario de Neurociencias de Valparaíso, Universidad de Valparaíso, Valparaíso, Chile

ARTICLE INFO

Keywords:

Connexins
Hemichannels
Glial
Brain injuries
Spreading depression

ABSTRACT

Cortical spreading depression (CSD) is an intriguing phenomenon consisting of massive slow brain depolarizations that affects neurons and glial cells. It has been recognized since 1944, but its pathogenesis has only been uncovered during the last decade. Acute brain injuries can be further complicated by CSD in > 50% of severe cases. This phenomenon is repetitive and produces a metabolic overload that increments secondary damage. Propagation of CSD is known to be linked to excitotoxicity, but the mechanisms associated with its initiation remain less understood. It has been shown that CSD can be initiated by increases in extracellular $[K^+]_e$ ($[K^+]_e$), and animal models use high $[K^+]_e$ to promote CSD. Connexin hemichannel activity increases due to high $[K^+]_e$ and low extracellular $[Ca^{2+}]_e$, conditions that occur after brain injury. Moreover, glial cell gap junction channels are fundamental in controlling extracellular medium composition, particularly in maintaining normal extracellular glutamate and K^+ concentrations through “spatial buffering”. However, the role of astrocytic gap junctions under tissue stress can change to damage spread in the acute damage zone whereas the reduced communication in adjacent zone would reduce cell death propagation. Here, we review the main findings associated with CSD, and discuss the possible involvement of astrocytic connexin-based channels in secondary damage propagation. This article is part of a Special Issue entitled: Gap Junction Proteins edited by Jean Claude Herve.

1. Introduction

Acute brain injuries, including stroke, subarachnoid hemorrhage (SAH), hypoxic encephalopathy after cardiac arrest (HECA) and traumatic brain injury (TBI) are prevalent diseases [1]. They constitute a heterogeneous group of diseases, but exhibit several common properties, including a similar pathophysiology. They are globally distributed and associated with high mortality and devastating sequelae. Stroke is the second and third leading cause of death and disability worldwide, respectively [2]. TBI is the primary cause of death and permanent brain damage in individuals younger than 45 years old. In United States, 1.7 million cases of TBI occur annually, which result in a burden of about 275,000 hospitalizations, 52,000 deaths and more than USD\$60 billion in costs [3,4]. Hypoxic encephalopathy occurs in > 80% of survivors of cardiac arrests [5]. There are approximately 365,000 treated cardiac arrests annually in the United States, both out of and in hospital settings [6,7]. SAH is the least prevalent disease of this group and affects 30,000 patients per year in the United States [8]. However, approximately 20% of deaths from SAH occur suddenly, resulting in a significant bias due to under-diagnosis [9].

Regardless of etiology, acute brain injuries are characterized by one or more primary damage zones at injury foci, which propagate to neighboring parenchyma, and are initially not compromised by ischemia, inflammation, oxidative stress, excitotoxicity or cellular tumefaction [10,11]. To date, there is only a specific treatment for ischemic stroke, namely, thrombolysis-based therapy. However, < 5% of candidate patients receive thrombolysis [12], mainly because of a substantial delay in arriving to the emergency room. Unfortunately, no specific treatment exists for the remaining acute brain injuries, and all neuroprotective trials have failed in the previous two decades [1,13]. Thus, the mortality rate associated with severe cases remains high at 25%, 30%, 35% and 50% for stroke, SAH, TBI and HECA [14–17], respectively, despite the full support management provided in critical care.

Patients with acute brain injuries in critical care are often clinically and physiologically monitored, which include the evaluation of variables such as arterial and intracranial pressure, electroencephalographic recordings and brain images with transcranial Doppler ultrasonography, computed scanner or magnetic resonance, with variations depending on the specific disease [18,19]. Stroke patients may be

* Corresponding author at: Departamento de Fisiología, Facultad de Biología, Pontificia Universidad Católica de Chile, Santiago, Chile.
E-mail address: jsaez@bio.puc.cl (J.C. Sáez).

<http://dx.doi.org/10.1016/j.bbamem.2017.08.014>

Received 24 February 2017; Received in revised form 8 August 2017; Accepted 23 August 2017
Available online 31 August 2017

0005-2736/ © 2017 Elsevier B.V. All rights reserved.

There is a huge gap between preclinical and clinical trials, in terms of translation into an effective drug or action. There are several reasons for this discrepancy. They come from difference in the type of animal used, the model of brain injury, the time between damage and therapy, and the heterogeneity of diseases studied or treated, among others. In addition, there is another hidden possibility: our limited knowledge of concomitant phenomena occurring after injury. CSDs can complicate the evolution of acute brain injuries, which could explain, at least in part, the differences between preclinical and clinical results. Understand its initiation and propagation is critical to design effective neuroprotective therapy. On the other hand, Cx HCs are responsible of damage propagation in acute conditions such as inflammation, oxidative stress, hypoxia or ischemia. A possible candidate is an acute increase of Cx HC activity in CSD generation (Fig. 2).

Transparency document

The <http://dx.doi.org/10.1016/j.bbame.2017.08.014> associated with this article can be found, in online version.

Acknowledgments

This work was partially funded by grant Inicio 2016 of Vicerrectoría de Investigación, Pontificia Universidad Católica de Chile (to M.R.) and grant N° 1150291 (to JCS), and P09-022-F from Iniciativa Científica Milenio (ICM)-ECONOMIA, Chile (to JCS).

References

- [1] N. Stocchetti, F.S. Taccone, G. Citerio, P.E. Pope, P.D. Le Roux, M. Oddo, K.H. Polhemus, R.D. Stevens, W. Boman, A.I. Maas, G. Meyfroidt, M.J. Bell, R. Silbergeld, P.M. Vespa, A.J. Paden, R. Holbrook, S. Tiberman, E.R. Zanier, T. Valenzuela, J. Wenden, D.K. Menon, J.L. Vincent, Neuroprotection in acute brain injury: an up-to-date review, *Crit. Care* 19 (2015) 186.
- [2] G.J. Hanley, The global and regional burden of stroke, *Lancet. Glob. Heal.* 1 (2013) e239–40.
- [3] J. Santopietro, J.A. Yoonessi, J.P. Niemeier, J.K. White, C.M. Coughlin, Traumatic brain injury and behavioral health: the state of treatment and policy, *N.C. Med. J.* 76 (2015) 96–100.
- [4] J.A. Langlois, W. Rutland-Brown, M.M. Wald, The epidemiology and impact of traumatic brain injury: a brief overview, *J. Head Trauma Rehabil.* 21 (2006) 375–378.
- [5] C. Mead, M. Holzer, Brain function after resuscitation from cardiac arrest, *Curr. Opin. Crit. Care* 10 (2004) 213–217.
- [6] R.M. Merchant, L. Yang, L.B. Becker, R.A. Berg, V. Nadkarni, G. Nichol, R.G. Carr, N. Mitta, S.M. Bradley, B.S. Ahluwalia, P.W. Gronowald, American Heart Association Get With The Guidelines-Resuscitation Investigators, Incidence of treated cardiac arrest in hospitalized patients in the United States, *Crit. Care Med.* 39 (2011) 2401–2406.
- [7] T.D. Rex, M.S. Eisenberg, G. Sinibaldi, R.D. White, Incidence of EMS-treated out-of-hospital cardiac arrest in the United States, *Resuscitation* 63 (2004) 17–24.
- [8] B.E. Zacharia, Z.L. Hickman, B.T. Gombel, P. Deltom, I. Kotchetov, A.F. Ducruet, E.S. Connolly, Epidemiology of a nontraumatic subarachnoid hemorrhage, *Neurosurg. Clin. N. Am.* 21 (2010) 221–233.
- [9] M. Kojia, J. Kaprio, Controversies in epidemiology of intracranial aneurysms and SAH, *Nat. Rev. Neurol.* 12 (2016) 50–55.
- [10] A. Kuntz, U. Dirnagl, P. Menzies, Acute pathophysiological processes after ischaemic and traumatic brain injury, *Best Pract. Res. Clin. Anaesthesiol.* 24 (2010) 495–509.
- [11] M. Rovegna, P.A. Soto, J.C. Soto, R. von Bormann, Biological mechanisms involved in the spread of traumatic brain damage, *Med. Int.* 36 (2012) 37–44.
- [12] R. Mikulic, P. Kadlecová, A. Odolcovská, A. Kolářová, M. Benčan, V. Štegl, I. Čížka, K. Fiksová, J. Křivá, V. Domato, A. Vilianová, D. Játun, Y. Kroupí, N. Ahmed, Factors influencing in-hospital delay in treatment with intravenous thrombolysis, *Stroke* 43 (2012) 1578–1583.
- [13] K.K. Jain, Neuroprotection in traumatic brain injury, *Drug Discov. Today* 13 (2008) 1082–1089.
- [14] V.L. Feigin, R.V. Krishnamurthi, P. Parmar, B. Norving, G.A. Mensah, D.A. Bennett, S. Barker-Collo, A.E. Mens, R.L. Sacco, T. Truelsen, S. Davis, J.D. Pandian, M. Naghavi, M.H. Forouzanfar, G. Nguyen, C.O. Johnson, T. Vos, A. Mente, C.J. Murray, G.A. Roth, GBD 2013 Writing Group, GBD 2013 Stroke Panel Experts Group, Update on the global burden of ischemic and hemorrhagic stroke in 1990–2013: the GBD 2013 study, *Neuroepidemiology* 45 (2015) 161–176.
- [15] T.K. Mulholland, A.J. Molloy, N. Hall, D.R. Yates, R. Goldacre, M. Senade, A. Chelton, M.J. Goldacre, The falling rate of hospital admission, case fatality, and population-based mortality for subarachnoid hemorrhage in England, 1990–2010, *J. Neurosurg.* (2016) 1–7.
- [16] N. Nilsson, J. Wetterberg, T. Cronberg, D. Erlinge, Y. Gueche, C. Hassager, J. Hom, J. Hvidt, J. Kjaergaard, M. Kuiper, T. Pellis, P. Stammet, M. Waeber, M.P. Wais, A. Åsman, N. Al-Salmi, S. Boogaard, J. Bro-Jørgensen, I. Brunetti, J.F. Hugue, C.D. Hingston, N.P. Juffermans, M. Koopmans, L. Køber, J. Langergren, G. Lilja, J.F. Möller, M. Rundgren, C. Rylander, O. Seid, C. Werer, P. Winkel, H. Friberg, Targeted temperature management at 33°C versus 36°C after cardiac arrest, *N. Engl. J. Med.* 369 (2013) 2197–2206.
- [17] H.C. Paul, O. Bouamra, M. Woodford, A.T. King, D.W. Yates, F.E. Lecky, Trends in head injury outcome from 1989 to 2003 and the effect of neurosurgical care: an observational study, *Lancet* 366 (2005) 1538–1544.
- [18] N. Stocchetti, A.I. Maas, Traumatic intracranial hypotension, *N. Engl. J. Med.* 370 (2014) 2121–2130.
- [19] P. Le Roux, D.K. Menon, G. Citerio, P. Vespa, M.K. Bader, G. Brophy, M.N. Diringer, N. Stocchetti, W. Videtta, R. Ammonia, N. Badjatia, J. Bodd, R. Chennu, S. Choi, J. Claassen, M. Czornyj, M. De Georgia, A. Figini, J. Figini, R. Hillenkamp, D. Horowitz, P. Hutchinson, M. Kumar, M. McNeill, C. Miller, A. Nadeau, M. Oddo, D.W. Olson, K. O'Phelan, J.J. Povungu, C. Pappo, R. Riller, C. Robertson, M. Schmidt, F. Taccone, The international multidisciplinary consensus conference on multimodal monitoring in neurocritical care: a list of recommendations and additional conclusions: a statement for healthcare professionals from the neurocritical care society and the European Neurocrit. Care 21 (2014) 282–296.
- [20] A. Bastamante, T. Garcia-Bernardo, N. Rodriguez, V. Lombard, M. Ribó, C. Molina, J. Montaner, Ischemic stroke outcome: a review of the influence of post-stroke complications within the different scenarios of stroke care, *Eur. J. Intern. Med.* 29 (2016) 9–21.
- [21] C.D. Baggott, B. Asgaard-Klein, Cerebral vasospasm, *Neurosurg. Clin. N. Am.* 25 (2014) 497–528.
- [22] J.A. Hartings, A.J. Strong, M. Fabricius, A. Manning, R. Bhatia, J.P. Dwyer, A.T. Mason, F.C. Tortella, M.R. Bullock, Spreading depolarizations and late secondary insults after traumatic brain injury, *J. Neurotrauma* 26 (2009) 1857–1866.
- [23] J.A. Hartings, M.R. Bullock, D.O. Okonkwo, L.S. Murry, G.D. Murry, M. Fabricius, A.I. Maas, J. Weitzel, O. Sakowitz, B. Mathern, B. Rosenbush, H. Ilanguma, J.P. Dwyer, A.M. Purcell, L.A. Shetter, C. Pahl, A.J. Strong, Spreading depolarizations and outcome after traumatic brain injury: a prospective observational study, *Lancet Neurol.* 10 (2011) 1058–1064.
- [24] J.P. Dwyer, The role of spreading depression, spreading depolarization and spreading ischemia in neurological disease, *Nat. Med.* 17 (2011) 430–447.
- [25] A.A. Leão, Spreading depression of activity in the cerebral cortex, *J. Physiol.* (1944).
- [26] S. Canale, I. Makarova, L. López-Aguado, C. Largo, J.M. Baro, O. Herreras, Longitudinal depolarization gradients along the somatodendritic axis of CA1 pyramidal cells: a novel feature of spreading depression, *J. Neurophysiol.* 94 (2005) 943–951.
- [27] R.P. Kraig, C. Nicholson, Extracellular ionic variations during spreading depression, *Neuroscience* 3 (1978) 1045–1059.
- [28] T. Takano, G.F. Tian, W. Peng, N. Lou, D. Lovatt, A.J. Hansen, K.A. Kierulff, M. Nedergaard, Cortical spreading depression causes and coincides with tissue hypoxia, *Nat. Neurosci.* 10 (2007) 754–762.
- [29] G.G. Somjen, Mechanisms of spreading depression and hypoxic spreading depression-like depolarization, *Physiol. Rev.* 81 (2001) 1065–1096.
- [30] D. Pietrobon, M.A. Moskowitz, Cause and consequence in the wake of cortical spreading depression and spreading depolarizations, *Nat. Rev. Neurosci.* 15 (2014) 379–393.
- [31] S.E. Hopwood, M.C. Packin, E.L. Rizzini, M.G. Bostville, A.J. Strong, Transient changes in cortical glucose and lactate levels associated with post-ischemic depolarizations, studied with rapid-sampling microdialysis, *J. Cereb. Blood Flow Metab.* 25 (2005) 391–401.
- [32] L. von Baumgarten, R. Tschöhl, S. Thal, T. Back, N. Hossfeld, Role of cortical spreading depolarizations for secondary brain damage after traumatic brain injury in mice, *J. Cereb. Blood Flow Metab.* 28 (2008) 1253–1260.
- [33] D. Resorcin, A. Manning, P. Hühner, R. Bhatia, M. Fabricius, C. Tollie, C. Pahl, M. Ervine, A.J. Strong, M.G. Bostville, Dynamic metabolic response to multiple spreading depolarizations in patients with acute brain injury: an online microdialysis study, *J. Cereb. Blood Flow Metab.* 30 (2010) 1343–1359.
- [34] P.C. Told-Hansen, Review: history of migraine with aura and cortical spreading depression from 1941 and onwards, *Cephalalgia* 30 (2010) 780–792.
- [35] K.S. Lashley, Patterns of cerebral integration indicated by the symptoms of migraine, *Arch. Neurol. Psychiatr.* 46 (1941) 331.
- [36] G. Menzies, C.K. Tong, M. Chesser, Extracellular pH changes and accompanying cation shifts during ouabain-induced spreading depression, *J. Neurophysiol.* 83 (2000) 1338–1345.
- [37] A.M. van den Maagdenberg, D. Pietrobon, T. Pizzorosso, S. Kaja, L.A. Bove, T. Coats, R.C. van de Ven, A. Tottem, J. van der Kaai, J.J. Plant, R.R. Frants, M.D. Ferrari, A. Cacciatore, A knock-in migraine mouse model with increased susceptibility to cortical spreading depression, *Neuron* 41 (2004) 701–710.
- [38] L.G. Wu, R.E. Wootenbrook, J.G. Boon, W.A. Catterall, B. Salzman, Calcium channel types with distinct postsynaptic localization couple differentially to transmitter release in single calyx-type synapses, *J. Neurosci.* 19 (1999) 726–736.
- [39] S.J. Caldwell, C. Wang, C.F. Fletcher, N.A. Jenkins, N.G. Copeland, D.A. Hooford, Excitatory but not inhibitory synaptic transmission is reduced in lethargic (Ca_v2.1^{0/0}) and tottering (Ca_v2.1^{+/lat}) mouse thalamus, *J. Neurophysiol.* 81 (1999) 2066–2074.
- [40] A. Tottem, T. Pullin, S. Pagnani, S. Lavietto, J. Strassman, C. Fletcher, D. Pietrobon, Familial hemiplegic migraine mutations increase Ca_v2+ influx



Contents lists available at ScienceDirect

Data in Brief

journal homepage: www.elsevier.com/locate/dib

Data Article

Experimental and theoretical structural/spectroscopical correlation of enterobactin and catecholamide

M. Moreno^{b,*}, A. Zacarias^{a,*}, L. Velasquez^{c,h}, G. Gonzalez^{d,e},
M. Alegría-Arcos^{f,g}, F. Gonzalez-Nilo^f, E.K.U. Gross^a^a Max Planck Institute of Microstructure Physics, Weinberg 2, D06120 Halle, Germany and ETSF.^b University of the Basque Country, Barrio Sarriena, s/n, 48940 Leioa, Bizkaia, Spain^c Universidad Andres Bello, Facultad de Medicina, Center for Integrative Medicine and Innovative Science, Echaurren 183, Santiago, Chile^d Center for Development of Nanoscience and Nanotechnology, CEDENNA, Casilla 653, Santiago, Chile^e Universidad de Chile, Facultad de Ciencias, Departamento de Química, Laboratorio de Síntesis Inorgánica y electroquímica, Las Palmeras 3425, Nuñoa, Santiago, Chile^f Universidad Andres Bello, Facultad de Ciencias Biológicas, Center for Bioinformatic and Integrative Biology, Av Republica 239, Santiago, Chile^g Centro Interdisciplinario de Neurociencias de Valparaíso (CINV), Facultad de Ciencias, Universidad de Valparaíso, Valparaíso, Chile^h Facultad Ciencias de la Salud, Universidad SEK, Chile, Fernando Manterola 0789, Providencia, Santiago

ARTICLE INFO

Article history:

Received 23 February 2018

Received in revised form

9 May 2018

Accepted 24 August 2018

Available online 29 August 2018

Keywords:

Catecholate FeEnterobactin

FTIR

DFT

MD

ABSTRACT

Here we report the IR spectra of FeEnterobactin in catecholate conformations ($[\text{CatFeEB}]^{3-}$) obtained by DFT calculations using PBE/QZVP and their correlation it with its experimental counterpart $[\text{SalH}_3\text{FeEB}]^0$. Fragments of FeEnterobactin and Enterobactin (H_6EB) are elucidated from their MALDI-TOF mass spectrometry, and the dependence of the frontier orbitals (HOMO and LUMO) with the catecholamide dihedral angles of H_6EB is reported. The frequency distribution of catecholamide dihedral angle of H_6EB was carried-out using molecular dynamics (MD). The data presented enriches the understanding of $[\text{CatFeEB}]^{3-}$ and H_6EB frequency distribution and reactivity.

© 2018 Published by Elsevier Inc. This is an open access article under the CC BY license (<http://creativecommons.org/licenses/by/4.0/>).

DOI of original article: <https://doi.org/10.1016/j.saa.2018.02.060>

* Corresponding authors.

E-mail addresses: mmoreno043@ikasle.ehu.eus (M. Moreno), zacarias@mpi-halle.mpg (A. Zacarias).<https://doi.org/10.1016/j.dib.2018.08.114>2352-3409/© 2018 Published by Elsevier Inc. This is an open access article under the CC BY license (<http://creativecommons.org/licenses/by/4.0/>).

Acknowledgments

We thank next funding sources; Lamellar Nanostructure and Bio Nanomedicine groups of the Center for the Development of Nanoscience and Nanotechnology (CEDENNA) Chile, and the Experimental II Department of the Max Planck Institute for Microstructure Physics in 2011.

ACT-1107 Project titled “Integration of Structural Biology to the development of Bionanotechnology” funded by CONICYT, Chile. FGN acknowledge the support of FONDECYT Grant 1170733 and MAA is funded by CONICYT PCHA/Doctorado Nacional 2017-21172039 fellowship. The Centro Interdisciplinario de Neurociencia de Valparaíso (CINV) is a Millennium Institute supported by the Millennium Scientific Initiative of the Ministerio de Economía, Fomento y Turismo.

We also thank the Computer facilities of the MPI Halle and the CBIB of Universidad Andres Bello, and Dr. Andrea Porzel from Leibniz Institute of Plant Biochemistry for help with MALDI-TOF MS interpretation.

Transparency document. Supporting information

Transparency data associated with this article can be found in the online version at <https://doi.org/10.1016/j.dib.2018.08.114>.

References

- [1] M. Moreno, A. Zacarias, A. Porzel, A. Velasquez, G. Gonzalez, M. Alegría-Arcos, F. Gonzalez-Nilo, E.K.U. Gross, IR and NMR spectroscopic correlation of enterobactin by DFT, *Spectrochim. Acta A* 18 (2018) 264–277.
- [2] W.L. Jorgensen, J. Chandrasekhar, J.D. Madura, R.W. Impey, M.L. Klein, Development of an improved four-site water model for biomolecular simulations: tip4p-ew, *J. Chem. Phys.* 79 (1983) 926–935.
- [3] W.L. Jorgensen, D.S. Maxwell, J. Tirado-Rives, Development and testing of the OPLS all-atom force field on conformational energetics and properties of organic liquids, *J. Am. Chem. Soc.* 118 (1996) 11225–11236.
- [4] Desmond Molecular Dynamics System, Desmond Molecular Dynamics System Version 3.6, D.E. Shaw Research, New York, NY, 2013.
- [5] W. Humphrey, A. Dalke, K. Schulten, VMD: visual molecular dynamics, *J. Mol. Graph.* 14 (1996) 33–38.
- [6] J.P. Perdew, K. Burke, M. Ernzerhof, *Phys. Rev. Lett.* 77 (1996) 3865–3868.
- [7] F. Weigend, R. Ahlrichs, Balanced basis sets of split valence, triple zeta valence and quadruple zeta valence quality for H to Rn: design and assessment of accuracy, *Phys. Chem. Chem. Phys.* 18 (2005) 3297–3305.
- [8] F. Weigend, F. Furche, R. Ahlrichs, Gaussian basis sets of quadruple zeta valence quality for atoms H–Kr, *J. Chem. Phys.* 24 (2003) 12753–12762.
- [9] J. Frisch, et al., Gaussian 09, revision B.01, Gaussian Inc., Wallingford CT, 2010.
- [10] V.L. Pecoraro, W.R. Harris, G.B. Wong, C.J. Carrano, K.N. Raymond, Coordination chemistry of microbial iron transport compounds. 23. Fourier transform infrared spectroscopy of ferric catechylamide analogues of enterobactin, *J. Am. Chem. Soc.* 14 (1983) 4623–4633.
- [11] W.R. Harris, C.J. Carrano, S.R. Cooper, S.R. Sofen, A.E. Avdeef, J.V. McArdle, K.N. Raymond, Coordination chemistry of microbial iron transport compounds. 19. Stability constants and electrochemical behavior of ferric enterobactin and model complexes, *J. Am. Chem. Soc.* 20 (1979) 6097–6104.
- [12] M.E. Wieser, N. Holden, T.B. Coplen, J.K. Böhlke, M. Berglund, W.A. Brand, P. De Bièvre, M. Gröning, R.D. Loss, J. Meija, T. Hirata, Atomic weights of the elements 2011 (IUPAC Technical Report), *Pure Appl. Chem.* 5 (2013) 1047–1078.
- [13] D. Vonlanthen, A. Mishchenko, M. Elbing, M. Neuburger, T. Wandlowski, M. Mayor, Chemically controlled conductivity: torsion-angle dependence in a single-molecule biphenyldithiol junction, *Angew. Chem. Int. Ed.* 48 (2009) 8886–8890.
- [14] A. Mishchenko, L.A. Zotti, D. Vonlanthen, M. Bürkle, F. Pauly, J.C. Cuevas, M. Mayor, T. Wandlowski, Single-molecule junctions based on nitrile-terminated biphenyls: a promising new anchoring group. Single-molecule junctions based on nitrile-terminated biphenyls: a promising new anchoring group, *J. Am. Chem. Soc.* 133 (2010) 1184–1187.
- [15] T.M. Hoette, R.J. Abergel, J. Xu, R.K. Strong, K.N. Raymond, The role of electrostatics in siderophore recognition by the immunoprotein siderocalin 1, *J. Am. Chem. Soc.* 51 (2008) 17584–17592.
- [16] L. Patiny, A. Borel, ChemCalc: a building block for tomorrow's chemical infrastructure, *J. Chem. Inf. Model.* 53 (2013) 1223–1228.



Editorial

Involvement of Connexin Hemichannels in the Inflammatory Response of Chronic Diseases

Juan C. Sáez ^{1,2,*} and Colin Green ^{3,*}

¹ Departamento de Fisiología, Facultad de Ciencias Biológicas, Pontificia Universidad Católica de Chile, Alameda 340, 8331150 Santiago, Chile

² Instituto de Neurociencias, Centro Interdisciplinario de Neurociencias de Valparaíso, Universidad de Valparaíso, 2381850 Valparaíso, Chile

³ Department of Ophthalmology, New Zealand National Eye Centre, University of Auckland, Auckland 1142, New Zealand

* Correspondence: jsaez@bio.puc.cl (J.C.S.); c.green@auckland.ac.nz (C.G.)

Received: 3 August 2018; Accepted: 20 August 2018; Published: 21 August 2018



Over the last decade it has become evident that under normal conditions connexin hemichannels are either not expressed (e.g., skeletal muscle) or are expressed in very low numbers with low open probability in various mammalian tissues (e.g., liver and central nervous system (CNS)). However, both the number and activity of these non-selective channels are drastically increased in different cell types under pathological conditions. Since the inflammatory response is a consequence and/or the cause of most diseases, connexin hemichannels have been implicated as a common factor in numerous chronic pathological indications (including muscular dystrophy, amyotrophic lateral sclerosis, ongoing effects of CNS trauma, stroke or ischemia, glaucoma, diabetic retinopathy and macular degeneration, Alzheimer's and Parkinson's disease, epilepsy, chronic pain, brain and other tumors, and infectious diseases). However, further work is needed to fully understand hemichannel regulatory mechanisms and their involvement in the outcome of the different disease conditions.

Currently, the molecular target of different clinically available anti-inflammatory agents block one (or at most two) intracellular inflammatory signaling pathways, leaving several others active, and which persist despite chronic treatment, and alter the phenotype of inflamed cells. The phenotypic changes explain why cells stop performing their normal functions and subsequently lead to organ dysfunction. Consequently, the chronic use of many available anti-inflammatory compounds can result in kidney, liver, or heart dysfunction, amongst other complications. Connexin hemichannel regulation offers an alternative approach. Connexin hemichannels have been shown to be permeable to calcium ions and ATP which activate intracellular inflammatory signaling pathways. Therefore, selective inhibitors of connexin hemichannels are expected to be useful for the long-term treatment of inflammatory disease. These agents may provide an entire new generation of anti-inflammatory pharmaceuticals. Indeed, it is important to emphasize the evidence for connexin hemichannels as new molecular targets in order to prevent the activation of most intracellular inflammatory pathways.

This issue of the *International Journal of Molecular Sciences* focuses on the involvement of connexin hemichannels in the inflammatory response, emphasising chronic pathological conditions. It brings together substantial evidence for connexin hemichannel-mediated tissue dysfunction associated with a diverse range of chronic disease indications, thus supporting the translation of hemichannel regulation into clinical application.

For instance, Valdebenito and co-workers [1] have provided novel information revealing the importance of a cell–cell communication pathways mediated by connexin-based channels in cancer, including gap junction channels, hemichannels, and tunneling nanotubes. Artificial intelligence and machine learning are proposed as new approaches that could provide insights into the intercellular transfer of cell signals. They also proposed that the identification of these cell–cell communication



Connexin 43 Hemichannel Activity Promoted by Pro-Inflammatory Cytokines and High Glucose Alters Endothelial Cell Function

Juan C. Sáez^{1,2}, Susana Contreras-Duarte^{1,3}, Gonzalo I. Gómez⁴, Valeria C. Labra⁴, Cristian A. Santibañez⁴, Rosario Gajardo-Gómez⁴, Beatriz C. Avendaño⁴, Esteban F. Díaz⁴, Trinidad D. Montero⁴, Victoria Velarde⁴ and Juan A. Orellana^{4*}

¹Departamento de Fisiología, Pontificia Universidad Católica de Chile, Santiago de Chile, Chile, ²Instituto de Neurociencias, Centro Interdisciplinario de Neurociencias de Valparaíso, Universidad de Valparaíso, Valparaíso, Chile, ³Departamento de Ginecología y Obstetricia, Escuela de Medicina, Facultad de Medicina, Pontificia Universidad Católica de Chile, Santiago, Chile, ⁴Departamento de Neurología, Escuela de Medicina and Centro Interdisciplinario de Neurociencias, Facultad de Medicina, Pontificia Universidad Católica de Chile, Santiago, Chile

OPEN ACCESS

Edited by:

Robert Murray Hamilton,
Hospital for Sick Children, Canada

Reviewed by:

Bo-Zong Shao,
Second Military Medical University,
China

Nicolas Riteau,
UMR7355 Immunologie et
neurogénétique expérimentales et
moléculaires (INEM), France
Alex Rafacho,
Universidade Federal de Santa
Catarina, Brazil

*Correspondence:

Juan A. Orellana
jaorella@uc.cl

Specialty section:

This article was submitted to
Inflammation,
a section of the journal
Frontiers in Immunology

Received: 26 February 2018

Accepted: 31 July 2018

Published: 15 August 2018

Citation:

Sáez JC, Contreras-Duarte S,
Gómez GI, Labra VC, Santibañez CA,
Gajardo-Gómez R, Avendaño BC,
Díaz EF, Montero TD, Velarde V
and Orellana JA (2018)
Connexin 43 Hemichannel Activity
Promoted by Pro-Inflammatory
Cytokines and High Glucose Alters
Endothelial Cell Function.
Front. Immunol. 9:1899.
doi: 10.3389/fimmu.2018.01899

The present work was done to elucidate whether hemichannels of a cell line derived from endothelial cells are affected by pro-inflammatory conditions (high glucose and IL-1 β /TNF- α) known to lead to vascular dysfunction. We used EAhy 926 cells treated with high glucose and IL-1 β /TNF- α . The hemichannel activity was evaluated with the dye uptake method and was abrogated with selective inhibitors or knocking down of hemichannel protein subunits with siRNA. Western blot analysis, cell surface biotinylation, and confocal microscopy were used to evaluate total and plasma membrane amounts of specific proteins and their cellular distribution, respectively. Changes in intracellular Ca²⁺ and nitric oxide (NO) signals were estimated by measuring FURA-2 and DAF-FM probes, respectively. High glucose concentration was found to elevate dye uptake, a response that was enhanced by IL-1 β /TNF- α . High glucose plus IL-1 β /TNF- α -induced dye uptake was abrogated by connexin 43 (Cx43) but not pannexin1 knockdown. Furthermore, Cx43 hemichannel activity was associated with enhanced ATP release and activation of p38 MAPK, inducible NO synthase, COX₂, PGE₂ receptor EP₁, and P2X₇/P2Y₁ receptors. Inhibition of the above pathways prevented completely the increase in Cx43 hemichannel activity of cells treated high glucose and IL-1 β /TNF- α . Both synthetic and endogenous cannabinoids (CBs) also prevented the increment in Cx43 hemichannel opening, as well as the subsequent generation and release of ATP and NO induced by pro-inflammatory conditions. The counteracting action of CBs also was extended to other endothelial alterations evoked by IL-1 β /TNF- α and high glucose, including increased ATP-dependent Ca²⁺ dynamics and insulin-induced NO production. Finally, inhibition of Cx43 hemichannels also prevented the ATP release from endothelial cells treated with IL-1 β /TNF- α and high glucose. Therefore, we propose that reduction of hemichannel activity could represent a strategy against the activation of deleterious pathways that lead to endothelial dysfunction and possibly cell damage evoked by high glucose and pro-inflammatory conditions during cardiovascular diseases.

Keywords: connexins, endothelium, inflammation, cytokines, gap junctions

novel CB agonists that could preserve their positive role without having side effects in general physiology.

ETHICS STATEMENT

This study was carried out in accordance with the recommendations of the Animal Care Guidelines of the Research Ethic Committee from the Pontificia Universidad Católica de Chile. The protocol was approved by Research Ethic Committee from the Pontificia Universidad Católica de Chile.

AUTHOR CONTRIBUTIONS

Conceived, performed, and analyzed the experiments: JAO, JCS, VV, SC-D, GG, VL, CS, RG-G, BA, ED, and TM. Wrote and edited the manuscript: JAO, JCS, and VV. All authors read and approved the final manuscript.

ACKNOWLEDGMENTS

CONICYT, PIA, FONDECYT, ICM, and Pontificia Universidad Católica de Chile.

FUNDING

This work was supported by the Fondo Nacional de Desarrollo Científico y Tecnológico (FONDECYT) Grant 1160710 (to JAO), 1150291 (to JCS), the Comisión Nacional de Investigación Científica y Tecnológica (CONICYT) and Programa de Investigación Asociativa (PIA) Grant Anillo de Ciencia y Tecnología ACT1411 (to JAO), P09-022-F from ICM-ECONOMIA, Chile (to JCS).

REFERENCES

- McCarron JG, Lee MD, Wilson C. The endothelium solves problems that endothelial cells do not know exist. *Trends Pharmacol Sci* (2017) 38:322–38. doi:10.1016/j.tips.2017.01.008
- Pober JS, Sessa WC. Inflammation and the blood microvascular system. *Cold Spring Harb Perspect Biol* (2014) 7:a016345. doi:10.1101/cshperspect.a016345
- Vestweber D. How leukocytes cross the vascular endothelium. *Nat Rev Immunol* (2015) 15:692–704. doi:10.1038/nri3908
- Cahill PA, Redmond EM. Vascular endothelium – gatekeeper of vessel health. *Atherosclerosis* (2016) 248:97–109. doi:10.1016/j.atherosclerosis.2016.03.007
- Hansen NW, Hansen AJ, Sams A. The endothelial border to health: mechanistic evidence of the hyperglycemic culprit of inflammatory disease acceleration. *IUBMB Life* (2017) 69:148–61. doi:10.1002/iub.1610
- Meunier C, Wang N, Yi C, Dallerac G, Ezan P, Koulakoff A, et al. Contribution of astroglial Cx43 hemichannels to the modulation of glutamatergic currents by D-serine in the mouse prefrontal cortex. *J Neurosci* (2017) 37:9064–75. doi:10.1523/JNEUROSCI.2204-16.2017
- Bol M, Wang N, De Bock M, Wacquier B, Decrock E, Gadicherla A, et al. At the cross-point of connexins, calcium, and ATP: blocking hemichannels inhibits vasoconstriction of rat small mesenteric arteries. *Cardiovasc Res* (2017) 113:195–206. doi:10.1093/cvr/cvw215
- Orellana JA, Sáez PJ, Cortes-Campos C, Elizondo RJ, Shoji KF, Contreras-Duarte S, et al. Glucose increases intracellular free Ca(2+) in tanyocytes via ATP released through connexin 43 hemichannels. *Glia* (2012) 60:53–68. doi:10.1002/glia.21246
- Sáez JC, Leybaert L. Hunting for connexin hemichannels. *FEBS Lett* (2014) 588:1205–11. doi:10.1016/j.febslet.2014.03.004
- Sáez JC, Berthoud VM, Branes MC, Martínez AD, Beyer EC. Plasma membrane channels formed by connexins: their regulation and functions. *Physiol Rev* (2003) 83:1359–400. doi:10.1152/physrev.00007.2003
- Leybaert L, Lampe PD, Dhein S, Kwak BR, Ferdinandy P, Beyer EC, et al. Connexins in cardiovascular and neurovascular health and disease: pharmacological implications. *Pharmacol Rev* (2017) 69:396–478. doi:10.1124/pr.115.012062
- Kim Y, Davidson JO, Gunn KC, Phillips AR, Green CR, Gunn AJ. Role of hemichannels in CNS inflammation and the inflammasome pathway. *Adv Protein Chem Struct Biol* (2016) 104:1–37. doi:10.1016/bs.apcsb.2015.12.001
- Esposito K, Nappo F, Marfella R, Giugliano G, Giugliano F, Ciotola M, et al. Inflammatory cytokine concentrations are acutely increased by hyperglycemia in humans: role of oxidative stress. *Circulation* (2002) 106:2067–72. doi:10.1161/01.CIR.0000034509.14906.AE
- Stentz FB, Umpierrez GE, Cuervo R, Kitabchi AE. Proinflammatory cytokines, markers of cardiovascular risks, oxidative stress, and lipid peroxidation in patients with hyperglycemic crises. *Diabetes* (2004) 53:2079–86. doi:10.2337/diabetes.53.8.2079
- Ling PR, Mueller C, Smith RJ, Bistrian BR. Hyperglycemia induced by glucose infusion causes hepatic oxidative stress and systemic inflammation, but not STAT3 or MAP kinase activation in liver in rats. *Metabolism* (2003) 52:868–74. doi:10.1016/S0026-0495(03)00057-X
- Li J, Huang M, Shen X. The association of oxidative stress and pro-inflammatory cytokines in diabetic patients with hyperglycemic crisis. *J Diabetes Complications* (2014) 28:662–6. doi:10.1016/j.jdiacomp.2014.06.008
- Urata Y, Yamamoto H, Goto S, Tsushima H, Akazawa S, Yamashita S, et al. Long exposure to high glucose concentration impairs the responsive expression of gamma-glutamylcysteine synthetase by interleukin-1beta and tumor necrosis

SUPPLEMENTARY MATERIAL

The Supplementary Material for this article can be found online at <https://www.frontiersin.org/articles/10.3389/fimmu.2018.01899/full#supplementary-material>.

FIGURE S1 | Etd uptake induced by high glucose and IL-1 β /TNF- α is not related to osmolarity changes, whereas high glucose/IL-1 β /TNF- α plus WIN do not affect connexin 43 (Cx43) distribution in endothelial cells. **(A)** Averaged Etd uptake rate normalized with respect to control condition (dashed line) of EAhy cells treated for 72 h with 5 mM glucose and IL-1 β /TNF- α alone or in combination with 20 or 40 mM sucrose or 20 or 40 mM mannitol. Data were obtained from three independent experiments (see scatter dot plot) with two repeats each one (≥ 35 cells analyzed for each repeat). **(B,C)** Representative fluorescence images depicting Cx43 (green), tubulin (red), and DAPI (blue) immunolabeling of EAhy cells treated for 72 h with 25 mM glucose plus IL-1 β /TNF- α and 5 μ M WIN. Insets: 1.7 \times magnification of the indicated area of panels **(C)**. Calibration bars: white = 35 μ m, yellow = 60 μ m, and green = 25 μ m.

FIGURE S2 | High glucose and IL-1 β /TNF- α increase the activity of connexin 43 hemichannels and nitric oxide production in HUVEC endothelial cells. **(A)** Averaged Etd uptake rate normalized with control condition (dashed line) by HUVEC cells treated for 72 h with 25 mM glucose and IL-1 β /TNF- α alone or in combination with the following blockers: 100 μ M gap26, 100 μ M 10 panx1, 10 μ M WIN or 5 μ M WIN plus 5 μ M SR-141716A (SR1). * $p < 0.05$, IL-1 β /TNF- α and high glucose compared to control; * $p < 0.05$, effect of blockers compared IL-1 β /TNF- α and high glucose. **(B)** Average of DAF fluorescence by HUVEC cells treated for 72 h with 5 mM glucose (control; white bars), 25 mM glucose and IL-1 β /TNF- α (red bars) alone or with different combinations of the following compounds: 5 μ M WIN (WIN), 5 μ M SR-141716A (SR1), 1 μ M insulin or 100 μ M gap26. * $p < 0.05$, IL-1 β /TNF- α and high glucose compared to control; * $p < 0.05$, effect of each compound compared to the effect induced by IL-1 β /TNF- α and high glucose; * $p < 0.05$, effect of each cannabinoid receptor antagonist compared to the effect of the respective cannabinoid; * $p < 0.05$, effect of insulin compared to the respective control (one-way analysis of variance followed by Tukey's *post hoc* test). Data were obtained from three independent experiments (see scatter dot plot) with three repeats each one (≥ 35 cells analyzed for each repeat).



Gating-induced large aqueous volumetric remodeling and aspartate tolerance in the voltage sensor domain of Shaker K⁺ channels

Ignacio Díaz-Franulic^{a,b,c,1}, Vivian González-Pérez^d, Hans Moldenhauer^{a,b}, Nieves Navarro-Quezada^{a,b}, and David Naranjo^{a,1}

^aInstituto de Neurociencia, Facultad de Ciencias, Universidad de Valparaíso, 2360102 Valparaíso, Chile; ^bCentro Interdisciplinario de Neurociencia de Valparaíso, Universidad de Valparaíso, 2360103 Valparaíso, Chile; ^cCenter for Bioinformatics and Integrative Biology, Universidad Andrés Bello, 8370186 Santiago, Chile; and ^dDepartment of Anesthesiology, Washington University School of Medicine, St. Louis, MO 63110

Edited by Richard W. Aldrich, The University of Texas at Austin, Austin, TX, and approved June 26, 2018 (received for review April 25, 2018)

Neurons encode electrical signals with critically tuned voltage-gated ion channels and enzymes. Dedicated voltage sensor domains (VSDs) in these membrane proteins activate coordinately with an unresolved structural change. Such change conveys the transmembrane translocation of four positively charged arginine side chains, the voltage-sensing residues (VSRs; R1–R4). Countercharges and lipid phosphohead groups likely stabilize these VSRs within the low-dielectric core of the protein. However, the role of hydration, a sign-independent charge stabilizer, remains unclear. We replaced all VSRs and their neighboring residues with negatively charged aspartates in a voltage-gated potassium channel. The ensuing mild functional effects indicate that hydration is also important in VSR stabilization. The voltage dependency of the VSR aspartate variants approached the expected arithmetic summation of charges at VSR positions, as if negative and positive side chains faced similar pathways. In contrast, aspartates introduced between R2 and R3 did not affect voltage dependence as if the side chains moved outside the electric field or together with it, undergoing a large displacement and volumetric remodeling. Accordingly, VSR performed osmotic work at both internal and external aqueous interfaces. Individual VSR contributions to volumetric works approached arithmetical additivity but were largely dissimilar. While R1 and R4 displaced small volumes, R2 and R3 volumetric works were massive and vectorially opposed, favoring large aqueous remodeling during VSD activation. These diverse volumetric works are, at least for R2 and R3, not compatible with VSR translocation across a unique stationary charge transfer center. Instead, VSRs may follow separated pathways across a fluctuating low-dielectric septum.

voltage sensor | charge hydration | osmotic work | conformational change | Shaker

Voltage-dependent K⁺ (Kv) ion channels are membrane proteins involved in a myriad of physiological processes exquisitely regulated by membrane potential (1–4). By allowing the permeation of potassium ions, they drive the membrane voltage toward the K⁺ equilibrium potential, modulating cell excitability (5). Assembled as tetramers, each Kv channel subunit has six transmembrane segments (S1–S6), of which S1–S4 constitute the voltage sensor domain (VSD) and S5 and S6, placed at the channel fourfold symmetry axis, form the ion conduction pathway (6). In Shaker Kv channels, voltage sensitivity is mostly due to the electrophoretic transmembrane migration of four arginine residues [voltage-sensing residues (VSRs); R1–R4] placed in VSD's S4 (7–10). The total charge displaced per channel for the native Shaker is 12–13 e₀, while for the R2Q, R3N, and R4Q variants, it is about three-quarters of the total (8, 9). These amounts agreed with the measures of the electrical valence of the voltage dependence of pore opening (Z). Thus, almost all of the charge movement is used to open the ion conduction pore (8). This concept applies to other Kv, Cav, and Nav ion channels also (2, 4, 11).

Because charged particles are energetically disfavored in the low-dielectric membrane environment, electrostatic stabilization of VSR should occur through contacts with negative side chains in the protein core and/or lipid phosphohead groups (12–16). Because these charge stabilization mechanisms are sign-specific, charge reversions in VSR should lead to dramatic alteration of the VSD structure. We performed an aspartate scanning along the S4 region hosting R1–R4 of the Shaker K⁺ channel. Because all aspartate variants displayed moderate functional alterations, sign-independent VSR charge stabilization mechanisms as hydration must exist. Then, VSD activation implies water mobilization between compartments, such that we could expect osmotic work. By challenging the VSD with unilateral and bilateral hyperosmolarity, we found that each VSR contributes in a unique and vectorially different manner to the total osmotic work, perhaps across dissimilar trajectories.

Results

Sign-Independent Gating Charge Stabilization. We performed an aspartate scanning along the N-terminal half of S4 including all VSRs of Shaker (residues 359–371). Fig. 1A and *SI Appendix, Fig. S1* show K⁺-current traces for each aspartate-substituted

Significance

The neuronal action potential is a self-propagating transient depolarization traveling along the neuron membrane. This signal is produced by the coordinated activation of voltage-gated ion channels (VGICs), a family of ion-selective transmembrane proteins activated by depolarization. Sodium and calcium VGICs reinforce the signal, while potassium VGICs terminate it. A conserved voltage sensor domain (VSD) in VGICs responds with an unresolved conformational change driven by the transmembrane electrophoretic displacements of four arginine side chains. We show that those arginine side chains are stabilized by water impregnating the VSD and that, upon activation, displace large and dissimilar aqueous volumes at both protein faces. This charge translocation entails a transporter-like remodeling of water–protein interfaces that should create mechanical spikes accompanying action potentials.

Author contributions: I.D.-F., V.G.-P., H.M., and D.N. designed research; I.D.-F., V.G.-P., H.M., and D.N. performed research; I.D.-F., V.G.-P., H.M., N.N.-Q., and D.N. contributed new reagents/analytic tools; I.D.-F., V.G.-P., and D.N. analyzed data; and I.D.-F. and D.N. wrote the paper.

The authors declare no conflict of interest.

This article is a PNAS Direct Submission.

Published under the PNAS license.

¹To whom correspondence may be addressed. Email: david.naranjo@uv.cl or ignacio.diaz@cinv.cl.

This article contains supporting information online at www.pnas.org/lookup/suppl/doi:10.1073/pnas.1806578115/-DCSupplemental.

compartment in the active VSD. By moving perpendicular to the membrane plane, VSR, mostly R2 and R3, drags inwardly relative to VSRs, the boundaries of the hydrophobic septum (and of the electric field). Such movement could be a rotation along the axis of the inclined α -helical S4 segment (Fig. 5C), with 366 and 367 side chains being dragged inwardly while R2 and R3 move outward, respectively. Then, the charge transfer center behaves as a dynamic structure during VSD activation, in which R2 and R3 sense different molecular landscapes. This conclusion is in line with structural interpretations that compare VSD activation with transporter conformational change (21, 44) but contradicts molecular calculations suggesting stable electric field among different VSD structures (23).

By inward dragging the hydrophobic septum together with S4's outward activation movement, the Kv channel VSD would make a volumetric work that should produce cell swelling. Considering that we underestimate the enlargement, because it considers only sucrose-excluding compartments, in a 5- μ m-radius spherical cell with a density of $\sim 3,000$ Nav, Kv, and Cav channels per $1 \mu\text{m}^2$, an action potential would produce a >1 -Å transient radial cell swelling. This interpretation provides a molecular sustentation for the observed mechanical spikes associated with action potentials (45).

Materials and Methods

Site-Directed Mutagenesis, Channel Expression, and Electrophysiology. All Shaker mutant stems from Shaker B ($\Delta 64$ –6) were generated as before (3, 43).

Limiting Slope and Gating Currents. Limiting slope and gating currents recordings were performed with the patch clamp technique in inside-out configuration with an Axopatch 200B amplifier through a Digidata 1440 interface under control of pClamp 10 (Molecular Devices). For limiting slope recording, the pipette solution had 110 mM potassium methanesulfonate, 2 mM CaCl_2 , and 10 mM Hepes, pH 7.4, with CaCl_2 being replaced by MgCl_2 in the bath solution. Gating currents recording solution contained 100 mM *N*-methyl-D-glucamine, 5 mM EGTA, 2 mM KCl, and 10 mM Hepes, pH 7.4. The two-electrode voltage clamp recording solution contained 100 mM NaCl, 2 mM KCl, 2 mM CaCl_2 , 1 mM MgCl_2 , and 10 mM Hepes-NaOH, pH 7.4. Recordings were performed with an OC-725C amplifier (Warner Instruments) through a PCI-6035 interface (National Instruments) running WinWCP (Strathclyde University). All experiments were at room temperature (22°C to 24°C).

Data Analysis. Analysis was done with Clampfit 10. To compute conductance vs. voltage (G - V) relations, current amplitude measured at the end of the test voltage pulse was divided by the K^+ driving force, assuming a reversal potential of -100 mV. Offline analyses of single-channel activity were as before (3). The On phase of the gating currents was integrated, after correcting for leak, to construct the Q - V relations. The median voltage $V_{0.5}$ was calculated by the trapezoid rule, with a custom-made Excel routine (25). Additional experimental details and analysis are in [SI Appendix, SI Methods](#).

ACKNOWLEDGMENTS. We thank Chris Lingle and Yu Zhou (Washington University) for critical reading of the manuscript and Victoria Prado for *Xenopus* care and oocyte preparation. We also thank Millennium Scientific Initiative P029-022-F. This work was supported by Fondecyt Postdoctoral Grants 3170599 (to I.D.-F.) and 3160321 (to H.M.).

- Islas LD, Sigworth FJ (1999) Voltage sensitivity and gating charge in Shaker and Shab family potassium channels. *J Gen Physiol* 114:723–742.
- Nocelet F, et al. (1996) Effective gating charges per channel in voltage-dependent K^+ and Ca^{2+} channels. *J Gen Physiol* 108:143–155.
- González-Pérez V, Stack K, Boric K, Naranjo D (2010) Reduced voltage sensitivity in a K^+ -channel voltage sensor by electric field remodeling. *Proc Natl Acad Sci USA* 107:5178–5183.
- Ishida IG, Rangel-Yescas GE, Carrasco-Zanini J, Islas LD (2015) Voltage-dependent gating and gating charge measurements in the Kv1.2 potassium channel. *J Gen Physiol* 145:345–358.
- González C, et al. (2012) K^+ channels: Function-structural overview. *Compr Physiol* 2:2087–2149.
- Long SB, Tao X, Campbell EB, MacKinnon R (2007) Atomic structure of a voltage-dependent K^+ channel in a lipid membrane-like environment. *Nature* 450:376–382.
- Yang N, George AL, Jr, Horn R (1996) Molecular basis of charge movement in voltage-gated sodium channels. *Neuron* 16:113–122.
- Seoh SA, Sigg D, Papazian DM, Bezanilla F (1996) Voltage-sensing residues in the S2 and S4 segments of the Shaker K^+ channel. *Neuron* 16:1159–1167.
- Aggarwal SK, MacKinnon R (1996) Contribution of the S4 segment to gating charge in the Shaker K^+ channel. *Neuron* 16:1169–1177.
- Larsson HP, Baker OS, Dhillon DS, Isacoff EY (1996) Transmembrane movement of the shaker K^+ channel S4. *Neuron* 16:387–397.
- Hirschberg B, Rovner A, Lieberman M, Patlak J (1995) Transfer of twelve charges is needed to open skeletal muscle Na^+ channels. *J Gen Physiol* 106:1053–1068.
- Papazian DM, et al. (1995) Electrostatic interactions of S4 voltage sensor in Shaker K^+ channel. *Neuron* 14:1293–1301.
- Tiwari-Woodruff SK, Schulteis CT, Mock AF, Papazian DM (1997) Electrostatic interactions between transmembrane segments mediate folding of Shaker K^+ channel subunits. *Biophys J* 72:1489–1500.
- Xu Y, Ramu Y, Lu Z (2008) Removal of phospho-head groups of membrane lipids immobilizes voltage sensors of K^+ channels. *Nature* 451:826–829.
- Schmidt D, Jiang QX, MacKinnon R (2006) Phospholipids and the origin of cationic gating charges in voltage sensors. *Nature* 444:775–779.
- DeCaen PG, Yarov-Yarovsky V, Sharp EM, Scheuer T, Catterall WA (2009) Sequential formation of ion pairs during activation of a sodium channel voltage sensor. *Proc Natl Acad Sci USA* 106:22498–22503.
- Giollo M, Martin AJ, Walsh I, Ferrari C, Tosatto SC (2014) NeEMO: A method using residue interaction networks to improve prediction of protein stability upon mutation. *BMC Genomics* 15(Suppl 4):S7.
- Barlow DJ, Thornton JM (1983) Ion-pairs in proteins. *J Mol Biol* 168:867–885.
- Almers W (1978) Gating currents and charge movements in excitable membranes. *Rev Physiol Biochem Pharmacol* 82:96–190.
- Naranjo D, Wen H, Brehm P (2015) Zebrafish $\text{CaV}2.1$ calcium channels are tailored for fast synchronous neuromuscular transmission. *Biophys J* 108:578–584.
- Li Q, et al. (2014) Structural mechanism of voltage-dependent gating in an isolated voltage-sensing domain. *Nat Struct Mol Biol* 21:244–252.
- Vargas E, et al. (2012) An emerging consensus on voltage-dependent gating from computational modeling and molecular dynamics simulations. *J Gen Physiol* 140:587–594.
- Souza CS, Amaral C, Treptow W (2014) Electric fingerprint of voltage sensor domains. *Proc Natl Acad Sci USA* 111:17510–17515.
- Armstrong CM, Bezanilla F (1973) Currents related to movement of the gating particles of the sodium channels. *Nature* 242:459–461.
- Chowdhury S, Chanda B (2012) Estimating the voltage-dependent free energy change of ion channels using the median voltage for activation. *J Gen Physiol* 139:3–17.
- Zimmerberg J, Bezanilla F, Parsegian VA (1990) Solute inaccessible aqueous volume changes during opening of the potassium channel of the squid giant axon. *Biophys J* 57:1049–1064.
- Kitaguchi T, Sukhareva M, Swartz KJ (2004) Stabilizing the closed S6 gate in the Shaker Kv channel through modification of a hydrophobic seal. *J Gen Physiol* 124:319–332.
- Jiang X, Bett GC, Li X, Bondarenko VE, Rasmussen RL (2003) C-type inactivation involves a significant decrease in the intracellular aqueous pore volume of Kv1.4 K^+ channels expressed in *Xenopus* oocytes. *J Physiol* 549:683–695.
- Ahern CA, Horn R (2004) Specificity of charge-carrying residues in the voltage sensor of potassium channels. *J Gen Physiol* 123:205–216.
- Hidalgo P, MacKinnon R (1995) Revealing the architecture of a K^+ channel pore through mutant cycles with a peptide inhibitor. *Science* 268:307–310.
- Schreiber G, Fersht AR (1995) Energetics of protein-protein interactions: Analysis of the barnase-barstar interface by single mutations and double mutant cycles. *J Mol Biol* 248:478–486.
- Lee SY, Banerjee A, MacKinnon R (2009) Two separate interfaces between the voltage sensor and pore are required for the function of voltage-dependent K^+ channels. *PLoS Biol* 7:e47.
- Lu Z, Klem AM, Ramu Y (2002) Coupling between voltage sensors and activation gate in voltage-gated K^+ channels. *J Gen Physiol* 120:663–676.
- Chakrapani S, Cuellar LG, Cortes DM, Perozo E (2008) Structural dynamics of an isolated voltage-sensor domain in a lipid bilayer. *Structure* 16:398–409.
- Krepkiy D, et al. (2009) Structure and hydration of membranes embedded with voltage-sensing domains. *Nature* 462:473–479.
- Lacroix JJ, Campos FV, Frezza L, Bezanilla F (2013) Molecular bases for the asynchronous activation of sodium and potassium channels required for nerve impulse generation. *Neuron* 79:651–657.
- Tao X, Lee A, Umapathat W, Dougherty DA, MacKinnon R (2010) A gating charge transfer center in voltage sensors. *Science* 328:67–73.
- Lin MC, Hsieh JY, Mock AF, Papazian DM (2011) R1 in the Shaker S4 occupies the gating charge transfer center in the resting state. *J Gen Physiol* 138:155–163.
- Villalba-Galea CA, Frezza L, Sandtner W, Bezanilla F (2013) Sensing charges of the Ciona intestinalis voltage-sensing phosphatase. *J Gen Physiol* 142:543–555.
- Starace DM, Bezanilla F (2001) Histidine scanning mutagenesis of basic residues of the S4 segment of the shaker K^+ channel. *J Gen Physiol* 117:469–490.
- Zhao H (2006) Viscosity B-coefficients and standard partial molar volumes of amino acids, and their roles in interpreting the protein (enzyme) stabilization. *Biophys Chem* 122:157–183.
- Moldenhauer H, Diaz-Franulic I, González-Nilo F, Naranjo D (2016) Effective pore size and radius of capture for K^+ ions in K-channels. *Sci Rep* 6:19893.
- Diaz-Franulic I, Sepúlveda RV, Navarro-Quezada N, González-Nilo F, Naranjo D (2015) Pore dimensions and the role of occupancy in unitary conductance of Shaker K channels. *J Gen Physiol* 146:133–146.
- Chanda B, Asamoah OK, Blunck R, Roux B, Bezanilla F (2005) Gating charge displacement in voltage-gated ion channels involves limited transmembrane movement. *Nature* 436:852–856.
- Kim GH, Kosterin P, Obaid AL, Salzberg BM (2007) A mechanical spike accompanies the action potential in mammalian nerve terminals. *Biophys J* 92:3122–3129.
- Seber GAF, Lee AJ (2003) *Linear Regression Analysis* (Wiley, Hoboken, NJ), 2nd Ed.

Santiago, 27 July 2018

Experimental and computational characterization of the interaction between gold nanoparticles and PAMAM dendrimers

M.B. Camarada^{1*}, J. Comer^{2*}, H. Poblete³, E.R. Azhagiya Singam², V. Marquez-Miranda^{4,5}, C. Morales-Verdejo¹, F.D. Gonzalez-Nilo⁵

¹*Centro de Nanotecnología Aplicada, Facultad de Ciencias, Universidad Mayor, Camino la Pirámide 5750, Huechuraba, Santiago, Chile*

²*Nanotechnology Innovation Center of Kansas State, Institute of Computational Comparative Medicine, Department of Anatomy and Physiology, Kansas State University, 1800 Denison Ave, Manhattan, Kansas, KS 66506, United States of America*

³*Centro de Bioinformática y Simulación Molecular, Facultad de Ingeniería; Nucleo Científico Multidisciplinario-DI; Millennium Nucleus of Ion Channels-Associated Diseases (MINICAD), Universidad de Talca, 2 Norte 685, Casilla 721, Talca, Chile*

⁴*Current address: uBiome SpA, Av. Santa María 2810, Providencia, Santiago, Chile.*

⁵*Universidad Andrés Bello, Center for Bioinformatics and Integrative Biology (CBIB), Facultad de Ciencias de la Vida, Av. República 330, Santiago, Chile*

Abstract

Dendrimers provide a means to control the synthesis of gold nanoparticles and stabilize their suspensions. However, design of improved dendrimers for this application is hindered by a lack of understanding how the dendrimers and synthesis conditions determine nanoparticle morphology and suspension stability. In the present work, we evaluate the effect of polyamidoamine (PAMAM) dendrimers terminated with different functional groups (–OH or –NH₃⁺) and different synthesis conditions on the morphology of the resulting gold nanoparticles and their stability in solution. We leverage molecular dynamics simulations to identify the atomic interactions that underlie adsorption of PAMAM dendrimers to gold surface and how the thermodynamics of this adsorption depends on the terminal functional groups of the dendrimers. We find that gold nanoparticles formed with hydroxyl-terminated PAMAM (PAMAM–OH) rapidly aggregate, while those formed with PAMAM–NH₃⁺ are stable in solution for months of storage. Synthesis under ultrasound sonication is shown to be more rapid than under agitation, with sonication producing smaller nanoparticles. Free-energy calculations in molecular dynamics simulations show that all dendrimers have a high affinity for the gold surface, although PAMAM–OH and its oxidized aldehyde form (PAMAM–CHO) have a greater affinity for the nanoparticle surface than PAMAM–NH₃⁺. While adsorption of PAMAM–OH and PAMAM–CHO has both favorable entropy and enthalpy, adsorption of PAMAM–NH₃⁺ is driven by a strong enthalpic component subject to an unfavorable entropic component.

Keywords

dendrimers, PAMAM, gold nanoparticles, adaptive biasing force, sonication

email: maria.camarada@umayor.cl, jeffcomer@ksu.edu

Acknowledgements

M.B.C. is grateful to Fondecyt for funding support (Project N° 1180023). Powered@NLHPC: This research was partially supported by the supercomputing infrastructure of the NLHPC (ECM-02). H.P. thanks to Fondecyt grant No. 1171155, also, to the Millennium Nucleus of Ion Channels-Associated Diseases (MiNICAD) is a Millennium Nucleus supported by the Iniciativa Científica Milenio of the Ministry of Economy, Development and Tourism (Chile). This material is based upon work supported by the National Science Foundation (USA) under grant number CHE-1726332.

Supporting Information. UV-vis spectra of the synthesized nanoparticles in the absence of reducing agent and AFM images of gold nanoparticles.

References

1. Zhang, L.; Gu, F.; Chan, J.; Wang, A.; Langer, R.; Farokhzad, O., Nanoparticles in medicine: therapeutic applications and developments. *Clinical pharmacology and therapeutics* **2008**, *83* (5), 761-769.
2. Xu, Y. Y.; Bian, C.; Chen, S.; Xia, S., A microelectronic technology based amperometric immunosensor for α -fetoprotein using mixed self-assembled monolayers and gold nanoparticles. *Anal. Chim. Acta* **2006**, *561* (1), 48-54.
3. Ayati, A.; Ahmadpour, A.; Bamoharram, F. F.; Tanhaei, B.; Mänttari, M.; Sillanpää, M., A review on catalytic applications of Au/TiO₂ nanoparticles in the removal of water pollutant. *Chemosphere* **2014**, *107*, 163-174.
4. Dinali, R.; Ebrahimezhad, A.; Manley-Harris, M.; Ghasemi, Y.; Berenjian, A., Iron oxide nanoparticles in modern microbiology and biotechnology. *Critical Reviews in Microbiology* **2017**, 1-15.
5. Jin, R.; Charles Cao, Y.; Hao, E.; Metraux, G. S.; Schatz, G. C.; Mirkin, C. A., Controlling anisotropic nanoparticle growth through plasmon excitation. *Nature* **2003**, *425* (6957), 487-490.
6. Roduner, E., Size matters: why nanomaterials are different. *Chem. Soc. Rev.* **2006**, *35* (7), 583-592.
7. Lewis, L. N., Chemical catalysis by colloids and clusters. *Chemical Reviews* **1993**, *93* (8), 2693-2730.
8. Sauter, C.; Emin, M. A.; Schuchmann, H. P.; Tavman, S., Influence of hydrostatic pressure and sound amplitude on the ultrasound induced dispersion and de-agglomeration of nanoparticles. *Ultrasonics Sonochemistry* **2008**, *15* (4), 517-523.
9. Grillo, R.; Rosa, A. H.; Fraceto, L. F., Engineered nanoparticles and organic matter: A review of the state-of-the-art. *Chemosphere* **2015**, *119*, 608-619.
10. Crooks, R. M.; Zhao, M.; Sun, L.; Chechik, V.; Yeung, L. K., Dendrimer-encapsulated metal nanoparticles: synthesis, characterization, and applications to catalysis. *Accounts of chemical research* **2001**, *34* (3), 181-190.

Engineering Atrazine Loaded Poly (lactic-co-glycolic Acid) Nanoparticles to Ameliorate Environmental Challenges

Brian Schnoor,^{*,†,‡} Ahmad Elhendawy,^{†,‡} Suzanna Joseph,^{†,‡} Mark Putman,^{†,‡} Randall Chacón-Cerdas,[§] Dora Flores-Mora,[§] Felipe Bravo-Moraga,^{||} Fernando Gonzalez-Nilo,^{||} and Carolina Salvador-Morales^{*,†,‡,||}

[†]Bioengineering Department, George Mason University, 4400 University Drive MS 1J7, Fairfax, Virginia 22030, United States

[‡]Institute of Advanced Biomedical Research, George Mason University, 10920 George Mason Circle, MS1A9, Manassas, Virginia 20110, United States

[§]Instituto Tecnológico de Costa Rica, Biotechnology Research Center, Cartago, Costa Rica

^{||}Center for Bioinformatics and Integrative Biology, Facultad de Ciencias Biológicas, Universidad Andres Bello, Santiago 8370146, Chile

S Supporting Information

ABSTRACT: The use of herbicides plays a vital role in controlling weeds and conserving crops; however, its usage generates both environmental and economic problems. For example, herbicides pose a financial issue as farmers must apply large quantities to protect crops due to absorption rates of less than 0.1%. Therefore, there is a great need for the development of new methods to mitigate these issues. Here, we report for the first time the synthesis of poly(lactic-co-glycolic-acid) (PLGA) nanoherbicides loaded with atrazine as an active ingredient. We used potato plants as a biological model to assess the herbicidal activity of the engineered PLGA nanoherbicides. Our method produced nanoherbicides with an average size of 110 ± 10 nm prior to lyophilization. Fifty percent of the loaded atrazine in the PLGA matrix is released in 72 h. Furthermore, we performed Monte Carlo simulations to determine the chemical interaction among atrazine, PLGA, and the solvent system. One of the most significant outcomes of these simulations was to find the formation of a hydrogen bond of 1.9 Å between PLGA and atrazine, which makes this interaction very stable. Our *in vitro* findings showed that as atrazine concentration is increased in PLGA nanoparticles, potato plants undergo a significant decrease in stem length, root length, fresh weight, dry weight, and the number of leaves, with root length being the most affected. These experimental results suggest the herbicidal effectiveness of atrazine-loaded PLGA nanoherbicides in inhibiting the growth of the potato plant. Hence, we present the proof-of-concept for using PLGA nanoherbicides as an alternative method for inhibiting weed growth. Future studies will involve a deep understanding of the mechanism of plant–nanoherbicide interaction as well as the role of PLGA as a growth potentiator.

KEYWORDS: environmental technology, nanoherbicides, poly(lactic-co-glycolic-acid) (PLGA), atrazine, polymers, nanoparticles

■ INTRODUCTION

Protecting crops from nutrient stealing weeds is an essential part of agriculture. Herbicides play a vital role in controlling weeds and conserving crops. However, the use of herbicides generates many environmental and economic problems. Current herbicides pose a significant risk to the environment since vast quantities of herbicides are washed into streams and rivers as runoff, which can kill nontarget organisms and disrupt ecosystems.^{1–4} The widespread use of herbicides, such as atrazine, also presents economic problems because these herbicides evaporate quickly and are readily trapped in the top layer of soil due to soil absorption.^{5,6} Therefore, less than 0.1% of the applied herbicides reach the target organisms.⁷ Even the herbicide that reaches the target weed can be ineffective due to poor translocation in the weed and the development of herbicide resistant weeds. Because of this phenomenon, larger amounts of herbicides are required, which can exacerbate environmental damage. To overcome these problems, a new delivery system is needed to protect the herbicides, ensure that they reach the weed, and improve transport of the herbicide within the target weed.

Atrazine is the second most popular herbicide in the United States since it is very efficient in controlling weeds and has proven to be harmless toward corn crops.⁸ Nevertheless, atrazine can cause severe environmental damage. For instance, in the United States, it contaminates more water sources than any other pesticide.⁹ In the European Union, atrazine has already been banned because atrazine contamination in the groundwater exceeded the maximum limits set by law.¹⁰ Furthermore, studies indicated that atrazine has harmful effects on nontarget organisms in aquatic ecosystems.^{3,4,11}

Nanoparticle-based delivery systems for herbicides also known as “nanoherbicides” have shown great promise to improve herbicidal efficacy.^{8,12–14} Nanoherbicides consist of a traditional herbicide encapsulated within a nanoparticle’s core, which protects and directs the herbicide to the target organism. Nanoherbicides have the potential to prevent the fast

Received: April 14, 2018

Revised: June 14, 2018

Accepted: July 13, 2018

polymer is an excellent option for the synthesis of novel nanoherbicides because of its biocompatibility, FDA approval, customized herbicide release, and tunable biodegradable profile. We would expect to achieve higher efficacy in inhibiting the growth as we increase the herbicides' encapsulation efficiency. We found that lyophilized nanoherbicides whose size is around 500 nm \pm 10 nm affect plant growth. Since the nanoherbicides are made of the PLGA polymer, and this polymer degrades in the presence of water, we had to lyophilize the nanoherbicides to conduct the in vitro plant studies. The 50% encapsulation efficiency of atrazine in the PLGA matrix produced a decrement of 40% in root length. Also, we observed that the PLGA nanoherbicides are as effective as unencapsulated atrazine to reduce growth but substantially less toxic because after the PLGA matrix undergoes degradation, it will be metabolized by the Krebs cycle releasing only CO₂ and water as final products. Therefore, PLGA nanoherbicides will not induce detrimental effects in the environment compared to other types of nanoherbicides or naked herbicides. Equally important, because PLGA nanoherbicides control the release of the active ingredient, they will greatly reduce toxicity in the environment. Notably, we observed that PLGA serves as a growth potentiator for plants. Thus, in this article we presented the proof-of-concept of using PLGA nanoherbicides as an alternative method for inhibiting weed growth and PLGA nanoparticles as a potential growth factor for plants. For atrazine-resistant crops such as corn, the PLGA nanoparticles could serve to promote crop growth while the encapsulated atrazine inhibits weed growth. Additionally, this growth effect could serve to counterbalance some of the effect of the herbicide on nontarget plants without atrazine resistance. Future studies will involve an in-depth understanding of the mechanism of plant–nanoherbicide interaction as well as the role of PLGA as a growth potentiator.

■ ASSOCIATED CONTENT

■ Supporting Information

The Supporting Information is available free of charge on the ACS Publications website at DOI: 10.1021/acs.jafc.8b01911.

TEM micrograph and average hydrodynamic diameter of lyophilized nanoherbicides (PDF)

■ AUTHOR INFORMATION

Corresponding Author

*Tel: 703-993-5895. E-mail: csalvado@gmu.edu.

ORCID

Carolina Salvador-Morales: 0000-0002-2588-6608

Funding

This work was supported by a CSM startup fund (162904). This project was also funded in part through the Undergraduate Research Scholars Program sponsored by the George Mason Office of Student Scholarship Creativity and Research.

Notes

The authors declare no competing financial interest.

■ ACKNOWLEDGMENTS

We thank Dr. Thomas Huff for assistance in developing the protocol for the LC-MS measurements. Furthermore, we thank Drs. Mikell Paige and Barney Bishop for giving access to the FT-IR and DLS instruments.


■ ABBREVIATIONS USED

PLGA, poly(lactic-co-glycolic acid); DSPEPEG-NH₂, 1,2-distearoyl-1-*sn*-glycero-3-phosphoethanolamine-*N*-[amino-(polyethylene glycol)]; DLS, dynamic light scattering; TEM, transmission electron microscopy; LC-MS, liquid chromatography/mass spectroscopy; diH₂O, deionized water

■ REFERENCES

- (1) Nicodemo, D.; Maioli, M. A.; Medeiros, H. C. D.; Guelfi, M.; Balieira, K. V. B.; De Jong, D.; Mingatto, F. E. Fipronil and Imidacloprid Reduce Honeybee Mitochondrial Activity *Environ. Toxicol. Environ. Toxicol. Chem.* **2014**, *33*, 2070–2075.
- (2) Corsini, E.; Sokooti, M.; Galli, C. L.; Moretto, A.; Colosio, C. Pesticide Induced Immunotoxicity in Humans: A Comprehensive Review of the Existing Evidence. *Toxicology* **2013**, *307*, 123–135.
- (3) Jie, G.; Yu, W.; Bin, G.; Lei, W.; Hao, C. Environmental Fate and Transport of Pesticides. *Pesticides*; CRC Press: Boca Raton, FL, 2012; pp 29–46.
- (4) Wauchope, R. D. The Pesticide Content of Surface Water Draining from Agricultural Fields – A Review. *J. Environ. Qual.* **1978**, *7*, 459–472.
- (5) Mudhoo, A.; Garg, V. K. Sorption, Transport and Transformation of Atrazine in Soils Minerals and Composts: A Review. *Pedosphere* **2011**, *21*, 11–25.
- (6) Gamble, D. S. Atrazine Sorption Kinetics in a Characterized Soil: Predictive Calculations. *Environ. Sci. Technol.* **2008**, *42*, 1537–1541.
- (7) Otlavaro, J. O.; Brigante, M. Interaction of Pesticides with Natural and Synthetic Solids. Evaluation in Dynamic and Equilibrium Conditions. *Environ. Sci. Pollut. Res.* **2018**, *25*, 6707–6719.
- (8) Pereira, A. E. S.; Grillo, R.; Mello, N. F. S.; Rosa, A. H.; Fraceto, L. F. Application of Poly(epsilon-caprolactone) Nanoparticles Containing Atrazine Herbicide as an Alternative Technique to Control Weeds and Reduce Damage to the Environment. *J. Hazard. Mater.* **2014**, *268*, 207–215.
- (9) Giliom, R. J.; Barbash, J. E.; Crawford, C. G.; Hamilton, P. A.; Martin, J. D.; Nakagaki, N.; Nowell, L.; Scott, J. C.; Stackleberg, P. E.; Thelin, G. P.; Wolock, D. M. The Quality of Our Nation's Waters: Pesticides in the Nation's Streams and Ground Water, 1992–2001. *United States Geological Survey* **2006**, *1291*, 41–66.
- (10) 2004/248/EC: Commission Decision of 10 March 2004 concerning the noninclusion of atrazine in Annex I to Council Directive 91/414/EEC and the withdrawal of authorizations for plant protection products containing this active substance (Text with EEA relevance) (notified under document number C (2004) 731).
- (11) Schulz, R. Field Studies on Exposure, Effects, and Risk Mitigation of Aquatic Nonpoint-Source Insecticide Pollution: A Review. *J. Environ. Qual.* **2004**, *33*, 419–448.
- (12) Grillo, R.; Pereira, A. E. S.; Nishisaka, C. S.; de Lima, R.; Oehlke, K.; Greiner, R.; Fraceto, L. F. Chitosan/tripolyphosphate Nanoparticles Loaded with Paraquat Herbicide: An Environmentally Safer Alternative for Weed Control. *J. Hazard. Mater.* **2014**, *278*, 163–171.
- (13) Silva, M. S.; Cocenza, D. S.; Grillo, R.; de Melo, N. F. S.; Tonello, P. S.; de Oliveira, L. C.; Cassimiro, D. L.; Rosa, A. H.; Fraceto, L. F. Paraquat-Loaded Alginate/chitosan Nanoparticles: Preparation, Characterization and Soil Sorption Studies. *J. Hazard. Mater.* **2011**, *190*, 366–374.
- (14) Kah, M.; Beulke, S.; Tiede, K.; Hofmann, T. K. Nanopesticides: State of Knowledge, Environmental Fate and Exposure Modelling. *Crit. Rev. Environ. Sci. Technol.* **2013**, *43*, 1823–1867.
- (15) de Oliveira, J. L.; Campos, E. V.; Gonçalves da Silva, C. M.; Pasquoto, T.; Lima, R.; Fraceto, L. F. Solid Lipid Nanoparticles Co-Loaded with Simazine and Atrazine: Preparation, Characterization, and Evaluation of Herbicidal Activity. *J. Agric. Food Chem.* **2015**, *63*, 422–432.
- (16) Grillo, R.; dos Santos, N. Z. P.; Maruyama, C. R.; Rosa, A. H.; de Lima, R.; Fraceto, L. F. Poly(epsilon-caprolactone) Nanocapsules as

Neonatal exposure to oestradiol increases dopaminergic transmission in nucleus accumbens and morphine-induced conditioned place preference in adult female rats

C. Bonansco¹ | J. Martínez-Pinto¹ | R. A. Silva¹ | V. B. Velásquez¹ |
A. Martorell^{1,2} | M. V. Selva¹ | P. Espinosa¹ | P. R. Moya^{1,3,4} | G. Cruz¹ |
M. E. Andrés⁵ | R. Sotomayor-Zárate¹ 

¹Centro de Neurobiología y Plasticidad Cerebral, Instituto de Fisiología, Facultad de Ciencias, Universidad de Valparaíso, Valparaíso, Chile

²Escuela de Fonoaudiología, Facultad de Ciencias de la Rehabilitación, Universidad Andres Bello, Viña del Mar, Chile

³Núcleo Milenio Biología de Enfermedades Neuropsiquiátricas (NUMIND), Valparaíso, Chile

⁴Centro Interdisciplinario de Neurociencia de Valparaíso, Valparaíso, Chile

⁵Departamento de Biología Celular y Molecular, Facultad de Ciencias Biológicas, Pontificia Universidad Católica de Chile, Santiago, Chile

Correspondence

Ramón Sotomayor-Zárate, Laboratorio de Neuroquímica y Neurofarmacología, CNPC, Instituto de Fisiología, Facultad de Ciencias, Universidad de Valparaíso, Valparaíso, Chile. Email: ramon.sotomayor@uv.cl

Funding information

DIUV-CI, Grant/Award Number: 01/2006; Fondo Nacional de Desarrollo Científico y Tecnológico, Grant/Award Number: 113-0491, 114-1272 and 116-0398; Millennium Institute, Grant/Award Number: P09-022-F

Steroid sex hormones produce physiological effects in reproductive tissues and also in nonreproductive tissues, such as the brain, particularly in cortical, limbic and mid-brain areas. Dopamine (DA) neurones involved in processes such as prolactin secretion (tuberoinfundibular system), motor circuit regulation (nigrostriatal system) and driving of motivated behaviour (mesocorticolimbic system) are specially regulated by sex hormones. Indeed, sex hormones promote neurochemical and behavioural effects induced by drugs of abuse by tuning midbrain DA neurones in adult animals. However, the long-term effects induced by neonatal exposure to sex hormones on dopaminergic neurotransmission have not been fully studied. The present study aimed to determine whether a single neonatal exposure with oestradiol valerate (EV) results in a programming of dopaminergic neurotransmission in the nucleus accumbens (NAcc) of adult female rats. To answer this question, electrophysiological, neurochemical, cellular, molecular and behavioural techniques were used. The data show that frequency but not amplitude of the spontaneous excitatory postsynaptic current is significantly increased in NAcc medium spiny neurones of EV-treated rats. In addition, DA content and release are both increased in the NAcc of EV-treated rats, caused by an increased synthesis of this neurotransmitter. These results are functionally associated with a higher percentage of EV-treated rats conditioned to morphine, a drug of abuse, compared to controls. In conclusion, neonatal programming with oestradiol increases NAcc dopaminergic neurotransmission in adulthood, which may be associated with increased reinforcing effects of drugs of abuse.

KEYWORDS

dopamine, microdialysis, morphine, oestradiol, programming

1 | INTRODUCTION

Sex hormones such as oestrogens exert their biological actions in reproductive (gonads) and nonreproductive tissues (liver, bones, muscle and brain) via activation of nuclear oestrogen receptor (ER) α and ER β ¹ and plasmatic membrane G protein-coupled receptors.² In the

central nervous system, ERs are localised in different brain areas,^{3,4} including the nigrostriatal and the mesocorticolimbic pathways.^{5,6}

The mesocorticolimbic pathway or reward circuit is activated by natural rewards such as sex⁷ and food,⁸ as well as by drugs of abuse.^{9,10} The main neurotransmitter in the mesocorticolimbic pathway is dopamine (DA), which is released by midbrain dopaminergic

release in PFC induced by acute stress in female rats, associated with and potentiated by a decrease in cortical and plasmatic allopregnanolone levels, a GABA_A receptor positive allosteric modulator. Noteworthy, administration of progesterone (ie, a sex hormone precursor of the brain allopregnanolone synthesis) decreases the PFC DA release induced by acute stress in control and EB rats.⁵⁴ Neonatal exposure to EV produces a lack of corpus luteum in the ovary and a significant decrease in serum progesterone levels in adult female rats.^{24,27} Considering the results of Porcu et al.,⁵⁴ we can hypothesise that low levels of serum progesterone result in a reduction of NAcc allopregnanolone and a decrease in the hyperpolarising effect of this neurosteroid. This hypothesis cannot be ruled out and should be investigated in further studies.

Our electrophysiological studies show that the stimulation of dopaminergic afferents from VTA increases the frequency but not amplitude of the spontaneous EPSC on MSNs, which could be explained by a presynaptic mechanism, such as an increase of release probability and/or in terminal excitability. Because dopaminergic stimulation does not modify either the action potential-threshold (data not show) or sEPSC amplitude in MSNs in both groups, it is unlikely that modulatory effects occur postsynaptically. However, we cannot rule out postsynaptic effects induced by oestrogens. In this sense, oestrogens can modulate pre- and postsynaptic currents produced by glutamate via the specific activation of oestrogen receptors in each sex.⁵⁵ Indeed, further electrophysiological experiments will be necessary to establish the mechanisms of this dopaminergic potentiation, including minimal evoked and miniature EPSC recordings. These findings suggest that the neonatal exposure to EV potentiates the dopaminergic modulation onto excitatory currents, which may be a result of either increased DA release or increased D₁ receptor expression in glutamatergic terminals, in agreement with previous studies.^{38,56} Nevertheless, further experiments are required to clarify which mechanism is responsible for strengthening glutamatergic inputs. By contrast to our data, a recently study showed that neonatal exposure to E₂ or testosterone reduced the mEPSC frequency of MSNs in the NAcc of prepubertal female rats.⁵⁷ Several methodological differences may explain the dissimilarity between both works. First, the age of the rats in which the electrophysiological recordings were performed was different (PND60–62 vs PND16–23). Second, our work was performed in sagittal slices that preserve the integrity of the dopaminergic afferents to NAcc from VTA, whereas the work of Cao et al.⁵⁷ was performed in coronal slices. Finally, we used an ester of E₂ (valerate or pentanoate of E₂) that has different pharmacokinetics from E₂, such as half-life time and duration of effect.⁵⁸ These differences may be responsible for brain long-term effects that might favor an overstimulation of dopaminergic neurotransmission in NAcc.

To determine whether the electrophysiological, neurochemical, cellular and molecular changes observed in EV-treated rats are related to effects at the behavioural level, a morphine-induced CPP was performed to evaluate the degree of drug-induced conditioning.

Similar to other drugs of abuse, morphine increases NAcc DA release⁹ via hyperpolarisation of VTA GABAergic neurones that express μ opioid receptors.^{59,60} Our results show that morphine increases the percentage of conditioning in EV-treated rats respect to controls. B. Velásquez, G. Zamorano and R. Sotomayor-Zárate, unpublished results. obtained in our laboratory show that adult EV male rats have increased NAcc DA release and morphine-induced locomotor activity.

In summary, the results of the present study show that neonatal programming by EV modulates the dopaminergic neurotransmitter system and enhances morphine-induced conditioning. We have shown that neonatal programming with sex hormones (EV and TP) affects long-term mesolimbic and nigrostriatal pathways.²⁵ In humans, it has been recently demonstrated that prenatal exposure to androgens correlates with an increased dependence on alcohol in adult life.⁶¹ On the other hand, children who have developed precocious puberty (an early activation of the reproductive axis leading to an onset of puberty near to 8 and 9 years in girls and boys, respectively) show an increase in risky behaviours, such as drug abuse, sexual risk and anti-social behaviours in adolescence.⁶² Our data from animal studies highlight the strong influence of early exposure of E₂ on neurotransmission in adulthood, particularly on the dopaminergic system, which could be a factor of susceptibility with respect to dependence on drugs of abuse, such as alcohol and opioids.

ACKNOWLEDGEMENTS

This work was primarily funded by FONDECYT Grant No. 116-0398 to RS-Z. Partial support was received from DIUV-CI Grant No. 01/2006 (to RS-Z, CB, GC and PRM), FONDECYT Grants No. 113-0491 (to CB) and No. 114-1272 (to PRM), and The Centro Interdisciplinario de Neurociencia de Valparaíso is a Millennium Institute Grant No. P09-022-F (to PRM).

ORCID

R. Sotomayor-Zárate  <http://orcid.org/0000-0002-1239-5367>

REFERENCES

- Alexander SP, Cidlowski JA, Kelly E, et al. The Concise Guide to PHARMACOLOGY 2015/16: nuclear hormone receptors. *Br J Pharmacol*. 2015;172:5956–5978.
- Filardo EJ, Quinn JA, Frackelton AR Jr, Bland KI. Estrogen action via the G protein-coupled receptor, GPR30: stimulation of adenylyl cyclase and cAMP-mediated attenuation of the epidermal growth factor receptor-to-MAPK signaling axis. *Mol Endocrinol*. 2002;16:70–84.
- Sheridan PJ. Autoradiographic localization of steroid receptors in the brain. *Clin Neuropharmacol*. 1984;7:281–295.
- Laflamme N, Nappi RE, Drolet G, Labrie C, Rivest S. Expression and neuropeptidergic characterization of estrogen receptors (ERalpha and ERbeta) throughout the rat brain: anatomical evidence of distinct roles of each subtype. *J Neurobiol*. 1998;36:357–378.



ORIGINAL ARTICLE

Selecting optimal mixtures of natural sweeteners for carbonated soft drinks through multi-objective decision modeling and sensory validation

Waldo Acevedo^{1,2} | Chloé Capitaine³ | Ricardo Rodríguez³ | Ingrid Araya-Durán⁴ |
Fernando González-Nilo⁴ | José R. Pérez-Correa¹ | Eduardo Agosin^{1,3}

¹Department of Chemical and Bioprocess Engineering, School of Engineering, Pontificia Universidad Católica de Chile, Santiago, Chile

²Institute of Chemistry, Pontificia Universidad Católica de Valparaíso, Valparaíso, Chile

³Centro de Aromas y Sabores, DICTUC, Santiago, Chile

⁴Universidad Andrés Bello, Faculty of Biological Sciences, Center for Bioinformatics and Integrative Biology, Santiago, Chile

Correspondence

Eduardo Agosin, Department of Chemical and Bioprocess Engineering, School of Engineering, Pontificia Universidad Católica de Chile, Avenida Vicuña Mackenna 4860, Santiago, Chile.

Email: agosin@ing.puc.cl

Funding information

Chilean National Council of Scientific and Technological Research (CONICYT), Grant/Award Number: 21130688

Abstract

The objective of this study was to develop a methodology to optimize mixtures of natural, non-caloric sweeteners—with the highest sweetness and the lowest bitterness—for carbonated soft drinks. To this end, and with the aid of a trained sensory panel, we first determined the most suitable mixtures of tagatose, sucrose, and stevia in a soft drink matrix, using a three-component simplex lattice mixture design. Then, we developed a multi-objective thermodynamically-based decision model to this purpose. Results indicate that both, sucrose and tagatose, were able to reduce stevia's bitterness. However, an increase of bitterness intensity was found above 0.23 g/L of stevia (sucrose equivalency or SE >5). Both, sensory analysis and multi-objective decision modeling identified similar optimal mixtures, corresponding to 23–39 g/L sucrose, 0.19–0.34 g/L stevia, and 34–42 g/L tagatose, depending on the desired sweetness/bitterness balance. Within this constrained area, a reduction of almost 60% of sucrose can be achieved in both approaches, keeping bitterness intensity low.

Practical applications

Current demand of low-calorie beverages has significantly raised as a result of consumer concerns on the negative effects of refined sugars present in carbonated soft drinks. Consequently, natural sweeteners, and their mixtures, are being increasingly used for these product developments. This study provides a methodology to optimize mixtures of natural, noncaloric sweeteners for preparing carbonated soft drinks with the lowest possible caloric content, while maintaining the tastiness—high sweetness and low bitterness—of full caloric ones, containing the bulk sweetener tagatose and the high-intensity sweetener stevia.

1 | INTRODUCTION

The consumption of carbonated sugary drinks has been a constant matter of concern to public health, due to the negative contribution of refined sugars and calories to diet. In recent decades, the intake of these beverages has increased considerably around the world. From 1997 to 2010, average annual consumption of soft drinks worldwide increased by 20%, mainly sugar-sweetened carbonated drinks (Basu, McKee, Galea, & Stuckler, 2013). This increase has been related with rising rates of obesity and other health outcomes, like type 2 diabetes mellitus and cardiovascular diseases (Basu et al., 2013; Malik, Popkin,

Bray, Després, & Hu, 2010; Vartanian, Schwartz, & Brownell, 2007). These health trends are increasing awareness among consumers about the intake of carbonated sugary drinks, encouraging them to shift their preferences toward products with less sugar and caloric content. To meet this demand, beverages sweetened with a large variety of noncaloric artificial sweeteners, like potassium acesulfame and aspartame, have been developed by the industry as healthier alternatives. Their sweetening power at very low concentrations and their limited caloric contribution made these compounds an excellent alternative to replace sugar. However, consumer's reports and studies with animals have claimed that the consumption of these high-intensity,

the proposed optimal area, the optimal combinations of sucrose–stevioside–tagatose and sucrose–rebA–tagatose correspond to relative fractions of 0.27/0.45/0.28 and 0.26/0.45/0.29, respectively (Supporting Information Table S4). However, the cost of production and the amount of tagatose makes these mixtures less suitable. When price and calories reduction are incorporated, then relative fractions of 0.24/0.50/0.26 and 0.23/0.50/0.27 would be more appealing.

In conclusion, in this work, we demonstrated that a multi-objective decision model could be successfully used to identify optimal mixtures of natural sweeteners—highest sweetness and lowest bitterness—based on the interaction energies of sweetener–receptor and sweetener–sweetener complexes. The optimal mixtures predicted by multi-objective thermodynamic modeling were similar to those obtained through DOE and sensory analysis, demonstrating the robustness of the developed model. Therefore, the most suitable combinations, depending on the sweetness/bitterness balance, were those containing 23–39 g/L sucrose, 0.19–0.34 g/L stevia, and 34–42 g/L tagatose. It is worth mentioning at this level that consumer research studies would be necessary to further validate the acceptability of the selected optimal mixtures.

Experimental sensory optimization validated the results predicted by the multi-objective decision model. A reduction of almost 60% of sucrose can be achieved using both stevia and tagatose, keeping bitterness intensity low. If further reduction is desired, ternary mixtures with a higher proportion of tagatose are a good option. This could result in a 79% reduction of total calories compared to a regular soft drink (pure sucrose). However, if an economically feasible product is required, the reduction of the amount of tagatose would be mandatory.

Finally, multi-objective optimization will be a useful tool for developing new sweetener mixtures with other natural sweeteners, such as *Luo Han Guo* (also known as monk-fruit) or to reduce other unwanted attributes besides bitterness.

ACKNOWLEDGMENTS

We are grateful to Professor Piero Andrea Temussi, from University of Naples, for his valuable comments that contributed significantly to improve the final manuscript; to Javier Sainz, from Prodalya, Inc. in Santiago, Chile, for his recommendations and suggestions during the course of this work; to Felipe Bravo, from Center for Bioinformatics and Integrative Biology at University Andrés Bello, Santiago, for theoretical calculations of ternary interaction energy of sweeteners. This work was supported by a doctoral fellowship from the Chilean National Council of Scientific and Technological Research (CONICYT) [grant number 21130688 to W.A.].

CONFLICT OF INTEREST

The authors declare no conflict of interest.

REFERENCES

- Acevedo, W., Gonzalez-Nilo, F., & Agosin, E. (2016). Docking and molecular dynamics of Steviol glycosides-human bitter receptors interactions. *Journal of Agricultural and Food Chemistry*, 64(40), 7585–7596.
- Acevedo, W., Ramirez-Sarmiento, C. A., & Agosin, E. (2018). Identifying the interactions between natural, non-caloric sweeteners and the human sweet receptor by molecular docking. *Food Chemistry*, 264, 164–171.
- Andersen, H., & Vigh, M. (2002). Synergistic combination of sweeteners including D-tagatose.
- Avila-Salas, F., Sandoval, C., Caballero, J., Guíñez-Molinos, S., Santos, L. S., Cachau, R. E., & González-Nilo, F. D. (2012). Study of interaction energies between the PAMAM dendrimer and nonsteroidal anti-inflammatory drug using a distributed computational strategy and experimental analysis by ESI-MS/MS. *The Journal of Physical Chemistry*, 116(7), 2031–2039.
- Bassoli, A., Drew, M. G. B., Merlini, L., & Morini, G. (2002). General Pseudoreceptor model for sweet compounds: A semiquantitative prediction of binding affinity for sweet-tasting molecules. *Journal of Medicinal Chemistry*, 45(20), 4402–4409.
- Basu, S., McKee, M., Galea, G., & Stuckler, D. (2013). Relationship of soft drink consumption to global overweight, obesity, and diabetes: A cross-national analysis of 75 countries. *American Journal of Public Health*, 103(11), 2071–2077.
- Bertelsen, H., Jensen, B. B., & Buemann, B. (1999). D-tagatose—A novel low-calorie bulk sweetener with prebiotic properties. *World Review of Nutrition and Dietetics*, 85, 98–109.
- Biasini, M., Bienert, S., Waterhouse, A., Arnold, K., Studer, G., Schmidt, T., ... Schwede, T. (2014). SWISS-MODEL: Modelling protein tertiary and quaternary structure using evolutionary information. *Nucleic Acids Research*, 42(W1), W252–W258.
- Bradstock, M. K., Serdula, M. K., Marks, J. S., Barnard, R. J., Crane, N. T., Remington, P. L., & Trowbridge, L. (1986). Evaluation aspartame of reactions to food additives: The aspartame experience. *American Journal of Clinical Nutrition*, 43(3), 464–469.
- Buemann, B., Toubro, S., Raben, A., & Astrup, A. (1999). Human tolerance to a single, high dose of D-tagatose. *Regulatory Toxicology and Pharmacology*, 29(2), S66–S70.
- Carakostas, M., Prakash, I., Kinghorn, A. D., Wu, C. D., & Soejarto, D. D. (2012). Steviol glycosides. In L. B. Nabors (Ed.), *Alternative sweeteners* (4th ed., pp. 159–180). New York, NY: Marcel Dek.
- Choi, J. h., & Chung, S. j. (2014). Optimal sensory evaluation protocol to model concentration–response curve of sweeteners. *Food Research International*, 62, 886–893.
- Cowart, B. J. (1998). The addition of CO₂ to traditional taste solutions alters taste quality. *Chemical Senses*, 23(1984), 397–402.
- Deshmukh, M. M., Bartolotti, L. J., & Gadre, S. R. (2008). Intramolecular hydrogen bonding and cooperative interactions in carbohydrates via the molecular tailoring approach. *Journal of Physical Chemistry A*, 112(2), 312–321.
- Di Salle, F., Cantone, E., Savarese, M. F., Aragri, A., Prinster, A., Nicolai, E., ... Cuomo, R. (2013). Effect of carbonation on brain processing of sweet stimuli in humans. *Gastroenterology*, 145(3), 537–539.
- Donner, T. W., Wilber, J. F., & Ostrowski, D. (1999). D-tagatose, a novel hexose: Acute effects on carbohydrate tolerance in subjects with and without type 2 diabetes. *Diabetes, Obesity & Metabolism*, 1(5), 285–291.
- DuBois, G. E., Walters, D. E., Schiffman, S. S., Warwick, Z. S., Booth, B. J., Pecore, S. D., ... Brands, L. M. (1991). Concentration–response relationships of sweeteners. *ACS Symposium Series*, 450, 261–276.
- Espinoza, M. I., Vincken, J. P., Sanders, M., Castro, C., Stieger, M., & Agosin, E. (2014). Identification, quantification, and sensory characterization of steviol glycosides from differently processed *Stevia rebaudiana* commercial extracts. *Journal of Agricultural and Food Chemistry*, 62(49), 11797–11804.
- Fan, C. F., Olafson, B. D., Blanco, M., & Hsu, S. L. (1992). Application of molecular simulation to derive phase diagrams of binary mixtures, 25(14), 3667–3676.
- Findlay, C. J., Castura, J. C., & Lesschaeve, I. (2007). Feedback calibration: A training method for descriptive panels. *Food Quality and Preference*, 18, 321–328.
- Fujimaru, T., Park, J. H., & Lim, J. (2012). Sensory characteristics and relative sweetness of tagatose and other sweeteners. *Journal of Food Science*, 77(9), S323–S328.

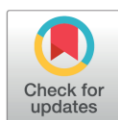
RESEARCH ARTICLE

3D similarities between the binding sites of monoaminergic target proteins

Gabriel Núñez-Vivanco^{1,2*}, Angélica Fierro³, Pablo Moya^{4,5}, Patricio Iturriaga-Vásquez⁶, Miguel Reyes-Parada^{7,8*}

1 Centro de Bioinformática y Simulación Molecular, Universidad de Talca, Talca, Chile, **2** Escuela de Ingeniería Civil en Bioinformática, Universidad de Talca, Talca, Chile, **3** Pontificia Universidad Católica de Chile, Santiago, Chile, **4** Instituto de Fisiología, Universidad de Valparaíso, Valparaíso, Chile, **5** Centro Interdisciplinario de Neurociencia de Valparaíso CINV, Universidad de Valparaíso, Valparaíso, Chile, **6** Facultad de Ingeniería y Ciencias, Universidad de la Frontera, Temuco, Chile, **7** School of Medicine, Faculty of Medical Sciences, University of Santiago de Chile, Santiago, Chile, **8** Facultad de Ciencias de la Salud, Universidad Autónoma de Chile, Talca, Chile

* ganunez@utalca.cl (GNV); miguel.reyes@usach.cl (MRP)



Abstract

The study of binding site similarities can be relevant to understand the interaction of different drugs at several molecular targets. The increasing availability of protein crystal structures and the development of novel algorithms designed to evaluate three-dimensional similarities, represent a great opportunity to explore the existence of electronic and shape features shared by clinically relevant proteins, which could assist drug design and discovery. Proteins involved in the recognition of monoaminergic neurotransmitters, such as monoamine transporters or monoamine oxidases (MAO) have been related to several psychiatric and neurological disorders such as depression or Parkinson's disease. In this work, we evaluated the possible existence of similarities among the binding sites of the serotonin transporter (SERT), the dopamine transporter (DAT), MAO-A and MAO-B. This study was carried out using molecular simulation methodologies linked to the statistical algorithm PocketMatch, which was modified in order to obtain similarities profiles. Our results show that DAT and SERT exhibit a high degree of 3-D similarities all along the pathway that is presumably involved in the substrate transport process. Distinct differences, on the other hand, were found both at the extracellular and the intracellular ends of the transporters, which might be involved in the selective initial recognition of the corresponding substrate. Similarities were also found between the active (catalytic) site of MAO-A and the extracellular vestibule of SERT (the S2 binding site). These results suggest some degree of structural convergence for these proteins, which have different functions, tissue distribution and genetic origin, but which share the same endogenous ligand (serotonin). Beyond the functional implications, these findings are valuable for the design of both selective and non-selective ligands.

OPEN ACCESS

Citation: Núñez-Vivanco G, Fierro A, Moya P, Iturriaga-Vásquez P, Reyes-Parada M (2018) 3D similarities between the binding sites of monoaminergic target proteins. PLoS ONE 13(7): e0200637. <https://doi.org/10.1371/journal.pone.0200637>

Editor: Manuela Helmer-Citterich, Università degli Studi di Roma Tor Vergata, ITALY

Received: November 15, 2017

Accepted: June 30, 2018

Published: July 20, 2018

Copyright: © 2018 Núñez-Vivanco et al. This is an open access article distributed under the terms of the [Creative Commons Attribution License](https://creativecommons.org/licenses/by/4.0/), which permits unrestricted use, distribution, and reproduction in any medium, provided the original author and source are credited.

Data Availability Statement: All relevant data are within the paper and its Supporting Information files.

Funding: This project was partially supported by Fondecyt (Fondo Nacional de Desarrollo Científico y Tecnológico) grants 1170662 (MRP), 1141272 (PM), 1150615 (PIV), 1161375 (AF) and the ICM MINECOM (Iniciativa Científica Milenio, Ministerio de Economía) grants NC130011 and P09-022-F, www.conicyt.cl/fondecyt, <http://www.iniciativamilenio.cl/>. The funders had no role in

the catalytic site of MAOs [28] and the key residues Glu, Thr and Asp that form the S2 binding site of SERT. However, it should be noted that this consensus binding site must be cautiously considered in terms of drug design, since it might not reflect some specific physicochemical features of each isolated binding site. For instance, although negatively charged residues are contained in the common binding site, there are not such type of residues at the active site of MAO-A.

Concluding remarks

3D similarities between SERT and DAT were found all along the pathway that is presumably involved in the substrate transport process. This agrees with the idea that these proteins share a similar mechanism for the transport of substrates from the extracellular domain to the cytoplasm [7,64]. In addition, 3D differences between SERT and DAT were found both at the extracellular and the intracellular ends of the transporters, in regions that, remarkably, are relatively distant from the S1 or S2 binding sites. These results are in agreement with recent computational and mutagenesis data showing that selective binding of substrates is not associated with the non-conserved SERT/DAT residues at S1 or S2 binding sites [66], but rather suggest that selectivity might be related to the initial recognition of substrates at the areas that we have found to show 3D differences. Altogether, similarities and differences detected when comparing SERT and DAT might be useful for both a better understanding of monoamine transporter function and for the design of selective and non-selective ligands.

Similarities were also found between the active (catalytic) site of MAO-A and the extracellular vestibule of SERT (the S2 binding site). These results suggest some degree of structural convergence [67] for these proteins which have different functions, tissue distribution and genetic origin, but which share the same endogenous ligand (5-HT). Hence, we propose the existence of a serotonergic “receptophore” in both proteins (the consensus binding site shown in Fig 8), which by analogy with the pharmacophore concept can be defined as a 3D ensemble, at the binding site(s) of two or more receptors, of molecular, steric and electronic features that ensure the optimal molecular interactions with a common promiscuous ligand. Further studies are necessary to determine if this 3D ensemble is also present in metabotropic and/or ionotropic 5-HT receptors, and if this concept can be extrapolated to other ligand-receptor systems.

Finally, from a methodological perspective, we want to emphasize that the use of dummy atoms instead of typical ligands to study binding site characteristics can be particularly appropriate in those cases where the ligand binding site is unknown.

Supporting information

S1 File. Supplementary information. Figure A: RMSD of MAO-A. Figure B: RMSD of MAO-B. Figure C: RMSD of SERT. Figure D: RMSD of DAT. Figure E: ProsaII evaluation of DAT. Figure F: Procheck evaluation of DAT. Figure G: RMSD between SERT and DAT. Figure H: Average of Similarity between all dummy atoms in DAT and MAO-B. Figure I: Average of Similarity between all dummy atoms in SERT and MAO-A. Table A: Binding sites similarities between MAOA/SERT, MAOA/DAT, MAOB/SERT and MAOB/DAT. Figure J: Representation of a sequence-based alignment between SERT and MAO-A. (PDF)

Acknowledgments

This project was partially supported by Fondecyt (Fondo Nacional de Desarrollo Científico y Tecnológico) Grants 1170662 (M. R-P), 1141272 (P. M), 1150615 (P. I-V), 1161375 (A. F) and

the ICM MINECOM (Iniciativa Científica Milenio, Ministerio de Economía) Grants NC130011 and P09-022-F.

Author Contributions

Conceptualization: Gabriel Núñez-Vivanco, Pablo Moya, Miguel Reyes-Parada.

Data curation: Gabriel Núñez-Vivanco, Patricio Iturriaga-Vásquez.

Formal analysis: Gabriel Núñez-Vivanco, Angélica Fierro.

Funding acquisition: Pablo Moya.

Investigation: Gabriel Núñez-Vivanco, Patricio Iturriaga-Vásquez, Miguel Reyes-Parada.

Methodology: Angélica Fierro, Patricio Iturriaga-Vásquez.

Software: Gabriel Núñez-Vivanco.

Validation: Angélica Fierro.

Writing – original draft: Gabriel Núñez-Vivanco, Miguel Reyes-Parada.

Writing – review & editing: Gabriel Núñez-Vivanco, Pablo Moya, Miguel Reyes-Parada.

References

1. Purves D, Augustine GJ, Fitzpatrick D, Hall WC, LaMantia A-S, McNamara JO WS, editor. *Neuroscience*. 3rd ed. Sinauer Associates: Sunderland; 2004.
2. De Deurwaerdere P, Ramsay RR, Di Giovanni G. Neurobiology and neuropharmacology of monoaminergic systems. *Prog Neurobiol*. 2017; 151: 1–3. <https://doi.org/10.1016/j.pneurobio.2017.02.001> PMID: 28259728
3. Stahl SM. *Stahl's Essential Psychopharmacology*. 4th ed. Cambridge University Press; 2013.
4. Kristensen AS, Andersen J, Jørgensen TN, Sørensen L, Eriksen J, Loland CJ, et al. SLC6 Neurotransmitter Transporters: Structure, Function, and Regulation. *Pharmacol Rev*. 2011; 63: 585–640. <https://doi.org/10.1124/pr.108.000869> PMID: 21752877
5. Rudnick G, Krämer R, Blakely RD, Murphy DL, Verrey F. The SLC6 transporters: Perspectives on structure, functions, regulation, and models for transporter dysfunction. *Pflügers Arch*. 2014. pp. 25–42. <https://doi.org/10.1007/s00424-013-1410-1> PMID: 24337881
6. Brøer S, Gether U. The solute carrier 6 family of transporters. *Br J Pharmacol*. 2012. pp. 256–278. <https://doi.org/10.1111/j.1476-5381.2012.01975.x> PMID: 22519513
7. Penmatsa A, Gouaux E. How LeuT shapes our understanding of the mechanisms of sodium-coupled neurotransmitter transporters. *J Physiol*. 2014; 592: 863–869. <https://doi.org/10.1113/jphysiol.2013.259051> PMID: 23878376
8. Loland CJ. The use of LeuT as a model in elucidating binding sites for substrates and inhibitors in neurotransmitter transporters. *Biochimica et Biophysica Acta—General Subjects*. 2015. pp. 500–510. <https://doi.org/10.1016/j.bbagen.2014.04.011> PMID: 24769398
9. Yamashita A, Singh SK, Kawate T, Jin Y, Gouaux E. Crystal structure of a bacterial homologue of Na⁺/Cl[−]-dependent neurotransmitter transporters. *Nature*. 2005; 437: 215–23. <https://doi.org/10.1038/nature03978> PMID: 16041361
10. Coleman JA, Green EM, Gouaux E. X-ray structures and mechanism of the human serotonin transporter. *Nature*. 2016; 532: 334–339. <https://doi.org/10.1038/nature17629> PMID: 27049939
11. Wang KH, Penmatsa A, Gouaux E. Neurotransmitter and psychostimulant recognition by the dopamine transporter. *Nature*. 2015; 521: 322–327. <https://doi.org/10.1038/nature14431> PMID: 25970245
12. Penmatsa A, Wang KH, Gouaux E. X-ray structures of *Drosophila* dopamine transporter in complex with nisoxetine and reboxetine. *Nat Struct Mol Biol*. 2015; 22: 506–508. <https://doi.org/10.1038/nsmb.3029> PMID: 25961798
13. Grouleff J, Ladefoged LK, Koldse H, Schiøtt B. Monoamine transporters: Insights from molecular dynamics simulations. *Frontiers in Pharmacology*. 2015. <https://doi.org/10.3389/fphar.2015.00235> PMID: 26528185



RCAN1 Knockdown Reverts Defects in the Number of Calcium-Induced Exocytotic Events in a Cellular Model of Down Syndrome

Jacqueline Vásquez-Navarrete¹, Agustín D. Martínez¹, Stéphane Ory², Ximena Baéz-Matus¹, Arlek M. González-Jamett¹, Sebastián Brauchi³, Pablo Caviedes^{4,5*} and Ana M. Cárdenas^{1*}

¹Centro Interdisciplinario de Neurociencia de Valparaíso, Facultad de Ciencias, Universidad de Valparaíso, Valparaíso, Chile, ²Centre National de la Recherche Scientifique (CNRS UPR 3212), Institut des Neurosciences Cellulaires et Intégratives (INCI), Strasbourg, France, ³Department of Physiology, Faculty of Medicine, Universidad Austral de Chile, Valdivia, Chile, ⁴Programa de Farmacología Molecular y Clínica, ICBM, Facultad de Medicina, Universidad de Chile, Santiago, Chile, ⁵Centro de Biotecnología y Bioingeniería (CeBiB), Departamento de Ingeniería Química, Biotecnología y Materiales, Facultad de Ciencias Físicas y Matemáticas, Universidad de Chile, Santiago, Chile

OPEN ACCESS

Edited by:

Francesco Moccia,
University of Pavia, Italy

Reviewed by:

Sungho Chang,
Seoul National University,
South Korea
Damien Keating,
Flinders University, Australia

*Correspondence:

Pablo Caviedes
pcaviede@med.uchile.cl
Ana M. Cárdenas
ana.cardenas@uv.cl

Received: 06 February 2018

Accepted: 12 June 2018

Published: 06 July 2018

Citation:

Vásquez-Navarrete J, Martínez AD, Ory S, Baéz-Matus X, González-Jamett AM, Brauchi S, Caviedes P and Cárdenas AM (2018) RCAN1 Knockdown Reverts Defects in the Number of Calcium-Induced Exocytotic Events in a Cellular Model of Down Syndrome. *Front. Cell. Neurosci.* 12:189. doi: 10.3389/fncel.2018.00189

In humans, Down Syndrome (DS) is a condition caused by partial or full trisomy of chromosome 21. Genes present in the DS critical region can result in excess gene dosage, which at least partially can account for DS phenotype. Although regulator of calcineurin 1 (RCAN1) belongs to this region and its ectopic overexpression in neurons impairs transmitter release, synaptic plasticity, learning and memory, the relative contribution of RCAN1 in a context of DS has yet to be clarified. In the present work, we utilized an *in vitro* model of DS, the CTb neuronal cell line derived from the brain cortex of a trisomy 16 (Ts16) fetal mouse, which reportedly exhibits acetylcholine release impairments compared to CNh cells (a neuronal cell line established from a normal littermate). We analyzed single exocytotic events by using total internal reflection fluorescence microscopy (TIRFM) and the vesicular acetylcholine transporter fused to the pH-sensitive green fluorescent protein (VACHT-pHluorin) as a reporter. Our analyses showed that, compared with control CNh cells, the trisomic CTb cells overexpress RCAN1, and they display a reduced number of Ca²⁺-induced exocytotic events. Remarkably, RCAN1 knockdown increases the extent of exocytosis at levels comparable to those of CNh cells. These results support a critical contribution of RCAN1 to the exocytosis process in the trisomic condition.

Keywords: down syndrome, exocytosis, cholinergic vesicles, RCAN1, trisomy 16, total internal reflection fluorescence microscopy, vesicular acetylcholine transporter, pHluorin

INTRODUCTION

Down Syndrome (DS), a condition caused by the presence of an extra copy of chromosome 21, is manifested by multiple abnormalities, the most prominent features being neurological and cognitive disabilities. Although cognitive impairments vary in DS individuals from mild to moderate, working memory, language and comprehension are the most greatly impaired functions

Abbreviations: DS, Down syndrome; DSCR1, Down syndrome critical region 1; NT, non-targeting siRNA; RCAN1, regulator of calcineurin 1; Ts16, trisomy 16; TIRFM, total internal reflection fluorescence microscopy; VACHT-pHluorin, vesicular acetylcholine transporter fused to the pH-sensitive green fluorescent protein.

compared to CNh cells (Figure 4), and to address its contribution to the regulation of exo/endocytosis, we reduced its expression by transfecting specific Rcan1 siRNAs. In this condition, Rcan1 abundance reached levels comparable to those observed in CNh cells. Interestingly, although Rcan1 knockdown in CTb cells did not affect spontaneous exocytosis, it increased the number of non-lateral diffusion events induced by ionomycin, reaching values similar to those of CNh cells. Therefore, as in chromaffin cells, our study indicates that Rcan1 is involved in the control of regulated exocytosis.

The effects of the Rcan1 overexpression on exocytosis in chromaffin cells seem to be a consequence of the chronic inhibition of calcineurin. Indeed, chronic exposure of chromaffin cells to calcineurin inhibitors reduced the total amount of exocytosis and impaired vesicle recycling (Zanin et al., 2013). Among the calcineurin substrates involved in vesicle recycling are dynamin, amphiphysin and synaptojanin (Cousin and Robinson, 2001). Of particular interest is dynamin, which in addition to its role in endocytosis, regulates exocytosis and vesicle recycling (González-Jamett et al., 2010, 2013; Moya-Díaz et al., 2016). Rcan1 also regulates, via calcineurin, the actin cytoskeleton dynamics by regulating cofilin phosphorylation (Wang et al., 2016), a protein that disassembles actin filaments (Maciver and Hussey, 2002; Pavlov et al., 2007; Pfaendtner et al., 2010). It is known that Rcan1 overexpression reduces the levels of active cofilin (Wang et al., 2016), and cofilin knockdown decreases G-actin/F-actin ratio (Hotulainen et al., 2005). Since actin plays critical roles at different stages of exocytosis (Porat-Shliom et al., 2013; Olivares et al., 2014) Rcan1 overexpression could have affected exocytosis in CTb cells by impairing actin remodeling. Interestingly, CTb cells exhibit increased F-actin/G-actin ratio when compared with CNh cells (Pérez-Núñez et al., 2016) and it has been observed that a reduced F-actin disassembly negatively impacts exocytosis (Meunier and Gutiérrez, 2016).

CONCLUSION

Hundreds of genes are overexpressed in DS (Hattori et al., 2000), which have a variable contribution to the phenotypes associated with the trisomic condition. Although the molecular mechanisms remain to be addressed, we found that the overexpression of

Rcan1 contributes to the reduced exocytosis function in the trisomic condition. Rcan1 knockdown is apparently sufficient to restore such impaired exocytosis, even when other genes of the DS critical region, such as the amyloid precursor protein and the DS cell adhesion molecule, are also overexpressed (Opazo et al., 2006; Rojas et al., 2008; Pérez-Núñez et al., 2016).

AUTHOR CONTRIBUTIONS

JV-N performed experiments and statistical analysis. AM designed and interpreted results. SO interpreted results and critically revised the manuscript. XB-M performed experiments. AG-J performed experiments and critically revised the manuscript. SB designed constructs, interpreted results and critically revised the manuscript. PC conceived the study, interpreted results and critically revised the manuscript. AC conceived the study, designed experiments, interpreted results and drafted the manuscript. All authors read and approved the final manuscript.

FUNDING

This work has been supported by the grants Fondo Nacional de Desarrollo Científico y Tecnológico (FONDECYT; Chile) 1130241 and 1160495, CONICYT for funding of Basal Centre, CeBiB, FB0001 and P09-022-F from ICM-ECONOMIA, Chile.

ACKNOWLEDGMENTS

JV-N was awarded with a CONICYT scholarship 22141340 for Master Degree studies. The Centro Interdisciplinario de Neurociencia de Valparaíso (CINV) is a Millennium Institute supported by the Millennium Scientific Initiative of the Ministerio de Economía, Fomento y Turismo.

SUPPLEMENTARY MATERIAL

The Supplementary Material for this article can be found online at: <http://www.frontiersin.org/articles/10.3389/fncel.2018.00189/full#supplementary-material>

REFERENCES

- Acuña, M. A., Pérez-Núñez, R., Noriega, J., Cárdenas, A. M., Bacigalup, J., Delgado, R., et al. (2012). Altered voltage dependent calcium currents in a neuronal cell line derived from the cerebral cortex of a trisomy 16 fetal mouse, an animal model of Down syndrome. *Neurotox. Res.* 22, 59–68. doi: 10.1007/s12640-011-9304-5
- Alabi, A. A., and Tsien, R. W. (2013). Perspectives on kiss-and-run: role in exocytosis, endocytosis and neurotransmission. *Annu. Rev. Physiol.* 75, 393–422. doi: 10.1146/annurev-physiol-020911-153305
- Albillos, A., Dernick, G., Horstmann, H., Almers, W., Alvarez de Toledo, G., and Lindau, M. (1997). The exocytotic event in chromaffin cells revealed by patch amperometry. *Nature* 389, 509–512. doi: 10.1038/39081
- Alés, E., Tabares, L., Poyato, J. M., Valero, V., Lindau, M., and Alvarez de Toledo, G. (1999). High calcium concentrations shift the mode of exocytosis to the kiss-and-run mechanism. *Nat. Cell Biol.* 1, 40–44. doi: 10.1038/9012
- Allen, D. D., Martin, J., Arriagada, C., Cárdenas, A. M., Rapoport, S. I., Caviedes, R., et al. (2000). Impaired cholinergic function in cell lines derived from the cerebral cortex of normal and trisomy 16 mice. *Eur. J. Neurosci.* 12, 3259–3364. doi: 10.1046/j.1460-9568.2000.00221.x
- Atluri, P. P., and Ryan, T. A. (2006). The kinetics of synaptic vesicle reacidification at hippocampal nerve terminals. *J. Neurosci.* 26, 2313–2320. doi: 10.1523/JNEUROSCI.4425-05.2006
- Belichenko, P. V., Kleschevnikov, A. M., Salehi, A., Epstein, C. J., and Mobley, W. C. (2007). Synaptic and cognitive abnormalities in mouse models of Down syndrome: exploring genotype-phenotype relationships. *J. Comp. Neurol.* 504, 329–345. doi: 10.1002/cne.21433
- Bowser, D. N., and Khakh, B. S. (2007). Two forms of single-vesicle astrocyte exocytosis imaged with total internal reflection fluorescence microscopy. *Proc. Natl. Acad. Sci. U S A* 104, 4212–4217. doi: 10.1073/pnas.0607625104

RESEARCH ARTICLE

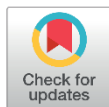
Calcium and cAMP directly modulate the speed of the *Drosophila* circadian clock

Angelina Palacios-Muñoz[‡], John Ewer^{*}

Centro Interdisciplinario de Neurociencia de Valparaíso, Facultad de Ciencias, Universidad de Valparaíso, Gran Bretaña 1111, Valparaíso, Chile

[‡] Current address: Departamento de Psiquiatría, Escuela de Medicina, Centro Interdisciplinario de Neurociencia, Pontificia Universidad Católica de Chile, Diagonal Paraguay 362, Santiago, Chile

^{*} john.ewer@uv.cl



Abstract

Circadian clocks impose daily periodicities to animal behavior and physiology. At their core, circadian rhythms are produced by intracellular transcriptional/translational feedback loops (TTFL). TTFLs may be altered by extracellular signals whose actions are mediated intracellularly by calcium and cAMP. In mammals these messengers act directly on TTFLs via the calcium/cAMP-dependent transcription factor, CREB. In the fruit fly, *Drosophila melanogaster*, calcium and cAMP also regulate the periodicity of circadian locomotor activity rhythmicity, but whether this is due to direct actions on the TTFLs themselves or are a consequence of changes induced to the complex interrelationship between different classes of central pacemaker neurons is unclear. Here we investigated this question focusing on the peripheral clock housed in the non-neuronal prothoracic gland (PG), which, together with the central pacemaker in the brain, controls the timing of adult emergence. We show that genetic manipulations that increased and decreased the levels of calcium and cAMP in the PG caused, respectively, a shortening and a lengthening of the periodicity of emergence. Importantly, knockdown of CREB in the PG caused an arrhythmic pattern of eclosion. Interestingly, the same manipulations directed at central pacemaker neurons caused arrhythmicity of eclosion and of adult locomotor activity, suggesting a common mechanism. Our results reveal that the calcium and cAMP pathways can alter the functioning of the clock itself. In the PG, these messengers, acting as outputs of the clock or as second messengers for stimuli external to the PG, could also contribute to the circadian gating of adult emergence.

OPEN ACCESS

Citation: Palacios-Muñoz A, Ewer J (2018) Calcium and cAMP directly modulate the speed of the *Drosophila* circadian clock. PLoS Genet 14(6): e1007433. <https://doi.org/10.1371/journal.pgen.1007433>

Editor: Paul H. Taghert, Washington University in Saint Louis School of Medicine, UNITED STATES

Received: March 26, 2018

Accepted: May 18, 2018

Published: June 7, 2018

Copyright: © 2018 Palacios-Muñoz, Ewer. This is an open access article distributed under the terms of the [Creative Commons Attribution License](https://creativecommons.org/licenses/by/4.0/), which permits unrestricted use, distribution, and reproduction in any medium, provided the original author and source are credited.

Data Availability Statement: All relevant data are within the paper and its Supporting Information files.

Funding: This work was supported by the Comisión Nacional de Investigación Científica y Tecnológica (CONICYT; <http://www.conicyt.cl/>) doctoral scholarship (#24110076) to APM, Fondo Nacional de Desarrollo Científico y Tecnológico (FONDECYT; <http://www.conicyt.cl/fondecyt/>) postdoctoral grant (#3160177) to APM, and Fondo Nacional de Desarrollo Científico y Tecnológico (FONDECYT; <http://www.conicyt.cl/fondecyt/>) grant

Author summary

Circadian clocks impose daily periodicities to animal behavior and physiology. At their core, circadian rhythms are produced by intracellular transcriptional/translational feedback loops (TTFL). TTFLs may be altered by extracellular signals whose actions are mediated intracellularly by calcium and cAMP. In *Drosophila*, calcium and cAMP levels affect the periodicity of *Drosophila* circadian rhythms, but whether this is due to direct actions on the TTFLs themselves or is a consequence of changes induced to the complex interrelationship between different classes of central pacemaker neurons is unclear. Here we used

corresponding MESA analyses of timecourse of eclosion behavior of animals expressing *Epac1* sensor in the PG (a); records of controls are shown below: *phm-gal4* driver (b) and *UAS-Epac1* sensor alone (c). (B) Free-running periodicity values for genotypes shown in (A); each circle indicates results from separate experiments; average is indicated by horizontal line; same letters indicate no statistically different groups (one-way ANOVA, Tukey's *post hoc* multiple comparison analyses). (C) Average rhythmicity index (RI) values (\pm SEM) for genotypes shown in (A); numbers in parenthesis indicate number of separate experiments; same letters indicate no statistically different groups (one-way ANOVA, Tukey's *post hoc* multiple comparison analyses). (D) Representative records of adult locomotor activity in DD (left) and Auto-correlation analyses (right) of normal (*per*⁺) fly expressing *Epac1* sensor in the PG (a) and of *per*⁰¹ adult expressing *Epac1* sensor in the PG (b). (E) Free-running period values for results shown in (D); each circle indicates individual flies tested; average is indicated by horizontal line. (F) Average (\pm SEM) RI, ****p*<0.0001 (two-tailed Student *t*-test with confidence interval of 95%). Numbers in parenthesis indicate total number of flies tested. (TIF)

Acknowledgments

We thank Julie Simpson for UAS-GCaMP3.2 calcium sensor and Paul Taghert for UAS-*Epac1* cAMP sensor, and for *pdf-GAL4* and *tim-GAL4* drivers.

Author Contributions

Conceptualization: Angelina Palacios-Muñoz, John Ewer.

Data curation: Angelina Palacios-Muñoz, John Ewer.

Formal analysis: Angelina Palacios-Muñoz, John Ewer.

Funding acquisition: John Ewer.

Investigation: Angelina Palacios-Muñoz, John Ewer.

Methodology: Angelina Palacios-Muñoz, John Ewer.

Project administration: John Ewer.

Resources: John Ewer.

Supervision: John Ewer.

Validation: Angelina Palacios-Muñoz.

Writing – original draft: Angelina Palacios-Muñoz, John Ewer.

Writing – review & editing: Angelina Palacios-Muñoz, John Ewer.

References

1. Takahashi JS (2017) Transcriptional architecture of the mammalian circadian clock. *Nat Rev Genet* 18: 164–179. <https://doi.org/10.1038/nrg.2016.150> PMID: 27990019
2. Hardin PE (2011) Molecular genetic analysis of circadian timekeeping in *Drosophila*. *Adv Genet* 74: 141–173. <https://doi.org/10.1016/B978-0-12-387690-4.00005-2> PMID: 21924977
3. Frenkel L, Muraro NI, Beltran Gonzalez AN, Marcora MS, Bernabo G, et al. (2017) Organization of Circadian Behavior Relies on Glycinergic Transmission. *Cell Rep* 19: 72–85. <https://doi.org/10.1016/j.celrep.2017.03.034> PMID: 28380364

Please cite this article in press as: Carrasquel-Ursulaez et al., Determination of the Stoichiometry between α - and γ 1 Subunits of the BK Channel Using LRET, Biophysical Journal (2018), <https://doi.org/10.1016/j.bpj.2018.04.008>

Biophysical Journal

Biophysical Letter



Determination of the Stoichiometry between α - and γ 1 Subunits of the BK Channel Using LRET

Willy Carrasquel-Ursulaez,¹ Osvaldo Alvarez,^{1,2} Francisco Bezanilla,^{1,3,4} and Ramon Latorre^{1,*}

¹Centro Interdisciplinario de Neurociencia de Valparaíso, Universidad de Valparaíso, Valparaíso, Chile; ²Departamento de Biología, Facultad de Ciencias, Universidad de Chile, Santiago, Chile; ³Department of Biochemistry and Molecular Biology and ⁴Institute for Biophysical Dynamics, University of Chicago, Chicago, Illinois

ABSTRACT Two families of accessory proteins, β and γ , modulate BK channel gating and pharmacology. Notably, in the absence of internal Ca^{2+} , the γ 1 subunit promotes a large shift of the BK conductance-voltage curve to more negative potentials. However, very little is known about how α - and γ 1 subunits interact. In particular, the association stoichiometry between both subunits is unknown. Here, we propose a method to answer this question using lanthanide resonance energy transfer. The method assumes that the kinetics of lanthanide resonance energy transfer-sensitized emission of the donor double-labeled α/γ 1 complex is the linear combination of the kinetics of the sensitized emission in single-labeled complexes. We used a lanthanide binding tag engineered either into the α - or the γ 1 subunits to bind Tb^{3+} as the donor. The acceptor (BODIPY) was attached to the BK pore-blocker iberiotoxin. We determined that γ 1 associates with the α -subunit with a maximal 1:1 stoichiometry. This method could be applied to determine the stoichiometry of association between proteins within heteromultimeric complexes.

BK channels are homotetramers of the pore-forming α -subunit, which is broadly expressed in mammal tissues and its distinctive physiological function is to dampen the effects of the cytosolic increase of Ca^{2+} concentration due to the opening of voltage-dependent Ca^{2+} channels (1–4). Although BK channels are coded by a single gene (*KCNMA1*), they display a remarkable functional diversity, largely due to their interaction with accessory subunits. Two families of BK channel accessory subunits, the β -family (β 1– β 4) (5–8) and the γ -family (γ 1– γ 4) (9,10), confer new and physiological relevant phenotypes to the BK channel. Within the γ -family, the most remarkable effects are produced by the γ 1 subunit (9). This accessory subunit greatly increases the allosteric coupling between voltage sensors and pore, shifting the conductance-voltage (G-V) curve >150 mV to the left along the voltage axis (9,10).

Although the structure of the *Aplysia* BK channel was determined by the cryo-electron microscopy technique (11,12), little is known about the detailed structure of the accessory subunits beyond their secondary structure and putative membrane topology (10,13). Regarding the stoichiometry between the α -subunit and its accessory subunits, it is known that the tetramer formed by α can hold from one to

four β 1 or β 2 subunits (14). However, the stoichiometry between α - and any of the γ -subunits is unknown at present. Interestingly, the γ 1 subunit displays an all-or-none effect on the BK channel. However, there is not a definite test of how many γ 1 subunits are necessary to cause this effect (15).

Lanthanide resonance energy transfer (LRET) technique, together with symmetric nanopositioning system (SNPS) analysis (16), have been previously used to study conformational changes in ion channels in response to a stimulus like, for example, a change in membrane voltage (16,17). LRET/SNPS calculates the positions of terbium ions chelated by lanthanide binding tag (LBT) motifs (18), which are strategically inserted in different positions of the protein of interest. In the case of β 1, LRET/SNPS was used to determine the structural rearrangements due to the interaction between the α - with β 1 subunits (19). Given the tetrameric structure of BK, the LBT-labeled channel contains four LBT- Tb^{3+} donors interacting with a single toxin-BODIPY acceptor. Two alternatives strategies were used to study the ($\alpha + \beta$ 1)BK channel complex (19). In the first approach, the α -subunits were LBT-labeled to explore the Tb^{3+} positions in the absence and the presence of β 1 subunit. In the second strategy, β 1 was LBT-labeled to determine its position relative to the α -subunit. In both cases, because the acceptor is located outside the center of symmetry of the channel, there are four different donor-acceptor distances. Therefore, one way to analyze the LRET/SNPS results is

Submitted February 12, 2018, and accepted for publication April 5, 2018.

*Correspondence: ramon.latorre@uv.cl

Editor: William Kobertz.

<https://doi.org/10.1016/j.bpj.2018.04.008>

© 2018 Biophysical Society.

Please cite this article in press as: Carrasquel-Ursulaez et al., Determination of the Stoichiometry between α - and γ 1 Subunits of the BK Channel Using LRET, Biophysical Journal (2018), <https://doi.org/10.1016/j.bpj.2018.04.008>

Biophysical Letter

ACKNOWLEDGMENTS

We thank Mrs. Luisa Soto and Mrs. Victoria Prado (University of Valparaíso) for technical assistance.

This research was supported by The National Fund for Scientific and Technological Development (FONDECYT) grant 1150273 and the US Air Force Office of Scientific Research (AFOSR) under award No. FA9550-16-1-0384 to R.L.; Anillo Grant ACT-1107; and National Institutes of Health grants GM030376 and U54GM087519 to F.B. The Centro Interdisciplinario de Neurociencia de Valparaíso is a Millennium Institute supported by the Millennium Scientific Initiative of the Chilean Ministry of Economy, Development, and Tourism (P029-022-F).

SUPPORTING CITATIONS

Reference (24) appears in the Supporting Material.

REFERENCES

- Contreras, G. F., K. Castillo, ..., R. Latorre. 2013. A BK (Slo1) channel journey from molecule to physiology. *Channels (Austin)*. 7:442–458.
- Cui, J., H. Yang, and U. S. Lee. 2009. Molecular mechanisms of BK channel activation. *Cell. Mol. Life Sci.* 66:852–875.
- Latorre, R., and S. Brauchi. 2006. Large conductance Ca^{2+} -activated K^+ (BK) channel: activation by Ca^{2+} and voltage. *Biol. Res.* 39:385–401.
- Latorre, R., K. Castillo, ..., O. Alvarez. 2017. Molecular determinants of BK channel functional diversity and functioning. *Physiol. Rev.* 97:39–87.
- Orio, P., P. Rojas, ..., R. Latorre. 2002. New disguises for an old channel: MaxiK channel β -subunits. *News Physiol. Sci.* 17:156–161.
- Sun, X., M. A. Zaydman, and J. Cui. 2012. Regulation of voltage-activated K^+ channel gating by transmembrane β subunits. *Front. Pharmacol.* 3:63.
- Toro, L., M. Wallner, ..., Y. Tanaka. 1998. Maxi-K(Ca), a unique member of the voltage-gated K channel superfamily. *News Physiol. Sci.* 13:112–117.
- Torres, Y. P., F. J. Morera, ..., R. Latorre. 2007. A marriage of convenience: β -subunits and voltage-dependent K^+ channels. *J. Biol. Chem.* 282:24485–24489.
- Yan, J., and R. W. Aldrich. 2012. BK potassium channel modulation by leucine-rich repeat-containing proteins. *Proc. Natl. Acad. Sci. USA.* 109:7917–7922.
- Yan, J., and R. W. Aldrich. 2010. LRRC26 auxiliary protein allows BK channel activation at resting voltage without calcium. *Nature.* 466:513–516.
- Hite, R. K., X. Tao, and R. MacKinnon. 2017. Structural basis for gating the high-conductance Ca^{2+} -activated K^+ channel. *Nature.* 541:52–57.
- Tao, X., R. K. Hite, and R. MacKinnon. 2017. Cryo-EM structure of the open high-conductance Ca^{2+} -activated K^+ channel. *Nature.* 541:46–51.
- Knaus, H. G., K. Folander, ..., R. Swanson. 1994. Primary sequence and immunological characterization of β -subunit of high conductance Ca^{2+} -activated K^+ channel from smooth muscle. *J. Biol. Chem.* 269:17274–17278.
- Wang, Y. W., J. P. Ding, ..., C. J. Lingle. 2002. Consequences of the stoichiometry of Slo1 α and auxiliary β subunits on functional properties of large-conductance Ca^{2+} -activated K^+ channels. *J. Neurosci.* 22:1550–1561.
- Gonzalez-Perez, V., X. M. Xia, and C. J. Lingle. 2014. Functional regulation of BK potassium channels by γ 1 auxiliary subunits. *Proc. Natl. Acad. Sci. USA.* 111:4868–4873.
- Hyde, H. C., W. Sandtner, ..., F. Bezanilla. 2012. Nano-positioning system for structural analysis of functional homomeric proteins in multiple conformations. *Structure.* 20:1629–1640.
- Kubota, T., T. Durek, ..., A. M. Correa. 2017. Mapping of voltage sensor positions in resting and inactivated mammalian sodium channels by LRET. *Proc. Natl. Acad. Sci. USA.* 114:E1857–E1865.
- Nitz, M., M. Sherawat, ..., B. Imperiali. 2004. Structural origin of the high affinity of a chemically evolved lanthanide-binding peptide. *Angew. Chem. Int. Engl.* 43:3682–3685.
- Castillo, J. P., J. E. Sánchez-Rodríguez, ..., R. Latorre. 2016. β 1-subunit-induced structural rearrangements of the Ca^{2+} - and voltage-activated K^+ (BK) channel. *Proc. Natl. Acad. Sci. USA.* 113:E3231–E3239.
- Takahashi, T., E. Neher, and B. Sakmann. 1987. Rat brain serotonin receptors in *Xenopus* oocytes are coupled by intracellular calcium to endogenous channels. *Proc. Natl. Acad. Sci. USA.* 84:5063–5067.
- Posson, D. J., P. Ge, ..., P. R. Selvin. 2005. Small vertical movement of a K^+ channel voltage sensor measured with luminescence energy transfer. *Nature.* 436:848–851.
- Posson, D. J., and P. R. Selvin. 2008. Extent of voltage sensor movement during gating of SHAKER K^+ channels. *Neuron.* 59:98–109.
- Heyduk, T., and E. Heyduk. 2001. Luminescence energy transfer with lanthanide chelates: interpretation of sensitized acceptor decay amplitudes. *Anal. Biochem.* 289:60–67.
- Cox, D. H., J. Cui, and R. W. Aldrich. 1997. Allosteric gating of a large conductance Ca -activated K^+ channel. *J. Gen. Physiol.* 110:257–281.



Contents lists available at ScienceDirect

Spectrochimica Acta Part A: Molecular and Biomolecular Spectroscopy

journal homepage: www.elsevier.com/locate/saa

IR and NMR spectroscopic correlation of enterobactin by DFT

M. Moreno^{a,*}, A. Zacarias^b, A. Porzel^c, L. Velasquez^d, G. Gonzalez^{e,f}, M. Alegría-Arcos^{g,h}, F. Gonzalez-Nilo^g, E.K.U. Gross^b^a University of the Basque Country, Barrio Sarriena, s/n, 48940 Leioa, Bizkaia, Spain^b Max Planck Institute of Microstructure Physics, Weinberg 2, D 06120, Halle, Germany and ETSF^c Leibniz Institute of Plant Biochemistry, Weinberg 3, D 06120 Halle, Germany^d Universidad Andres Bello, Facultad de Medicina, Center for Integrative Medicine and Innovative Science, Echaurren 183, Santiago, Chile^e Center for Development of Nanoscience and Nanotechnology, CEDENNA, Casilla 653, Santiago, Chile^f Universidad de Chile, Facultad de Ciencias, Departamento de Química, Laboratorio de Síntesis Inorgánica y electroquímica, Las Palmeras 3425, Nuñoa, Santiago, Chile^g Universidad Andres Bello, Facultad de Ciencias Biológicas, Center for Bioinformatic and Integrative Biology, Av Republica 239, Santiago, Chile^h Centro Interdisciplinario de Neurociencias de Valparaíso (CINV), Facultad de Ciencias, Universidad de Valparaíso, Valparaíso, Chile

ARTICLE INFO

Article history:

Received 19 July 2017

Received in revised form 19 January 2018

Accepted 22 February 2018

Available online 2 March 2018

Keywords:

Enterobactin

NMR

FT-IR

DFT

MALDI-TOF MS

ABSTRACT

Emerging and re-emerging epidemic diseases pose an ongoing threat to global health. Currently, Enterobactin and Enterobactin derivatives have gained interest, owing to their potential application in the pharmaceutical field. As it is known [J. Am. Chem. Soc. (1979) 101, 20, 6097–6104], Enterobactin (H₆EB) is an efficient iron carrier synthesized and secreted by many microbial species. In order to facilitate the elucidation of enterobactin and its analogues, here we propose the creation of a H₆EB standard set using Density Functional Theory Infrared (IR) and NMR spectra. We used two exchange-correlation (xc) functionals (PBE including long-range corrections—LC-PBE— and mPW1), 2 basis sets (QZVP and 6-31G(d)) and 2 grids (fine and ultrafine) for most of the H₆EB structures dependent of dihedral angles. The results show a significant difference between the O—H and N—H bands, while the C=O amide and O—(C=O)— IR bands are often found on top of each other. The NMR DFT calculations show a strong dependence on the xc functional, basis set, and grid used for the H₆EB structure. Calculated ¹H and ¹³C NMR spectra enable the effect of the solvent to be understood in the context of the experimental measurements. The good agreement between the experimental and the calculated spectra using LC-PBE/QZVP and ultra-fine grid suggest the possibility of the systems reported here to be considered as a standard set. The dependence of electrostatic potential and frontier orbitals with the catecholamide dihedral angles of H₆EB is described. The matrix-assisted laser desorption/ionization time of the flight mass spectrometry (MALDI-TOF MS) of H₆EB is also reported of manner to enrich the knowledge about its reactivity.

© 2018 The Authors. Published by Elsevier B.V. This is an open access article under the CC BY-NC-ND license (<http://creativecommons.org/licenses/by-nc-nd/4.0/>).

1. Introduction

Siderophores in general, are efficient iron carriers synthesized and secreted by microbial species [1,2]. The Siderophore Enterobactin (H₆EB) is a C₃-symetric triscatechol composed of a backbone of a trilactone ring and three catecholate units attached through amide linkages (Fig. 1). The catecholate units embed the guest ion in an octahedral cavity, leaving a partially free amide group [1]. Its particular conformation allows a high iron-binding affinity and ion carrier (log K_f: 51) [1]. Catecholates are among nature's most sophisticated structures that are found in granular cuticles of marine mussels, flavonoids, plant enzymes and hormone neurotransmitters. Mimicking these natural structures has led to the synthesis of advanced materials, such as catalytic surfaces, polymeric resins, biosensors, dyes and fuel cells [3,4], as well

as modified complex molecules with potential medical applications like the Enterobactin [5,6].

Commonly, all Fe-siderophore complexes require an active protein transport, FepA is a channel protein composed of an N-terminal gate protein and a β-barrel [7]. FepA is connected to an outer membrane receptor (TonB-dependent receptor), which extends into the periplasm. The final step requires the Fe-Enterobactin (FeH₆EB) to be carried through the periplasmic by FepB, which is connected to FepD and FepG cytoplasmic transmembrane proteins, which deliver it through an ATPase to FepC, which provides energy to assist with its uptake through the inner membrane [8,9]. In 2003, R. Chakraborty et al [10] reported that triccatechols are required to be recognized by FepA, making their spectroscopic details relevant for ferric catecholamide analogs of Enterobactin, owing to their potential applications in the pharmaceutical field [11]. Later in 2008, K.N. Raymond [12] illustrate that siderocalin binds both bare and ferric siderophores in order to intercept the delivery of iron to the bacteria, impeding in this manner their virulence.

* Corresponding author.

E-mail address: mmoreno043@ikasle.ehu.es (M. Moreno).

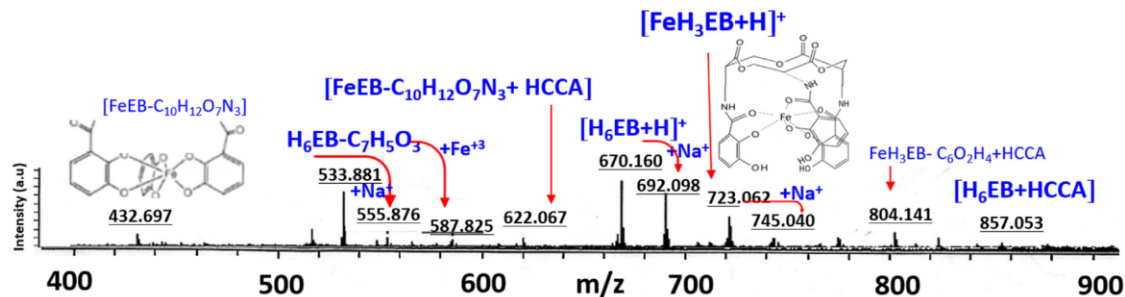


Fig. 18. MALDI-TOF MS spectra of $[\text{FeH}_3\text{Enterobactin}]^0$ (FeH_3EB).

with a slope and a correlation factor (R^2) of 1.017 and 0.998, respectively, with an SD of 7.13 cm^{-1} (see Fig. 17). The data here obtained, allows also to localize the N—H and O—H fingerprint regions ($1500\text{--}400 \text{ cm}^{-1}$) and although it is complicated by the large number of different vibrational modes that occur here, and under the conditions in which the theoretical IR were performed (gas phase, low temperature), we can “highlight” that the calculated N—H and O—H fingerprints at 1396.55 , 1181.15 , 895.47 , 754.06 and 652.43 cm^{-1} corresponds exclusively to N—H, while 1332.90 , 980.66 , 793.27 , 695.61 and 562.56 overlapped with OH bands and 1224.43 , 1126.23 , 1040.44 , 858.27 cm^{-1} for OH bands, match with those reported for L-D serine and catechol group bands [16,6], see video SI. Experimental and calculated FeH_3EB IR was also performed of manner to support the suitability of this study. Figures from S10 to S12 in SI reveal similitude between H_6EB and FeEB IR spectrums for both experimental and calculated. IR theoretical study of FeEnterobactin , with Fe, linked to different donor groups will be published elsewhere. FeEnterobactin (FeH_3EB) was purchased in Genaxxon Bioscience GmbH and the measurement conditions for IR and MALDI-TOF-MS were similar to H_6EB . The utility of the IR calculation at solvent-free is that this offers an almost accurate correlation with experimental IR spectra which also is obtained using solvent-free environment, this allows predict the reactivity of H_6EB with chemical reagent in gas phase at room temperature by advanced processes of functionalization as those based on vapour phase metalation (VPM) process at room temperature.

4.4. FeH_3EB MALDI-TOF MS Spectra Analysis

Work in progress of the FeH_3EB compound shows (see spectrum displayed in Fig. 18) a good agreement for the most abundant isotope localized at 723.062 m/z , with a calculated value of 723.414 m/z for $[\text{FeH}_3\text{EB} + \text{H}]^+$, this allows iron to be designed in the triprotonated salicylate conformation (Fe linked at C4,4',4'' and C6,6',6'') rather than in the six-unprotonated catecholate conformation, with a calculated value of 719.382 m/z (Fe linked at C7,7',7'' and C6,6',6''), which is common in the liquid state. Similar catechols are linked to Fe, and a novel form of fragmenting is observed at 432.697 m/z , with a calculated value of 433.188 m/z ; this is designated here as $[\text{FeEB-C}_{10}\text{H}_{12}\text{O}_7\text{N}_3]$, which considers the loss of the crown ester skeleton with the amide group, forcing Fe to move to C7—C6 rather than the C4—C6 position and changing its preference to the catecholate conformation. At 622.067 m/z , the existence of the same fragment mixture as HCCA can be confirmed, designated here as $[\text{FeEB-C}_{10}\text{H}_{12}\text{O}_7\text{N}_3 + \text{HCCA}]$, with a calculated value of 622.328 m/z . The expected cleavage is also seen at 587.825 m/z and 804.141 m/z with the loss of catechol and catechol + carbonyls groups, with calculated values of 587.301 and 804.492 m/z for $[\text{FeH}_3\text{EB-C}_7\text{H}_5\text{O}_3]$ and $[\text{FeH}_3\text{EB-C}_6\text{H}_5\text{O}_2]$, respectively. Details in Fig. S13 in SI.

5. Conclusions

MALDI-TOF MS spectra reveal a marked difference in the reactivity of H_6EB when matrix-assisted laser desorption/ionization-time is used. Specifically, we emphasize the fragmentation change when H_6EB is linked to iron, passing the incision selectivity since the amide group in H_6EB to C4 and C5 in FeH_3EB . This is rational considering that FeH_3EB contains Fe coordinated to O4,4',4'' and O6,6',6''. The results show significant differences between the O—H and N—H bands, and the C=O amide and O—C(=O) IR bands which are often on top of each other. The NMR DFT calculations reported here show a strong dependence of the exchange-correlation functional, basis set, grid and the dihedral angles considered in H_6EB structure. Thus, the good agreement between both IR and NMR spectra for the xc LC-PBE functional with QZVP basis set using ultrafine grid of both H_6EB structure-1 and average with the experimental results compared with the others DFT methods (mPW91/QZVP and mPW91/6-31G(d)) here utilized, in spite of the absence of solvent, our results allowed to consider that the calculated IR spectra and ^1H and ^{13}C chemical shifts form a reliable standard set for the spectroscopic characterization of Enterobactin systems.

Supplementary data to this article can be found online at <https://doi.org/10.1016/j.saa.2018.02.060>.

Funding Sources

Lamellar Nanostructure and BioNanomedicine groups of the Center for the Development of Nanoscience and Nanotechnology (CEDENNA) Chile, and the Max Planck Institute for Microstructure Physics. ACT-1107 Project titled “Integration of Structural Biology to the development of Bionanotechnology” funded by CONICYT Chile. FGN acknowledge the support of FONDECYT Grant 1170733 and MAA is funded by CONICYT PCHA/Doctorado Nacional 2017-21172039 fellowship. The Centro Interdisciplinario de Neurociencia.

Notes

This research began during M.A. Moreno's time in Dr. M. Knez's group at Experimental Department II of the Max Planck Institute for Microstructure Physics in 2011.

Acknowledgment

We thank Prof. Dr. Peter Fratzl, acting Director of the Experimental Department 2 from the Max Planck Institute of Microstructure Physics, Dr. M. Knez, from CIC-Nanogune and the Computer facilities of the Max Planck Institute for Microstructure Physics and the CBIB of Universidad Andres Bello.



Role of calcium permeable channels in dendritic cell migration

Pablo J Sáez^{1,2}, Juan C Sáez^{3,4}, Ana-María Lennon-Duménil⁵ and Pablo Vargas^{1,2}



Calcium ion (Ca^{2+}) is an essential second messenger involved in multiple cellular and subcellular processes. Ca^{2+} can be released and sensed globally or locally within cells, providing complex signals of variable amplitudes and time-scales. The key function of Ca^{2+} in the regulation of actin-myosin contractility has provided a simple explanation for its role in the regulation of immune cell migration. However, many questions remain, including the identity of the Ca^{2+} stores, channels and upstream signals involved in this process. Here, we focus on dendritic cells (DCs), because their immune sentinel function heavily relies on their capacity to migrate within tissues and later on between tissues and lymphoid organs. Deciphering the mechanisms by which cytoplasmic Ca^{2+} regulate DC migration should shed light on their role in initiating and tuning immune responses.

Addresses

¹ Institut Curie, PSL Research University, CNRS, UMR144, F-75005, France

² Institut Pierre-Gilles de Gennes, PSL Research University, F-75005, France

³ Departamento de Fisiología, Facultad de Ciencias Biológicas, Pontificia Universidad Católica, Santiago 6513677, Chile

⁴ Instituto Milenio, Centro Interdisciplinario de Neurociencias de Valparaíso, Valparaíso 2360103, Chile

⁵ Institut Curie, PSL Research University, INSERM, U932, F-75005, France

Corresponding authors: Sáez, Pablo J (pablo.saez@curie.fr), Vargas, Pablo (pablo.vargas@curie.fr)

Current Opinion in Immunology 2018, 52:74–80

This review comes from a themed issue on **Special section on ion channels and immune cells**

Edited by **Pablo Pelegrín** and **Florence Velge-Roussel**

<https://doi.org/10.1016/j.coi.2018.04.005>

0952-7915/© 2018 Published by Elsevier Ltd.

Introduction

Calcium ion (Ca^{2+}) is a ubiquitous and highly versatile second messenger, which plays a crucial role in many cellular functions [1]. Increases in free cytosolic Ca^{2+} trigger a series of cellular responses, including signaling, intracellular trafficking, non-muscular myosin IIA (MyoII)-

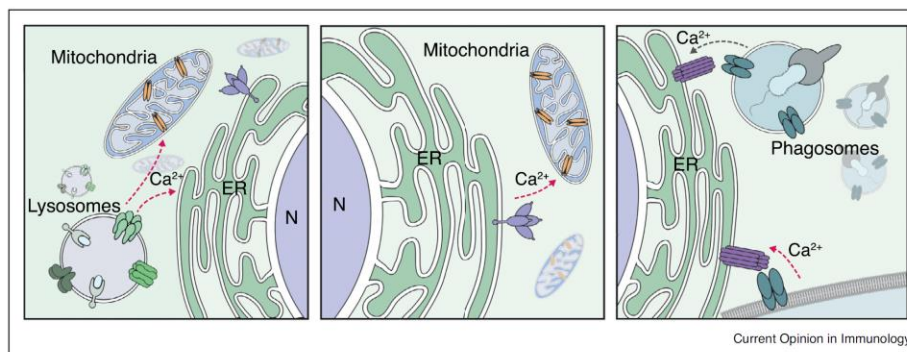
induced contractility, actin reorganization and cell migration [2–4]. The rise in free cytosolic Ca^{2+} occurs either by influx from the extracellular microenvironment or release from intracellular Ca^{2+} stores. Remarkably, each Ca^{2+} response is an encrypted message with specific speed, amplitude and spatio-temporal pattern that cells decode to transform in a coordinated function [5]. Cell migration is one of the key functions in which Ca^{2+} signaling plays a pivotal role [3]. During this process, rises in the free cytosolic Ca^{2+} concentration are integrated by the cells triggering MyoII-mediated contractility, resulting in fast cell locomotion [3]. MyoII activity is particularly important for migration of leukocytes in tissues [6], as its activation facilitates fast cell migration in confined geometries [7]. However, how leukocytes integrate distinct Ca^{2+} signals is not well understood. In particular, how cell motility is coordinated based on mobilization of Ca^{2+} from different compartments remains unsolved. This phenomenon might be particularly important in tissues, in which the complex physical and chemical properties of the microenvironment can trigger a diversity of Ca^{2+} -dependent responses.

Among leukocytes, dendritic cell (DC) migration plays a pivotal role in the initiation of adaptive immune responses [8]. During inflammation, DCs migrate from damaged or infected tissues to lymph nodes (LNs) in order to activate T cells, the effectors of the adaptive immune system. At the cellular level, homing of DCs to lymphoid tissues is a complex multistep process during which cells adapt to the dynamic properties of the microenvironment [7]. These steps include DC migration in the interstitial space of tissues, chemotaxis, the passage through the tight endothelium and the final colonization of the target organ. Ca^{2+} signaling is required for a plethora of functions in DCs, to explore them we recommend the following articles [9–11]. In this review, we focus on the role of Ca^{2+} signaling in the various steps of DC migration from peripheral tissues to LNs. More precisely, we will discuss recent advances on the role of Ca^{2+} release from different stores in the coordination of DC motility. We will further analyze the mechanical responses of DCs to microenvironmental changes, to finally provide a perspective on the role of Ca^{2+} dynamics in the coordination of immune responses.

Tissue exploration

Immature DCs (iDCs) randomly patrol tissues in search for danger signals [8]. Owing to the complexity of

Figure 2



Inter-organelle communication. Closely apposed organelles allow communication between different Ca^{2+} stores that in migratory cells have a specific intracellular organization and might be essential to modulate the migratory features of dendritic cells. *Left:* At the cell rear Ca^{2+} release from the lysosomes via transient receptor potential-mucolipin 1 channel (TRPML1) or transient receptor potential cation member 2 (TRPM2) channel might be quickly taken up by the endoplasmic reticulum (ER, pumps are not shown) or mitochondria (mitochondrial Ca^{2+} uniporter, MCU). *Middle:* Mitochondria located at the cell front can also interact with the ER, regulating local Ca^{2+} release via inositol-trisphosphate receptor (IP_3R) to locally modulate cell signaling. *Right:* During store-operated Ca^{2+} entry (SOCE), the ER resident protein stromal interaction molecules (STIM) bind CRAC channels located in the plasma membrane allowing Ca^{2+} influx and consequent refilling of the ER. In addition, at the cell front fusion of phagosomes with the ER triggers local Ca^{2+} signaling through CRAC channels. Arrows indicate the Ca^{2+} flux direction.

Furthermore, unlike DCs, T cells stop with increases in the cytosolic Ca^{2+} [63,64]. An interesting hypothesis is that during the immune response the cell-cell Ca^{2+} transfer via gap junctions from DCs to T cells [34,65,66], might be a stop signal to stabilize immune synapses in LNs [67].

Future challenges concern the visualization of Ca^{2+} dynamics in migrating DCs. Indeed, the lack of transgenic mice and the fact that fluorescent Ca^{2+} probes might directly affect cell migration [68], has hampered the analysis of Ca^{2+} dynamics at various spatio-temporal scales in DCs. The development of new tools to study Ca^{2+} signaling during DC migration, as it happened in other leukocytes [69,70], shall therefore help the field moving forward.

Concluding remarks

In the present review, we summarize the complexity of the Ca^{2+} code for the regulation of DC migration at different stages of the immune response. Ca^{2+} stores differentially contribute to increments in the cytosolic Ca^{2+} concentration, generating responses that depend on the cellular state [71]. While iDCs rely mostly in Ca^{2+} from the ER for cell motility, mDCs required Ca^{2+} from the lysosomes, although membrane channels also contribute depending on the stimulus. This differential response is probably linked to the different functions of these cells. At the immature state, DCs are dedicated to antigen internalization, function that can lead to the interaction of nascent phagosomes with the ER to regulate antigen

processing. The use of ER as store for the regulation of cell motility in iDCs might serve to couple both functions, helping to coordinate the early events of the immune response. On the other side, mDCs are specialized in antigen presentation, which occurs upon degradation of the ingested particles in lysosomes and the consequent generation of antigenic peptides. The use of this store to control cell motility might allow the coupling of antigen presentation with the homing of mDCs to the LNs, favoring the specific migration of cells endowed with the potential to mount immune responses. Once at the LNs, cell-cell communication mechanisms, such as gap junction channels, might allow Ca^{2+} transfer from mDCs to T cells, contributing to their efficient activation. We hypothesize that the fine regulation of Ca^{2+} release from intracellular stores generates a precise Ca^{2+} code, which is required to coordinate the multiple cellular functions leading to the spatio-temporal organization of immune responses.

Conflict of interest

No conflict of interest.

References and recommended reading

Papers of particular interest, published within the period of review, have been highlighted as:

- of special interest
 - of outstanding interest
1. Berridge MJ: **The inositol trisphosphate/calcium signaling pathway in health and disease.** *Physiol Rev* 2016, **96**:1261-1296.

Anionic Carbosilane Dendrimers Destabilize the GP120-CD4 Complex Blocking HIV-1 Entry and Cell to Cell Fusion

Carlos Guerrero-Beltrán,^{†,•,§,¶,||} Ignacio Rodríguez-Izquierdo,^{†,•,§} Ma Jesús Serramia,^{†,•} Ingrid Araya-Durán,^{§,□,||} Valeria Márquez-Miranda,^{§,□,||} Rafael Gómez,^{‡,§,¶,||} Francisco Javier de la Mata,^{‡,§,¶,||} Manuel Leal,^{■,▽} Fernando González-Nilo,^{§,□,||} and M. Angeles Muñoz-Fernández^{*,†,•,§,¶,||}

[†]Laboratorio Inmunobiología Molecular, Hospital General Universitario Gregorio Marañón and Instituto de Investigación Sanitaria Gregorio Marañón (IISGM), 28007 Madrid, Spain

[•]Spanish HIV HGM BioBank, 28009 Madrid, Spain

[‡]Plataforma de Laboratorio, Hospital General Universitario Gregorio Marañón, 28007 Madrid, Spain

[§]Center for Bioinformatics and Integrative Biology (CBIB), Facultad de Ciencias Biológicas, Universidad Andres Bello, Av. República 239, Santiago, Chile, 8370146

[□]Fundación Fraunhofer Chile Research, Las Condes, Chile, 7550296

^{||}Centro Interdisciplinario de Neurociencia de Valparaíso, Facultad de Ciencias, Universidad de Valparaíso, Valparaíso, Chile, 2360102

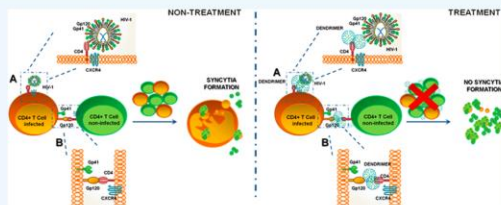
[‡]Department of Química Orgánica y Química Inorgánica and ^{||}Instituto de Investigación Química “Andrés M. del Río” (IQAR), Universidad de Alcalá (IRYCIS), Campus Universitario, 28871 Madrid, Spain

[¶]Networking Research Center on Bioengineering, Biomaterials and Nanomedicine (CIBER-BBN), Instituto de Salud Carlos III, Av. de Monforte de Lemos, 5, 28029 Madrid, Spain

[■]Instituto de Biomedicina de Sevilla (IBiS). Hospital Universitario Virgen del Rocío, Av. Manuel Siurot, s/n, 41013 Sevilla, Spain

[▽]Servicio de Medicina Interna. Hospital Viamed Santa Ángela, Av. de Jerez, 59, 41014 Sevilla, Spain

ABSTRACT: Cell-to-cell transmission is the most effective pathway for the spread of human immunodeficiency virus (HIV-1). Infected cells expose virus-encoded fusion proteins on their surface as a consequence of HIV-1 replicative cycle that interacts with noninfected cells through CD4 receptor and CXCR4 coreceptor leading to the formation of giant multinucleated cells known as syncytia. Our group previously described the potent activity of dendrimers against CCR5-tropic viruses. Nevertheless, the study of G1-S4, G2-S16, and G3-S16 dendrimers in the context of X4-HIV-1 tropic cell–cell fusion referred to syncytium formation remains still unknown. These dendrimers showed a suitable biocompatibility in all cell lines studied and our results demonstrated that anionic carbosilane dendrimers G1-S4, G2-S16, and G3-S16 significantly inhibit the X4-HIV-1 infection, as well as syncytia formation, in a dose dependent manner. We also demonstrated that G2-S16 and G1-S4 significantly reduced syncytia formation in HIV-1 Env-mediated cell-to-cell fusion model. Molecular modeling and in silico models showed that G2-S16 dendrimer interfered with gp120-CD4 complex and demonstrated its potential use for a treatment.



INTRODUCTION

Human immunodeficiency virus type 1 (HIV-1) continues to be a major global public health problem. The UNAIDS program on HIV/AIDS estimated that 36.7 million people lived with HIV-1 worldwide, highlighting that around one-third of all people did not know their HIV-positive status.¹ The percentage of anti-retroviral naïve individuals harboring X4 viruses varies between 10% and 38%. Some studies estimated the prevalence of CXCR4-using virus in primary HIV infection at 6–19%.² Therefore, it is important encourage treatment during this phase of infection. Otherwise, the anti-retroviral therapy coverage according to data from UNAIDS is increasing in over

two-thirds of infected patients; however, in regions like Eastern Europe and Central Asia, those data do not reach 30%,¹ so they are more susceptible to CXCR4-tropic viruses and developing AIDS.

The envelope glycoproteins (*Env*) of HIV-1 are the key elements involved in viral entry. *Env* derives from gp160 precursors generating noncovalently associated trimers of gp120 and gp41 heterodimers. Thus, the entry of HIV-1 into susceptible cells begins with the initial binding of the HIV-1

Received: February 12, 2018

Revised: March 23, 2018

Published: March 23, 2018

systems considering G2-S16 dendrimer. Then, the gp120-CD4 binding free energy, $\Delta G_{\text{binding}}$, was calculated using the Molecular Mechanics/Generalized Born surface area method (MM-GBSA)⁴⁵ as previously reported,^{34,46,47} considering the following equation:

$$\begin{aligned}\Delta G_{\text{binding}} &= G_{\text{TOTAL}}(\text{gp120} - \text{CD4complex}) \\ &\quad - (G_{\text{TOTAL}}(\text{gp120}) + G_{\text{TOTAL}}(\text{CD4}))G_{\text{TOTAL}} \\ &= H_{\text{MM}} + G_{\text{solv}} - T\Delta S_{\text{conf}}\end{aligned}$$

where H_{MM} contribution was calculated by summing the in vacuo gas-phase nonbond energies ($H_{\text{MM}} = E_{\text{vdW}} + E_{\text{ele}}$) and the solvation free energies ($G_{\text{solv}} = G_{\text{GB}} + G_{\text{NP}}$) for each component, e.g., gp120-CD4 complex, gp120 protein, and CD4 protein. Polar solvation free energy G_{GB} was calculated using Generalized Born approach and nonpolar solvation G_{NP} was calculated as γ (SASA) + β , in which $\gamma = 0.00542 \text{ kcal}/\text{\AA}^2$ and $\beta = 0.92 \text{ kcal/mol}$.⁴⁸ The conformational entropy was not included, because of the large low prediction accuracy and computational cost. $\Delta\Delta G_{\text{binding}}$ was obtained as a difference between $\Delta G_{\text{binding}}$ in bound-dendrimer and unbound-dendrimer state.

AUTHOR INFORMATION

Corresponding Author

*E-mail: mmunoz.hgugm@gmail.com or mmunoz.hgugm@salud.madrid.org. Telephone: +34 915 868 565.

ORCID

Rafael Gomez: 0000-0001-6448-2414

M. Angeles Muñoz-Fernández: 0000-0002-0813-4500

Author Contributions

•Guerrero-Beltran and Rodriguez-Izquierdo contributed equally to this work.

Notes

The authors declare no competing financial interest.

ACKNOWLEDGMENTS

This work has been (partially) funded by the RD12/0017/0037, RD16/0025/0019, projects as part of the Acción Estratégica en Salud, Plan Nacional de Investigación Científica, Desarrollo e Innovación Tecnológica (2008–2011; 2013–2016) and cofinanced by the Instituto de Salud Carlos III (Subdirección General de Evaluación) and Fondo Europeo de Desarrollo Regional (FEDER), RETIC PT13/0010/0028, Fondo de Investigación Sanitaria (FIS) (grant number PI16/01863), CYTED 214RT0482, EPIICAL Project and MINECO CTQ-2014-54004-P. CIBER-BBN is an initiative funded by the VI National R&D&I Plan 2008–2011, Iniciativa Ingenio 2010, the Consolider Program, and CIBER Actions and financed by the Instituto de Salud Carlos III with assistance from the European Regional Development Fund.

REFERENCES

- (1) UNAIDS (2017) UNAIDS DATA 2017; <http://www.unaids.org>.
- (2) Nozza, S., Pignataro, A. R., Galli, L., Ripa, M., Boeri, E., Chiappetta, S., Galli, A., Canducci, F., Sampaolo, M., Clementi, M., et al. (2014) Immunological recovery after 24 weeks of antiretroviral therapy in patients with X4 virus during primary HIV infection. *JAIDS, J. Acquired Immune Defic. Syndr.* 65, e27–9.
- (3) Martínez-Munoz, L., Barroso, R., Dyrhaug, S. Y., Navarro, G., Lucas, P., Soriano, S. F., Vega, B., Costas, C., Munoz-Fernandez, M. A., Santiago, C., et al. (2014) CCR5/CD4/CXCR4 oligomerization

prevents HIV-1 gp120IIIB binding to the cell surface. *Proc. Natl. Acad. Sci. U. S. A.* 111, E1960–9.

(4) Nankya, I. L., Tebit, D. M., Abraha, A., Kyeyune, F., Gibson, R., Jegede, O., Nickel, G., and Arts, E. J. (2015) Defining the fitness of HIV-1 isolates with dual/mixed co-receptor usage. *AIDS Res. Ther.* 12, 34.

(5) Delwart, E. L., Mullins, J. L., Gupta, P., Learn, G. H., Jr., Holodniy, M., Katzenstein, D., Walker, B. D., and Singh, M. K. (1998) Human immunodeficiency virus type 1 populations in blood and semen. *J. Virol.* 72, 617–23.

(6) Wenz, W., Noeldge, G., and Grosshans, U. M. (1979) [X-ray examination for the detection of complications after abdominal surgery (author's transl)]. *Prakt. Anaesth.* 14, 138–47.

(7) Zhu, T., Mo, H., Wang, N., Nam, D. S., Cao, Y., Koup, R. A., and Ho, D. D. (1993) Genotypic and phenotypic characterization of HIV-1 patients with primary infection. *Science* 261, 1179–81.

(8) Galli, G., Annunziato, F., Cosmi, L., Manetti, R., Maggi, E., and Romagnani, S. (2001) Th1 and th2 responses, HIV-1 coreceptors, and HIV-1 infection. *J. Biol. Regul. Homeost. Agents* 15, 308–13.

(9) Nardacci, R., Perfettini, J. L., Grieco, L., Thieffry, D., Kroemer, G., and Piacentini, M. (2015) Syncytial apoptosis signaling network induced by the HIV-1 envelope glycoprotein complex: an overview. *Cell Death Dis.* 6, e1846.

(10) Murooka, T. T., Sharaf, R. R., and Mempel, T. R. (2015) Large Syncytia in Lymph Nodes Induced by CCR5-Tropic HIV-1. *AIDS Res. Hum. Retroviruses* 31, 471–472.

(11) Symeonides, M., Murooka, T. T., Bellfy, L. N., Roy, N. H., Mempel, T. R., and Thali, M. (2015) HIV-1-Induced Small T Cell Syncytia Can Transfer Virus Particles to Target Cells through Transient Contacts. *Viruses* 7, 6590–603.

(12) Sepulveda-Crespo, D., Lorente, R., Leal, M., Gomez, R., De la Mata, F. J., Jimenez, J. L., and Munoz-Fernandez, M. A. (2014) Synergistic activity profile of carboxilane dendrimer G2-STE16 in combination with other dendrimers and antiretrovirals as topical anti-HIV-1 microbicide. *Nanomedicine* 10, 609–18.

(13) Cena-Diez, R., Vacas-Cordoba, E., Garcia-Broncano, P., de la Mata, F. J., Gomez, R., Maly, M., and Munoz-Fernandez, M. A. (2016) Prevention of vaginal and rectal herpes simplex virus type 2 transmission in mice: mechanism of antiviral action. *Int. J. Nanomed.* 11, 2147–62.

(14) Sepulveda-Crespo, D., Cena-Diez, R., Jimenez, J. L., and Angeles Munoz-Fernandez, M. (2017) Mechanistic Studies of Viral Entry: An Overview of Dendrimer-Based Microbicides As Entry Inhibitors Against Both HIV and HSV-2 Overlapped Infections. *Med. Res. Rev.* 37, 149–179.

(15) Sepulveda-Crespo, D., Jimenez, J. L., Gomez, R., De La Mata, F. J., Majano, P. L., Munoz-Fernandez, M. A., and Gastaminza, P. (2017) Polyanionic carboxilane dendrimers prevent hepatitis C virus infection in cell culture. *Nanomedicine* 13, 49–58.

(16) Sepulveda-Crespo, D., Serramia, M. J., Tager, A. M., Vrbanc, V., Gomez, R., De La Mata, F. J., Jimenez, J. L., and Munoz-Fernandez, M. A. (2015) Prevention vaginally of HIV-1 transmission in humanized BLT mice and mode of antiviral action of polyanionic carboxilane dendrimer G2-S16. *Nanomedicine* 11, 1299–308.

(17) Cena-Diez, R., Garcia-Broncano, P., Javier de la Mata, F., Gomez, R., Resino, S., and Munoz-Fernandez, M. (2017) G2-S16 dendrimer as a candidate for a microbicide to prevent HIV-1 infection in women. *Nanoscale* 9, 9732–9742.

(18) Garcia-Broncano, P., Cena-Diez, R., de la Mata, F. J., Gomez, R., Resino, S., and Munoz-Fernandez, M. A. (2017) Efficacy of carboxilane dendrimers with an antiretroviral combination against HIV-1 in the presence of semen-derived enhancer of viral infection. *Eur. J. Pharmacol.* 811, 155–163.

(19) Galan, I., Jimenez, J. L., Gonzalez-Rivera, M., De Jose, M. I., Navarro, M. L., Ramos, J. T., Mellado, M. J., Gurbindo, M. D., Bellon, J. M., Resino, S., et al. (2004) Virological phenotype switches under salvage therapy with lopinavir-ritonavir in heavily pretreated HIV-1 vertically infected children. *AIDS* 18, 247–55.

SCIENTIFIC REPORTS

OPEN

Synchronization transition in neuronal networks composed of chaotic or non-chaotic oscillators

Received: 20 December 2017

Accepted: 11 May 2018

Published online: 30 May 2018

Kesheng Xu¹, Jean Paul Maidana¹, Samy Castro¹ & Patricio Orio^{1,2}

Chaotic dynamics has been shown in the dynamics of neurons and neural networks, in experimental data and numerical simulations. Theoretical studies have proposed an underlying role of chaos in neural systems. Nevertheless, whether chaotic neural oscillators make a significant contribution to network behaviour and whether the dynamical richness of neural networks is sensitive to the dynamics of isolated neurons, still remain open questions. We investigated synchronization transitions in heterogeneous neural networks of neurons connected by electrical coupling in a small world topology. The nodes in our model are oscillatory neurons that – when isolated – can exhibit either chaotic or non-chaotic behaviour, depending on conductance parameters. We found that the heterogeneity of firing rates and firing patterns make a greater contribution than chaos to the steepness of the synchronization transition curve. We also show that chaotic dynamics of the isolated neurons do not always make a visible difference in the transition to full synchrony. Moreover, macroscopic chaos is observed regardless of the dynamics nature of the neurons. However, performing a Functional Connectivity Dynamics analysis, we show that chaotic nodes can promote what is known as multi-stable behaviour, where the network dynamically switches between a number of different semi-synchronized, metastable states.

Over the past decades, a number of observations of chaos have been reported in the analysis of time series from a variety of neural systems, ranging from the simplest to the more complex^{1,2}. It is generally accepted that the inherent instability of chaos in nonlinear systems dynamics, facilitates the extraordinary ability of neural systems to respond quickly to changes in their external inputs³, to make transitions from one pattern of behaviour to another when the environment is altered⁴, and to create a rich variety of patterns endowing neuronal circuits with remarkable computational capabilities⁵. These features are all suggestive of an underlying role of chaos in neural systems (For reviews, see^{6–7}), however these ideas may have not been put to test thoroughly.

Chaotic dynamics in neural networks can emerge in a variety of ways, including intrinsic mechanisms within individual neurons^{8–12} or by interactions between neurons^{13–21}. The first type of chaotic dynamics in neural systems is typically accompanied by microscopic chaotic dynamics at the level of individual oscillators. The presence of this chaos has been observed in networks of Hindmarsh-Rose neurons⁸ and biophysical conductance-based neurons^{9–12}. The second type of chaotic firing pattern is the synchronous chaos. Synchronous chaos has been demonstrated in networks of both biophysical and non-biophysical neurons^{13,15,17,22–24}, where neurons display synchronous chaotic firing-rate fluctuations. In the latter cases, the chaotic behaviour is a result of network connectivity, since isolated neurons do not display chaotic dynamics or burst firing. More recently, it has been shown that asynchronous chaos, where neurons exhibit asynchronous chaotic firing-rate fluctuations, emerge generically from balanced networks with multiple time scales in their synaptic dynamics²⁰.

Different modelling approaches have been used to uncover important conditions for observing these types of chaotic behaviour (in particular, synchronous and asynchronous chaos) in neural networks, such as the synaptic strength^{25–27}, heterogeneity of the numbers of synapses and their synaptic strengths^{28,29}, and lately the balance of excitation and inhibition³¹. The results obtained by Sompolinsky *et al.*²⁵ showed that, when the synaptic strength is increased, neural networks display a highly heterogeneous chaotic state via a transition from an inactive state. Other studies demonstrated that chaotic behaviour emerges in the presence of weak and strong heterogeneities, for example a coupled heterogeneous population of neural oscillators with different synaptic strengths^{28–30}. Recently, Kadmon *et al.*²¹ highlighted the importance of the balance between excitation and inhibition on a

¹Centro Interdisciplinario de Neurociencia de Valparaíso, Universidad de Valparaíso, Valparaíso, 2360102, Chile. ²Instituto de Neurociencia, Facultad de Ciencias, Universidad de Valparaíso, Valparaíso, 2360102, Chile. Correspondence and requests for materials should be addressed to P.O. (email: patricio.orio@uv.cl)

27. Ostojic, S. Two types of asynchronous activity in networks of excitatory and inhibitory spiking neurons. *Nature Neuroscience* **17**, 594–600 (2014).
28. Yazdankhah, A., Babadi, B., Rouhani, S., Arabzadeh, E. & Abbassian, A. New attractor states for synchronous activity in synfire chains with excitatory and inhibitory coupling. *Biological Cybernetics* **86**, 367–378 (2002).
29. Teramae, J.-N. & Fukai, T. Local cortical circuit model inferred from power-law distributed neuronal avalanches. *Journal of computational neuroscience* **22**, 301–312 (2007).
30. Pazó, D. & Montbrió, E. From quasiperiodic partial synchronization to collective chaos in populations of inhibitory neurons with delay. *Physical Review Letters* **116**, 238101 (2016).
31. Newman, M. E. & Watts, D. J. Renormalization group analysis of the small-world network model. *Physics Letters A* **263**, 341–346 (1999).
32. Orio, P. *et al.* Role of h in the firing pattern of mammalian cold thermoreceptor endings. *Journal of neurophysiology* **108**, 3009–3023 (2012).
33. Newman, M., Barabási, A.-L. & Watts, D. J. *The structure and dynamics of networks* (Princeton University Press, 2011).
34. Newman, M. *Networks: an introduction* (Oxford university press, 2010).
35. Chen, G., Wang, X. & Li, X. *Fundamentals of complex networks: models, structures and dynamics* (John Wiley & Sons, 2014).
36. Sprott, J. C. *Chaos and time-series analysis*, vol. 69 (Oxford: Oxford University Press, 2003).
37. Jones, D. S., Plank, M. & Sleeman, B. D. *Differential equations and mathematical biology* (CRC press, 2009).
38. Skokos, C. The lyapunov characteristic exponents and their computation. In *Dynamics of Small Solar System Bodies and Exoplanets*, 63–135 (Springer, 2010).
39. Lynch, S. *Dynamical systems with applications using MATLAB* (Springer, 2004).
40. Lee, D. T. & Yamamoto, A. Wavelet analysis: theory and applications. *Hewlett Packard journal* **45**, 44–52 (1994).
41. Addison, P. The illustrated wavelet transform handbook: Introductory theory and applications in science, engineering, *Medicine and Finance*. IOP Publishing, Bristol (2002).
42. Hramov, A. E., Koronovskii, A. A., Makarov, V. A., Pavlov, A. N. & Sitnikova, E. *Wavelets in Neuroscience* (Springer, 2015).
43. Shanahan, M. Metastable chimera states in community-structured oscillator networks. *Chaos: An Interdisciplinary Journal of Nonlinear Science* **20**, 013108 (2010).
44. Váša, F. *et al.* Effects of lesions on synchrony and metastability in cortical networks. *Neuroimage* **118**, 456–467 (2015).
45. Ponce-Alvarez, A. *et al.* Resting-state temporal synchronization networks emerge from connectivity topology and heterogeneity. *PLoS Comput Biol* **11**, e1004100 (2015).
46. Zhang, X., Zou, Y., Boccaletti, S. & Liu, Z. Explosive synchronization as a process of explosive percolation in dynamical phase space. *Scientific Reports* **4**, 5200 (2014).
47. IJansen, E. C., Battaglia, D., Spiegler, A., Deco, G. & Jirsa, V. K. Functional connectivity dynamics: modeling the switching behavior of the resting state. *Neuroimage* **105**, 525–535, <https://doi.org/10.1016/j.neuroimage.2014.11.001> (2015).
48. Preti, M. G., Bolton, T. A. & Van De Ville, D. The dynamic functional connectome: State-of-the-art and perspectives. *Neuroimage* (2016).
49. Wilcox, R. R. *Introduction to robust estimation and hypothesis testing* (Academic press, 2011).
50. Cabral, J., Kringelbach, M. & Deco, G. Functional connectivity dynamically evolves on multiple time-scales over a static structural connectome: Models and mechanisms. *Neuroimage* (2017).
51. Reyes, M. B., Carelli, P. V., Sartorelli, J. C. & Pinto, R. D. A modeling approach on why simple central pattern generators are built of irregular neurons. *PLoS one* **10**, e0120314 (2015).
52. Dingwell, J. B. *Lyapunov exponents*. Wiley Encyclopedia of Biomedical Engineering (2006).
53. Wainrib, G. & Touboul, J. Topological and dynamical complexity of random neural networks. *Physical Review Letters* **110**, 118101 (2013).
54. Anishchenko, V. S., Astakhov, V., Neiman, A., Vadivasova, T. & Schimansky-Geier, L. *Nonlinear dynamics of chaotic and stochastic systems: tutorial and modern developments* (Springer Science & Business Media, 2007).
55. Schuster, H. G. & Just, W. *Deterministic chaos: an introduction* (John Wiley & Sons, 2006).
56. Reynolds, A. M., Bartumeus, E., Kolzsch, A. & Van De Koppel, J. Signatures of chaos in animal search patterns. *Scientific Reports* **6**, 23492 (2016).
57. Mejias, J. E. & Longtin, A. Optimal heterogeneity for coding in spiking neural networks. *Physical Review Letters* **108**, <https://doi.org/10.1103/physrevlett.108.228102> (2012).
58. Mejias, J. E. & Longtin, A. Differential effects of excitatory and inhibitory heterogeneity on the gain and asynchronous state of sparse cortical networks. *Frontiers in Computational Neuroscience* **8**, <https://doi.org/10.3389/fncom.2014.00107> (2014).
59. Braiman, Y., Lindner, J. F. & Ditto, W. L. Taming spatiotemporal chaos with disorder. *Nature* **378**, 465 (1995).
60. Tessone, C. J., Mirasso, C. R., Toral, R. & Gunton, J. D. Diversity-induced resonance. *Physical Review Letters* **97**, 194101 (2006).
61. Valizadeh, A., Kolahchi, M. & Straley, J. Single phase-slip junction site can synchronize a parallel superconducting array of linearly coupled josephson junctions. *Physical Review B* **82**, 144520 (2010).
62. Faisal, A. A., Selen, L. P. & Wolpert, D. M. Noise in the nervous system. *Nature Reviews Neuroscience* **9**, 292–303 (2008).

Acknowledgements

KX is funded by Proyecto Fondecyt 3170342 (Chile). JM is Recipient Of A PhD Grant FIB-UV From UV. SC is recipient of a Ph.D. fellowship grant from CONICYT 21140603 (Chile). PO is partially funded by the Advanced Center for Electrical and Electronic Engineering (FB0008 Conicyt, Chile). The Centro Interdisciplinario de Neurociencia de Valparaíso (CINV) is a Millennium Institute supported by the Millennium Scientific Initiative of the Ministerio de Economía (ICM-MINECON, Proyecto Código P09-022-F, CINV, Chile).

Author Contributions

K.X. and P.O. performed numerical simulations and analysis. J.M., S.C. and P.O. performed Functional Connectivity Dynamics Analysis. K.X. and P.O. wrote the manuscript. K.X., J.M., S.C. and P.O. revised and approved the manuscript.

Additional Information

Supplementary information accompanies this paper at <https://doi.org/10.1038/s41598-018-26730-9>.

Competing Interests: The authors declare no competing interests.

Publisher's note: Springer Nature remains neutral with regard to jurisdictional claims in published maps and institutional affiliations.



Article

Self-Assembly Behavior of Amphiphilic Janus Dendrimers in Water: A Combined Experimental and Coarse-Grained Molecular Dynamics Simulation Approach

Mariana E. Elizondo-García ^{1,*}, Valeria Márquez-Miranda ², Ingrid Araya-Durán ²,
Jesús A. Valencia-Gallegos ^{1,*} and Fernando D. González-Nilo ^{2,3}

¹ Escuela de Ingeniería y Ciencias, Tecnológico de Monterrey, Av. Eugenio Garza Sada 2501 Sur, Monterrey 64849, Mexico

² Center for Bioinformatics and Integrative Biology (CBIB), Facultad de Ciencias Biológicas, Universidad Andrés Bello, Av. República 330, Santiago 8370186, Chile; valeria.marquez.m@gmail.com (V.M.-M.); ingrid.araya.duran@gmail.com (I.A.-D.); fernando.gonzalez@unab.cl (F.D.G.-N.)

³ Centro Interdisciplinario de Neurociencia de Valparaíso, Facultad de Ciencias, Universidad de Valparaíso, Gran Bretaña 1111, Playa Ancha, Valparaíso 2360102, Chile

* Correspondence: mariana.elizndo@gmail.com (M.E.E.-G); valencia@itesm.mx (J.A.V.-G); Tel.: +52-818-358-2000 (ext. 4511) (J.A.V.-G)

Received: 1 April 2018; Accepted: 16 April 2018; Published: 21 April 2018



Abstract: Amphiphilic Janus dendrimers (JDs) are repetitively branched molecules with hydrophilic and hydrophobic components that self-assemble in water to form a variety of morphologies, including vesicles analogous to liposomes with potential pharmaceutical and medical application. To date, the self-assembly of JDs has not been fully investigated thus it is important to gain insight into its mechanism and dependence on JDs' molecular structure. In this study, the aggregation behavior in water of a second-generation bis-MPA JD was evaluated using experimental and computational methods. Dispersions of JDs in water were carried out using the thin-film hydration and ethanol injection methods. Resulting assemblies were characterized by dynamic light scattering, confocal microscopy, and atomic force microscopy. Furthermore, a coarse-grained molecular dynamics (CG-MD) simulation was performed to study the mechanism of JDs aggregation. The obtaining of assemblies in water with no interdigitated bilayers was confirmed by the experimental characterization and CG-MD simulation. Assemblies with dendrimersome characteristics were obtained using the ethanol injection method. The results of this study establish a relationship between the molecular structure of the JD and the properties of its aggregates in water. Thus, our findings could be relevant for the design of novel JDs with tailored assemblies suitable for drug delivery systems.

Keywords: Janus dendrimers; amphiphilic; self-assembly; coarse-grained molecular dynamics

1. Introduction

Amphiphilic Janus dendrimers (JDs) are molecules composed of polar (hydrophilic) and non-polar (hydrophobic) dendritic blocks [1]. This characteristic is the key factor that favors the spontaneous self-assembly of JDs in water into complex supramolecular structures [2]. The variation in the chemical structure of JDs allows achieving a rich palette of morphologies in water, such as cubosomes, disks, tubular vesicles, helical ribbons and bilayered vesicles, termed as dendrimersomes [3].

For further research, a computational and experimental study of dendrimer structure modifications and their impact in the self-assembly process is in progress.

Supplementary Materials: The following are available online, Figure S1: Time stability of small assemblies from JD, Figure S2: Temperature stability of small assemblies from JD, Figure S3: Solvent accessible surface area (SASA) of the dendrimers during the simulation, Figure S4: Reaction scheme, Figure S5: ^1H NMR spectra (500 MHz, CDCl_3) of JD and peak assignments.

Acknowledgments: M.E.E.G. thank the Ph. D. scholarship (251115) from CONACyT. The authors would like to thank: Luis Elizalde-Herrera (CIQA) for his help running the NMR spectra; Gloria Macedo-Raygoza and Miguel J. Beltrán-García (UAG), for their help in the measuring of MALDI-TOF mass spectra; and Maricela Rodríguez-Nieto and Jorge Luis Menchaca (UANL), for their help with the AFM measurements. FDGN thanks to the USA Air Force Office of Scientific Research Awards.

Author Contributions: J.A.V.-G. conceived and supervised the project. M.E.E.-G. performed the experimental methods, analysis, and interpretation of the results and wrote the paper; V.M.-M. carried out the molecular dynamics simulations, analyzed the data and the results; I.A.-D. supported the molecular dynamics simulations, analysis, and interpretation of the results; F.D.G.-N. supported and supervised the project. All authors revised the paper.

Conflicts of Interest: The authors declare no conflict of interest.

References

- Kalhapure, R.S.; Kathiravan, M.K.; Akamanchi, K.G.; Govender, T. Dendrimers—From organic synthesis to pharmaceutical applications: An update. *Pharm. Dev. Technol.* **2013**, *20*, 22–40. [[CrossRef](#)] [[PubMed](#)]
- Fedeli, E.; Lancelot, A.; Serrano, J.L.; Calvo, P.; Sierra, T. Self-assembling amphiphilic Janus dendrimers: Mesomorphic properties and aggregation in water. *New J. Chem.* **2015**, *39*, 1960–1967. [[CrossRef](#)]
- Percec, V.; Wilson, D.A.; Leowanawat, P.; Wilson, C.J.; Hughes, A.D.; Kaucher, M.S.; Hammer, D.A.; Levine, D.H.; Kim, A.J.; Bates, F.S.; et al. Self-assembly of Janus dendrimers into uniform dendrimersomes and other complex architectures. *Science* **2010**, *328*, 1009–1014. [[CrossRef](#)] [[PubMed](#)]
- Sikwal, D.R.; Kalhapure, R.S.; Govender, T. An emerging class of amphiphilic dendrimers for pharmaceutical and biomedical applications: Janus amphiphilic dendrimers. *Eur. J. Pharm. Sci.* **2017**, *97*, 113–134. [[CrossRef](#)] [[PubMed](#)]
- Filippi, M.; Patrucco, D.; Martinelli, J.; Botta, M.; Castro-Hartmann, P.; Tei, L.; Terreno, E. Novel stable dendrimersome formulation for safe bioimaging applications. *Nanoscale* **2015**, *7*, 12943–12954. [[CrossRef](#)] [[PubMed](#)]
- Filippi, M.; Martinelli, J.; Mulas, G.; Ferraretto, M.; Teirlinck, E.; Botta, M.; Tei, L.; Terreno, E. Dendrimersomes: A new vesicular nano-platform for MR-molecular imaging applications. *Chem. Commun.* **2014**, *50*, 3453–3456. [[CrossRef](#)] [[PubMed](#)]
- Filippi, M.; Catanzaro, V.; Patrucco, D.; Botta, M.; Tei, L.; Terreno, E. First in vivo MRI study on theranostic dendrimersomes. *J. Control. Release* **2017**, *248*, 45–52. [[CrossRef](#)] [[PubMed](#)]
- Nazemi, A.; Gillies, E.R. Dendrimersomes with photodegradable membranes for triggered release of hydrophilic and hydrophobic cargo. *Chem. Commun.* **2014**, *50*, 11122–11125. [[CrossRef](#)] [[PubMed](#)]
- Peterca, M.; Percec, V.; Leowanawat, P.; Bertin, A. Predicting the size and properties of dendrimersomes from the lamellar structure of their amphiphilic Janus dendrimers. *J. Am. Chem. Soc.* **2011**, *133*, 20507–20520. [[CrossRef](#)] [[PubMed](#)]
- Zhang, S.; Sun, H.J.; Hughes, A.D.; Moussodia, R.O.; Bertin, A.; Chen, Y.; Pochan, D.J.; Heiney, P.A.; Klein, M.L.; Percec, V. Self-assembly of amphiphilic Janus dendrimers into uniform onion-like dendrimersomes with predictable size and number of bilayers. *Proc. Natl. Acad. Sci. USA* **2014**, *111*, 9058–9063. [[CrossRef](#)] [[PubMed](#)]
- Zhang, S.; Sun, H.J.; Hughes, A.D.; Draghici, B.; Lejnieks, J.; Leowanawat, P.; Bertin, A.; Otero De Leon, L.; Kulikov, O.V.; Chen, Y.; et al. “Single-Single” Amphiphilic Janus Dendrimers Self-Assemble into Uniform Dendrimersomes with Predictable Size. *ACS Nano* **2014**, *8*, 1554–1565. [[CrossRef](#)] [[PubMed](#)]
- Wang, P.; Ma, Y.; Liu, Z.; Yan, Y.; Sun, X.; Zhang, J. Vesicle formation of catanionic mixtures of CTAC/SDS induced by ratio: A coarse-grained molecular dynamic simulation study. *RSC Adv.* **2016**, *6*, 13442–13449. [[CrossRef](#)]

Novel Insights for Inhibiting Mutant Heterodimer IDH1^{wt-R132H} in Cancer: An In-Silico Approach

Ezequiel Iván Juritz¹ · Juan Pablo Bascur¹ · Daniel Eduardo Almonacid^{1,2} · Fernando Danilo González-Nilo^{1,3}

© Springer International Publishing AG, part of Springer Nature 2018

Abstract

Background Isocitrate dehydrogenase 1 (IDH1) is a dimeric enzyme responsible for supplying the cell's nicotinamide adenine dinucleotide phosphate (NADPH) reserves via dehydrogenation of isocitrate (ICT) and reduction of NADP⁺. Mutations in position R132 trigger cancer by enabling IDH1 to produce D-2-hydroxyglutarate (2-HG) and reduce inhibition by ICT. Mutant IDH1 can be found as a homodimer or a heterodimer.

Objective We propose a novel strategy to inhibit IDH1 R132 variants as a means not to decrease the concentration of 2-HG but to provoke a cytotoxic effect, as the cell malignancy at this point no longer depends on 2-HG. We aim to inhibit the activity of the mutant heterodimer to block the wild-type subunit. Limiting the NADPH reserves in a cancerous cell will enhance its susceptibility to the oxidative stress provoked by chemotherapy.

Methods We performed a virtual screening using all US FDA-approved drugs to replicate the loss of inhibition of mutant IDH1 by ICT. We characterized our results based on molecular interactions and correlated them with the described phenotypes.

Results We replicated the loss of inhibition by ICT in mutant IDH1. We identified 20 drugs with the potential to

inhibit the heterodimeric isoform. Six of them are used in cancer treatment.

Conclusions We present 20 FDA-approved drugs with the potential to inhibit IDH1 wild-type activity in mutated cells. We believe this work may provide important insights into current and new approaches to dealing with IDH1 mutations. In addition, it may be used as a basis for additional studies centered on drugs presenting differential sensitivities to different IDH1 isoforms.

Key Points

We describe a novel bioinformatics approach to inhibit isocitrate dehydrogenase 1 (IDH1) variant enzymes.

We performed a virtual screening of all US FDA-approved drugs to find potential inhibitors of the heterodimeric IDH1 R132H mutant enzyme.

We found 20 drugs with potential inhibiting properties for heterodimeric IDH1; six are used in cancer therapy and one presents enhanced activity in patients with IDH1 mutations.

✉ Ezequiel Iván Juritz
ejuritz@gmail.com

¹ Center for Bioinformatics and Integrative Biology, Facultad de Ciencias de la Vida, Universidad Andrés Bello, 8370146 Santiago, Chile

² uBiome, Inc., San Francisco, CA, USA

³ Centro Interdisciplinario de Neurociencia de Valparaíso, Facultad de Ciencias, Universidad de Valparaíso, 2366103 Valparaíso, Chile

1 Introduction

In humans, three enzymes have isocitrate dehydrogenase (IDH) activity: IDH1, IDH2, and the IDH3 complex [1], which is comprised of the IDH3a, IDH3b, and IDH3g subunits [2]. These enzymes transform isocitrate (ICT) into

Here, we provide results of an in silico screening procedure based on a novel approach of inhibiting IDH1 R132H mutants. We present 20 drugs derived from the FDA database with the potential to inhibit IDH1 wild-type activity in cells containing the mutation.

We believe this work may provide important insights into current and new approaches to deal with IDH1 mutations, particularly inhibiting the wild-type activity in cells presenting the IDH1 R132H mutation. In addition, it may be used as a basis for additional studies centered on drugs presenting differential sensitivities to different IDH1 isoforms.

4 Conclusions

Our docking results recreated, in silico, the loss of inhibition by ICT in IDH1 mutant enzymes, which represents strong evidence that the docking algorithm parameters are suitable for our studied system.

A total of 20 drugs presented potential inhibitory properties for the heterodimeric mutant IDH1^{wt-R132H}. As these drugs are approved by the FDA, the potential toxic or side effects they may present are limited and already characterized, although parameters such as administration and doses should be taken into account. The fact that five of these drugs are used in cancer treatment and that one presents antitumor activity is very encouraging. Moreover, one of these drugs (dasatinib) presents an exceptional sensitivity for IDH mutant tumor cell lines.

We believe the results of our simulations, which identified potential inhibitors of the wild-type activity of IDH1 R132H mutant heterodimers, is a promising approach and provides valuable insights for personalized medicine treatments. Further experimental analysis, such as proliferation assays and 2-HG quantifications, should be performed to support and validate our results.

5 Limitations

This work is a computational-based study of a new approach for inhibiting IDH1 mutants. We propose a list of 20 FDA-approved drugs that show theoretical potential to inhibit the heterodimeric mutant enzyme IDH1^{wt-R132H}. Further studies should be performed on these drugs to review the behavior with IDH1 mutants and to study their side effects. Regarding this last point, all drugs included in this study are FDA approved, limiting these potential problems.

Experimental procedures for selected drugs, including 2-HG measurements and calorimetry, are part of a proposal for continuing the present work.

Acknowledgements The authors wish to thank Dr. Elisabeth Bik for her help improving the manuscript. FDGN thanks to Centro Interdisciplinario de Neurociencia de Valparaíso (CINV) which is a Millennium Institute supported by the Millennium Scientific Initiative of the Ministerio de Economía, Fomento y Turismo, Chile.

Compliance with Ethical Standards

Conflict of interest The authors EIJ, JPB, DEA and FDGN have no conflicts of interest that are directly relevant to the content of this study. DEA is currently an employee of uBiome, Inc. and has received stock options as well as other compensations. FDGN is currently an advisor to uBiome, Inc. and has received stock options. uBiome had no influence on the design or execution of this study.

Funding This study was funded by FONDECYT postdoctoral Grant no. 3150671 (PI: EIJ) and FONDECYT Proyecto de Inicio no. 11130578 (PI: DEA).

References

- Krell D, Assoku M, Galloway M, Mulholland P, Tomlinson I, Bardella C. Screen for IDH1, IDH2, IDH3, D2HGDH and L2HGDH mutations in glioblastoma. *PLoS One*. 2011;6(5):e19868. <https://doi.org/10.1371/journal.pone.0019868>.
- Ma T, Peng Y, Huang W, Ding J. Molecular mechanism of the allosteric regulation of the $\alpha\gamma$ heterodimer of human NAD-dependent isocitrate dehydrogenase. *Sci Rep*. 2017;7:40921. <https://doi.org/10.1038/srep40921>.
- Reitman ZJ, Duncan CG, Poteet E, Winters A, Yan LJ, Gooden DM, Spasojevic I, Boros LG, Yang SH, Yan H. Cancer-associated isocitrate dehydrogenase 1 (IDH1) R132H mutation and D-2-hydroxyglutarate stimulate glutamine metabolism under hypoxia. *J Biol Chem*. 2014;289(34):23318–28. <https://doi.org/10.1074/jbc.M114.575183>.
- Xie X, Baird D, Bowen K, Capka V, Chen J, Chenail G, Cho Y, Dooley J, Farsidjani A, Fortin P, Kohls D, Kulathila R, Lin F, McKay D, Rodrigues L, Sage D, Touré BB, van der Plas S, Wright K, Xu M, Yin H, Levell J, Pagliarini RA. Allosteric mutant IDH1 inhibitors reveal mechanisms for IDH1 mutant and isoform selectivity. *Structure*. 2017;25(3):506–13. <https://doi.org/10.1016/j.str.2016.12.017>.
- Caims RA, Mak TW. Oncogenic isocitrate dehydrogenase mutations: mechanisms, models, and clinical opportunities. *Cancer Discov*. 2013;3(7):730–41. <https://doi.org/10.1158/2159-8290.CD-13-0083>.
- Parsons DW, Jones S, Zhang X, Lin JC, Leary RJ, Angenendt P, Mankoo P, Carter H, Siu IM, Gallia GL, Olivi A, McLendon R, Rasheed BA, Keir S, Nikolskaya T, Nikolsky Y, Busam DA, Tekleab H, Diaz LA Jr, Hartigan J, Smith DR, Strausberg RL, Marie SK, Shinjo SM, Yan H, Riggins GJ, Bigner DD, Karchin R, Papadopoulos N, Parmigiani G, Vogelstein B, Velculescu VE, Kinzler KW. An integrated genomic analysis of human glioblastoma multiforme. *Science*. 2008;321(5897):1807–12. <https://doi.org/10.1126/science.1164382>.
- Balss J, Meyer J, Mueller W, Korshunov A, Hartmann C, von Deimling A. Analysis of the IDH1 codon 132 mutation in brain tumors. *Acta Neuropathol*. 2008;116(6):597–602. <https://doi.org/10.1007/s00401-008-0455-2>.
- Kang MR, Kim MS, Oh JE, Kim YR, Song SY, Seo SI, Lee JY, Yoo NJ, Lee SH. Mutational analysis of IDH1 codon 132 in glioblastomas and other common cancers. *Int J Cancer*. 2009;125(2):353–5. <https://doi.org/10.1002/ijc.24379>.



Modulation of Connexin-36 Gap Junction Channels by Intracellular pH and Magnesium Ions

Lina Rimkute^{1*}, Tadas Kraujalis^{1,2}, Mindaugas Snipas^{1,3}, Nicolas Palacios-Prado^{4,5}, Vaidas Jotautis¹, Vytenis A. Skeberdis¹ and Feliksas F. Bukauskas¹

¹ Institute of Cardiology, Lithuanian University of Health Sciences, Kaunas, Lithuania, ² Department of Applied Informatics, Kaunas University of Technology, Kaunas, Lithuania, ³ Department of Mathematical Modelling, Kaunas University of Technology, Kaunas, Lithuania, ⁴ Centro Interdisciplinario de Neurociencias de Valparaíso, Universidad de Valparaíso, Valparaíso, Chile, ⁵ Department of Physiology, Pontificia Universidad Católica de Chile, Santiago, Chile

OPEN ACCESS

Edited by:

Fabio Mammano,
Istituto di Biologia Cellulare e
Neurobiologia (CNR), Italy

Reviewed by:

Richard David Veenstra,
State University of New York Upstate
Medical University, United States
Christian Giaume,
Collège de France, France

*Correspondence:

Lina Rimkute
lina.rimkute@ismuni.lt

[†]Deceased.

Specialty section:

This article was submitted to
Membrane Physiology and Membrane
Biophysics,
a section of the journal
Frontiers in Physiology

Received: 05 February 2018

Accepted: 23 March 2018

Published: 12 April 2018

Citation:

Rimkute L, Kraujalis T, Snipas M,
Palacios-Prado N, Jotautis V,
Skeberdis VA and Bukauskas FF
(2018) Modulation of Connexin-36
Gap Junction Channels by Intracellular
pH and Magnesium Ions.
Front. Physiol. 9:362.
doi: 10.3389/fphys.2018.00362

Connexin-36 (Cx36) protein forms gap junction (GJ) channels in pancreatic beta cells and is also the main Cx isoform forming electrical synapses in the adult mammalian brain. Cx36 GJs can be regulated by intracellular pH (pH_i) and cytosolic magnesium ion concentration ($[Mg^{2+}]_i$), which can vary significantly under various physiological and pathological conditions. However, the combined effect and relationship of these two factors over Cx36-dependent coupling have not been previously studied in detail. Our experimental results in HeLa cells expressing Cx36 show that changes in both pH_i and $[Mg^{2+}]_i$ affect junctional conductance (g_j) in an interdependent manner; in other words, intracellular acidification cause increase or decay in g_j depending on whether $[Mg^{2+}]_i$ is high or low, respectively, and intracellular alkalization cause reduction in g_j independently of $[Mg^{2+}]_i$. Our experimental and modelling data support the hypothesis that Cx36 GJ channels contain two separate gating mechanisms, and both are differentially sensitive to changes in pH_i and $[Mg^{2+}]_i$. Using recombinant Cx36 we found that two glutamate residues in the N-terminus could be partly responsible for the observed interrelated effect of pH_i and $[Mg^{2+}]_i$. Mutation of glutamate at position 8 attenuated the stimulatory effect of intracellular acidification at high $[Mg^{2+}]_i$, while mutation at position 12 and double mutation at both positions reversed stimulatory effect to inhibition. Moreover, Cx36*E8Q lost the initial increase of g_j at low $[Mg^{2+}]_i$ and double mutation lost the sensitivity to high $[Mg^{2+}]_i$. These results suggest that E8 and E12 are involved in regulation of Cx36 GJ channels by Mg^{2+} and H^+ ions.

Keywords: connexin-36, gap junctions, intracellular pH and Mg^{2+} , mutants, cell culture

INTRODUCTION

Cell-to-cell coupling through gap junction (GJ) channels is essential for intercellular communication in most cell types. GJ channels serve as an intercellular pathway for ions, small metabolites such as IP_3 and cAMP (Niessen et al., 2000; Bedner et al., 2006), and larger molecules such as small interfering RNAs (Valiunas et al., 2005; Antanaviciute et al., 2014) and peptides

that $[Mg^{2+}]_i$ and pH_i effect on Cx36 plays at least a partial role in the protective mechanisms. For example, the depletion of ATP during brain ischemia (Sato et al., 1984) could induce an increase of $[Mg^{2+}]_i$ (Henrich and Buckler, 2008), therefore these factors together might coordinate the regulation of electrical coupling. Presumably, under a mild ischemia it might be beneficial to maintain the normal electrical coupling, while the closure of Cx36 GJ channels during a severe ischemia could isolate the damaged regions of cells, thus preventing the further spread of apoptosis.

AUTHOR CONTRIBUTIONS

LR, VS, and FB: conception of the work, design of experiments, collection, analysis and interpretation of data, drafting of manuscript; TK and NP-P: recorded and analysed the experimental data; MS: constructed and applied mathematical

models; NP-P and MS: critically revised the manuscript; VJ: performed experiments.

FUNDING

This study was supported by grant No. MIP-76/2015 from the Research Council of Lithuania to FB, and partially supported by grant ICM-Economía P09-022-F Centro Interdisciplinario de Neurociencias de Valparaíso and Fondo Nacional de Desarrollo Científico y Tecnológico (FONDECYT) grants No. 3180272 to NP-P.

ACKNOWLEDGMENTS

We thank Alina Marandykina-Prakiene for generating mutants of Cx36 and Vytautas Raskevicius for performing structural modelling and evaluation of pK_a .

REFERENCES

- Acuña-Castillo, C., Coddou, C., Bull, P., Brito, J., and Huidobro-Toro, J. P. (2007). Differential role of extracellular histidines in copper, zinc, magnesium and proton modulation of the P2X7 purinergic receptor. *J. Neurochem.* 101, 17–26. doi: 10.1111/j.1471-4159.2006.04343.x
- Akopian, A., Atlasz, T., Pan, F., Wong, S., Zhang, Y., Völgyi, B., et al. (2014). Gap junction-mediated death of retinal neurons is connexin and insult specific: a potential target for neuroprotection. *J. Neurosci.* 34, 10582–10591. doi: 10.1523/JNEUROSCI.1912-14.2014
- Antanaviciute, L., Rysevaite, K., Liutkevicius, V., Marandykina, A., Rimkute, L., Sveikatiene, R., et al. (2014). Long-distance communication between laryngeal carcinoma cells. *PLoS ONE* 9:e9196. doi: 10.1371/journal.pone.009196
- Barbiroli, B., Martinelli, P., Patuelli, A., Lodi, R., Iotti, S., Cortelli, P., et al. (1999). Phosphorus magnetic resonance spectroscopy in multiple system atrophy and Parkinson's disease. *Mov. Disord.* 14, 430–435. doi: 10.1002/1531-8257(199905)14:3<430::AID-MDS10078>3.0.CO;2-S
- Bedner, P., Niessen, H., Odermatt, B., Kretz, M., Willecke, K., and Harz, H. (2006). Selective permeability of different connexin channels to the second messenger cyclic AMP. *J. Biol. Chem.* 281, 6673–6681. doi: 10.1074/jbc.M511235200
- Bennett, B. C., Purdy, M. D., Baker, K. A., Acharya, C., McIntire, W. E., Stevens, R. C., et al. (2016). An electrostatic mechanism for Ca^{2+} -mediated regulation of gap junction channels. *Nat. Commun.* 7, 8770. doi: 10.1038/ncomms9770
- Bennett, M. V., and Zukin, R. S. (2004). Electrical coupling and neuronal synchronization in the mammalian brain. *Neuron* 41, 495–511. doi: 10.1016/S0896-6273(04)00043-1
- Bevans, C. G., and Harris, A. L. (1999). Regulation of connexin channels by pH. Direct action of the protonated form of taurine and other aminosulfonates. *J. Biol. Chem.* 274, 3711–3719. doi: 10.1074/jbc.274.6.3711
- Beyer, E. C., Lipkind, G. M., Kyle, J. W., and Berthoud, V. M. (2012). Structural organization of intercellular channels II. Amino terminal domain of the connexins: sequence, functional roles, and structure. *Biochim. Biophys. Acta* 1818, 1823–1830. doi: 10.1016/j.bbame.2011.10.011
- Bissiere, S., Zelikowsky, M., Ponnusamy, R., Jacobs, N. S., Blair, H. T., and Fanselow, M. S. (2011). Electrical synapses control hippocampal contributions to fear learning and memory. *Science* 331, 87–91. doi: 10.1126/science.1193785
- Bukauskas, F. F., and Verselis, V. K. (2004). Gap junction channel gating. *Biochim. Biophys. Acta* 1662, 42–60. doi: 10.1016/j.bbame.2004.01.008
- Chesler, M., and Kaila, K. (1992). Modulation of pH by neuronal activity. *Trends Neurosci.* 15, 396–402. doi: 10.1016/0166-2236(92)90191-A
- Chesler, M., and Kraig, R. P. (1989). Intracellular pH transients of mammalian astrocytes. *J. Neurosci.* 9, 2011–2019.
- Chokshi, R., Matsushita, M., and Kozak, J. A. (2012). Detailed examination of Mg^{2+} and pH sensitivity of human TRPM7 channels. *Am. J. Physiol. Cell Physiol.* 302, C1004–C1011. doi: 10.1152/ajpcell.00422.2011
- Connors, B. W., and Long, M. A. (2004). Electrical synapses in the mammalian brain. *Annu. Rev. Neurosci.* 27, 393–418. doi: 10.1146/annurev.neuro.26.041002.131128
- Cruikshank, S. J., Hopperstad, M., Younger, M., Connors, B. W., Spray, D. C., and Srinivas, M. (2004). Potent block of Cx36 and Cx50 gap junction channels by mefloquine. *Proc. Natl. Acad. Sci. U.S.A.* 101, 12364–12369. doi: 10.1073/pnas.0402044101
- Del Corral, C., Iglesias, R., Zoidl, G., Dermietzel, R., and Spray, D. C. (2012). Calmodulin dependent protein kinase increases conductance at gap junctions formed by the neuronal gap junction protein connexin36. *Brain Res.* 1487, 69–77. doi: 10.1016/j.brainres.2012.06.058
- Durlach, J. (1990). Magnesium depletion and pathogenesis of Alzheimer's disease. *Magn. Res.* 3, 217–218.
- Farnsworth, N. L., and Benninger, R. K. (2014). New insights into the role of connexins in pancreatic islet function and diabetes. *FEBS Lett.* 588, 1278–1287. doi: 10.1016/j.febslet.2014.02.035
- Gajda, Z., Szupera, Z., Blazso, G., and Szente, M. (2005). Quinine, a blocker of neuronal cx36 channels, suppresses seizure activity in rat neocortex in vivo. *Epilepsia* 46, 1581–1591. doi: 10.1111/j.1528-1167.2005.00254.x
- Glaume, C., and Korn, H. (1982). Ammonium sulfate induced uncouplings of crayfish septate axons with and without increased junctional resistance. *Neuroscience* 7, 1723–1730. doi: 10.1016/0306-4522(82)90030-6
- González-Nieto, D., Gómez-Hernández, J. M., Larrosa, B., Gutiérrez, C., Muñoz, M. D., Fasciani, I., et al. (2008). Regulation of neuronal connexin-36 channels by pH. *Proc. Natl. Acad. Sci. U.S.A.* 105, 17169–17174. doi: 10.1073/pnas.0804189105
- Hanna, S. (1961). Plasma magnesium in health and disease. *J. Clin. Pathol.* 14, 410–414. doi: 10.1136/jcp.14.4.410
- Harks, E. G., de Roos, A. D., Peters, P. H., de Haan, L. H., Brouwer, A., Ypey, D. L., et al. (2001). Fenamates: a novel class of reversible gap junction blockers. *J. Pharmacol. Exp. Ther.* 298, 1033–1041.
- Harris, A. L., and Contreras, J. E. (2014). Motifs in the permeation pathway of connexin channels mediate voltage and Ca^{2+} sensing. *Front. Physiol.* 5:113. doi: 10.3389/fphys.2014.00113
- Harris, A. L., Spray, D. C., and Bennett, M. V. L. (1981). Kinetic properties of a voltage-dependent junctional conductance. *J. Gen. Physiol.* 77, 95–117. doi: 10.1085/jgp.77.1.95
- Henrich, M., and Buckler, K. J. (2008). Effects of anoxia, aglycemia, and acidosis on cytosolic Mg^{2+} , ATP, and pH in rat sensory neurons. *Am. J. Physiol. Cell Physiol.* 294, C280–C294. doi: 10.1152/ajpcell.00345.2007

Hereditary Myopathies

Arlek Marion González-Jamett,
Jorge Alfredo Bevilacqua and
Ana María Cárdenas Díaz

Additional information is available at the end of the chapter

<http://dx.doi.org/10.5772/intechopen.76076>

Abstract

Hereditary myopathies are inherited disorders primarily affecting the skeletal muscle tissue. These are caused by mutations in different genes encoding proteins that play important roles in muscle structure and function. Skeletal muscle weakness and hypotonia are typical clinical manifestations in most of hereditary myopathies. Histological features such as fiber type disproportion, myofibrillar disorganization, and structural abnormalities are usually observed in muscle biopsies of non-dystrophic myopathies, while fibrosis, fiber regeneration, wasting, and atrophy are characteristic of dystrophic myopathies. However, similar histopathological features may overlap in different hereditary myopathies. This is how mutations in a same gene can lead to different forms of hereditary myopathies and a same myopathic phenotype can derive from defects in different related genes making difficult a specific diagnosis. In this regard, understanding all aspects of hereditary myopathies can facilitate a better diagnosis and treatment. In this chapter, we offer a review of some of the most prevalent hereditary myopathies, highlighting clinical, histological, and molecular aspects of these muscle disorders.

Keywords: hereditary myopathy, muscle disease, congenital myopathy, muscular dystrophy

1. Introduction

Hereditary myopathies are a heterogeneous group of inherited diseases primarily affecting the skeletal muscle tissue. These are caused by mutations in genes encoding proteins critical for muscle structure and function, with X-linked, autosomal-recessive or -dominant inheritance pattern. Hereditary myopathies include several forms of dystrophic and non-dystrophic disorders with a wide spectrum of genetic, biochemical, histological, and clinical features. A common characteristic

IntechOpen

© 2018 The Author(s). Licensee IntechOpen. This chapter is distributed under the terms of the Creative Commons Attribution License (<http://creativecommons.org/licenses/by/3.0>), which permits unrestricted use, distribution, and reproduction in any medium, provided the original work is properly cited.



Acknowledgements

We thank Dr. Norma B. Romero from the Institute of Myology in Paris, France, and Prof. Anders Oldfors from the University of Gothenburg, in Gothenburg, Sweden for generously providing illustrative material. This work was supported by Grants Fondecyt 3160311 to AG-J, Fondecyt 1151383 to JAB and Fondecyt 1160495 to AMC.

Author details

Arlek Marion González-Jamett^{1*}, Jorge Alfredo Bevilacqua^{2,3} and Ana María Cárdenas Díaz¹

*Address all correspondence to: arlek.gonzalez@cinv.cl

1 Centro Interdisciplinario de Neurociencia de Valparaíso, Universidad de Valparaíso, Valparaíso, Chile

2 Departamento de Neurología y Neurocirugía Hospital Clínico Universidad de Chile, Universidad de Chile, Santiago, Chile

3 Unidad de Patología Neuromuscular, Departamento de Neurología y Neurocirugía, Clínica Dávila, Santiago, Chile

References

- [1] Cassandrini D et al. Congenital myopathies: Clinical phenotypes and new diagnostic tools. *Italian Journal of Pediatrics*. 2017;**43**(1):101
- [2] Jungbluth H et al. Current and future therapeutic approaches to the congenital myopathies. *Seminars in Cell & Developmental Biology*. 2017;**64**:191-200
- [3] North KN. Clinical approach to the diagnosis of congenital myopathies. *Seminars in Pediatric Neurology*. 2011;**18**(4):216-220
- [4] Romero NB. Recent advances in nemaline myopathy. *Current Opinion in Neurology*. 2013;**26**(5):519-526
- [5] Malfatti E et al. Muscle histopathology in nebulin-related nemaline myopathy: Ultrastructural findings correlated to disease severity and genotype. *Acta Neuropathologica Communications*. 2014;**2**:44
- [6] Clarkson E et al. Congenital myopathies: Diseases of the actin cytoskeleton. *The Journal of Pathology*. 2004;**204**(4):407-417
- [7] Sewry CA et al. Myopathology in congenital myopathies. *Neuropathology and Applied Neurobiology*. 2017;**43**(1):5-23

RESEARCH ARTICLE

The syndromic deafness mutation G12R impairs fast and slow gating in Cx26 hemichannels

Isaac E. García^{1,2}, Felipe Villanelo^{1,3}, Gustavo F. Contreras¹, Amaury Pupo¹, Bernardo I. Pinto¹, Jorge E. Contreras⁴, Tomás Pérez-Acle^{1,3}, Osvaldo Alvarez^{2,4}, Ramon Latorre¹, Agustín D. Martínez⁵, and Carlos González¹

Mutations in connexin 26 (Cx26) hemichannels can lead to syndromic deafness that affects the cochlea and skin. These mutations lead to gain-of-function hemichannel phenotypes by unknown molecular mechanisms. In this study, we investigate the biophysical properties of the syndromic mutant Cx26G12R (G12R). Unlike wild-type Cx26, G12R macroscopic hemichannel currents do not saturate upon depolarization, and deactivation is faster during hyperpolarization, suggesting that these channels have impaired fast and slow gating. Single G12R hemichannels show a large increase in open probability, and transitions to the subconductance state are rare and short-lived, demonstrating an inoperative fast gating mechanism. Molecular dynamics simulations indicate that G12R causes a displacement of the N terminus toward the cytoplasm, favoring an interaction between R12 in the N terminus and R99 in the intracellular loop. Disruption of this interaction recovers the fast and slow voltage-dependent gating mechanisms. These results suggest that the mechanisms of fast and slow gating in connexin hemichannels are coupled and provide a molecular mechanism for the gain-of-function phenotype displayed by the syndromic G12R mutation.

Introduction

A family of proteins called connexins forms vertebrate gap junction channels and hemichannels. They are encoded by a multigene family that contains 21 members in humans (Söhl and Willecke, 2003). Connexins have four transmembrane segments (TM1–4) connected by two extracellular loops (EL1–2) and one intracellular loop, with cytosolic N- and C-terminal segments. Hemichannels are formed by oligomerization of six connexin monomers and communicate between the cytoplasm and the extracellular milieu. At plasma membrane appositional zones, hemichannels can dock to compatible hemichannels in the adjacent cell to form gap junction channels, providing a direct pathway for intercellular communication (Goodenough et al., 1996; Gaietta et al., 2002; Segretain and Falk, 2004). Connexin hemichannels are regulated by pH (Bevans and Harris, 1999), phosphorylation (Lampe and Lau, 2000), and divalent cations (Verselis et al., 1994; Verselis and Srinivas, 2008) and exhibit two voltage-dependent gating mechanisms: loop (slow) gating, which closes hemichannels at hyperpolarizing voltages, and Vj (fast) gating, which drives hemichannels into a subconductance state at depolarizing voltages (Trexler et al., 1996; Bargiello et al., 2012; Oh and Bargiello, 2015).

Mutations in the Cx26 gene are the main cause of genetic deafness (Bergoffen et al., 1993; Kelsell et al., 1997, 2000; Arita et al., 2006; Arora et al., 2008; Dobrowolski and Willecke, 2009), with a prevalence of ~50% of cases worldwide (Kelsell et al., 1997). Some mutations in Cx26 produce syndromic deafness in which severe deafness is accompanied by extensive damage in other tissues, such as in keratitis ichthyosis deafness (KID) syndrome, in which patients also present skin abnormalities (such as palmoplantar keratoderma and erythrokeratoderma) and strong inflammation of the cornea (Yotsumoto et al., 2003; van Steensel et al., 2004; Arita et al., 2006; Mazereeuw-Hautier et al., 2007). To date, there is agreement that nonsyndromic deafness-associated Cx26 mutations reduce gap junction channel function, the degree of which correlates well with deafness severity. In contrast, Cx26 mutations associated with syndromic deafness produce hyperactive or leaky hemichannels in their homomeric (Gerido et al., 2007; Lee et al., 2009; Sánchez et al., 2010, 2013, 2016) and heteromeric (García et al., 2015) configurations. KID-associated mutations cluster at the N terminus and the TM1/EL1 segment of Cx26 in amino acid residues that face the channel pore (García et al., 2016). These regions are critical for regulation of gating.

¹Centro Interdisciplinario de Neurociencia de Valparaíso, Facultad de Ciencias, Universidad de Valparaíso, Valparaíso, Chile; ²Laboratory of Molecular Physiology and Biophysics, Facultad de Odontología, Universidad de Valparaíso, Valparaíso, Chile; ³Computational Biology Laboratory, Fundación Ciencia & Vida, Santiago, Chile; ⁴Department of Pharmacology, Physiology, and Neuroscience, New Jersey Medical School, Rutgers University, Newark, NJ; ⁵Departamento de Biología, Facultad de Ciencias, Universidad de Chile, Santiago, Chile.

Correspondence to Carlos González: carlos.gonzalez@uv.cl; Agustín D. Martínez: agustin.martinez@uv.cl; Ramon Latorre: ramon.latorre@uv.cl.

© 2018 García et al. This article is distributed under the terms of an Attribution–Noncommercial–Share Alike–No Mirror Sites license for the first six months after the publication date (see <http://www.rupress.org/terms/>). After six months it is available under a Creative Commons License (Attribution–Noncommercial–Share Alike 4.0 International license, as described at <https://creativecommons.org/licenses/by-nc-sa/4.0/>).

Acknowledgments

We thank Dr. José Ignacio García-Palacios and Dr. Viviana Berthoud for helpful discussions on the manuscript. We thank Claudia Pareja-Barrueto for helpful discussions on molecular dynamic simulations. We thank the National Laboratory of High Performance Computing–Chile center for providing computing time for molecular dynamic simulations, Powered@NLHPC.

This work was supported by Programa de Atracción e Inserción de Capital Humano Avanzado a la Academia (PAI 79170081) to I.E. García, Fondo Nacional de Desarrollo Científico y Tecnológico (3150634 to I.E. García, 1171240 to A.D. Martínez, 3140590 to G.F. Contreras, 1180434 to C. González, 1160574 to T. Pérez-Acle, and 1150273 to R. Latorre), Beca Comisión Nacional de Investigación Científica y Tecnológica–Programa Formación de Capital Humano Avanzado/Doctorado Nacional/2017 to B.I. Pinto, Programa de Financiamiento Basal PFB16 Fundación Ciencia para la Vida, and the National Institutes of Health (R01-GM099490 to J.E. Contreras). This work was partially supported by the Air Force Office of Scientific Research under award number FA9550-16-1-0384 to R. Latorre. The Centro Interdisciplinario de Neurociencia de Valparaíso is a Millennium Institute supported by the Millennium Scientific Initiative of the Chilean Ministry of Economy, Development, and Tourism (P029-022-F).

The authors declare no competing financial interests.

Author contributions: I.E. García, R. Latorre, A.D. Martínez, and C. González conceived this work. I.E. García, F. Villanelo, O. Alvarez, R. Latorre, and A.D. Martínez cowrote and coedited the final version of the manuscript. I.E. García, O. Alvarez, and R. Latorre designed the experimental strategies. I.E. García performed all the electrophysiological experiments. I.E. García, F. Villanelo, A. Pupo, and T. Pérez-Acle performed molecular dynamic simulations. All authors contributed to data analysis.

Merritt C. Maduke served as editor.

Submitted: 6 March 2017

Revised: 13 November 2017

Accepted: 21 March 2018

References

- Arita, K., M. Akiyama, T. Aizawa, Y. Umetsu, I. Segawa, M. Goto, D. Sawamura, M. Demura, K. Kawano, and H. Shimizu. 2006. A novel N14Y mutation in Connexin26 in keratitis-ichthyosis-deafness syndrome: Analyses of altered gap junctional communication and molecular structure of N terminus of mutated Connexin26. *Am. J. Pathol.* 169:416–423. <https://doi.org/10.2353/ajpath.2006.051242>
- Arora, A., P.J. Minogue, X. Liu, P.K. Addison, I. Russel-Eggitt, A.R. Webster, D.M. Hunt, L. Ebi-hara, E.C. Beyer, V.M. Berthoud, and A.T. Moore. 2008. A novel connexin50 mutation associated with congenital nuclear pulverulent cataracts. *J. Med. Genet.* 45:155–160. <https://doi.org/10.1136/jmg.2007.051029>
- Bargiello, T.A., Q. Tang, S. Oh, and T. Kwon. 2012. Voltage-dependent conformational changes in connexin channels. *Biochim. Biophys. Acta.* 1818:1807–1822. <https://doi.org/10.1016/j.bbame.2011.09.019>
- Batir, Y., T.A. Bargiello, and T.L. Dowd. 2016. Structural studies of N-terminal mutants of connexin 26 and connexin 32 using 1H NMR spectroscopy. *Arch. Biochem. Biophys.* 608:8–19.
- Bennett, B.C., M.D. Purdy, K.A. Baker, C. Acharya, W.E. McIntire, R.C. Stevens, Q. Zhang, A.L. Harris, R. Abagyan, and M. Yeager. 2016. An electrostatic mechanism for Ca(2+)-mediated regulation of gap junction channels. *Nat. Commun.* 7:8770. <https://doi.org/10.1038/ncomms9770>

- Bergoffen, J., S.S. Scherer, S. Wang, M.O. Scott, L.J. Bone, D.L. Paul, K. Chen, M.W. Lensch, P.F. Chance, and K.H. Fischbeck. 1993. Connexin mutations in X-linked Charcot-Marie-Tooth disease. *Science.* 262:2039–2042. <https://doi.org/10.1126/science.8266101>
- Bevans, C.G., and A.L. Harris. 1999. Regulation of connexin channels by pH. Direct action of the protonated form of taurine and other aminosulfonates. *J. Biol. Chem.* 274:3711–3719. <https://doi.org/10.1074/jbc.274.6.3711>
- Dobrowolski, R., and K. Willecke. 2009. Connexin-caused genetic diseases and corresponding mouse models. *Antioxid. Redox Signal.* 11:283–295. <https://doi.org/10.1089/ars.2008.2128>
- Ebihara, L. 1996. Xenopus connexin38 forms hemi-gap-junctional channels in the nonjunctional plasma membrane of Xenopus oocytes. *Biophys. J.* 71:742–748. [https://doi.org/10.1016/S0006-3495\(96\)79273-1](https://doi.org/10.1016/S0006-3495(96)79273-1)
- Gaietta, G., T.J. Deerinck, S.R. Adams, J. Bouwer, O. Tour, D.W. Laird, G.E. Sosinsky, R.Y. Tsien, and M.H. Ellisman. 2002. Multicolor and electron microscopic imaging of connexin trafficking. *Science.* 296:503–507. <https://doi.org/10.1126/science.1068793>
- García, I.E., J. Maripillán, O. Jara, R. Ceriani, A. Palacios-Muñoz, J. Ramachandran, P. Olivero, T. Perez-Acle, C. González, J.C. Sáez, et al. 2015. Keratitis-ichthyosis-deafness syndrome-associated Cx26 mutants produce nonfunctional gap junctions but hyperactive hemichannels when co-expressed with wild type Cx43. *J. Invest. Dermatol.* 135:1338–1347. <https://doi.org/10.1038/jid.2015.20>
- García, I.E., F. Bosen, P. Mujica, A. Pupo, C. Flores-Munoz, O. Jara, C. González, K. Willecke, and A.D. Martínez. 2016. From hyperactive Connexin26 hemichannels to impairments in epidermal calcium gradient and permeability barrier in the keratitis-ichthyosis-deafness syndrome. *J. Invest. Dermatol.* 136:574–583.
- Gerido, D.A., A.M. DeRosa, G. Richard, and T.W. White. 2007. Aberrant hemichannel properties of Cx26 mutations causing skin disease and deafness. *Am. J. Physiol. Cell Physiol.* 293:C337–C345. <https://doi.org/10.1152/ajpcell.00626.2006>
- Goodenough, D.A., J.A. Goliger, and D.L. Paul. 1996. Connexins, connexons, and intercellular communication. *Annu. Rev. Biochem.* 65:475–502. <https://doi.org/10.1146/annurev.bi.65.070196.002355>
- Kelsell, D.P., J. Dunlop, H.P. Stevens, N.J. Lench, J.N. Liang, G. Parry, R.F. Mueller, and I.M. Leigh. 1997. Connexin 26 mutations in hereditary non-syndromic sensorineural deafness. *Nature.* 387:80–83. <https://doi.org/10.1038/387080a0>
- Kelsell, D.P., A.L. Wilgoss, G. Richard, H.P. Stevens, C.S. Munro, and I.M. Leigh. 2000. Connexin mutations associated with palmoplantar keratoderma and profound deafness in a single family. *Eur. J. Hum. Genet.* 8:141–144. <https://doi.org/10.1038/sj.ejhg.5200407>
- Kwon, T., A.L. Harris, A. Rossi, and T.A. Bargiello. 2011. Molecular dynamics simulations of the Cx26 hemichannel: Evaluation of structural models with Brownian dynamics. *J. Gen. Physiol.* 138:475–493. <https://doi.org/10.1085/jgp.20110679>
- Kyle, J.W., P.J. Minogue, B.C. Thomas, D.A. Domowicz, V.M. Berthoud, D.A. Hanck, and E.C. Beyer. 2008. An intact connexin N-terminus is required for function but not gap junction formation. *J. Cell Sci.* 121:2744–2750. <https://doi.org/10.1242/jcs.032482>
- Lagree, V., K. Brunschwig, P. Lopez, N.B. Gilula, G. Richard, and M.M. Falk. 2003. Specific amino-acid residues in the N-terminus and TM3 implicated in channel function and oligomerization compatibility of connexin43. *J. Cell Sci.* 116:3189–3201. <https://doi.org/10.1242/jcs.00604>
- Lampe, P.D., and A.F. Lau. 2000. Regulation of gap junctions by phosphorylation of connexins. *Arch. Biochem. Biophys.* 384:205–215. <https://doi.org/10.1006/abbi.2000.2131>
- Lee, J.R., A.M. Derosa, and T.W. White. 2009. Connexin mutations causing skin disease and deafness increase hemichannel activity and cell death when expressed in Xenopus oocytes. *J. Invest. Dermatol.* 129:870–878. <https://doi.org/10.1038/jid.2008.335>
- Lomize, M.A., A.L. Lomize, I.D. Pogozheva, and H.I. Mosberg. 2006. OPM: Orientations of proteins in membranes database. *Bioinformatics.* 22:623–625. <https://doi.org/10.1093/bioinformatics/btk023>
- Lopez, W., J. Gonzalez, Y. Liu, A.L. Harris, and J.E. Contreras. 2013. Insights on the mechanisms of Ca²⁺ regulation of connexin26 hemichannels revealed by human pathogenic mutations (D50N/Y). *J. Gen. Physiol.* 142:23–35. <https://doi.org/10.1085/jgp.201210893>
- Lopez, W., J. Ramachandran, A. Alamarah, Y. Luo, A.L. Harris, and J.E. Contreras. 2016. Mechanism of gating by calcium in connexin hemichannels. *Proc. Natl. Acad. Sci. USA.* 113:E7986–E7995. <https://doi.org/10.1073/pnas.1609378113>
- Maeda, S., S. Nakagawa, M. Suga, E. Yamashita, A. Oshima, Y. Fujiyoshi, and T. Tsukihara. 2009. Structure of the connexin 26 gap junction

García et al.

Altered fast and slow gating elicited by Cx26G12R

Journal of General Physiology
<https://doi.org/10.1085/jgp.201711782>

14



Lack of Pannexin 1 Alters Synaptic GluN2 Subunit Composition and Spatial Reversal Learning in Mice

Ivana Gajardo¹, Claudia S. Salazar², Daniela Lopez-Espíndola^{3,4}, Carolina Estay^{1,2}, Carolina Flores-Muñoz², Claudio Elgueta⁵, Arlek M. Gonzalez-Jamett^{2,6}, Agustín D. Martínez², Pablo Muñoz^{1,4,7} and Álvaro O. Ardiles^{1,2,8*}

¹Departamento de Patología y Fisiología, Facultad de Medicina, Universidad de Valparaíso, Valparaíso, Chile,

²Centro Interdisciplinario de Neurociencia de Valparaíso, Facultad de Ciencias, Universidad de Valparaíso, Valparaíso, Chile,

³Escuela de Tecnología Médica, Facultad de Medicina, Universidad de Valparaíso, Valparaíso, Chile, ⁴Centro de Investigaciones Biomédicas, Escuela de Medicina, Universidad de Valparaíso, Valparaíso, Chile, ⁵Institute for Physiology I, University of Freiburg, Freiburg, Germany, ⁶Programa de Farmacología Molecular y Clínica, Instituto de Ciencias Biomédicas (ICBM), Facultad de Medicina, Universidad de Chile, Santiago, Chile, ⁷Center for Applied Neurological Sciences, Faculty of Medicine, Universidad de Valparaíso, Valparaíso, Chile, ⁸Centro Interdisciplinario de Estudios en Salud, Facultad de Medicina, Universidad de Valparaíso, Viña del Mar, Chile

Long-term potentiation (LTP) and long-term depression (LTD) are two forms of synaptic plasticity that have been considered as the cellular substrate of memory formation. Although LTP has received considerable more attention, recent evidences indicate that LTD plays also important roles in the acquisition and storage of novel information in the brain. Pannexin 1 (Panx1) is a membrane protein that forms non-selective channels which have been shown to modulate the induction of hippocampal synaptic plasticity. Animals lacking Panx1 or blockade of Pannexin 1 channels precludes the induction of LTD and facilitates LTP. To evaluate if the absence of Panx1 also affects the acquisition of rapidly changing information we trained Panx1 knockout (KO) mice and wild type (WT) littermates in a visual and hidden version of the Morris water maze (MWM). We found that KO mice find the hidden platform similarly although slightly quicker than WT animals, nonetheless, when the hidden platform was located in the opposite quadrant (OQ) to the previous learned location, KO mice spent significantly more time in the previous quadrant than in the new location indicating that the absence of Panx1 affects the reversion of a previously acquired spatial memory. Consistently, we observed changes in the content of synaptic proteins critical to LTD, such as GluN2 subunits of N-methyl-D-aspartate receptors (NMDARs), which changed their contribution to synaptic plasticity in conditions of Panx1 ablation. Our findings give further support to the role of Panx1 channels on the modulation of synaptic plasticity induction, learning and memory processes.

Keywords: Pannexin 1, long-term depression, GluN2 subunits, behavioral flexibility, synaptic plasticity

INTRODUCTION

N-methyl-D-aspartate receptor (NMDAR)-dependent long-term potentiation (LTP) and long-term depression (LTD) are two opposing forms of activity-dependent synaptic plasticity which have emerged as putative cellular mechanisms underlying learning and memory in the central nervous system (CNS; Lynch, 2004; Collingridge et al., 2010). Whereas a plethora of studies support the

OPEN ACCESS

Edited by:

Juan Andrés Orellana,
Pontificia Universidad Católica de
Chile, Chile

Reviewed by:

Georg Zoidl,
York University, Canada
Michael F. Jackson,
University of Manitoba, Canada

*Correspondence:

Álvaro O. Ardiles
alvaro.ardiles@uv.cl

Received: 15 November 2017

Accepted: 22 March 2018

Published: 10 April 2018

Citation:

Gajardo I, Salazar CS,
Lopez-Espíndola D, Estay C,
Flores-Muñoz C, Elgueta C,
Gonzalez-Jamett AM, Martínez AD,
Muñoz P and Ardiles AO (2018) Lack
of Pannexin 1 Alters Synaptic
GluN2 Subunit Composition and
Spatial Reversal Learning in Mice.
Front. Mol. Neurosci. 11:114.
doi: 10.3389/fnmol.2018.00114

hippocampus, and they have key roles in synaptic function and plasticity (Yashiro and Philpot, 2008). The identity of GluN2 subunits determines some of the biophysical properties of NMDARs important for synaptic plasticity. For instance, GluN2A-containing receptors show lower affinity for glutamate, higher sensitivity to Mg^{2+} blockade, greater channel open probability and Ca^{2+} desensitization than GluN2B (Yashiro and Philpot, 2008). This has important implications because these properties can determine the responses to stimulation at different frequencies and hence the directionality of the synaptic modifications (Erreger et al., 2005). In other words, at low frequencies typically used to induce LTD (1 Hz), GluN2B makes a larger contribution to the total charge transfer and calcium influx than GluN2A (Erreger et al., 2005). However, under high-frequency stimulation, typically used to induce LTP (100 Hz), the current mediated by GluN2A considerably exceeds that of GluN2B (Erreger et al., 2005). Currently, there is contrasting evidence regarding the differential roles of GluN2 subunits to LTP and LTD induction. For instance, it has been speculated that GluN2B favors more LTP induction than GluN2A (Tang et al., 1999; Hendricson et al., 2002; Wong et al., 2002; Philpot et al., 2003; Barria and Malinow, 2005; Bartlett et al., 2007; Morishita et al., 2007; Philpot et al., 2007; Wang et al., 2009). However, it has also been reported that GluN2A-, but not GluN2B-containing receptors, mediate LTP (Liu et al., 2004; Massey et al., 2004). On the other hand, some reports indicate that induction of LTD does not require GluN2B-containing NMDARs activation (Hendricson et al., 2002; Bartlett et al., 2007; Morishita et al., 2007). Indeed, a LFS protocol (900 pulses, 1 Hz) induces LTP instead LTD in a GluN2A KO mice (Bartlett et al., 2007). In contrast, other evidences suggest that GluN2B but not GluN2A subunits are important for LTD (Liu et al., 2004; Kollen et al., 2008). It should be noted that the contribution of these GluN2 subunits also depends on the developmental, regional and behavioral experience context in which they are studied. Notwithstanding, these evidences suggest that the threshold for the induction of LTD and LTP is governed by the ratio of GluN2A/GluN2B (Yashiro and Philpot, 2008) and alterations in this ratio might generate, in turn, impairments in synaptic plasticity and brain mechanisms underlying learning and memory. Thus, it has been proposed that synapses exhibiting a high GluN2A/GluN2B ratio, would favor the induction of LTD, while synapses with a low GluN2A/GluN2B ratio would be more prone to express LTP (Yashiro and Philpot, 2008). Our results suggest that *Panx1* loss might modify GluN2A/GluN2B ratio which generates the observed changes in LTP and LTD expression. Indeed, we found that the synaptic content of GluN2B-subunit of NMDAR was significantly increased in hippocampal PSD-enriched fractions, whereas GluN2A subunit was significantly increased in synaptosomes obtained from KO mice compared to WT animals. Although comparison between groups revealed no significant differences in the GluN2A/GluN2B ratio in PSD and synaptosomal fractions, we observed a tendency to a reduction in the ratio in KO PSDs compared to WT. The latter suggests that GluN2B levels are higher than GluN2A in KO PSDs. On the contrary, in KO synaptosomes the ratio tended to be higher than

WT, suggesting in this case that GluN2B levels are lower than GluN2A in KO synaptosomes. These assumptions were supported by visualization of hippocampal Sch-CA1 synapses by electron microscopy, where we observed a redistribution of gold particles positive for GluN2A- and GluN2B-subunits (Figures 4I,J). It is noteworthy that in KO synapses, most of gold particles positive to GluN2A subunits accumulate in non-synaptic sites, whereas GluN2B particles localize overlying spine membrane.

According with these results, we observed a lower contribution of extra-synaptic GluN2B-containing NMDARs to LTD, revealed by TBOA incubation, in KO slices compared to WT animals (Figures 3E,F), suggesting a modification either in traffic or expression of GluN2 subunits from/toward non-synaptic sites. Indeed, we found a tendency to greater surface level of both GluN2 subunits in KO mice compared to WT animals (Figure 4F). Nevertheless, we did not found changes in total levels of GluN2 subunits evaluated in hippocampal homogenates (Figure 4E). In agreement with that, an earlier report by Prochnow et al. (2012), using *Panx1*^{-/-} mice, showed no changes in synaptic plasticity related-genes including GluN2 subunits of NMDARs indicating that expression of GluN2 is not affected.

In summary, our data revealed novel functions of *Panx1* channels in synaptic plasticity and memory flexibility. Furthermore, these results are in line with a modification in the LTD mechanism thought to be implied in these cognitive processes. For instance, we found that KO mice display a modification in synaptic proteins, some of which are critical for the induction or expression of LTD. Based on the current findings we propose that *Panx1* channels modulate the induction of synaptic plasticity by changing the distribution of subunit-specific NMDARs, ultimately leading to deficiencies in learning and memory processes.

AUTHOR CONTRIBUTIONS

IG, CSS, DL-E and ÁOA designed the research. IG, CSS, DL-E, CEstay, CF-M and ÁOA performed experiments, analyzed data and contributed to figures. CELgueta, PM, AMG-J and ADM contributed analytic tools. ÁOA wrote the article.

FUNDING

This work was supported by grants Fondo Nacional de Desarrollo Científico y Tecnológico (FONDECYT) N° 3130759, N° 11150776 and Comisión Nacional de Investigación Científica y Tecnológica, PAI N° 79150045 to ÁOA, and CINV ICM P09-022-F to ÁOA and ADM.

ACKNOWLEDGMENTS

We thank Dr. Adrian Palacios for kindly sharing the equipment. We also thank Daniela Ponce, Alejandro Munizaga, Juan Francisco Varas, Elena Mery, Barbara Gomez and Renato Pardo for technical assistance.

Large Conductance Potassium Channels in the Nervous System

Oxford Handbooks Online

Large Conductance Potassium Channels in the Nervous System FREE

Willy Carrasquel-Ursulaez, Yenisleidy Lorenzo, Felipe Echeverria, and Ramon Latorre

The Oxford Handbook of Neuronal Ion Channels

Edited by Arin Bhattacharjee

Subject: Neuroscience, Molecular and Cellular Systems Online Publication Date: Apr 2018

DOI: 10.1093/oxfordhb/9780190669164.013.11

Abstract and Keywords

The Slowpoke (Slo) family of large conductance K⁺ channels comprises four structurally and functionally related members (Slo1, Slo2.1, Slo2.2, and Slo3). With the exception of Slo3, all Slo channels are expressed in neurons, where their diverse functions include influencing the shape, frequency, and propagation of action potentials, as well as neurotransmitter release. The Slo1 channel (KCa1.1; KCNMA1, BK) is Ca²⁺- and voltage-activated, while the two Slo2 channels, Slo2.1 (KNa1.2, KCNT2, Slick) and Slo2.2 (KNa1.1, KCNT1, Slack), are activated by internal Na⁺. The functional diversity of the Slo family is greatly increased through alternative splicing, metabolic regulation, and the formation of heterotetramers (Slo2 channels). Co-expression of the pore-forming α subunit of Slo1 with its accessory subunits β and γ further increases channel diversity. This chapter focuses on the role of the Slo channel family in neurons under both physiological and pathological conditions.

Keywords: Slo channels, BK channel, Slick channel, Slack channel, Neurons, Neuronal channels, Beta subunits, Beta 2, Beta 4

Large Conductance Potassium Channels in the Nervous System

about the specific structural determinants of the Slo channel function. However, the answers to several important problems, such as that of the molecular determinants of these channel's unusually large conductance, remain elusive.

Future Directions

Several key questions currently remain unanswered about the Slo channel family and its role in the nervous system. Among the major recent advances of this field was the determination of the structures of Slo1 and Slo2.2. Without doubt, these structures will greatly help the design of new and more potent agonists and inhibitors of these channels in a major step towards a structurally oriented Slo channel pharmacology. In addition, the newly available information on their structures will help reveal the molecular determinants of their large conductance and exquisitely high selectivity. It seems likely that these open questions can be resolved by focusing future studies on the molecular characteristics of the internal vestibule. Finally, the precise role of Slo channels in neuronal diseases should be further pinpointed, in order to aid the rational approach to the treatment of these ailments.

Acknowledgements

This work was supported by Fondo Nacional de Desarrollo Científico y Tecnológico (FONDECYT) Grant No. 1150273 to RL, Comisión Nacional de Investigación Científica y Tecnológica (CONICYT) doctoral fellowship to YL, and the Air Force Office of Scientific Research under award number FA9550-16-1-0384 to RL. The Centro Interdisciplinario de Neurociencia de Valparaíso is a Millennium Institute (P09-022-F) supported by the Millennium Scientific Initiative of Ministerio de Economía, Fomento y Turismo of Chile.

References

- Adelman, J. P., Shen, K. Z., Kavanaugh, M. P., Warren, R. A., Wu, Y. N., Lagrutta, A., ... North, R. A. (1992). Calcium-activated potassium channels expressed from cloned complementary DNAs. *Neuron*, 9(2), 209–216.
- Aggarwal, S. K., & MacKinnon, R. (1996). Contribution of the S4 segment to gating charge in the Shaker K⁺ channel. *Neuron*, 16(6), 1169–1177.
- Ahrendt, E., Kyle, B., Braun, A. P., & Braun, J. E. (2014). Cysteine string protein limits expression of the large conductance, calcium-activated K⁺ (BK) channel. *PLoS One*, 9(1), e86586. doi:10.1371/journal.pone.0086586



An integrate-and-fire model to generate spike trains with long-range dependence

Alexandre Richard¹ · Patricio Orio^{2,3} · Etienne Tanré⁴Received: 5 May 2017 / Revised: 22 February 2018 / Accepted: 23 February 2018
© Springer Science+Business Media, LLC, part of Springer Nature 2018

Abstract

Long-range dependence (LRD) has been observed in a variety of phenomena in nature, and for several years also in the spiking activity of neurons. Often, this is interpreted as originating from a non-Markovian system. Here we show that a purely Markovian integrate-and-fire (IF) model, with a noisy slow adaptation term, can generate interspike intervals (ISIs) that appear as having LRD. However a proper analysis shows that this is not the case asymptotically. For comparison, we also consider a new model of individual IF neuron with fractional (non-Markovian) noise. The correlations of its spike trains are studied and proven to have LRD, unlike classical IF models. On the other hand, to correctly measure long-range dependence, it is usually necessary to know if the data are stationary. Thus, a methodology to evaluate stationarity of the ISIs is presented and applied to the various IF models. We explain that Markovian IF models may seem to have LRD because of non-stationarities.

Keywords Interspike interval statistics · Stochastic integrate-and-fire model · Long-range dependence · Stationarity

1 Introduction

The modeling of neuronal activity has a long and rich history whose first successes date back to the 50's and the seminal work of Hodgkin and Huxley (1952). A few years later, a simpler probabilistic model based on the passage times of a random walk was introduced by Gerstein and

Mandelbrot (1964), corresponding to a stochastic version of the Perfect Integrate-and-Fire (PIF) model.

The activity of a neuron is characterized by the electrical potential of its membrane, and more precisely by spikes whose amplitude and duration are very similar to one another. Therefore, it is rather the sequence of times at which these spikes occur which is believed to carry the neuronal information. While temporal (and spatial) correlations between interspike intervals (ISIs) have been observed for a long time (see Chacron et al. 2003 and references therein), the presence of fractal behavior (Teich 1992; Bair et al. 1994) and LRD phenomena in the spiking activity of neurons has been acknowledged for only two decades: see Teich et al. (1996, 1997), Lewis et al. (2001), Lowen et al. (2001), Bhattacharya et al. (2005), including artificially grown neuronal networks in Segev et al. (2002), etc. (see the introduction of Jackson 2004 for a very comprehensive list of references). This LRD phenomenon is ubiquitous in nature, and takes the form of power-law correlations between interspike intervals rather than exponentially decaying correlations. In particular, LRD implies that the present neuronal activity is correlated with a very distant past.

Until recently in the neuroscience literature, long-range dependence, also called long memory, has been quantified

Action Editor: A. Compte

✉ Alexandre Richard
alexandre.richard@centralesupelec.frPatricio Orio
patricio.orio@uv.clEtienne Tanré
Etienne.Tanre@inria.fr¹ CentraleSupélec, Université Paris-Saclay, Laboratoire MICS et Fédération CNRS - FR3487, Gif-sur-Yvette, France² Instituto de Neurociencia, Facultad de Ciencias, Universidad de Valparaíso, Valparaíso, Chile³ Centro Interdisciplinario de Neurociencia de Valparaíso, Universidad de Valparaíso, Valparaíso, Chile⁴ Université Côte d'Azur, Inria, 2004 Route des Lucioles BP 93, 06902 Sophia-Antipolis, France

From Doukhan (1994), Chapter 1.5, it is known that any stationary and mixing sequence satisfies an invariance principle. This is enough to apply Theorem 4 of Mandelbrot (1975), which gives the convergence of $N^{-1/2}R/S(N)$ to a non-trivial random variable. Therefore we conjecture the following result that we plan to prove in a separate work, that is:

If $\alpha = 0.5$, the sequence of interspike intervals generated by the PIF/LIF model (2) has a stationary regime, and $N^{-1/2}R/S(N)$ converges to a non-degenerate random variable (i.e. $\hat{H}_N \rightarrow 0.5$).

Our second heuristics is about the approximation of the fractional Brownian motion by a sequence of n -dimensional Ornstein-Uhlenbeck processes, as n increases. In Schwalger et al. (2015), the general idea is that the covariance of a general Gaussian process can be approximated by an Ornstein-Uhlenbeck with sufficiently many components. In Carmona et al. (2000), it is proven that the fBm is indeed an infinite-dimensional Ornstein-Uhlenbeck process. Therefore, we can consider our model with fractional noise as a natural limit to the model proposed in Schwalger et al. (2015). Although this is not the only possible limit in their approach, the fBm is the most sensible choice to obtain long-range dependence.

Acknowledgements Part of this work was carried out while A.R. was a postdoc at Inria Sophia-Antipolis and at Ecole Polytechnique (the support from ERC 321111 Rofirm is gratefully acknowledged). A.R. and E.T. acknowledge the support from the ECOS-Sud Program Chili-France C15E05 and from the European Union's Horizon 2020 Framework Program for Research and Innovation under Grant Agreement No. 720270 (Human Brain Project SGA1). P.O. acknowledges the support from the Advanced Center for Electrical and Electronic Engineering (Basal Funding FB0008, Conicyt) and the project P09-022-F from the Millennium Scientific Initiative of the Chilean Ministry of Economy, Development, and Tourism.

We thank the reviewers for their remarks which helped to improve significantly the quality of this paper.

Compliance with Ethical Standards

Conflict of Interest The authors declare that they have no conflict of interest.

References

- Abry, P., Gonçalves, P., Flandrin, P. (1995). *Wavelets, spectrum analysis and Itô processes*, (pp. 15–29). New York: Springer.
- Baddeley, R., Abbott, L.F., Booth, M.C., Sengpiel, F., Freeman, T., Wakeman, E.A., Rolls, E.T. (1997). Responses of neurons in primary and inferior temporal visual cortices to natural scenes, (Vol. 264 pp. 1775–1783).
- Bair, W., Koch, C., Newsome, W., Britten, K. (1994). Power spectrum analysis of bursting cells in area mt in the behaving monkey. *Journal of Neuroscience*, 14(5), 2870–2892.
- Beran, J., Feng, Y., Ghosh, S., Kulik, R. (2013). *Long-memory processes*. Heidelberg: Springer. Probabilistic properties and statistical methods.
- Bhattacharya, R.N., Gupta, V.K., Waymire, E. (1983). The Hurst effect under trends. *Journal of Applied Probability*, 20(3), 649–662.
- Bhattacharya, J., Edwards, J., Mamelak, A., Schuman, E. (2005). Long-range temporal correlations in the spontaneous spiking of neurons in the hippocampal-amygdala complex of humans. *Neuroscience*, 131(2), 547–555.
- Brunel, N., & Sergi, S. (1998). Firing frequency of leaky integrate-and-fire neurons with synaptic current dynamics. *Journal of Theoretical Biology*, 195(1), 87–95.
- Cardinali, A., & Nason, G.P. (2010). Costationarity of locally stationary time series. *Journal of Time Series Econometrics*, 2(2), Article 1.
- Cardinali, A., & Nason, G.P. (2018). Practical powerful wavelet packet tests for second-order stationarity. *Applied and Computational Harmonic Analysis* 44(3), 558–583.
- Carmona, P., Coutin, L., Montseny, G. (2000). Approximation of some Gaussian processes. *Statistical Inference for Stochastic Processes*, 3(1-2), 161–171. 19th “Rencontres Franco-Belges de Statisticiens” (Marseille, 1998).
- Chacron, M.J., Pakdaman, K., Longtin, A. (2003). Interspike interval correlations, memory, adaptation, and refractoriness in a leaky integrate-and-fire model with threshold fatigue. *Neural Computation*, 15(2), 253–278.
- Churilla, A.M., Gottschalk, W.A., Liebovitch, L.S., Selector, L.Y., Todorov, A.T., Yeandle, S. (1995). Membrane potential fluctuations of human t-lymphocytes have fractal characteristics of fractional brownian motion. *Annals of Biomedical Engineering*, 24(1), 99–108.
- Coeurjolly, J.-F. (2000). Simulation and identification of the fractional brownian motion: a bibliographical and comparative study. *Journal of Statistical Software*, 5(1), 1–53.
- de Oliveira, R.C., Barbosa, C., Consoni, L., Rodrigues, A., Varanda, W., Nogueira, R. (2006). Long-term correlation in single calcium-activated potassium channel kinetics. *Physica A: Statistical Mechanics and its Applications*, 364, 13–22.
- Decreusefond, L., & Nualart, D. (2008). Hitting times for Gaussian processes. *The Annals of Probability*, 36(1), 319–330.
- Delorme, M., & Wiese, K.J. (2015). Maximum of a fractional Brownian motion: analytic results from perturbation theory. *Physical Review Letters*, 115(21), 210601, 5.
- Destexhe, A., Rudolph, M., Paré, D. (2003). The high-conductance state of neocortical neurons *in vivo*. *Nature Reviews Neuroscience*, 4(9), 739–751.
- Doukhan, P. (1994). *Mixing, properties and examples, volume 85 of lecture notes in statistics*. New York: Springer.
- Drew, P.J., & Abbott, L.F. (2006). Models and properties of power-law adaptation in neural systems. *Journal of Neurophysiology*, 96(2), 826–833.
- Fairhall, A.L., Lewen, G.D., Bialek, W., de Ruyter van Steveninck, R.R. (2001). Efficiency and ambiguity in an adaptive neural code. *Nature*, 412, 787–792.
- Gerstein, G.L., & Mandelbrot, B. (1964). Random walk models for the spike activity of a single neuron. *Biophysical Journal*, 4(1), 41–68.
- Hammond, A., & Sheffield, S. (2013). Power law Pólya's urn and fractional Brownian motion. *Probability Theory and Related Fields*, 157(3–4), 691–719.
- Hodgkin, A.L., & Huxley, A.F. (1952). A quantitative description of membrane current and its application to conduction and excitation in nerve. *The Journal of Physiology*, 117(4), 500–544.



Article

Angiotensin II-Induced Mesangial Cell Damage Is Preceded by Cell Membrane Permeabilization Due to Upregulation of Non-Selective Channels

Gonzalo I. Gómez ^{1,*} , Paola Fernández ¹, Victoria Velarde ¹ and Juan C. Sáez ^{1,2,*}¹ Departamento de Fisiología, Facultad de Ciencias Biológicas, Pontificia Universidad Católica de Chile, Alameda #340, 8331150 Santiago, Chile; paolafernandezbq@gmail.com (P.F.); vvelarde@bio.puc.cl (V.V.)² Instituto Milenio, Centro Interdisciplinario de Neurociencias de Valparaíso, Universidad de Valparaíso, 2381850 Valparaíso, Chile* Correspondence: gggomez@uc.cl (G.I.G.); jcsaez@gmail.com (J.C.S.);
Tel.: +56-2-2354-6185 (G.I.G.); +56-2-2354-2860 (J.C.S.)

Received: 16 February 2018; Accepted: 20 March 2018; Published: 23 March 2018



Abstract: Connexin43 (Cx43), pannexin1 (Panx1) and P2X₇ receptor (P2X₇R) are expressed in kidneys and are known to constitute a feedforward mechanism leading to inflammation in other tissues. However, the possible functional relationship between these membrane channels and their role in damaged renal cells remain unknown. In the present work, we found that MES-13 cells, from a cell line derived from mesangial cells, stimulated with angiotensin II (AngII) developed oxidative stress (OS, thiobarbituric acid reactive species (TBARS) and generated pro-inflammatory cytokines (ELISA; IL-1 β and TNF- α). The membrane permeability increased progressively several hours before the latter outcome, which was a response prevented by Losartan, indicating the involvement of AT₁ receptors. Western blot analysis showed that the amount of phosphorylated MYPT (a substrate of RhoA/ROCK) and Cx43 increased progressively and in parallel in cells treated with AngII, a response followed by an increase in the amount in Panx1 and P2X₇R. Greater membrane permeability was partially explained by opening of Cx43 hemichannels (Cx43 HCs) and Panx1 channels (Panx1 Chs), as well as P2X₇R activation by extracellular ATP, which was presumably released via Cx HCs and Panx1 Chs. Additionally, inhibition of RhoA/ROCK blocked the progressive increase in membrane permeability, and the remaining response was explained by the other non-selective channels. The rise of activity in the RhoA/ROCK-dependent pathway, as well as in Cx HCs, P2X₇R, and to a minor extent in Panx1 Chs led to higher amounts of TBARS and pro-inflammatory cytokines. We propose that AngII-induced mesangial cell damage could be effectively inhibited by concomitantly inhibiting the RhoA/ROCK-dependent pathway and one or more non-selective channel(s) activated through this pathway.

Keywords: connexin hemichannel; gap junction; P2X₇ receptor; pannexin1 channel; extracellular ATP; oxidative stress; angiotensin receptors; Fasudil; Y-27632

1. Introduction

In chronic kidney disease, hypertension is one of the most common complications that generate predispositions to other health problems, affecting several organs. Hypertensive nephropathy begins in the glomerulus by increasing intraglomerular pressure. These early events activate and damage mesangial cells, epithelial cells and podocytes in the glomerulus. In turn, these cells produce vasoactive and pro-inflammatory agents, which increase cell damage and promote fibrosis, reducing renal blood flow, permeability and, eventually, glomerular filtration [1].

4.6. Thiobarbituric Acid Reactive Substances (TBARS) Measurement

The amount of TBARS was estimated using the method described by Ramanathan and collaborators [68] with slight modifications. Culture medium was mixed with SDS (8% *w/v*), thiobarbituric acid (0.8% TBA *w/v*), and acetic acid (20% *v/v*), and heated for 60 min at 90 °C. Precipitated material was removed by centrifugation, and the absorbance of the supernatant was evaluated at 532 nm. The amount of TBARS was calculated using a calibration curve obtained with malondialdehyde (MDA) as standard. MDA was obtained from Merck (Darmstadt, Germany).

4.7. Enzyme-Linked Immunosorbent Assay

IL-1 β and TNF- α ELISA assays were performed to determine the amount of IL-1 β and TNF- α in the extracellular medium under different conditions, following the manufacturer's protocol (IL-1 β and TNF- α EIA kit, Enzo Life Science, Farmingdale, NY, USA). Results were normalized by protein amount in ng/mL.

4.8. Statistical Analysis

Results were evaluated by ANOVA, and the Tuckey's post-test was used to evaluate the difference between the two groups. Results below are expressed as the average of values from each independent experiment \pm SE, and considered significantly different if $p < 0.05$. Analyses were performed with the GraphPad Prism 5 software for Windows (1992–2007, GraphPad Software, 12 March, 2007, La Jolla, CA, USA).

Acknowledgments: This work was partially supported by a CONICYT Ph.D. fellowship No. 21120081 (to Gonzalo I. Gómez), a FONDECYT grant No. 1150291 (to Juan C. Sáez), and P09-022-F from Iniciativa Científica Milenio (ICM)-ECONOMIA, Chile (to Juan C. Sáez). The data of this work will be presented by Gonzalo I. Gómez as partial fulfillment of the requirements to obtain a Ph.D. degree in Physiological Sciences at Pontificia Universidad Católica de Chile.

Author Contributions: Gonzalo I. Gómez, Victoria Velarde and Juan C. Sáez conceived and designed the experiments; Gonzalo I. Gómez and Paola Fernández performed the experiments; Gonzalo I. Gómez and Juan C. Sáez analyzed the data; Juan C. Sáez and Victoria Velarde contributed reagents/materials/analysis tools; Gonzalo I. Gómez and Juan C. Sáez wrote the paper.

Conflicts of Interest: The authors declare no conflict of interest.

Abbreviations

Cx43	Connexin 43
Panx1	Pannexin 1
P2X ₇ R	P2X ₇ Receptor
OS	Oxidative stress
TBARS	Thiobarbituric reactive species
AngII	Angiotensin II
ROCK	Rho kinase
NF κ B	Nuclear factor kappa-light-chain-enhancer of activated B cells
Cx GJs	Connexin gap junctions
Cx HCs	Connexin hemichannels
Panx Chs	Pannexin channels
FBS	Fetal bovine serum
CBX	Carbenoxolone
PBC	Probenecid
MDA	Malondialdehyde
Etd ⁺	Ethidium

SCIENTIFIC REPORTS

OPEN

Electrical coupling between A17 cells enhances reciprocal inhibitory feedback to rod bipolar cells

Claudio Elgueta^{1,2}, Felix Leroy³, Alex H. Vielma², Oliver Schmachtenberg² & Adrian G. Palacios²

Received: 9 February 2017
Accepted: 29 January 2018
Published online: 15 February 2018

A17 amacrine cells are an important part of the scotopic pathway. Their synaptic varicosities receive glutamatergic inputs from rod bipolar cells (RBC) and release GABA onto the same RBC terminal, forming a reciprocal feedback that shapes RBC depolarization. Here, using patch-clamp recordings, we characterized electrical coupling between A17 cells of the rat retina and report the presence of strongly interconnected and non-coupled A17 cells. In coupled A17 cells, evoked currents preferentially flow out of the cell through GJs and cross-synchronization of presynaptic signals in a pair of A17 cells is correlated to their coupling degree. Moreover, we demonstrate that stimulation of one A17 cell can induce electrical and calcium transients in neighboring A17 cells, thus confirming a functional flow of information through electrical synapses in the A17 coupled network. Finally, blocking GJs caused a strong decrease in the amplitude of the inhibitory feedback onto RBCs. We therefore propose that electrical coupling between A17 cells enhances feedback onto RBCs by synchronizing and facilitating GABA release from inhibitory varicosities surrounding each RBC axon terminal. GJs between A17 cells are therefore critical in shaping the visual flow through the scotopic pathway.

The mammalian retina can elicit behavioral responses after the detection and processing of just a few photons¹. This is accomplished by the scotopic pathway, a highly efficient microcircuit formed by distinct sets of dedicated excitatory and inhibitory cells^{2–5}. Although the multiple synaptic steps that compose the scotopic pathway should theoretically add noise to the transmitted information, low-level luminous signals can faithfully be interpreted by the visual cortex¹. One mechanism which is proposed to help in discriminating light-induced from randomly-generated spurious signals is the generation of a code of highly synchronized action potentials at the output of retinal ganglion cells (RGCs)^{6–9}. Correlated firing can be supported by the existence of common convergent synaptic inputs with high release probability^{6,10,11} and by electrical coupling between RGCs or between populations of presynaptic neurons^{6,12–14}. Therefore, synchronous activity could be a critical feature in earlier steps of retinal signal processing, allowing faithful transmission of weak luminous signals.

The second synapse of the main scotopic pathway is located between RBCs and AII amacrine cells. Glutamate released from RBC ribbon synapses depolarizes glycinergic AII cells, which in turn use the cone bipolar circuitry to convey scotopic signals towards RGCs^{4,5,15,16}. RBCs also contact A17 amacrine cell dendrites forming a tripartite synapse with AII and A17 cells^{17,18}. Glutamate from RBCs triggers GABA release from A17 cells onto RBC axon terminals¹⁹. This reciprocal feedback modulates the gain and kinetics of the RBC-AII synapse^{20,21} by curtailing RBC cell depolarization²². A17 cells receive inputs from around 100 RBCs, but each RBC makes only one contact with a given A17 cell^{23–25}. The depolarization induced by a single RBC remains electrically confined at the postsynaptic varicosity thanks to the morphological and electrophysiological properties of A17 cells^{23,26}. This arrangement could potentially introduce noise to the output of RBCs due to the variability between isolated reciprocal inhibitory synapses.

Interestingly, GABAergic A17 cells are known to be electrically interconnected^{25,27–29} and dendro-dendritic electrical coupling between neurons could support the homogenization of voltage fluctuations and enhance signal synchrony in downstream targets^{30–33}. However, in spite of the central role of A17 cells in the scotopic circuitry^{20,21} and the relevance and prevalence of electrical synapses in this circuit^{34–38}, a detailed characterization of how the

¹Centro Interdisciplinario de Neurociencia de Valparaíso, Universidad de Valparaíso, Valparaíso, Chile. ²Physiology Institute I, Alberts Ludwig University, Freiburg, Germany. ³Neuroscience department, Columbia University Medical Center, 1051 Riverside Drive, New York, NY, 10032, USA. Correspondence and requests for materials should be addressed to C.E. (email: claudioez@gmail.com)

52. Veruki, M. L. & Hartveit, E. All (Rod) amacrine cells form a network of electrically coupled interneurons in the mammalian retina. *Neuron* **33**, 935–946 (2002).
53. Güldenagel, M. *et al.* Expression patterns of connexin genes in mouse retina. *Journal of Comparative Neurology* **425**, 193–201 (2000).
54. Kamasawa, N. *et al.* Abundance and ultrastructural diversity of neuronal gap junctions in the OFF and ON sublaminae of the inner plexiform layer of rat and mouse retina. *Neuroscience* **142**, 1093–1117 (2006).
55. Vaney, D. I., Nelson, J. C. & Pow, D. V. Neurotransmitter coupling through gap junctions in the retina. *The Journal of neuroscience* **18**, 10594–10602 (1998).
56. Lin, B., Jakobs, T. C. & Masland, R. H. Different functional types of bipolar cells use different gap-junctional proteins. *The Journal of neuroscience* **25**, 6696–6701 (2005).
57. Schubert, T., Maxeiner, S., Krüger, O., Willecke, K. & Weiler, R. Connexin45 mediates gap junctional coupling of bistratified ganglion cells in the mouse retina. *Journal of Comparative Neurology* **490**, 29–39 (2005).
58. Bloomfield, S. A., Xin, D. & Osborne, T. Light-induced modulation of coupling between All amacrine cells in the rabbit retina. *Visual neuroscience* **14**, 565–576 (1997).
59. Beierlein, M., Gibson, J. R. & Connors, B. W. A network of electrically coupled interneurons drives synchronized inhibition in neocortex. *Nature neuroscience* **3**, 904–910 (2000).
60. Galarreta, M. & Hestrin, S. A network of fast-spiking cells in the neocortex connected by electrical synapses. *Nature* **402**, 72–75 (1999).
61. Tamás, G., Buhl, E. H., Lörincz, A. & Somogyi, P. Proximally targeted GABAergic synapses and gap junctions synchronize cortical interneurons. *Nature neuroscience* **3**, 366–371 (2000).
62. Sterling, P., Freed, M. A. & Smith, R. G. Architecture of rod and cone circuits to the on-beta ganglion cell. *The Journal of neuroscience* **8**, 623–642 (1988).
63. Singer, J. H. & Diamond, J. S. Sustained Ca²⁺ entry elicits transient postsynaptic currents at a retinal ribbon synapse. *The Journal of Neuroscience* **23**, 10923–10933 (2003).
64. Oesch, N. W. & Diamond, J. S. Ribbon synapses compute temporal contrast and encode luminance in retinal rod bipolar cells. *Nature neuroscience* **14**, 1555–1561 (2011).
65. Singer, J. H. & Diamond, J. S. Vesicle depletion and synaptic depression at a mammalian ribbon synapse. *Journal of neurophysiology* **95**, 3191–3198 (2006).
66. Chapot, C. A., Euler, T. & Schubert, T. How do horizontal cells “talk” to cone photoreceptors? Different levels of complexity at the cone–horizontal cell synapse. *The Journal of Physiology* (2017).
67. Völgyi, B., Xin, D. & Bloomfield, S. A. Feedback inhibition in the inner plexiform layer underlies the surround-mediated responses of All amacrine cells in the mammalian retina. *The Journal of Physiology* **539**, 603–614 (2002).
68. Van Rijen, H., Wilders, R., Van Ginneken, A. C. & Jongsma, H. J. Quantitative analysis of dual whole-cell voltage-clamp determination of gap junctional conductance. *Pflügers Archiv* **436**, 141–151 (1998).

Acknowledgements

This study was supported by CINV, a Millennium Institute (P09-022-F) funded by the Millennium Scientific Initiative of the Ministry of Economy, Development and Tourism (Chile), a graduate MECESUP fellowship and a CONYCIIT PhD support grant to CE and a FONDECYT No. 1171228. We thank Dr. Pepe Alcamí, Dr. Michael Strüder and Dr. Shakuntala Savanthrapadian for their comments and suggestions on the manuscript.

Author Contributions

C.E. designed the project, obtained the data and wrote the manuscript. F.I. and A.V. obtained data and contributed in writing the manuscript. O.S. and A.P. contributed in project design and writing of the manuscript.

Additional Information

Competing Interests: The authors declare no competing interests.

Publisher's note: Springer Nature remains neutral with regard to jurisdictional claims in published maps and institutional affiliations.



Open Access This article is licensed under a Creative Commons Attribution 4.0 International License, which permits use, sharing, adaptation, distribution and reproduction in any medium or format, as long as you give appropriate credit to the original author(s) and the source, provide a link to the Creative Commons license, and indicate if changes were made. The images or other third party material in this article are included in the article's Creative Commons license, unless indicated otherwise in a credit line to the material. If material is not included in the article's Creative Commons license and your intended use is not permitted by statutory regulation or exceeds the permitted use, you will need to obtain permission directly from the copyright holder. To view a copy of this license, visit <http://creativecommons.org/licenses/by/4.0/>.

© The Author(s) 2018

SCIENTIFIC REPORTS

OPEN

Demonstration of ion channel synthesis by isolated squid giant axon provides functional evidence for localized axonal membrane protein translation

Received: 1 November 2017
Accepted: 18 January 2018
Published online: 02 February 2018

Chhavi Mathur¹, Kory R. Johnson², Brian A. Tong¹, Pablo Miranda¹, Deepa Srikumar¹, Daniel Basilio^{1,3}, Ramon Latorre⁴, Francisco Bezanilla⁵ & Miguel Holmgren¹

Local translation of membrane proteins in neuronal subcellular domains like soma, dendrites and axon termini is well-documented. In this study, we isolated the electrical signaling unit of an axon by dissecting giant axons from mature squids (*Dosidicus gigas*). Axoplasm extracted from these axons was found to contain ribosomal RNAs, ~8000 messenger RNA species, many encoding the translation machinery, membrane proteins, translocon and signal recognition particle (SRP) subunits, endomembrane-associated proteins, and unprecedented proportions of SRP RNA (~68% identical to human homolog). While these components support endoplasmic reticulum-dependent protein synthesis, functional assessment of a newly synthesized membrane protein in axolemma of an isolated axon is technically challenging. Ion channels are ideal proteins for this purpose because their functional dynamics can be directly evaluated by applying voltage clamp across the axon membrane. We delivered *in vitro* transcribed RNA encoding native or *Drosophila* voltage-activated Shaker K_v channel into excised squid giant axons. We found that total K⁺ currents increased in both cases; with added inactivation kinetics on those axons injected with RNA encoding the Shaker channel. These results provide unambiguous evidence that isolated axons can exhibit *de novo* synthesis, assembly and membrane incorporation of fully functional oligomeric membrane proteins.

Neurons are morphologically compartmentalized cells. Their cell bodies possess the nucleus and organelles to synthesize proteins, many of which are transported to axons and dendrites. Nonetheless, cumulative evidence has suggested that local protein translation is essential^{1–3} for dendritic function^{4–13}, axonal maintenance^{14,15}, as well as for external stimuli-induced responses in specialized axonal structures, such as in growth cones during axonal development^{16–20} and navigation^{15,21–24}, and in axon termini during axonal regeneration^{25,26} and synaptic plasticity²⁷. Consistently, large number of mRNA transcripts have been reported in these compartments^{28–36}.

Using genomewide microarrays or next-generation sequencing with pure axonal preparations^{30,33,35}, the number of unique transcripts in axons are now believed to be in the thousands; and likely many are actively translated locally³⁷. In this study, we aimed to obtain a transcriptome using axoplasm, exclusively derived from the giant axon of the Humboldt squid (*Dosidicus gigas*). These axons are known to be formed by fusion of axons originating from cell bodies residing in the stellate ganglion³⁸ that gives rise to a large electrical signal transmission unit, normally larger than 1.0 mm in diameter (Fig. 1). Axoplasm was separated from axolemma and surrounding Schwann cells to assess the population of RNA transcripts present in one single axon. Total RNA from axoplasm

¹National Institute of Neurological Disorders and Stroke, National Institutes of Health, Bethesda, Maryland, 20892, USA. ²Bioinformatics Section, National Institute of Neurological Disorders and Stroke, National Institutes of Health, Bethesda, Maryland, 20892, USA. ³Facultad de Ciencias, Universidad de Chile, Santiago, 7750000, Chile. ⁴Centro Interdisciplinario de Neurociencias de Valparaíso, Universidad de Valparaíso, Valparaíso, 2366103, Chile. ⁵Department of Biochemistry and Molecular Biology, University of Chicago, Gordon Center for Integrative Sciences, Chicago, Illinois, 60637, USA. Correspondence and requests for materials should be addressed to R.L. (email: ramon.latorre@uv.cl) or F.B. (email: fbezanilla@peds.bsd.uchicago.edu) or M.H. (email: holmgren@ninds.nih.gov)

45. Deutsch, C. The birth of a channel. *Neuron* **40**, 265–276 (2003).
46. Khanna, R., Myers, M. P., Laine, M. & Papazian, D. M. Glycosylation increases potassium channel stability and surface expression in mammalian cells. *J Biol Chem* **276**, 34028–34034, <https://doi.org/10.1074/jbc.M105248200> (2001).
47. Larsen, N. & Zwiebel, C. SRP-RNA sequence alignment and secondary structure. *Nucleic Acids Res* **19**, 209–215 (1991).
48. Frankenhaeuser, B. & Hodgkin, A. L. The after-effects of impulses in the giant nerve fibres of Loligo. *J Physiol* **131**, 341–376 (1956).
49. Demo, S. D. & Yellen, G. The inactivation gate of the Shaker K⁺ channel behaves like an open-channel blocker. *Neuron* **7**, 743–753 (1991).
50. Hoshi, T., Zagotta, W. N. & Aldrich, R. W. Biophysical and molecular mechanisms of Shaker potassium channel inactivation. *Science* **250**, 533–538 (1990).
51. Zagotta, W. N., Hoshi, T. & Aldrich, R. W. Restoration of inactivation in mutants of Shaker potassium channels by a peptide derived from ShB. *Science* **250**, 568–571 (1990).
52. Zhou, M., Morais-Cabral, J. H., Mann, S. & MacKinnon, R. Potassium channel receptor site for the inactivation gate and quaternary amine inhibitors. *Nature* **411**, 657–661, <https://doi.org/10.1038/35079500> (2001).
53. MacKinnon, R. Determination of the subunit stoichiometry of a voltage-activated potassium channel. *Nature* **350**, 232–235, <https://doi.org/10.1038/350232a0> (1991).
54. Gomez-Lagunas, F. & Armstrong, C. M. Inactivation in ShakerB K⁺ channels: a test for the number of inactivating particles on each channel. *Biophys J* **68**, 89–95, [https://doi.org/10.1016/S0006-3495\(95\)80162-1](https://doi.org/10.1016/S0006-3495(95)80162-1) (1995).
55. MacKinnon, R., Aldrich, R. W. & Lee, A. W. Functional stoichiometry of Shaker potassium channel inactivation. *Science* **262**, 757–759 (1993).
56. Li, M., Jan, Y. N. & Jan, L. Y. Specification of subunit assembly by the hydrophilic amino-terminal domain of the Shaker potassium channel. *Science* **257**, 1225–1230 (1992).
57. Shen, N. V. & Pfaffinger, P. J. Molecular recognition and assembly sequences involved in the subfamily-specific assembly of voltage-gated K⁺ channel subunit proteins. *Neuron* **14**, 625–633, doi:0896-6273(95)90319-4 (1995).
58. Cornejo, V. H., Luarte, A. & Couve, A. Global and local mechanisms sustain axonal proteostasis of transmembrane proteins. *Traffic*. <https://doi.org/10.1111/tra.12472> (2017).
59. Lin, A. C. & Holt, C. E. Function and regulation of local axonal translation. *Curr Opin Neurobiol* **18**, 60–68, <https://doi.org/10.1016/j.conb.2008.05.004> (2008).
60. Giuditta, A., Cupello, A. & Lazzarini, G. Ribosomal RNA in the axoplasm of the squid giant axon. *J Neurochem* **34**, 1757–1760 (1980).
61. Giuditta, A., Kaplan, B. B., van Minnen, J., Alvarez, J. & Koenig, E. Axonal and presynaptic protein synthesis: new insights into the biology of the neuron. *Trends Neurosci* **25**, 400–404 (2002).
62. Taylor, A. M. *et al.* Axonal mRNA in uninjured and regenerating cortical mammalian axons. *J Neurosci* **29**, 4697–4707, <https://doi.org/10.1523/JNEUROSCI.6130-08.2009> (2009).
63. Jung, H., Yoon, B. C. & Holt, C. E. Axonal mRNA localization and local protein synthesis in nervous system assembly, maintenance and repair. *Nat Rev Neurosci* **13**, 308–324, <https://doi.org/10.1038/nrn3210> (2012).
64. Giuditta, A. *et al.* Active polysomes in the axoplasm of the squid giant axon. *J Neurosci Res* **28**, 18–28, <https://doi.org/10.1002/jnr.490280103> (1991).
65. Metuzals, J., Chang, D., Hammar, K. & Reese, T. S. Organization of the cortical endoplasmic reticulum in the squid giant axon. *J Neurocytol* **26**, 529–539 (1997).
66. Wu, Y. *et al.* Contacts between the endoplasmic reticulum and other membranes in neurons. *Proc Natl Acad Sci USA* **114**, E4859–E4867, <https://doi.org/10.1073/pnas.1701078114> (2017).
67. Nagaya, N. & Papazian, D. M. Potassium channel alpha and beta subunits assemble in the endoplasmic reticulum. *J Biol Chem* **272**, 3022–3027 (1997).
68. Hodgkin, A. L. & Huxley, A. F. A quantitative description of membrane current and its application to conduction and excitation in nerve. *J Physiol* **117**, 500–544 (1952).
69. Venkataraman, G., Srikanth, D. & Holmgren, M. Quasi-specific access of the potassium channel inactivation gate. *Nat Commun* **5**, 4050, <https://doi.org/10.1038/ncomms5050> (2014).
70. Rapallino, M. V., Cupello, A. & Giuditta, A. Axoplasmic RNA species synthesized in the isolated squid giant axon. *Neurochem Res* **13**, 625–631 (1988).

Acknowledgements

We thank Oliver Schmachtenberg, Alan Neely, Ana Maria Navia, Rodrigo Toro and David Parada for *in situ* Montemar logistics and to John Ewer for critical reading of the manuscript. This work was partially supported by a Fogarty International Research Collaboration Award grant (RO3 TW008351) and by the Air Force Office of Scientific Research under award number FA9550-16-1-0384 to RL, FB and MH. Additional funding was obtained from NIH grant R01-GM030376 (FB). RL was supported by FONDECYT grant 1150273. The Centro Interdisciplinario de Neurociencia de Valparaíso (CINV) is a Millennium Institute supported by the Millennium Scientific Initiative of the Chilean Ministry of Economy, Development and Tourism. MH and KRJ are supported by the Intramural Research Program of the NIH (NINDS). We thank the Section on Instrumentation of the National Institute of Mental Health for squid chambers construction. We thank NIH Intramural Sequencing Center (NISC) for performing sequencing runs on the Illumina platform and Weiwei Wu for assistance with Bioanalyzer runs.

Author Contributions

M.H., F.B. and C.M. conceived the project. C.M. and D.S. designed and performed molecular biology experiments. C.M., M.H., B.A.T. and K.R.J. performed the bioinformatics analysis. F.B., M.H., D.B. and R.L. performed squid giant axon electrophysiology experiments and analyzed the data. P.M. performed *Xenopus* oocytes experiments and analyzed the data. All authors contributed to write the manuscript.

Additional Information

Supplementary information accompanies this paper at <https://doi.org/10.1038/s41598-018-20684-8>.

Competing Interests: The authors declare that they have no competing interests.

Publisher's note: Springer Nature remains neutral with regard to jurisdictional claims in published maps and institutional affiliations.

Sepsis-Induced Channelopathy in Skeletal Muscles is Associated with Expression of Non-Selective Channels

Balboa, Elisa^{*,†}; Saavedra-Leiva, Fujiko^{*,†}; Cea, Luis, A.^{*}; Vargas, Aníbal, A.^{*}; Ramírez, Valeria[†]; Escamilla, Rosalba^{*,§}; Sáez, Juan, C.^{*,§}; Regueira, Tomás[†]

SHOCK: February 2018 - Volume 49 - Issue 2 - p 221–228

doi: 10.1097/SHK.0000000000000916

Basic Science Aspects (Animal Subjects)

Abstract Author InformationAuthors Article MetricsMetrics

ABSTRACT Skeletal muscles (~50% of the body weight) are affected during acute and late sepsis and represent one sepsis associate organ dysfunction. Cell membrane changes have been proposed to result from a channelopathy of yet unknown cause associated with mitochondrial dysfunction and muscle atrophy. We hypothesize that the channelopathy might be explained at least in part by the expression of non-selective channels. Here, this possibility was studied in a characterized mice model of late sepsis with evident skeletal muscle atrophy induced by cecal ligation and puncture (CLP). At day seven after CLP, skeletal myofibers were found to present *de novo* expression (immunofluorescence) of connexins 39, 43, and 45 and 7 receptor² P2X₇ receptor whereas pannexin1 did not show significant changes. These changes were associated with increased sarcolemma permeability (~4 fold higher dye uptake assay), ~25% elevated in intracellular free-Ca²⁺ concentration (FURA-2), activation of protein degradation via ubiquitin proteasome pathway (Murf and Atrogin 1 reactivity), moderate reduction in oxygen consumption not explained by changes in levels of relevant respiratory proteins, ~3 fold decreased mitochondrial membrane potential (MitoTracker Red CMXRos) and ~4 fold increased mitochondrial superoxide production (MitoSox). Since connexin hemichannels and P2X₇ receptors are permeable to ions and small molecules, it is likely that they are main protagonists in the channelopathy by reducing the electrochemical gradient across the cell membrane resulting in detrimental metabolic changes and muscular atrophy.

^{*}Departamento de Fisiología, Pontificia Universidad Católica de Chile, Santiago, Chile

[†]Centro de pacientes críticos, Clínica las Condes, Santiago, Chile

^{*}Institute of Biomedical Sciences, Faculty of Medicine, University of Chile, Santiago, Chile

[§]Centro Interdisciplinario de Neurociencias de Valparaíso, Valparaíso, Chile

Address reprint requests to Dr Tomás Regueira, PhD, Centro de pacientes críticos, Clínica las Condes, Estoril 450, Las Condes, Santiago, Chile. E-mail: tregueira@gmail.com; or Dr Juan C. Sáez, PhD, Department of Physiology, Pontificia Universidad Católica de Chile, Alameda 340, Santiago, Chile. E-mail: jsaez@bio.puc.cl

Received 14 March, 2017

Revised 3 April, 2017

Accepted 25 May, 2017

EB and FS equally contributed to this work.

CINV ANNUAL PROGRESS REPORT – 2018

23-11-2018

Sepsis-Induced Channelopathy in Skeletal Muscles is Associat... : Shock

This work was partially funded by Fondo Nacional de Ciencia y Tecnología (FONDECYT) grants 1141092 (to TR and JCS), 1150291 (to JCS), post-doctoral FONDECYT grant 3160594 (to EB), FONDECYT 11160739 and CONICYT/PAI 79140023 (to LC), and as well as ICM-Economía P09-022-F Centro Interdisciplinario de Neurociencias de Valparaíso (to JCS).

The authors report no conflicts of interest.

Supplemental digital content is available for this article. Direct URL citation appears in the printed text and is provided in the HTML and PDF versions of this article on the journal's Web site (www.shockjournal.com).

© 2018 by the Shock Society

This website uses cookies. By continuing to use this website you are giving consent to cookies being used. For information on cookies and how you can disable them visit our Privacy and Cookie Policy.

Got it, thanks!



Contents lists available at ScienceDirect

BBA - Biomembranes

journal homepage: www.elsevier.com/locate/bbamem

Review

Redox-mediated regulation of connexin proteins; focus on nitric oxide[☆]Isaac E. García^a, Helmuth A. Sánchez^a, Agustín D. Martínez^{a,*}, Mauricio A. Retamal^{b,*}^a Centro Interdisciplinario de Neurociencia de Valparaíso, Instituto de Neurociencia, Facultad de Ciencias, Universidad de Valparaíso, Valparaíso, Chile^b Centro de Fisiología Celular e Integrativa, Facultad de Medicina, Clínica Alemana Universidad del Desarrollo, Santiago, Chile

ARTICLE INFO

Keywords:
Gap junction channel
Hemichannel
Redox potential
Nitric oxide

ABSTRACT

Connexins are membrane proteins that form hemichannels and gap junction channels at the plasma membrane. Through these channels connexins participate in autocrine and paracrine intercellular communication. Connexin-based channels are tightly regulated by membrane potential, phosphorylation, pH, redox potential, and divalent cations, among others, and the imbalance of this regulation have been linked to many acquired and genetic diseases. Concerning the redox potential regulation, the nitric oxide (NO) has been described as a modulator of the hemichannels and gap junction channels properties. However, how NO regulates these channels is not well understood. In this mini-review, we summarize the current knowledge about the effects of redox potential focused in NO on the trafficking, formation and functional properties of hemichannels and gap junction channels.

1. Introduction

1.1. General characteristics of hemichannels and gap junction channels formed by Cxs

In humans there are 21 genes encoding different connexin (Cx) protein isoforms which can make gap junction channels (GJCs) and hemichannels (HCs) [1]. A GJC forms an aqueous pore that connects directly the cytoplasm of adjacent cells; and is made of two HCs each provided by one of the contacting cells. HCs are formed by the oligomerization of six Cx protein subunits organized around a central pore. In the unopposed cell membrane, HCs communicate the cytoplasm with the extracellular milieu, providing a paracrine and autocrine intercellular signaling pathway. Both HCs and GJCs are permeable to ions and small molecules, like ATP, glucose, NAD⁺, second messengers (e.g., cAMP, IP₃, cGMP), nucleotides, small peptides and siRNAs [2,3]. Malfunctioning of these intercellular communication has been linked to many acquired and genetic diseases from heart disease to genetic deafness, and neurodegenerative diseases like Parkinson and Alzheimer (for revision see [4,5]).

Compared to the majority of the integral membrane proteins, Cxs exhibit a short half-life (< 5 h), which demand fast regulation of their synthesis, trafficking and internalization/degradation rate in order to maintain suitable levels of GJCs and HCs at the plasma membrane [2]. The signaling pathways involved in these key regulatory processes have their target in intracellular Cxs domains such as its C-terminal [6,7].

Mutations on these segments have been linked to several diseases [4,8,9].

Among the modulators of the functional state of GJCs and HCs, membrane potential, intra and extracellular [Ca²⁺], pH, and phosphorylation have been extensively studied (for comprehensive reviews see [10–12]). However, recently has been growing interest to study the role of redox potential as a Cxs modulator [13]. Redox modulation of Cxs can be exerted by oxidation of several potentially oxidizable amino acids, like cysteine, methionine, tyrosine, and tryptophan. These residues could be oxidized by several molecules such as NO, HO, ROO, CO₃, NO₂, O₂, peroxyntous (ONOOH) and H₂O₂. From all these possibilities only NO and/or its by-products have been consistently shown to affect Cx-based channels properties [14]. In the next sections we summarize the current knowledge regarding to the effects of NO and NO-mediated signaling pathways on the formation and functional activity of HCs and GJCs formed by Cxs.

1.2. Nitric oxide and its role in the HC trafficking and GJC formation

It is well known that Cxs oligomerize in the trans Golgi network or in the ER [15]. After oligomerization the formed HCs traffic to the plasma membrane through a Golgi-dependent or -independent sorting mechanism [16]. Once in the plasma membrane, HCs and GJCs are quickly recycled which is consistent with its very short half-life (few hours; 3–5 h). Therefore, the intercellular communication through HCs and GJCs can be effectively controlled by changes in the rate of

[☆] This article is part of a Special Issue entitled: Gap Junction Proteins edited by Jean Claude Herve.

* Corresponding authors.

E-mail addresses: agustin.martinez@uv.cl (A.D. Martínez), mretamal@udd.cl (M.A. Retamal).

<http://dx.doi.org/10.1016/j.bbamem.2017.10.006>

Received 8 May 2017; Received in revised form 25 August 2017; Accepted 6 October 2017

Available online 07 October 2017

0005-2736/ © 2017 Elsevier B.V. All rights reserved.

suggest that redox signaling molecules such as NO, could modulate the HC oligomerization and its trafficking to the plasma membrane, as occur in other proteins. In addition, the requirement of extracellular cysteines to the serial docking of two HCs to form a GJC, open the possibility that any modification on these cysteines may affect GJC assembly. Moreover, this has been shown that NO modulates the electrical properties and permeability of Cx46 HCs [45]. However, it is not clear if NO modulates the slow gating and/or the fast gating or if any intra and extracellular cysteines could modulate the pore diameter and/or its electrostatic profile. Therefore, we propose a model with possible mechanisms of action of NO on Cxs based channels (Fig. 1), but with many open questions to be solved. On the other hand, it is clear that NO may exert its effect on Cx-based channels through two pathways, activation the guanylyl cyclase and/or the S-nitrosylation of free cysteines. As mentioned in this review, it seems that NO affect different Cxs types through these two molecular mechanisms, and the final effect seems to be cell type dependent. Thus, it could be plausible to suggest that depending on the proximity of a given Cx to the NO's source, it will be S-nitrosylated or affected by phosphorylations dependent of cGMP. Additionally, it is well known that the NOSs can be compartmentalized, thus the NO production also can be confined to certain zones or organelles into the cell, affecting different pool of Cxs e.g. those in appositional or non-appositional plasma membranes.

In summary, it is clear that molecules associated to redox potential affect the properties of channels formed by Cxs. The search for the regulatory mechanisms is a new challenge in the Cx field that needs to be addressed.

Transparency document

The [Transparency document](#) associated with this article can be found, in online version.

Acknowledgments

This manuscript was supported by grant Fondecyt #1160227 (MAR); Fondecyt #1130855 and 1171240 (ADM); Fondecyt #3150634 (IEG). The Centro Interdisciplinario de Neurociencia de Valparaíso is a Millennium Institute supported by the Millennium Scientific Initiative of the Chilean Ministry of Economy, Development, and Tourism (P029-022-F).

Competing interest

The authors declare no competing interest.

References

- [1] G. Sohl, K. Willecke, Gap junctions and the connexin protein family, *Cardiovasc. Res.* 62 (2004) 228–232.
- [2] J.C. Saez, V.M. Berthoud, M.C. Branes, et al., Plasma membrane channels formed by connexins: their regulation and functions, *Physiol. Rev.* 83 (2003) 1359–1400.
- [3] L. Zong, Y. Zhu, R. Liang, et al., Gap junction mediated miRNA intercellular transfer and gene regulation: a novel mechanism for intercellular genetic communication, *Sci Rep* 6 (2016) 19884.
- [4] I.E. García, P. Prado, A. Pupo, et al., Connexinopathies: a structural and functional glimpse, *BMC Cell Biol.* 17 (Suppl. 1) (2016) 17.
- [5] M.A. Retamal, E.P. Reyes, I.E. García, et al., Diseases associated with leaky hemichannels, *Front. Cell. Neurosci.* 9 (2015) 267.
- [6] E. Leithe, M. Mesnil, T. Aasen, The connexin 43 C-terminus: a tail of many tales, *Biochim. Biophys. Acta* (2017), <http://dx.doi.org/10.1016/j.bbame.2017.05.008> (In press).
- [7] J.W. Smyth, S.S. Zhang, J.M. Sanchez, et al., A 14-3-3 mode-1 binding motif initiates gap junction internalization during acute cardiac ischemia, *Traffic* 15 (2014) 684–699.
- [8] I.E. García, F. Bosen, P. Mujica, et al., From hyperactive connexin26 hemichannels to impairments in epidermal calcium gradient and permeability barrier in the keratitis-ichthyosis-deafness syndrome, *J. Invest. Dermatol.* 136 (2016) 574–583.
- [9] A.D. Martínez, R. Acuna, V. Figueroa, et al., Gap-junction channels dysfunction in deafness and hearing loss, *Antioxid. Redox Signal.* 11 (2009) 309–322.
- [10] A.L. Harris, Emerging issues of connexin channels: biophysics fills the gap, *Q. Rev. Biophys.* 34 (2001) 325–472.
- [11] P.D. Lampe, A.F. Lau, Regulation of gap junctions by phosphorylation of connexins, *Arch. Biochem. Biophys.* 384 (2000) 205–215.
- [12] S. Oh, T.A. Bargiello, Voltage regulation of connexin channel conductance, *Yonsei Med. J.* 56 (2015) 1–15.
- [13] M.A. Retamal, I.E. García, B.I. Pinto, et al., Extracellular cysteine in connexins: role as redox sensors, *Front. Physiol.* 7 (2016) 1.
- [14] M.A. Retamal, Connexin and pannexin hemichannels are regulated by redox potential, *Front. Physiol.* 5 (2014) 80.
- [15] J.A. Diez, S. Ahmad, W.H. Evans, Assembly of heteromeric connexons in guinea-pig liver en route to the Golgi apparatus, plasma membrane and gap junctions, *Eur. J. Biochem.* 262 (1999) 142–148.
- [16] M. Koval, Pathways and control of connexin oligomerization, *Trends Cell Biol.* 16 (2006) 159–166.
- [17] J.W. Brewer, R.B. Corley, Quality control in protein biogenesis: thiol-mediated retention monitors the redox state of proteins in the endoplasmic reticulum, *J. Cell Sci.* 109 (Pt 9) (1996) 2383–2392.
- [18] L. Moldovan, N.I. Moldovan, Oxygen free radicals and redox biology of organelles, *Histochem. Cell Biol.* 122 (2004) 395–412.
- [19] A. Hoffmann, T. Gloe, U. Pohl, et al., Nitric oxide enhances de novo formation of endothelial gap junctions, *Cardiovasc. Res.* 60 (2003) 421–430.
- [20] P. Kameritsch, A. Hoffmann, U. Pohl, Opposing effects of nitric oxide on different connexins expressed in the vascular system, *Cell Commun. Adhes.* 10 (2003) 305–309.
- [21] R.J. Anand, S. Dai, C. Rippel, et al., Activated macrophages inhibit enterocyte gap junctions via the release of nitric oxide, *Am. J. Physiol. Gastrointest. Liver Physiol.* 294 (2008) G109–19.
- [22] W. Malorni, F. Iosi, M.T. Santini, et al., Menadione-induced oxidative stress leads to a rapid down-modulation of transferrin receptor recycling, *J. Cell Sci.* 106 (Pt 1) (1993) 309–318.
- [23] W. Malorni, U. Testa, G. Rainaldi, et al., Oxidative stress leads to a rapid alteration of transferrin receptor intravesicular trafficking, *Exp. Cell Res.* 241 (1998) 102–116.
- [24] R.M. Dekroon, P.J. Amati, Endocytosis of apoE-EGFP by primary human brain cultures, *Cell Biol. Int.* 26 (2002) 761–770.
- [25] J.E. Contreras, H.A. Sanchez, E.A. Eugenin, et al., Metabolic inhibition induces opening of unapposed connexin 43 gap junction hemichannels and reduces gap junctional communication in cortical astrocytes in culture, *Proc. Natl. Acad. Sci. U. S. A.* 99 (2002) 495–500.
- [26] M.A. Retamal, C.J. Cortes, L. Reuss, et al., S-nitrosylation and permeation through connexin 43 hemichannels in astrocytes: induction by oxidant stress and reversal by reducing agents, *Proc. Natl. Acad. Sci. U. S. A.* 103 (2006) 4475–4480.
- [27] K. Abdelmohsen, P.A. Gerber, C. von Montfort, et al., Epidermal growth factor receptor is a common mediator of quinone-induced signaling leading to phosphorylation of connexin-43: role of glutathione and tyrosine phosphatases, *J. Biol. Chem.* 278 (2003) 38360–38367.
- [28] L.O. Klotz, P. Patak, N. Ale-Agha, et al., 2-Methyl-1,4-naphthoquinone, vitamin K (3), decreases gap-junctional intercellular communication via activation of the epidermal growth factor receptor/extracellular signal-regulated kinase cascade, *Cancer Res.* 62 (2002) 4922–4928.
- [29] D. Lin, D.J. Takemoto, Oxidative activation of protein kinase Cgamma through the C1 domain. Effects on gap junctions, *J. Biol. Chem.* 280 (2005) 13682–13693.
- [30] J. Hu, L. Engman, I.A. Cotgreave, Redox-active chalcogen-containing glutathione peroxidase mimetics and antioxidants inhibit tumour promoter-induced down-regulation of gap junctional intercellular communication between WB-F344 liver epithelial cells, *Carcinogenesis* 16 (1995) 1815–1824.
- [31] N. Rouach, C.F. Calvo, H. Duquenois, et al., Hydrogen peroxide increases gap junctional communication and induces astrocyte toxicity: regulation by brain macrophages, *Glia* 45 (2004) 28–38.
- [32] C. Lu, D.G. McMahon, Modulation of hybrid bass retinal gap junctional channel gating by nitric oxide, *J. Physiol.* 499 (Pt 3) (1997) 689–699.
- [33] K.K. Ball, L. Harik, G.K. Gandhi, et al., Reduced gap junctional communication among astrocytes in experimental diabetes: contributions of altered connexin protein levels and oxidative-nitrosative modifications, *J. Neurosci. Res.* 89 (2011) 2052–2067.
- [34] G.K. Gandhi, K.K. Ball, N.F. Cruz, et al., Hyperglycaemia and diabetes impair gap junctional communication among astrocytes, *ASN Neuro* 2 (2010) e00030.
- [35] A.C. Straub, M. Billaud, S.R. Johnstone, et al., Compartmentalized connexin 43 s-nitrosylation/denitrosylation regulates heterocellular communication in the vessel wall, *Arterioscler. Thromb. Vasc. Biol.* 31 (2011) 399–407.
- [36] P. Kameritsch, N. Khandoga, W. Nagel, et al., Nitric oxide specifically reduces the permeability of Cx37-containing gap junctions to small molecules, *J. Cell. Physiol.* 203 (2005) 233–242.
- [37] R.L. McKinnon, M.L. Bolon, H.X. Wang, et al., Reduction of electrical coupling between microvascular endothelial cells by NO depends on connexin37, *Am. J. Physiol. Heart Circ. Physiol.* 297 (2009) H93–H101.
- [38] K. Pogoda, M. Fuller, U. Pohl, et al., NO, via its target Cx37, modulates calcium signal propagation selectively at myoendothelial gap junctions, *Cell Commun. Signal* 12 (2014) 33.
- [39] L.S. Patel, C.K. Mitchell, W.P. Dubinsky, et al., Regulation of gap junction coupling through the neuronal connexin Cx35 by nitric oxide and cGMP, *Cell Commun. Adhes.* 13 (2006) 41–54.
- [40] M.A. Retamal, K.A. Schalper, K.F. Shoji, et al., Opening of connexin 43 hemichannels is increased by lowering intracellular redox potential, *Proc. Natl. Acad. Sci. U. S. A.* 104 (2007) 8322–8327.
- [41] M.A. Retamal, K.A. Schalper, K.F. Shoji, et al., Possible involvement of different

Optocapacitive Generation of Action Potentials by Microsecond Laser Pulses of Nanojoule Energy

João L. Carvalho-de-Souza,¹ Bernardo I. Pinto,^{1,3} David R. Pepperberg,^{4,*} and Francisco Bezanilla^{1,2,*}

¹Department of Biochemistry and Molecular Biology and ²Institute for Biophysical Dynamics, The University of Chicago, Chicago, Illinois;

³Centro Interdisciplinario de Neurociencias de Valparaíso, Universidad de Valparaíso, Valparaíso, Chile; and ⁴Lions of Illinois Eye Research Institute, Department of Ophthalmology and Visual Sciences, University of Illinois at Chicago, Chicago, Illinois

ABSTRACT Millisecond pulses of laser light delivered to gold nanoparticles residing in close proximity to the surface membrane of neurons can induce membrane depolarization and initiate an action potential. An optocapacitance mechanism proposed as the basis of this effect posits that the membrane-interfaced particle photothermally induces a cell-depolarizing capacitive current, and predicts that delivering a given laser pulse energy within a shorter period should increase the pulse's action-potential-generating effectiveness by increasing the magnitude of this capacitive current. Experiments on dorsal root ganglion cells show that, for each of a group of interfaced gold nanoparticles and microscale carbon particles, reducing pulse duration from milliseconds to microseconds markedly decreases the minimal pulse energy required for AP generation, providing strong support for the optocapacitance mechanism hypothesis.

The artificial stimulation of neuronal activity with light is a topic of major interest in neuroscience research. Recently, we presented a technique that enables light-induced depolarization and resulting action potential (AP) generation by excitable cells. Unlike optogenetics or optopharmacology (1–10), it does not require either genetic modification of the neuron or the development/preparation of a chemical photoswitch. The mechanism whereby the technique works was unveiled by Shapiro et al. (11), who demonstrated that IR radiation is able to increase the cell membrane temperature and increase its electric capacitance. The current needed to satisfy the equation $Q = C \times V$ depolarizes the membrane, reaching its excitation voltage threshold and eliciting an action potential. The amount of change in temperature is small, but it occurs quickly, a property that led Shapiro et al. (11) to hypothesize and show a capacitance change during IR pulses. However, IR radiation is absorbed by water in the bulk medium, yielding slow and spatially imprecise photostimulation and requiring more light energy to boost the generated capacitive current. As a means of increasing the spatial localization and, potentially, the physiological effectiveness of the photostimulus, we have investigated the ability of 20 nm spherical gold nanoparticles (AuNPs) to serve as light-to-heat transducers

when positioned close to neuronal membranes by specific binders (12). These experiments, which involved 532 nm laser pulses (a wavelength that penetrates water well and is near the peak of the plasmon absorbance band of these AuNPs), indicated robust light-induced AP generation with millisecond flashes, and provided further evidence for the dependence of this photoresponsiveness on a thermally induced change in membrane capacitance. Based on the evident role of membrane capacitance change in transducing light energy into cell depolarization and AP generation, we have adopted the term “optocapacitance” to refer to the technique and the hypothesized operative mechanism.

The optocapacitance mechanism posits that a temperature-induced change in capacitance (C_m) establishes a charge debt that is met by depolarization of the membrane. It is then reasonable to suspect that if the capacitance changes more quickly, the necessary charge debt can be achieved within a shorter time (t) period of stimulation (the duration of the light pulse). Conceptually, the greater the value of dC_m/dt , the larger is the current which, in turn, will produce more membrane depolarization, thus making it easier to reach excitation threshold. Most importantly, at the moment of initiation of a virtually square pulse of laser energy to the preparation, the system exhibits a maximum rate of temperature change and thus of capacitance change. Over the duration of the pulse, the rate of change in temperature, and thus the rate of capacitance change, decreases continuously, making necessary the delivery of more energy to the

Submitted September 13, 2017, and accepted for publication November 14, 2017.

*Correspondence: davipepp@uic.edu or fbezanilla@uchicago.edu

Editor: Brian Salzberg.

<https://doi.org/10.1016/j.bpj.2017.11.018>

© 2017 Biophysical Society.

This is an open access article under the CC BY-NC-ND license (<http://creativecommons.org/licenses/by-nc-nd/4.0/>).



Carvalho-de-Souza et al.

ACKNOWLEDGMENTS

We thank Ms. Li Tang for assistance with DRG cell preparations.

J.L.C.-d.-S., B.I.P., D.R.P., and F.B. acknowledge support by National Institutes of Health (NIH) grants R01-GM030376, R21-EY023430, and R21-EY027101. D.R.P. acknowledges funding received from Research to Prevent Blindness (New York, NY) and Search for Vision (Cicero, IL). B.I.P. acknowledges fellowship support from CONICYT-PFCHA Doctorado Nacional 2017 and the Centro Interdisciplinario de Neurociencia de Valparaíso, a Millennium Institute (P09-022-F).

REFERENCES

1. Boyden, E. S., F. Zhang, ..., K. Deisseroth. 2005. Millisecond-timescale, genetically targeted optical control of neural activity. *Nat. Neurosci.* 8:1263–1268.
2. Hochbaum, D. R., Y. Zhao, ..., A. E. Cohen. 2014. All-optical electrophysiology in mammalian neurons using engineered microbial rhodopsins. *Nat. Methods.* 11:825–833.
3. Cosentino, C., L. Alberio, ..., A. Moroni. 2015. Optogenetics. Engineering of a light-gated potassium channel. *Science.* 348:707–710.
4. Deisseroth, K. 2015. Optogenetics: 10 years of microbial opsins in neuroscience. *Nat. Neurosci.* 18:1213–1225.
5. Valeeva, G., T. Tressard, ..., R. Khazipov. 2016. An optogenetic approach for investigation of excitatory and inhibitory network GABA actions in mice expressing Channelrhodopsin-2 in GABAergic neurons. *J. Neurosci.* 36:5961–5973.
6. Lester, H. A., M. E. Krouse, ..., B. F. Erlanger. 1980. A covalently bound photoisomerizable agonist: comparison with reversibly bound agonists at Electrophorus electropores. *J. Gen. Physiol.* 75:207–232.
7. Volgraf, M., P. Gorostiza, ..., D. Trauner. 2006. Allosteric control of an ionotropic glutamate receptor with an optical switch. *Nat. Chem. Biol.* 2:47–52.
8. Fortin, D. L., M. R. Banghart, ..., R. H. Kramer. 2008. Photochemical control of endogenous ion channels and cellular excitability. *Nat. Methods.* 5:331–338.
9. Yue, L., M. Pawlowski, ..., D. R. Pepperberg. 2012. Robust photoregulation of GABA_A receptors by allosteric modulation with a propofol analogue. *Nat. Commun.* 3:1095.
10. Levitz, J., J. Broichhagen, ..., E. Y. Isacoff. 2017. Dual optical control and mechanistic insights into photoswitchable group II and III metabotropic glutamate receptors. *Proc. Natl. Acad. Sci. USA.* 114:E3546–E3554.
11. Shapiro, M. G., K. Homma, ..., F. Bezanilla. 2012. Infrared light excites cells by changing their electrical capacitance. *Nat. Commun.* 3:736.
12. Carvalho-de-Souza, J. L., J. S. Treger, ..., F. Bezanilla. 2015. Photosensitivity of neurons enabled by cell-targeted gold nanoparticles. *Neuron.* 86:207–217.
13. Taylor, R. E. 1965. Impedance of the squid axon membrane. *J. Cell. Comp. Physiol.* 66:21–25.
14. Geddes, L. A. 2004. Accuracy limitations of chronaxie values. *IEEE Trans. Biomed. Eng.* 51:176–181.
15. Cole, K. S., R. Guttman, and F. Bezanilla. 1970. Nerve membrane excitation without threshold. *Proc. Natl. Acad. Sci. USA.* 65:884–891.
16. Eom, K., J. Kim, ..., S. J. Kim. 2014. Enhanced infrared neural stimulation using localized surface plasmon resonance of gold nanorods. *Small.* 10:3853–3857.
17. Paviolo, C., A. C. Thompson, ..., P. R. Stoddart. 2014. Nanoparticle-enhanced infrared neural stimulation. *J. Neural Eng.* 11:065002.
18. Eom, K., C. Im, ..., S. J. Kim. 2016. Synergistic combination of near-infrared irradiation and targeted gold nanoheaters for enhanced photothermal neural stimulation. *Biomed. Opt. Express.* 7:1614–1625.
19. Paviolo, C., and P. R. Stoddart. 2017. Gold nanoparticles for modulating neuronal behavior. *Nanomaterials (Basel).* 7. <https://doi.org/10.3390/nano704009>.
20. Jiang, Y., J. L. Carvalho-de-Souza, ..., B. Tian. 2016. Heterogeneous silicon mesostructures for lipid-supported bioelectric interfaces. *Nat. Mater.* 15:1023–1030.
21. Rajavel, K., R. Gomathi, ..., R. T. Rajendra Kumar. 2014. In vitro bacterial cytotoxicity of CNTs: reactive oxygen species mediate cell damage edges over direct physical puncturing. *Langmuir.* 30:592–601.
22. Cohen, L. B., and B. M. Salzberg. 1978. Optical measurement of membrane potential. In *Reviews of Physiology, Biochemistry and Pharmacology*, Vol. 83. Springer, Berlin, Germany, pp. 35–88.

Input-Specific NMDAR-Dependent Potentiation of Dendritic GABAergic Inhibition

Chiayu Q. Chiu,^{1,2} James S. Martenson,^{1,3} Maya Yamazaki,⁴ Rie Natsume,⁴ Kenji Sakimura,⁴ Susumu Tomita,^{1,3} Steven J. Tavalin,⁵ and Michael J. Higley^{1,5,*}

¹Department of Neuroscience, Program in Cellular Neuroscience, Neurodegeneration, and Repair, Kavli Institute for Neuroscience, Yale University School of Medicine, New Haven, CT 06510, USA

²Centro Interdisciplinario de Neurociencia de Valparaíso, Universidad de Valparaíso, Valparaíso 2360102, Chile

³Department of Cellular and Molecular Physiology, Yale University School of Medicine, New Haven, CT 06510, USA

⁴Department of Cellular Neurobiology, Brain Research Institute, Niigata University, Niigata 951-8585, Japan

⁵Department of Pharmacology, University of Tennessee Health Science Center, Memphis, TN 38103, USA

*Lead Contact

*Correspondence: m.higley@yale.edu

<https://doi.org/10.1016/j.neuron.2017.12.032>

SUMMARY

Preservation of a balance between synaptic excitation and inhibition is critical for normal brain function. A number of homeostatic cellular mechanisms have been suggested to play a role in maintaining this balance, including long-term plasticity of GABAergic inhibitory synapses. Many previous studies have demonstrated a coupling of postsynaptic spiking with modification of perisomatic inhibition. Here, we demonstrate that activation of NMDA-type glutamate receptors leads to input-specific long-term potentiation of dendritic inhibition mediated by somatostatin-expressing interneurons. This form of plasticity is expressed postsynaptically and requires both CaMKII α and the $\beta 2$ subunit of the GABA-A receptor. Importantly, this process may function to preserve dendritic inhibition, as genetic deletion of NMDAR signaling results in a selective weakening of dendritic inhibition. Overall, our results reveal a new mechanism for linking excitatory and inhibitory input in neuronal dendrites and provide novel insight into the homeostatic regulation of synaptic transmission in cortical circuits.

INTRODUCTION

The balance of synaptic excitation and inhibition is central to normal brain function and is disrupted in a variety of neurodevelopmental disorders (Gogolla et al., 2009; Isaacson and Scanziani, 2011; Lewis and Hashimoto, 2007). In the neocortex, this balance is hypothesized to be maintained via an array of mechanisms that regulate synaptic strength and excitability (Kullmann et al., 2012; Malenka and Bear, 2004; Turigiano, 2011). Mechanistic studies of synaptic plasticity have largely focused on potentiation and depression of excitatory glutamatergic connections. More recently, plasticity of inhibitory GABAergic synapses

has also begun to receive attention, although the underlying cellular targets and molecular mechanisms are less well understood (Castillo et al., 2011; Kullmann et al., 2012).

A major challenge to understanding the contribution of inhibitory plasticity to brain development and function is the diversity of cortical GABAergic interneurons (INs) (Ascoli et al., 2008). Recent work suggests three principal groups: cells co-expressing the calcium (Ca^{2+})-binding protein parvalbumin (PV), the peptide transmitter somatostatin (SOM), or the serotonin 5HT3a receptor (Rudy et al., 2011). The latter class includes the vasoactive intestinal peptide (VIP)-expressing cells. PV-INs make inhibitory contacts onto the perisomatic and proximal dendritic regions of excitatory pyramidal neurons (PNs) and exert well-documented control over the magnitude and timing of PN spike output (Cardin et al., 2009; Pouille and Scanziani, 2001). SOM-INs contact dendritic arbors, where they regulate Ca^{2+} signaling, synaptic integration, and dendritic spikes (Chiu et al., 2013; Murayama et al., 2009). VIP-INs largely, though not exclusively, target other INs and may drive state-dependent disinhibition of PNs (Fu et al., 2014; Pfeffer et al., 2013).

Recent evidence using two-photon imaging of fluorescently tagged inhibitory synapses *in vivo* suggests distinct learning rules for different populations of GABAergic inputs (Chen et al., 2012; Villa et al., 2016). In particular, inhibitory synapses onto dendritic spines, potentially formed by SOM-INs (Chiu et al., 2013), appear to be particularly plastic, as their basal turnover and response to sensory deprivation is significantly more dynamic than those onto dendritic shafts (Chen et al., 2012; van Versendaal et al., 2012). These findings suggest the intriguing possibility of GABAergic circuit-specific plasticity.

Notably, most studies of GABAergic plasticity have implicated perisomatic inhibition as a key locus for regulation. For example, synapses formed by PV-INs in primary visual cortex selectively exhibit long-term potentiation (LTP) in response to activity-dependent release of nitric oxide by postsynaptic PNs (Lourenço et al., 2014), and inputs from fast-spiking, putative PV-INs onto layer 4 PNs are selectively modified by visual experience (Maffei et al., 2006). Similarly, cholecystokinin (CCK)-expressing basket cells targeting proximal somatodendritic regions in the hippocampus are particularly sensitive to retrograde endocannabinoid



spine stability (Chen et al., 2015; Hayama et al., 2013). Thus, the homeostatic interaction of glutamatergic and GABAergic signaling may fine-tune excitatory synaptic integration at the level of individual synapses.

The critical role of inhibitory plasticity *in vivo* is also supported by recent work showing that GABAergic synapses formed in the dendrites of L2/3 PN of visual cortex are highly dynamic both spontaneously and in response to altered sensory experience (Chen et al., 2012; Kannan et al., 2016; Villa et al., 2016). Notably, GABAergic inputs to distal dendrites exhibit greater turnover than more proximal contacts, with synapses on dendritic spines among the most labile (Chen et al., 2012). This observation is consistent with our earlier findings that SOM-INs make a subset of their inputs directly onto spine heads (Chiu et al., 2013). Given these results and our present findings, it would be interesting to examine the role of NMDARs in visual experience-dependent reorganization of cortical GABAergic circuits.

The selective induction of NMDAR- and CaMKII α -dependent iLTP at synapses formed by SOM-INs might be solely explained by their structural proximity to glutamatergic inputs that also target PN dendrites. However, two results argue for a more complex explanation. First, loading either activated calmodulin or CaMKII α through the patch pipette was insufficient to trigger iLTP at PV-IN synapses despite robustly potentiating inputs from SOM-INs. Second, application of the $\beta 2/\beta 3$ subunit containing GABAergic receptor modulator etomidate selectively altered currents evoked by stimulation of SOM-INs, while genetic deletion of the $\beta 2$ subunit prevented induction of iLTP. Overall, these results suggest the tantalizing hypothesis that the molecular constituency of GABAergic synapses might differ across the somatodendritic arbor. The mechanisms underlying this molecular heterogeneity are unclear and could involve the differential trafficking of receptor subunits and accessory molecules to distinct pools of synapses across the somatodendritic arbor. In contrast to glutamatergic synapses, the structural organization of GABAergic inputs is not well characterized. Previous work has suggested the possibility that inhibitory scaffolding molecules may vary across synaptic subpopulations. In the neocortex, the cell adhesion molecule neuroligin-2 was reported to be necessary for synapses formed by PV-INs, but not SOM-INs (Gibson et al., 2009). In the cerebellum, the scaffolding molecule gephyrin was suggested to be critical for dendritic, but not perisomatic, GABAergic inputs to Purkinje cells (Viltoro et al., 2008). Recent studies have begun to reveal additional molecules involved in the structure and function of inhibitory synapses (Uezu et al., 2016; Yamasaki et al., 2017), and future investigation will be necessary to determine their selective roles in different cellular compartments.

Previous models of synaptic homeostasis often rely on a straightforward “balance” of overall excitation and inhibition that may be oversimplified. As we have shown, dysregulation of NMDAR signaling results in opposite alterations in putative PV- and SOM-IN-mediated inhibition. Importantly, these experiments do not rule out non-synaptic explanations for the links between NMDARs and GABAergic inputs *in vivo*. However, they are consistent with our iLTP data and highlight the possibility that the strength of inhibition can be redistributed along the somatodendritic axis in response to altered glutamatergic signaling. Indeed,

many studies have suggested that the functional roles of inhibition mediated by different IN populations are highly distinct (Atallah et al., 2012; Lee et al., 2012; Wilson et al., 2012). Thus, although the total amount of inhibition may remain “balanced,” the functional consequences for cellular and circuit activity may be considerable.

In conclusion, we present evidence for a novel synapse-specific mechanism for linking excitatory signaling to the potency of dendritic GABAergic inhibition. We expect that future studies into the cellular mechanisms governing such specificity will yield rich rewards into understanding both basic synaptic development and maintenance as well as circuit organization and function.

STAR★METHODS

Detailed methods are provided in the online version of this paper and include the following:

- KEY RESOURCES TABLE
- CONTACT FOR REAGENT AND RESOURCE SHARING
- EXPERIMENTAL MODEL AND SUBJECT DETAILS
- METHOD DETAILS
 - Slice Preparation
 - Electrophysiology
 - Synaptic Stimulation and GABA Uncaging
 - Conditional Deletion of Targeted Receptor Subunits
 - Generation of Conditional $\beta 2$ Knockout Mice
 - Pharmacology
 - Slice Resectioning for Immunofluorescence
- QUANTIFICATION AND STATISTICAL ANALYSIS

SUPPLEMENTAL INFORMATION

Supplemental Information includes four figures and can be found with this article online at <https://doi.org/10.1016/j.neuron.2017.12.032>.

ACKNOWLEDGMENTS

The authors wish to thank Dr. Jessica Cardin for helpful comments during the preparation of this manuscript and Dr. Ed Boyden for help with the use of ChrimsonR. This work was funded by the NIH (R01 MH099045 to M.J.H., R01 NS076637 to S.J.T., R01 MH115705 to S.T., F30 MH099742 to J.S.M., and K01 MH097961 to C.Q.C.), the March of Dimes Basil O'Connor Award to M.J.H., and funding agencies in Chile (FONDECYT No. 1171840 and MILENIO PROYECTO P09-022-F, CINV to C.Q.C.).

AUTHOR CONTRIBUTIONS

C.Q.C. and M.J.H. designed the experiments and wrote the manuscript. C.Q.C. performed all experiments. J.S.M., S.T., M.Y., K.S., and R.N. designed, generated, and validated the conditional $\beta 2$ subunit mouse. S.J.T. designed and synthesized constitutively active CaMKII α .

DECLARATION OF INTERESTS

The authors declare no competing interests.

Received: June 23, 2017
 Revised: November 16, 2017
 Accepted: December 21, 2017
 Published: January 17, 2018



Contents lists available at ScienceDirect

Carbohydrate Research

journal homepage: www.elsevier.com/locate/carres

Penicillium purpurogenum produces a novel endo-1,5-arabinanase, active on debranched arabinan, short arabinooligosaccharides and on the artificial substrate p-nitrophenyl arabinofuranoside

Felipe Vilches^a, María Cristina Ravanal^{a, b}, Felipe Bravo-Moraga^b, Danilo Gonzalez-Nilo^b, Jaime Eyzaguirre^{a, *}

^a Departamento de Ciencias Biológicas, Universidad Andrés Bello, República 217, Santiago, Chile

^b Center for Bioinformatics and Integrative Biology, Facultad de Ciencias Biológicas, Universidad Andrés Bello, República 239, Santiago, Chile



ARTICLE INFO

Article history:
Received 27 September 2017
Received in revised form
21 November 2017
Accepted 21 November 2017
Available online 26 November 2017

Keywords:
Endo-1,5-arabinanase
Penicillium purpurogenum
Pichia pastoris
Heterologous expression
GH family 43

ABSTRACT

Penicillium purpurogenum secretes numerous lignocellulose-degrading enzymes, including four arabinofuranosidases and an exo-arabinanase. In this work, the biochemical properties of an endo-arabinanase (ABN1) are presented. A gene, coding for a potential ABN was mined from the genome. It includes three introns. The cDNA is 975 bp long and codes for a mature protein of 324 residues. The cDNA was expressed in *Pichia pastoris*. The enzyme is active on debranched arabinan and arabinooligosaccharides. In contrast to other characterized ABNs, inactive on p-nitrophenyl- α -L-arabinofuranoside (pNPAra), ABN1 is active on this substrate. The enzyme has an optimal pH of 4.5 and an optimal temperature of 30–35 °C. Calcium does not activate ABN1. ABN1 belongs to GH family 43 sub-family 6, and a Clustal alignment with sequences of characterized fungal ABNs shows highest identity (54.6%) with an ABN from *Aspergillus aculeatus*. A three-dimensional model of ABN1 was constructed and the docking with pNPAra was compared with similar models of an enzyme very active on this substrate and another lacking activity, both from GH family 43. Differences in the number of hydrogen bonds between enzyme and substrate, and distance between the substrate and the catalytic residues may explain the differences in activity shown by these enzymes.

© 2017 Elsevier Ltd. All rights reserved.

1. Introduction

Along with D-xylose and D-ribose, L-arabinose is one of the most abundant pentoses in Nature. It is found as a component in the structure of arabinoxylan and pectin. Arabinoxylan, one of the hemicelluloses, is a constituent of plant lignocellulose, and L-arabinose participates in its structure as a substituent of the xylan backbone [1]. Pectin, another component of lignocellulose, is

present mainly in the primary cell-wall of plants. One of the pectin components, rhamnogalacturonan 1 (RG1) is rich in arabinose. In RG1, arabinose is present as arabinan and arabinogalactan, which are linked to the rhamnoses of the main chain of RG1 [2].

Arabinose is finding increased attention in biomedical applications. This sugar has been found to inhibit intestinal invertase, and in this way, it reduces the glycemic response after sucrose ingestion [3]. In addition, arabinooligosaccharides are considered potential prebiotics [4]. As a result, the production of L-arabinose and its oligosaccharides from natural sources containing polysaccharides rich in this sugar is of growing interest.

Polysaccharides can be hydrolyzed by means of acid or enzymes. The former has the disadvantage of producing side-products such as furfurals, and requires the disposal of the acid, which contaminates the environment. Enzymes, on the other hand, are very specific and can operate under milder conditions. Three groups of enzymes have been found to participate in the liberation of arabinose from arabinose-containing polysaccharides: 1) Endo-1,5-

Abbreviations: pNPAra, p-nitrophenyl- α -L-arabinofuranoside; pNPXyl, p-nitrophenyl- β -D-xylopyranoside; pNPGlu, p-nitrophenyl- β -D-glucopyranoside; pNPGal, p-nitrophenyl- β -D-galactopyranoside; pNPRham, p-nitrophenyl α -L-rhamnopyranoside; pNPFuc, p-nitrophenyl- α -L-fucopyranoside; pNPMan, p-nitrophenyl- β -D-mannopyranoside; GH, glycoside hydrolases; ABN, endo-arabinanase; RG1, rhamnogalacturonan 1; DNS, dinitrosalicylate.

* Corresponding author.

E-mail addresses: vilches.f@gmail.com (F. Vilches), cristina.ravanal@gmail.com (M.C. Ravanal), febravomoraga@gmail.com (F. Bravo-Moraga), fernando.gonzalez@unab.cl (D. Gonzalez-Nilo), jeyzaguirre@unab.cl (J. Eyzaguirre).

<https://doi.org/10.1016/j.carres.2017.11.014>
0008-6215/© 2017 Elsevier Ltd. All rights reserved.

temperature of 300 K. The minimization schema was set-up until convergence was reached. Then, a molecular dynamic was set-up to run for 10 ns using a restraint for the secondary structure. Finally, the last frame of the molecular dynamics was used for molecular docking simulations.

Docking studies were performed to predict the putative binding pocket of the protein. For this purpose, different docking simulations were performed using the AutodockVina program [35]. The grid box size was $60 \times 60 \times 60$, using a grid spacing of 0.375 Å. The center of the grid was located in the center of mass of the residues ASP30, ASP157 and GLU211 of ABN1 (numbering as in Supplementary Fig. 4) and equivalent residues at 5 Å for RmArase. The molecular model of pNPArA (ligand) was obtained from the simulations performed by in Ravanal et al. [25]. For docking simulations, the furanose ring of pNPArA was kept in a non-planar conformation, specifically the C-3-endo conformation, as was used successfully in Ref. [25]. At the same time, the rest of the single bonds were free to rotate during the sampling conformation. Using this strategy, 20 different ligand-protein conformations for RmArase and ABN1 were analyzed. The lowest energy conformations were selected and then filtered by the orientation of the ligand in the active site of RmArase and ABN1. ABF3 docking was recalculated using AutodockVina to compare results.

Conflicts of interest

The authors have no conflicts to disclose.

Acknowledgements

This work has been supported by grants from FONDECYT (1130180), Universidad Andrés Bello (DI-478-14/R, DI-31-12/R and PMIUB1301) and Neuromorphics Inspired Science [grant number FA9550-16-1-0384].

Appendix A. Supplementary data

Supplementary data related to this article can be found at <https://doi.org/10.1016/j.carres.2017.11.014>.

References

- [1] J.P. Joseleau, J. Comptat, K. Ruel, *Biotechnol. Progr.* 7 (1992) 1–15.
- [2] A.G.J. Voragen, G.-J. Coenen, R.P. Verhoef, H.A. Schols, *Struct. Chem.* 20 (2009) 263–275.
- [3] K. Seri, K. Sanai, N. Matsuo, K. Kawakubo, C. Xue, S. Inoue, *Metabolism* 45 (1996) 1368–1374.
- [4] M.A. Al-Tamimi, R.J. Palfreman, J.M. Cooper, G.R. Gibson, R.A. Rastall, *J. Appl. Microbiol.* 100 (2006) 407–414.
- [5] B.C. Saha, *Biotechnol. Adv.* 18 (2000) 403–423.
- [6] M.T. Numan, N.B. Bhosle, *J. Ind. Microbiol. Biotechnol.* 33 (2006) 247–260.
- [7] B. Seiboth, B. Metz, *Appl. Microbiol. Biotechnol.* 89 (2011) 1665–1673.
- [8] M.C. Ravanal, J. Eyzaguirre, *Fungal Biol.* 119 (2015) 641–647.
- [9] W. Mardones, E. Callegari, J. Eyzaguirre, *Fungal Biol.* 119 (2015) 1267–1278.
- [10] M. Skjöt, S. Kauppinen, L. Kofod, C. Fuglsang, M. Pauly, H. Dalbøge, L. Andersen, *Mol. Genet. Genomics* 265 (2001) 913–921.
- [11] K. Mewis, N. Lenfant, V. Lombard, B. Henrissat, *Appl. Environ. Microbiol.* 82 (2016) 1686–1692.
- [12] A. Yamaguchi, T. Tada, K. Wada, T. Nakaniwa, T. Kitatani, Y. Sogabe, M. Takao, T. Sakai, K. Nishimura, *J. Biochem.* 137 (2005) 587–592.
- [13] M.R. Proctor, E.J. Taylor, D. Nurizzo, J.P. Turkenburg, R.M. Lloyd, M. Vardakou, G.J. Davies, H.J. Gilbert, *PNAS* 102 (2005) 2697–2702.
- [14] D. Nurizzo, J.P. Turkenburg, S.J. Charnock, S.M. Roberts, E.J. Dodson, V.A. McKie, E.J. Taylor, H.J. Gilbert, G.J. Davies, *Nat. Struct. Biol.* 9 (2002) 665–668.
- [15] Z. Chen, Y. Liu, Q. Yan, S. Yang, Z. Jiang, *J. Agric. Food Chem.* 63 (2015) 1226–1233.
- [16] A.R. de L. Damásio, B.C. Pessela, C. Mateo, F. Segato, R.A. Prade, J.M. Guisan, M.T.M. Polizeli, *J. Mol. Catal. B* 77 (2012) 39–45.
- [17] S. Baue, P. Vasu, S. Persson, A.J. Mort, C.R. Somerville, *PNAS* 103 (2006) 11417–11422.
- [18] S. Kühnel, S.W.A. Hinz, L. Pouvreau, J. Wery, H.A. Schols, H. Gruppen, *Bioresour. Technol.* 101 (2010) 8300–8307.
- [19] T. Sakamoto, H. Ihara, S. Kozaki, H. Kawasaki, *Biochim. Biophys. Acta* 1624 (2003) 70–75.
- [20] T. Sakamoto, M. Inui, K. Yasui, S. Tokuda, M. Akiyoshi, Y. Kohori, T. Nakaniwa, T. Tada, *Appl. Microbiol. Biotechnol.* 93 (2012) 1087–1096.
- [21] N.D. Huy, S. Thiagarajan, Y.-E. Choi, D.-H. Kim, S.-M. Park, *Bioproc. Biosyst. Eng.* 36 (2013) 677–685.
- [22] C. Lang, R. Yang, Y. Yang, B. Gao, L. Zhao, W. Wei, H. Wang, S. Matsukawa, J. Xie, D. Wei, *Appl. Biochem. Biotechnol.* 180 (2016) 900–916.
- [23] F.M. Rombouts, A.G.J. Voragen, M.E. Searle-van Leeuwen, C.C.J.M. Geraeds, H.A. Schols, W. Pilnik, *Carbohydr. Polym.* 9 (1988) 25–47.
- [24] D. de Sanctis, J.M. Inacio, P.F. Lindley, I. de Sa-Nogueira, I. Bento, *FEBS J.* 277 (2010) 4562–4574.
- [25] M.C. Ravanal, M. Alegria-Arcos, F.D. González-Nilo, J. Eyzaguirre, *Arch. Biochem. Biophys.* 540 (2013) 117–124.
- [26] M. Hidalgo, J. Steiner, J. Eyzaguirre, *Biotechnol. Appl. Biochem.* 15 (1992) 185–191.
- [27] T.C. McIlvaine, *J. Biol. Chem.* 49 (1921) 183–186.
- [28] G.L. Miller, *Anal. Chem.* 31 (1959) 426–428.
- [29] U.K. Laemmli, *Nature* 22 (1970) 680–685.
- [30] S.F. Altschul, W. Gish, W. Miller, E.W. Myers, D.J. Lipman, *J. Mol. Biol.* 215 (1990) 403–410.
- [31] D.W.A. Buchan, F. Minneci, T.C.O. Nugent, K. Bryson, D.T. Jones, *Nucleic Acids Res.* 41 (W1) (2013) W340–W348.
- [32] A. Sali, T.L. Blundell, *J. Mol. Biol.* 234 (1993) 779–815.
- [33] A.D. MacKerell, D. Bashford, M. Bellott, R.L. Dunbrack, J.D. Evanseck, M.J. Field, S. Fischer, J. Gao, H. Guo, S. Ha, D. Joseph-McCarthy, L. Kuchnir, K. Kucera, F.T. Lau, C. Mattos, S. Michnick, T. Ngo, D.T. Nguyen, B. Prodhom, W.E. Reiher, B. Roux, M. Schlenkerich, J.C. Smith, R. Stote, J. Straub, M. Watanabe, J. Wiorkiewicz-Kuczera, D. Yin, M. Karplus, *J. Phys. Chem. B* 102 (1998) 3586–3616.
- [34] J.C. Phillips, R. Braun, W. Wang, J. Gumbart, E. Tajkhorshid, E. Villa, C. Chipot, R.D. Skeel, L. Kal, K. Schulten, *J. Comput. Chem.* 26 (2005) 1781–1802.
- [35] O. Trotter, A.J. Olson, *J. Comput. Chem.* 31 (2010) 455–461.

Trypanosoma cruzi Infection Induces Pannexin-1 Channel Opening in Cardiac Myocytes

Iván Barria,¹ Juan Güiza,¹ Fredi Cifuentes,¹ Pedro Zamorano,² Juan C. Sáez,^{3,4} Jorge González,⁵ and José L. Vega^{1*}

¹Experimental Physiology Laboratory (EPHYL), Antofagasta Institute, Universidad de Antofagasta, Antofagasta, Chile;

²Laboratory of Neurobiology, Department of Biomedicine, Universidad de Antofagasta, Antofagasta, Chile; ³Departamento de Fisiología, Facultad de Ciencias Biológicas, Pontificia Universidad Católica de Chile, Santiago, Chile;

⁴Centro Interdisciplinario de Neurociencias de Valparaíso, Valparaíso, Chile; ⁵Molecular Parasitology Unit, Faculty of Health Sciences, Universidad de Antofagasta, Antofagasta, Chile

Abstract. *Trypanosoma cruzi*, the etiological agent of Chagas diseases, invades the cardiac tissue causing acute myocarditis and heart electrical disturbances. In *T. cruzi* invasion, the parasite induces $[Ca^{2+}]_i$ transients in the host cells, an essential phenomenon for invasion. To date, knowledge on the mechanism that elicits transients of $[Ca^{2+}]_i$ during the infection of cardiac myocytes has not been fully characterized. Pannexin1 (Panx1) channels are poorly selective channels found in all vertebrates that serve as a pathway for ATP release. In this article, we demonstrate that *T. cruzi* infection results in the opening of Panx1 channels in cardiac myocytes. We show that pharmacological blockade of Panx1 channels inhibits *T. cruzi*-induced $[Ca^{2+}]_i$ transients and invasion in cardiac myocytes. Our results indicate that opening of Panx1 channels are required for *T. cruzi* invasion in cardiac myocytes, and we propose that targeting Panx1 channel could provide new potential therapeutic approaches to treat Chagas disease.

INTRODUCTION

The protozoan *Trypanosoma cruzi* is the etiological agent of Chagas disease, which is considered one of the most important neglected tropical diseases that causes approximately 10,600 deaths per year and 0.6 million disability-adjusted life per year.¹ *Trypanosoma cruzi* is an obligatory intracellular parasite, and therefore, it must activate mechanisms that enable its entrance into the host cells.^{2,3} Depletion of intracellular free calcium concentration ($[Ca^{2+}]_i$) in the host cell inhibits parasite invasion, indicating that increase in $[Ca^{2+}]_i$ is essential for *T. cruzi* infection.^{4,5} Previous studies have described that *T. cruzi*-induced $[Ca^{2+}]_i$ transients are not mediated by adrenergic receptor or L-type Ca^{2+} channel activation in cardiac cells.⁶ However, our understanding of the cellular mechanism involved in *T. cruzi*-induced $[Ca^{2+}]_i$ transients in cardiac myocytes remains unknown. Pannexin1 (Panx1) is a member of the gap junction family proteins and forms a plasma membrane channel that allows passage of anions, cations, dyes, and ATP.⁷ Panx1 channels are involved in a variety of cellular responses that includes apoptosis,⁸ inflammation,⁹ and innate immune response.¹⁰ Cardiac cells express Panx1, and other members of the gap junction family proteins such as connexin (Cx)40, Cx43, and Cx45.¹¹ Several publications indicate that *T. cruzi* infection reduces gap junctional communication due to a decrease in the amount of Cx43 protein and mRNA in cardiac myocytes.^{12,13} In agreement with these studies, we found that *T. cruzi* infection increases Cx43 hemichannel (a half of gap junction channel) activity in nonconfluent Cx43-HeLa cells.¹⁴ In addition, we demonstrated that *T. cruzi* invasion depends on host hemichannel types.¹⁴ Normally, Panx1 channels are mainly in a closed state; however, recent studies have demonstrated that pathogens such as *Chlamydia trachomatis* and HIV can induce opening of Panx1 channels during infection.^{15,16} In the current study, we provide first evidence that a pathogenic protozoan *T. cruzi* induces opening of Panx1 channels. In

addition, our data provide evidence that opening of Panx1 channels is necessary for Ca^{2+} transients during *T. cruzi* infection of cardiac myocytes. Furthermore, we show that pharmacological blockade of Panx1 channels inhibits *T. cruzi* invasion in cardiac myocytes.

MATERIALS AND METHODS

Antibodies and reagents. Polyclonal anti-Panx1 (#HPA016930), monoclonal anti- α -actin (#A5044), polyclonal anti-Cx43 (#C6219), and monoclonal anti-vimentin (#V6630) antibodies were purchased from Sigma-Aldrich (St. Louis, MO). Anti-rabbit (#111-095-003) or anti-mouse (#115-095-003) IgG antibodies coupled to FITC were purchased from Jackson ImmunoResearch (West Grove, PA). Carbenoxolone disodium salt (#C4790), adenosine 5'-triphosphate disodium salt hydrate (#A9187), probenecid (#P8761), and cytosine beta-D-arabinofuranoside (#C1768) from Sigma-Aldrich. MRS2179 tetrasodium salt (#0900), iso-PPADS tetrasodium salt (#0683), and ¹⁰Panx1 peptide (#3348) were purchased from Tocris (Bristol, United Kingdom). The Fluo-3 AM calcium indicator (#F1242) and cell viability assay kits (#L34969) were obtained from Thermo Fisher Scientific (Cambridge, MA). Ethidium bromide was obtained from Winkler (Santiago, Chile).

Parasites. H510 strain of *T. cruzi* was isolated in 1968 from a domiciliary *Triatoma dimidiata* found in an area endemic for Chagas disease in Costa Rica and cloned.¹⁷ *Trypanosoma cruzi*-virulent clone (H510 C8C3^{hvir}) were maintained for 30 years in an alternate mouse-cell culture passage, and avirulent clones (H510 C8C3^{lvir}) were maintained for 30 years in an axenic culture passage.¹⁸ Epimastigote forms were grown at 27°C in LIT medium (containing 5.4 mM KCl, 150 mM NaCl, 24 mM glucose, 5% [v/v] liver extract, 0.02% [w/v] hemin, 2% [w/v] yeast extract, and 1.5% [w/v] tryptose) and supplemented with 5% fetal bovine serum. For preparation of supernatant (SN) fraction, freshly harvested trypomastigotes were washed with phosphate-buffered saline (PBS) and resuspended in DMEM medium containing 0.5% FBS at 2×10^8 /mL. Trypomastigotes were then removed (15,000 rpm for 10 minutes at 4°C) and supernatants were stored at -80°C.

*Address correspondence to José L. Vega, Experimental Physiology Laboratory (EPHYL), Antofagasta Institute, Universidad de Antofagasta, Angamos 601, Antofagasta, Chile. E-mail: joseluis.vega@uantof.cl

(C8C3hvir); therefore, these factors could be responsible for the observed effects.¹⁸ Experimental studies will be required to confirm the participation of these virulent factors on Panx1 regulation.

Moreover, we found that Panx1 channel opening was required for *T. cruzi* invasion in cardiac myocytes. The involvement of the Panx1 channel in infections caused by obligate intracellular pathogens has already been demonstrated. For example, it has been described that probenecid (1.5 mM) inhibits *Chlamydia* growth in HeLa cells.¹⁵ In addition, ¹⁰Panx1 (200 μ M) has been demonstrated to abolish HIV replication in CD4⁺ T lymphocytes.¹⁶ *Trypanosoma cruzi* invades the cells, where it is transformed into amastigotes (replicative form) and begins to replicate intracellularly.²⁰ This invasion can be quantitatively examined via enumeration of intracellular amastigotes.²³ In agreement with previous studies, we found that ¹⁰Panx1 or probenecid reduced the number of intracellular amastigotes in cardiac myocytes. Interestingly, we found that the cells with the greatest number of amastigotes presented greater immunoreactivity to Panx1. In *Chlamydia* infection, recruitment of Panx1 into *Chlamydia*-containing parasitophorous vacuole membrane has been observed.¹⁵ The authors of the latter work suggested that Panx1 could contribute to maintaining an intracellular niche.¹⁵ Panx1 has been detected preferentially in the surface membrane but has also been found in intracellular compartments in rat atrial and ventricular primary cardiomyocytes.^{24,25} Unfortunately, our results do not allow us to identify if this greater expression occurs in the plasma membrane or at intracellular compartments of the cells.

Moreover, opening of Panx1 channel results in the release of ATP, which is a signaling molecule that can activate purinergic and adenosine receptors in an autocrine and paracrine manner.²⁶ Interestingly, ATP is a key molecule in *T. cruzi* host cell invasion. It has been demonstrated that depletion of ATP content decreases *T. cruzi* infectivity in HeLa cells.²⁷ In agreement with these studies, we found that ¹⁰Panx1 or probenecid reduced *T. cruzi*-evoked Ca²⁺ signal transients in cardiac myocytes. Although it is unknown whether Panx1 channel is permeable or not to Ca²⁺, it is well documented that Panx1 channel is permeable to ATP allowing its release to the extracellular milieu, which can induce transient Ca²⁺ signal by the activation of P2Y and/or P2X receptors.^{28–32} In addition, we found that *T. cruzi*-evoked Ca²⁺ signal transients were inhibited by a P2Y₁ but not a P2X antagonist, suggesting that Ca²⁺ signal transients resulted from Ca²⁺ release from intracellular stores. In HIV infection, it has been described that inhibition of any of the constituents of Panx1, ATP, or P2Y affected HIV replication, suggesting that this signaling may be important in the intracellular pathogen infection.³² Finally, we evaluated the cytotoxic effect of Panx1 blockers and P2 antagonist in *T. cruzi*, because probenecid has been demonstrated to induce chemosensitization of *Plasmodium falciparum* to antimalarial drugs³³ and suramin (a general P2 antagonist) used as an anti-trypanocidal drug.³⁴ For all drugs tested, none showed cytotoxic effects in *T. cruzi*.

In summary, our results strongly suggests that a virulence factor(s) from *T. cruzi* induces Ca²⁺ signal transients via Panx1 channel opening, putative ATP release, and subsequently activation of P2Y₁ receptors. Because cardiac myocytes are targets for *T. cruzi* in the vertebrate host, our study suggests

that Panx1 channel may play a critical role in the pathogenesis of Chagas disease.

Received April 9, 2017. Accepted for publication September 23, 2017.

Published online November 6, 2017.

Acknowledgments: We thank the staff of the microscopy and cytometer (CONICYT-FONDEQUIP EQM120137) facilities in Antofagasta Institute.

Financial support: This work was partially supported by FONDECYT grants 11130013 (to J. L. V.) and 1131007 (to J. G.) and Grant P09-022-F (to J. C. S.). The Centro Interdisciplinario de Neurociencia de Valparaíso is a Millennium Institute supported by the Millennium Scientific Initiative of the Chilean Ministry of Economy, Development, and Tourism (P029-022-F). Writing and preparation of this article was further supported by FONDECYT grants 11130013 (to J. L. V.). Iván Barria and Juan Guiza hold a CONICYT-Chile PhD Fellowship. This work will be presented as part of the PhD thesis of Iván Barria at the Universidad de Antofagasta.

Authors' addresses: Iván Barria, Juan Guiza, Fredi Cifuentes, and José L. Vega, Experimental Physiology Laboratory (EPHYL), Antofagasta Institute, Universidad de Antofagasta, Antofagasta, Chile, E-mails: ivan.barria.o@gmail.com, juan.igh@hotmail.com, fredi.cifuentes@uantof.cl, and joseluis.vega@uantof.cl. Pedro Zamorano, Department of Biomedicine, Universidad de Antofagasta, Antofagasta, Chile, E-mail: pzamorano@gmail.com. Juan C. Sáez, Departamento de Fisiología, Facultad de Ciencias Biológicas, Pontificia Universidad Católica de Chile, Santiago, Chile, E-mail: jsaez@bio.puc.cl. González, Molecular Parasitology Unit, Faculty of Health Sciences, Universidad de Antofagasta, Antofagasta, Chile, E-mail: jorge.gonzalez@uantof.cl.

REFERENCES

- Degenhardt L et al., 2013. Global burden of disease attributable to illicit drug use and dependence: findings from the Global Burden of Disease Study 2010. *Lancet* 382: 1564–1574.
- Calvet CM, Melo TG, Garzoni LR, Oliveira FO Jr, Silva Neto DT, Meirelles MNSL, Pereira MC, 2012. Current understanding of the *Trypanosoma cruzi*-cardiomyocyte interaction. *Front Immunol* 3: 327.
- Osorio L, Ríos I, Gutiérrez B, González J, 2012. Virulence factors of *Trypanosoma cruzi*: who is who? *Microbes Infect* 14: 1390–1402.
- Tardieux I, Nathanson MH, Andrews NW, 1994. Role in host cell invasion of *Trypanosoma cruzi*-induced cytosolic-free Ca²⁺ transients. *J Exp Med* 179: 1017–1022.
- Yoshida N, 2006. Molecular basis of mammalian cell invasion by *Trypanosoma cruzi*. *An Acad Bras Cienc* 78: 87–111.
- Barr SC, Hanm W, Andrews NW, Lopez JW, Ball BA, Pannabecker TL, Gilmour RF Jr, 1996. A factor from *Trypanosoma cruzi* induces repetitive cytosolic free Ca²⁺ transients in isolated primary canine cardiac myocytes. *Infect Immun* 64: 1770–1777.
- Penuela S, Gehi R, Laird DW, 2013. The biochemistry and function of pannexin channels. *Biochim Biophys Acta* 1828: 15–22.
- Chekeni FB et al., 2010. Pannexin 1 channels mediate 'find-me' signal release and membrane permeability during apoptosis. *Nature* 463: 863–867.
- Adamson SE, Leitinger N, 2014. The role of pannexin1 in the induction and resolution of inflammation. *FEBS Lett* 588: 1416–1422.
- Maslieva V, Thompson RJ, 2014. A critical role for pannexin-1 in activation of innate immune cells of the choroid plexus. *Channels (Austin)* 8: 131–141.
- Meens MJ, Kwak BR, Duffy HS, 2015. Role of connexins and pannexins in cardiovascular physiology. *Cell Mol Life Sci* 72: 2779–2792.
- de Carvalho A, Tanowitz H, Wittner M, Dermietzel R, Roy C, Hertzberg E, Spray D, 1992. Gap junction distribution is altered between cardiac myocytes infected with *Trypanosoma cruzi*. *Circ Res* 70: 733–742.
- Campos de Carvalho AC, Roy C, Hertzberg EL, Tanowitz HB, Kessler JA, Weiss LM, Wittner M, Dermietzel R, Gao Y, Spray DC, 1998. Gap junction disappearance in astrocytes and leptomeningeal cells as a consequence of protozoan infection. *Brain Res* 790: 304–314.

SENSING PAIN AND TEMPERATURE

RAMON LATORRE, KAREN CASTILLO, AND IGNACIO DÍAZ-FRANULIC¹

Introduction

Sensing pain and temperature is essential for life. However, the molecular nature of nociceptors or temperature receptor was a mystery until the end of the last century. Sherrington (Sherrington, 1906) postulated the existence of sensory receptors specialized in sensing noxious stimuli, and he called them nociceptors. In the skin, nociceptors are located in some A δ small myelinated axons that respond to intense mechanical but not to thermal or chemical stimuli. Others A δ fibers respond to noxious mechanical stimuli and noxious heat ($\sim 43^{\circ}\text{C}$). Unmyelinated C fibers give rise to nociceptors able to sense noxious mechanical, thermal and chemical stimuli but with a lower thermal threshold ($\sim 43^{\circ}\text{C}$). The conduction velocity of A δ and C is very different, 20 m/s and 1 m/s, respectively. When the noxious stimulus is applied to a mix A δ and C group of nociceptors, the subject may report two distinct pains separated in time: a “fast” or “first” pain and a “slow” or “second” pain (Patton, 1989). Isolation of fibers innervating the glabrous skin of the monkey’s hand indicates the presence of fibers responding to warming pulses from a base temperature of 34°C (innocuous warm) with a conduction velocity of 1.2 m/s suggesting that warm fibers are C-type fiber (Patton, 1989). The same region of the monkey skin gives rise to about the same number of fibers responding to a cold stimulus. Temperature sensing and pain converge in the same type of neurons in the dorsal root (DRG) and the trigeminus (TG) ganglia innervating the body and the head, respectively.

What are the cellular and molecular basis of thermosensation? What is the relationship between pain and temperature sensing? Not so many years ago researchers thought that the possibilities of finding an answer to this question were rather slim given the intensive properties of temperature. Temperature is a physical property that does not depend on the size of the system or the amount of material in the system. This situation, however, changed dramatically with the cloning and biophysical characteriza-

¹ Centro Interdisciplinario de Neurociencia de Valparaíso, Facultad de Ciencias, Universidad de Valparaíso, Valparaíso, Chile.

DOES INFLAMMATORY RESPONSE CAUSE TISSUE DYSFUNCTION IN CHRONIC DISEASES?

JUAN C. SÁEZ¹

Introduction

It is well accepted that protein subunits called connexins (Cxs) form gap junctions, which are membrane specializations made up of aggregates from a variable number of intercellular communication channels called *gap junction channels*. Each channel is formed by two hemichannels (Figure 1), which correspond to Cx oligohexamers that could be homomeric or heteromeric. While gap junctions formed by the same type of hemichannels are homotypic, those formed by different types of hemichannels are heterotypic. However, Cxs show different affinities when interacting with other Cxs, hence reducing the number of different possible hemichannel and gap junction channels that they can form.

Gap junctional communication can be established between cells of the same (homocellular) or different (heterocellular) type. While gap junction channels serve for direct communication between the cytoplasm of contacting cells, hemichannels serve as membrane pathways between intra and extracellular compartments. Vertebrates also express a more recently discovered protein family composed of three members termed pannexins (Panx1–3). Since evidence for Panx-formed gap junctions is very limited and most available data demonstrate that Panxs form hemichannel-like structures, the currently accepted name for these structures is Panx channels (Sosinsky *et al.*, 2011) (Figure 1). Although our knowledge regarding the permeability properties of these channels is still limited, it is well established that most cells express at least one Panx type, which is similar to what is known for Cxs.

Gap junction channels, Cx hemichannels and Panx1 channels are permeable to ions and small molecules and thus, are involved in coordinating electrical and metabolic responses among members of a cell community. Therefore, groups of cells communicated via gap junctions and hemichan-

¹ Departamento de Fisiología, Facultad de Biología, Pontificia Universidad Católica de Chile, Alameda 340, Santiago Chile. Instituto Interdisciplinario de Neurociencias de la Universidad de Valparaíso, Valparaíso, Chile.



INVITED REVIEW

How does the stimulus define exocytosis in adrenal chromaffin cells?

Fernando D. Marengo¹ · Ana M. Cárdenas²Received: 21 June 2017 / Revised: 28 July 2017 / Accepted: 1 August 2017 / Published online: 29 August 2017
© Springer-Verlag GmbH Germany 2017

Abstract The extent and type of hormones and active peptides secreted by the chromaffin cells of the adrenal medulla have to be adjusted to physiological requirements. The chromaffin cell secretory activity is controlled by the splanchnic nerve firing frequency, which goes from approximately 0.5 Hz in basal conditions to more than 15 Hz in stress. Thus, these neuroendocrine cells maintain a tonic release of catecholamines under resting conditions, massively discharge intravesicular transmitters in response to stress, or adequately respond to moderate stimuli. In order to adjust the secretory response to the stimulus, the adrenal chromaffin cells have an appropriate organization of Ca^{2+} channels, secretory granules pools, and sets of proteins dedicated to selectively control different steps of the secretion process, such as the traffic, docking, priming and fusion of the chromaffin granules. Among the molecules implicated in such events are the soluble *N*-ethylmaleimide-sensitive factor attachment protein receptor (SNARE) proteins, Ca^{2+} sensors like Munc13 and synaptotagmin-1, chaperon proteins such as Munc18, and the actomyosin complex. In the present review, we discuss how these

different actors contribute to the extent and maintenance of the stimulus-dependent exocytosis in the adrenal chromaffin cells.

Keywords Exocytosis · Chromaffin cells · Voltage-dependent Ca^{2+} channels · Vesicle pools · Catecholamines

Introduction

Adrenaline is the principal hormone released to the blood circulation during the acute response to stress. The key actions of this hormone comprise increase of heart rate and blood pressure, redistribution of blood to skeletal muscles, dilation of bronchia and pupils, and increase of blood glucose level. All these physiological changes prepare our body for a fight-or-flight response [29].

The biggest reservoir of adrenaline in the body is the medulla of the adrenal gland. Specifically, the functional unit of this tissue, the chromaffin cell, is in charge of producing and storing adrenaline. Indeed, the adrenal chromaffin cell (ACC) is equipped with the enzyme battery for the production of this hormone, including the enzymes tyrosine hydroxylase, L-aromatic amino-acid decarboxylase, dopamine-beta-hydroxylase, and phenylethanolamine-*N*-methyl-transferase, which respectively catalyze the synthesis of L-DOPA, dopamine, noradrenaline, and adrenaline from an initial precursor, tyrosine [70]. ACCs also produce enkephalins and other peptides, such as chromogranins and tissue plasminogen activator, which are packed in the secretory vesicles together with adrenaline, noradrenaline, small amount of dopamine, ATP, ascorbate and Ca^{2+} [38].

In response to stress, the splanchnic nerve releases acetylcholine into the adrenal medulla activating cholinergic receptors in the surface of the chromaffin cells. Then, the concomitant depolarization triggers the opening of voltage-dependent

This article is part of the special issue on Chromaffin Cells in Pflügers Archiv—European Journal of Physiology

✉ Fernando D. Marengo
fernando@fbmc.fcen.uba.ar

✉ Ana M. Cárdenas
ana.cardenas@uv.cl

¹ Departamento de Fisiología y Biología Molecular y Celular, Facultad de Ciencias Exactas y Naturales, Instituto de Fisiología, Biología Molecular y Neurociencias, Universidad de Buenos Aires, Consejo Nacional de Investigaciones Científicas y Técnicas, Buenos Aires, Argentina

² Centro Interdisciplinario de Neurociencia de Valparaíso, Facultad de Ciencias, Universidad de Valparaíso, Valparaíso, Chile

11], synaptotagmin-1 and its isoform synaptotagmin-7 [111, 115], and complexin-2 [32], indicating that molecules that modulate SNARE assembly regulate fusion pore dynamics. However, the fusion pore expansion is also influenced by F-actin [17, 54, 102] and myosin II [17, 92], which reportedly contribute to pull open the Ω shaped membrane profile formed by the vesicle during exocytosis [146].

The fusion pore can also close back resulting in the partial release of catecholamines [4]. This mechanism known as kiss-and-run is still unclear, but it is the predominant form of exocytosis at low frequency stimulations [36, 37, 43]. It appears that high Ca^{2+} concentrations avoid fusion pore closure [143]. It has been also proposed that dynamin, a GTPase that catalyzes membrane fission during endocytosis [55], promotes kiss-and-run exocytosis [24, 37, 53, 57] and rapid vesicle recycling [90]. However, dynamin has also reportedly been involved in favoring fusion pore expansion [8, 56] and stability [65, 129] and in facilitating full fusion of chromaffin granules [65, 113]. These divergent roles played by dynamin seem to depend on the intensity of the stimuli, the status of dynamin phosphorylation, and its interaction with the actomyosin cytoskeleton [56, 65, 113].

The diameter of the fusion pore also determines the amount and types of molecules released. Thus, a narrow fusion pore limits the outflow of catecholamines, but a more dilated fusion pore allows the passage of bigger molecules such as neuropeptide Y, and the full collapse of the granule on the plasma membrane permits the release of all intragranular transmitters [43, 109]. Therefore, considering that the transmitters stored in the chromaffin granules act on diverse types of receptors and tissues, the regulation of fusion pore dynamics and the mode of exocytosis could have important physiological consequences.

Concluding remarks

The release of hormones and active peptides from ACCs relies on a highly regulated sequence of events that leads to maintain a contingent of releasable chromaffin granules and finally to trigger their fusion. However, ACCs must respond to different physiological situations, such a massive response to stress, maintain a tonic release of transmitter under basal conditions, as well as to respond to moderate external stimuli. Therefore, the series of events conducting to the transmitter release should be sensitive to the magnitude and shape of the Ca^{2+} signals produced under such different situations. To support these actions, ACCs are equipped with a set of molecules and cellular elements that control the shape and spatial pattern of the Ca^{2+} signal and with Ca^{2+} -sensitive proteins that define the proper recruitment, priming, and fusion of chromaffin granules. As discussed in this article, several of those molecules and their contribution to the secretory process

have been identified. However, it remains to be further investigated how different Ca^{2+} -sensitive proteins, including synaptotagmins, Munc13s, and CAPSs, are coordinated and contribute to the exocytosis triggered by different types of stimuli. Future studies should be addressed to resolve these issues.

Acknowledgements This work has been supported by the grants FONDECYT 1160495 (Chile), P09-022-F from ICM-ECONOMIA (Chile), PICT 0524-2014 from Agencia Nacional de Promoción Científica y Tecnológica (Argentina), and UBACyT 2014-2017 from Universidad de Buenos Aires (Argentina). The Centro Interdisciplinario de Neurociencia de Valparaíso (CINV) is a Millennium Institute supported by the Millennium Scientific Initiative of the Ministerio de Economía, Fomento y Turismo.

References

1. Albillos A, Dermick G, Horstmann H, Almers W, Alvarez de Toledo G, Lindau M (1997) The exocytotic event in chromaffin cells revealed by patch amperometry. *Nature* 389(6650):509–512. doi:10.1038/39081
2. Albillos A, Neher E, Moser T (2000) R-type Ca^{2+} channels are coupled to the rapid component of secretion in mouse adrenal slice chromaffin cells. *J Neurosci* 20:8323–8330
3. Alés E, Fuentealba J, García AG, López MG (2005) Depolarization evokes different patterns of calcium signals and exocytosis in bovine and mouse chromaffin cells: the role of mitochondria. *Eur J Neurosci* 21:142–150. doi:10.1111/j.1460-9568.2004.03861.x
4. Alés E, Tabares L, Poyato JM, Valero V, Lindau M, Alvarez de Toledo G (1999) High calcium concentrations shift the mode of exocytosis to the kiss-and-run mechanism. *Nat Cell Biol* 1:40–44. doi:10.1038/9012
5. Alvarez YD, Belingheri AV, Perez Bay AE, Javis SE, Tedford HW, Zamponi G, Marengo FD (2013) The immediately releasable pool of mouse chromaffin cell vesicles is coupled to P/Q-type calcium channels via the synaptic protein interaction site. *PLoS One* 8:e54846. doi:10.1371/journal.pone.0054846
6. Alvarez YD, Ibáñez LI, Uchitel OD, Marengo FD (2008) P/Q Ca^{2+} channels are functionally coupled to exocytosis of the immediately releasable pool in mouse chromaffin cells. *Cell Calcium* 43:155–164. doi:10.1016/j.cecc.2007.04.014
7. Alvarez YD, Marengo FD (2011) The immediately releasable vesicle pool: highly coupled secretion in chromaffin and other neuroendocrine cells. *J Neurochem* 116:155–163. doi:10.1111/j.1471-4159.2010.07108.x
8. Anantharam A, Bittner MA, Aikman RL, Stuenkel EL, Schmid SL, Axelrod D, Holz RW (2011) A new role for the dynamin GTPase in the regulation of fusion pore expansion. *Mol Biol Cell* 22:1907–1918. doi:10.1091/mbc.E11-02-0101
9. Archer DA, Graham ME, Burgoyne RD (2002) Complexin regulates the closure of the fusion pore during regulated vesicle exocytosis. *J Biol Chem* 277:18249–18252. doi:10.1074/jbc.C200166200
10. Ardiles AO, González-Jamett AM, Maripillán J, Naranjo D, Caviedes P, Cárdenas AM (2007) Calcium channel subtypes differentially regulate fusion pore stability and expansion. *J Neurochem* 103:1574–1581. doi:10.1111/j.1471-4159.2007.04871.x
11. Ardiles AO, Maripillán J, Lagos VL, Toro R, Mora IG, Villarroel L, Alés E, Borges R, Cárdenas AM (2006) A rapid exocytosis



Contents lists available at ScienceDirect

Science of the Total Environment

journal homepage: www.elsevier.com/locate/scitotenv

The phenotypic variability in *Rana temporaria* decreases in response to drying habitats



Luz Calia Miramontes-Sequeiros ^{a,*}, Nicolás Palanca-Castán ^b,
Laura Caamaño-Chinchilla ^a, Antonio Palanca-Soler ^a

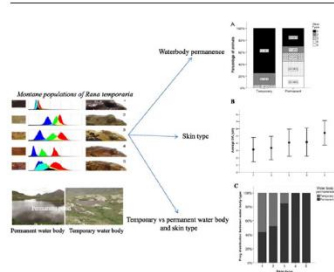
^a Laboratorio de Anatomía Animal, Departamento de Ecología y Biología Animal, Universidade de Vigo, Spain

^b Centro Interdisciplinario de Neurociencia de Valparaíso (CINV), Neuroscience of Circuits and Systems laboratory, Facultad de Ciencias, Universidad de Valparaíso, Chile

HIGHLIGHTS

- Drought is hypothesized to impact the phenotypic variability of *Rana temporaria*.
- A new non-invasive method was implemented to test such effect.
- Phenotypic variability decline was found in frogs developing in drying habitats.

GRAPHICAL ABSTRACT



ARTICLE INFO

Article history:
Received 26 June 2017
Received in revised form 20 August 2017
Accepted 26 August 2017
Available online xxxx

Editor: D. Barcelo

Keywords:
Anuran
Rana temporaria
Phenotypic plasticity
Animal coloration
Amphibian conservation

ABSTRACT

In this study, we evaluated the diversity of skin coloration as a proxy for phenotypic diversity. The European common frog (*Rana temporaria*) populations from the Southern slope of central Pyrenees lie at the limit of the species distribution in latitude and altitude. We analysed the relationship of skin color typology with different environmental variables and found a large decrease in skin type variety in frogs developing in temporary water bodies when compared to those developing in permanent water bodies. Our results show that our method can be used as a non-invasive way to study phenotypic diversity and suggest that adaptation to an early metamorphosis in a rapidly-drying habitat can have negative effects on adult phenotypic diversity. In light of these results, we argue that access to permanent water bodies is important to prevent loss of diversity in anuran populations and reduce their vulnerability to environmental impacts as well as pathogens.

© 2017 Elsevier B.V. All rights reserved.

1. Introduction

Amphibians have become a cause of great concern in the recent years due to their sharply declining populations worldwide and their high extinction rate. Some estimates suggest that current amphibian extinction rates are much higher than background rates (McCallum, 2007) and that loss of currently threatened species will lead to mass-

* Corresponding author at: Laboratorio de Anatomía Animal, Facultad de Biología, Universidade de Vigo, Campus Lagoas-Marcosende, 36310 Vigo, Spain.
E-mail address: kalya@uvigo.es (L.C. Miramontes-Sequeiros).

such as the introduction of non-native fish for recreational purposes or rising temperatures as a consequence of climate change will have a direct impact on the capacity of *R. temporaria* and other anurans to cope with further environmental change and will reduce the viability of vulnerable populations.

5. Conclusions

In conclusion, our study shows that the distribution of different skin colors in populations of *R. temporaria* is a non-random factor that can vary with geography and environmental conditions. The differences found between permanent and temporary water bodies suggest that skin color distribution is a suitable proxy to study phenotypic variability, and the variation encountered between separate geographical areas suggests a link to genetic variability that requires further study. The method presented in this paper allows for an objective measurement of frog skin color and the subsequent analysis of skin color distribution within and between populations. This method is easy to perform in the field along with other types of data sampling and can provide information about phenotypic diversity, which makes it a valuable tool for conservation-related monitoring of *R. temporaria* and other anurans.

Acknowledgements

This project was supported by the Animal Anatomy Laboratory Foundation (2014-001). We thank Ursicino Abajo, warden of the Respmuso mountain refuge, for his logistic and gastronomic support, and Krista L. Miramontes for her help reviewing the manuscript.

Funding

This research did not receive any specific grant from funding agencies in the public, commercial, or not-for-profit sectors.

References

- Bagnara, J.T., 1976. Color change. In: Lofts, B. (Ed.), *Physiology of the Amphibia*. vol. 3. Academic Press, New York, pp. 1–52.
- Bagnara, J.T., Hadley, M.E., 1973. *Chromatophores and Color Change: The Comparative Physiology of Animal Pigmentation*. Prentice-Hall, New Jersey.
- Barnosky, A.D., Matzke, N., Tomiya, S., et al., 2011. Has the earth's sixth mass extinction already arrived? *Nature* 471:51–57 (Mar 3). <http://dx.doi.org/10.1038/nature09678>.
- Bell, R.C., Zamudio, K.R., 2012. Sexual dichromatism in frogs: natural selection, sexual selection and unexpected diversity. *Proc. R. Soc. Lond. B Biol. Sci.* 279:4687–4693. <http://dx.doi.org/10.1098/rspb.2012.1609>.
- Bosch, J., Carrascal, L.M., Duran, L., et al., 2007. Climate change and outbreaks of amphibian chytridiomycosis in a montane area of Central Spain: is there a link? *Proc. R. Soc. Lond. B Biol. Sci.* 274:253–260. <http://dx.doi.org/10.1098/rspb.2006.3713>.
- Duellman, W.E., Trueb, L., 1994. *Biology of Amphibians*. The Johns Hopkins University Press, Baltimore, pp. 1–696.
- Endler, J.A., 1990. On the measurement and classification of color in studies of animal color patterns. *Biol. J. Linn. Soc.* 41:315–352. <http://dx.doi.org/10.1111/j.1095-8312.1990.tb00839.x>.
- Forsman, A., 2014. Effects of genotypic and phenotypic variation on establishment are important for conservation, invasion, and infection biology. *Proc. Natl. Acad. Sci.* 111:302–307. <http://dx.doi.org/10.1073/pnas.1317745111>.
- Gasc, J.P., Cabela, A., Crnobrnja-Isailovic, D., et al., 1997. Atlas of amphibians and reptiles in Europe. *Collection Patrimoines Naturels*, 29, Societas Europaea Herpetologica, Muséum National d'Histoire Naturelle et Service du Patrimoine Naturel, Paris, pp. 1–496.
- Hoffman, E.A., Blouin, M.S., 2000. A review of color and pattern polymorphisms in anurans. *Biol. J. Linn. Soc.* 70:633–665. <http://dx.doi.org/10.1111/j.1095-8312.2000.tb00221.x>.
- Knapp, R.A., Matthews, K.R., 2000. Non-native fish introductions and the decline of the mountain yellow-legged frog from within protected areas. *Conserv. Biol.* 14:428–438. <http://dx.doi.org/10.1046/j.1523-1739.2000.99099.x>.
- Lind, M.J., Johansson, F., 2007. The degree of adaptive phenotypic plasticity is correlated with the spatial environmental heterogeneity experienced by island populations of *Rana temporaria*. *J. Evol. Biol.* 20:1288–1297. <http://dx.doi.org/10.1111/j.1420-9101.2007.01353.x>.
- Lind, M.J., Johansson, F., 2011. Testing the role of phenotypic plasticity for local adaptation: growth and development in time-constrained *Rana temporaria* populations. *J. Evol. Biol.* 24:2696–2704. <http://dx.doi.org/10.1111/j.1420-9101.2011.02393.x>.
- Lind, M.J., Ingvarsson, P.K., Johansson, H., et al., 2011. Gene flow and selection on phenotypic plasticity in an island system of *Rana temporaria*. *Evolution* 65:684–697. <http://dx.doi.org/10.1111/j.1558-5646.2010.01122.x>.
- McCallum, M.L., 2007. Amphibian decline or extinction? Current declines dwarf background extinction rate. *J. Herpetol.* 41:483–491. [http://dx.doi.org/10.1670/0022-1511\(2007\)41\[483:ADOECD\]2.0.CO;2](http://dx.doi.org/10.1670/0022-1511(2007)41[483:ADOECD]2.0.CO;2).
- Montgomerie, R., 2006. Analyzing colors. In: Hill, G.E., Mc-Graw, K.J. (Eds.), *Bird Coloration*, Vol. 1: Mechanisms and Measurements. Harvard University Press, Cambridge, pp. 90–147.
- Newman, R.A., 1989. Developmental plasticity of *Scaphiopus couchii* tadpoles in an unpredictable environment. *Ecology* 70:1775–1787. <http://dx.doi.org/10.2307/1938111>.
- Palo, J.U., O'Hara, R.B., Laugen, A.T., et al., 2003. Latitudinal divergence of common frog (*Rana temporaria*) life history traits by natural selection: evidence from a comparison of molecular and quantitative genetic data. *Mol. Ecol.* 12:1963–1978. <http://dx.doi.org/10.1046/j.1365-294X.2003.01865.x>.
- Rowlands, A., 1952. The influence of water and light upon the color change of sightless frogs (*Rana temporaria*). *J. Exp. Biol.* 29, 127–136.
- Vences, M., Piqué, N., Lopez, A., et al., 1999. Summer habitat population estimate and body size variation in a high-altitude population of *Rana temporaria*. *Amphibia-Reptilia* 20, 431–435.
- Wake, D.B., Vredenburg, V.T., 2008. Are we in the midst of the sixth mass extinction? A view from the world of amphibians. *Proc. Natl. Acad. Sci. U. S. A.* 105:11466–11473. <http://dx.doi.org/10.1073/pnas.0801921105>.
- Wallace, H., Badawy, G.M.I., Wallace, B.M.N., 1999. Amphibian sex determination and sex reversal. *Cell. Mol. Life. Sci.* 55:901–909. <http://dx.doi.org/10.1007/s000180050343>.

Annex 12.- Organization of Scientific Events

MAX PLANCK MEETS VALPARAISO



Speakers

Iván Alfaro (Chile)
McLean Bolton (United States)
Andrea Calixto (Chile)
Andrés Chávez (Chile)
Chiayu Chiu (Chile)
John Ewer (Chile)
Claudio Fernández (Argentina)
David Fitzpatrick (United States)
Moritz Helmstaeder (Germany)
Michael Higley (United States)
Reinhard Jahn (Germany)
U. Benjamin Kaupp (Germany)

Ramón Latorre (Chile)
Antonia Marín-Burgin (Argentina)
Agustín Martínez (Chile)
Peter Mombaerts (Germany)
Nara Muraro (Argentina)
Damián Refojo (Argentina)
Juan Carlos Sáez (Chile)
Rodrigo Suárez (Australia)
Hiroki Taniguchi (United States)
Kathleen Whitlock (Chile)
Carsten Wotjak (Germany)
Ryohei Yasuda (United States)

Organizers



Support





1ª Jornada Chilena de Neurociencia Computacional


Valparaíso, 9-10 Agosto 2018

$$\frac{\partial^2 V}{\partial x^2} + \frac{\partial V}{\partial t} = \frac{V}{r_m}$$

$$\lambda^2 \frac{\partial^2 V}{\partial x^2} = \tau \frac{\partial V}{\partial t} + V$$


**INSTITUTO DE
Sistemas Complejos
DE VALPARAÍSO**

**CENTRO INTERDISCIPLINARIO DE
Neurociencia de
Valparaíso**



**Universidad
de Valparaíso
CHILE**

CINV ANNUAL PROGRESS REPORT – 2018

Annex 13.- Outreach activities throughout the period

**Tertulias
Porteñas**

CENTRO INTERDISCIPLINARIO DE
Neurociencia de
Valparaíso

¿SOMOS
LO QUE
COMEMOS?

JUEVES
5
ABRIL

19:00 | CENTEX

Centro de Extensión, del Ministerio
de las Culturas, las Artes y el Patrimonio
Plaza Sotomayor, Valparaíso

PARTICIPAN
Andrea Calixto,
Neurobióloga del CINV
Sofía Bustos,
Directora Ejecutiva Corporación Actueos

MODERA
Patricio Fernández, *Director de The Clinic*

ORGANIZA
CENTRO INTERDISCIPLINARIO DE
Neurociencia de
Valparaíso

CON EL RESPALDO DE

MEDIA PARTNERS

AUSPICIANTES

UNIVERSIDAD
de Valparaíso
CHILE

RVL
97.3fm

ALTAMIRA

CIRILO
FANSTRONG

ANIMACIÓN BOLSA

**Tertulias
Porteñas**

CENTRO DE INVESTIGACIONES EN
Neurociencia de
Valparaíso



¿QUÉ SABEMOS DE GÉNERO?

PARTICIPAN

Agustín Squella, Premio Nacional de Humanidades
y Ciencias Sociales de Chile 2009

Kathleen Whitlock, neurocientífica e
investigadora del CINV

Alessia Injoque, ingeniera industrial, mujer transgénero

MODERA

Patricio Fernández, director semanario *The Clinic*

JUEVES
2 AGOSTO
19:00 | CENTEX

Centro de Extensión, del Ministerio de las Culturas,
las Artes y el Patrimonio
Plaza Sotomayor, Valparaíso

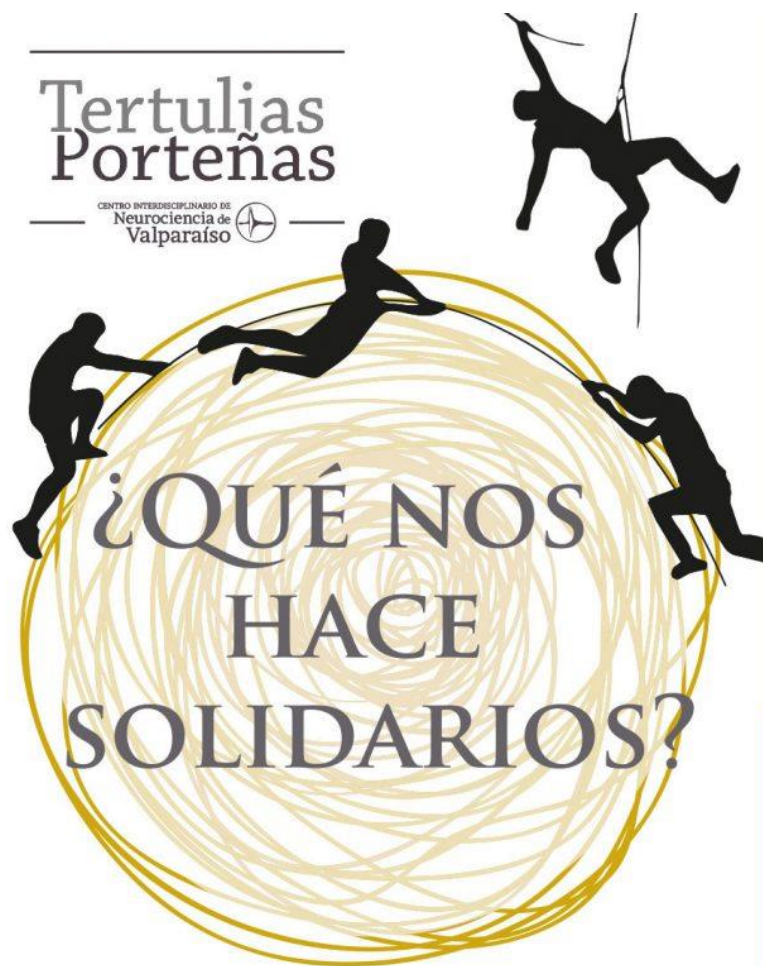
ORGANIZA

CON EL PATROCINIO DE

MECENAZOS

ALICIA CAL





NOVIEMBRE JUEVES
22 19:00 | TERRAZA CENTEX

Centro de Extensión del Ministerio de las Culturas,
las Artes y el Patrimonio.
Plaza Sotomayor 233, sexto piso.

PARTICIPAN
Carlos Rodríguez-Sickert
Doctor en Economía
Sasha Mudd
Doctora en Historia y Filosofía de las Ciencias
Alvaro Fischer
*Ingeniero en Matemáticas, emprendedor
y escritor*

MODERA
Patricio Fernández
Escritor, fundador del semanario The Clinic

ORGANIZA
CENTRO INTERDISCIPLINARIO DE
Neurociencia de Valparaíso

CON EL RESPALDO
Milenio

AUSPICIAN
ALTAMIRA
CIRILO
HOTEL
TRESPECES
I
FUSION
COCINAR

MEDIA PARTNERS
UNIVERSIDAD DE VALPARAÍSO CHILE
EL MERCURIO
RVL 97.3fm

GREAT MINDS 3 MINUTES 1 DAY

APPLY NOW!

[falling-walls.com/
lab/apply](http://falling-walls.com/lab/apply)

BE PART OF THE FALLING WALLS LAB CHILE ON 8 AUGUST 2018

YOUR PRESENTATION

- Present your research project, business plan or social initiative – in just 3 minutes!
- Get involved in exciting discussions and network with fellow innovators and experts from different disciplines.

WHO CAN APPLY

- We are looking for great ideas from all fields!
- Apply now if you are a Bachelor or Master student, PhD candidate, post-doc, young professional or entrepreneur.

APPLICATION DEADLINE

- Apply online at falling-walls.com/lab/apply
- Application deadline: **13 July 2018**

THE FALLING WALLS LAB CHILE

- The event will take place at the **DIN399**, Dinamarca 399, Cerro Panteón, Valparaíso.
- Start: 3 pm

SHARE YOUR INNOVATIVE IDEA AND WIN A TRIP TO BERLIN

A DISTINGUISHED JURY SELECTS THE WINNER WHO

- travels to Germany and qualifies directly for the global Lab Finale in Berlin on 8 November as one of 100 international winners (travel and accommodation are covered).
- wins a ticket for the Falling Walls Conference where leaders from science, industry and policy-making meet.

QUESTIONS?

Contact: fwlab@cienciajoven.cl

Tweet about the Lab: #FallingWalls18

The Falling Walls Lab Chile is hosted by Fundación Ciencia Joven, Centro Interdisciplinario de Neurociencia de Valparaíso, Universidad de Valparaíso and the German Academic Exchange Service (DAAD) with the support of the Federal Office of Germany.

**FALLING
WALLS
LAB**



Federal Foreign Office

DAAD

Deutscher Akademischer Austauschdienst
German Academic Exchange Service



FUNDACIÓN
CIENCIA JOVEN

CENTRO INTERDISCIPLINARIO DE
NEUROCIENCIA DE
Valparaíso



**Universidad
de Valparaíso**
CHILE



Annex 14.- Articles and Interviews

CINV ANNUAL PROGRESS REPORT – 2018

1) “Scientists again warn of the convenience of maintaining the winter schedule”

Web: Senado de Chile.

May 09, 2018

Link: <http://www.senado.cl/nuevamente-cientificos-advierten-conveniencia-de-mantener-horario-de-senado/2018-05-08/164540.html>

Scope: National



Usted está en: Inicio / Senadores

Nuevamente científicos advierten conveniencia de mantener horario de invierno todo el año

Los expertos colaborarán en la redacción de una moción, en la que se fundamentarían los efectos negativos que tiene para la salud adelantar y atrasar el despertador en distintos meses.

9 de mayo de 2018

A la medianoche de este sábado cuando lo relojes se atrasen una hora comenzará a regir el horario de invierno en todo el país, excepto en Isla de Pascua y Magallanes. El tema ha generado polémica cada vez que se ha puesto en la agenda porque no son pocos los que postulan que realizar dicho cambio no es conveniente.



En este contexto, el presidente de la [Comisión de Salud](#), el senador Guido Girardi recibió a un grupo de científicos que le entregaron un documento sobre los beneficios que tendría para la salud, mantener el horario de invierno y el negativo impacto que genera el uso del actual huso horario.

En el 2016, la Sala analizó el proyecto que establece la hora oficial en todo el territorio nacional ([Boletín N° 10181-06](#)), siendo remitido a la [Comisión de Minería y Energía](#) donde expertos analizaron los pros y contras de retrasar en una hora las manijas del reloj. Ver más detalles en nota relacionada: [“Analizan efectos del horario de verano: ¿sería conveniente volver al de invierno o intercambiar ambos?”](#)

Esta propuesta propone mantener los dos husos horarios, es decir, dejar las cosas tal y como están, pero ¿qué opinan los científicos?

“ENMENDAR UN ERROR”

subir

Hasta las dependencias del Congreso Nacional en Valparaíso, llegó el investigador del Centro Interdisciplinario de Neurociencia de la Universidad de Valparaíso, John Ewer, quien junto al Premio Nacional de Ciencias, el doctor Ramón Latorre, y la psiquiatra y académica de la Universidad de Concepción, doctora Carmen Gloria Betancourt, presentaron el citado documento. En él aseguran que “el cambio de horario que se decretó el 2017 para la Región Metropolitana es un error que debe ser enmendado”.

Esta medida busca aprovechar mejor la luz del día, pero según Ewer “cuando más tarde amanece, más tarde es el despertar biológico” y el desfase entre “el horario externo e interno” produce “alteraciones en el desempeño y aprendizaje” y afectaría principalmente a los “adolescentes”.

A Chile, según su posición planetaria, le corresponde el uso de horario de invierno que es similar a Perú, Colombia o Ecuador y no el que tenemos ahora que corresponde a Brasil.

PROYECTO DE LEY

subir

El senador Girardi afirmó que le parece “inaceptable que generemos patologías, que pueden ser muy graves para la salud, a causa de tomar medidas sin el sustento científico necesario”. Consideró “muy relevante que la Ciencia acuda al Congreso a pedir, con evidencia científica en la mano, que se corrijan medidas que se hicieron sin considerar su aporte”.

Frente a esto, el legislador anunció que presentará un proyecto “que haremos con la Academia de Ciencia y estos centros, para establecer un mecanismo respecto al cambio de horario que tenga evidencia y fundamentos científicos. A partir del 12 de mayo empieza el horario de invierno y ese debiera ser el horario permanente de este país”.

2) Title: “Chilean female neuroscientist is named member of The World Academy of Science”

Web: El Mostrador

October 22, 2018

Link: <https://www.elmostrador.cl/cultura/2018/10/22/neurocientifica-chilena-es-nombrada-miembro-de-la-academia-mundial-de-ciencias/>

Scope: National

Neurocientífica chilena es nombrada miembro de la Academia Mundial de Ciencias

por El Mostrador Cultura | 22 octubre, 2018



Actualmente, Karen Castillo está investigando el funcionamiento de una clase de proteínas que residen en la membrana de nuestras células y que, como antenas moleculares, actúan como receptores de la temperatura y el dolor. Son estas proteínas, las que llevan el extraño nombre de “canales receptores de potencial transitorio”, o TRP en la jerga de los expertos.

Karen Castillo, investigadora joven del Instituto Milenio, Centro Interdisciplinario de Neurociencia de la Universidad de Valparaíso, CINV, es la nueva integrante de la Academia Mundial de Ciencias (*The World Academy of Sciences* o TWAS) como Miembro Asociado y por un periodo de cinco años.

De acuerdo a cifras de la Organización de las Naciones Unidas para la Educación, la Ciencia y la Cultura, UNESCO, sólo el 32% de participación en ciencia y tecnología que se desarrolla en Chile es protagonizada por mujeres, uno de los índices más bajos de toda Latinoamérica en paridad de género. Considerando esta realidad, es que el nombramiento contribuye a potenciar el rol femenino en el ámbito científico nacional, especialmente en materia regional.

Los requisitos para llegar a ser un Miembro Asociado de la TWAS eran varios: ser investigador joven menor de 40 años, con una alta productividad científica y una contribución relevante como investigador independiente. “El hecho de ser una de las cinco científicas latinoamericanas jóvenes en ingresar a la Academia Mundial de Ciencias es un gran reconocimiento al trabajo científico que he desarrollado desde que egresé como ingeniero en Biotecnología Molecular de la Universidad de Chile, y hasta hoy, al interior del CINV. Por otro lado, esta distinción demuestra que es posible desarrollar ciencia de primer nivel en Chile fuera del centralismo de la capital, en regiones como Valparaíso”, enfatiza la investigadora, quien se desempeña como investigadora joven en el área de Biofísica del CINV.

“Karen Castillo señala que los fondos limitados para realizar investigación son una de las principales dificultades que deben enfrentar los científicos y académicos de Latinoamérica y el Caribe. Esta situación, a menudo, obliga a los profesionales a abandonar sus países de origen en busca de oportunidades económicas en el extranjero, impidiendo un adecuado impulso al desarrollo científico y económico del país, que termina proveyendo materias primas a países desarrollados, y sin darle un valor agregado sustentable a nuestros recursos, y al desarrollo tecnológico local.”

Karen Castillo señala que los fondos limitados para realizar investigación son una de las principales dificultades que deben enfrentar los científicos y académicos de Latinoamérica y el Caribe. Esta situación, a menudo, obliga a los profesionales a abandonar sus países de origen en busca de oportunidades económicas en el extranjero, impidiendo un adecuado impulso al desarrollo científico y económico del país, que termina proveyendo materias primas a países desarrollados, y sin darle un valor agregado sustentable a nuestros recursos, y al desarrollo tecnológico local.

“Es necesario crear redes de apoyo que beneficien el trabajo de investigación y la difusión científica de todas aquellas naciones

que aún no alcanzan un completo desarrollo. Necesitamos potenciar la ciencia en pos del conocimiento y las habilidades para enfrentar desafíos como la pobreza y las enfermedades en nuestros territorios. Promover la ciencia y el uso de datos científicos es lo que necesitamos en Chile y Latinoamérica para tomar decisiones, políticas, sociales y económicas acorde a las realidades locales. Así evitamos la fuga de capital humano y favorecemos el desarrollo global local”, agrega la investigadora.

Beneficios y redes de colaboración

Castillo explica que es habitual que los investigadores latinoamericanos realicen sus estudios en condiciones poco favorables y con equipamiento antiguo y que uno de los beneficios de pertenecer a la Academia Mundial de Ciencias radica en que, en caso de ser necesario, los científicos pueden acceder a instituciones europeas y con tecnología de punta para realizar sus estudios y análisis.

“También entrega la posibilidad de postular a proyectos de investigación competitivo para miembros de la asociación, es decir, existen fondos asegurados que permiten asociarse con determinado científico, financiando los viajes, equipos, reactivos y lo que tenga relación para facilitar la investigación científica con altos estándares. Eso mejora las interacciones colaborativas que uno como investigador y nuestro centro, a su vez, pueda tener, proporcionando acceso a fondos extranjeros fuera de Latinoamérica”, enfatiza la científica de CINV.

De esta manera es posible reconocer, apoyar y promover la excelencia en la investigación científica de América del Sur, facilitando el contacto entre científicos e instituciones latinoamericanas y europeas.

Brecha de género

La científica señala que hay un diagnóstico claro respecto a la inequidad de género en materia científica en Chile, en el cual “la balanza está fuertemente inclinada hacia los hombres, sobre todo en posiciones académicas y directivas que es donde más se percibe esta brecha”.

No obstante, considera que la masiva sensibilización que ha tenido el tema durante el último tiempo, ha abierto puertas para que se comience a discutir y legislar transversalmente sobre el tema.

Para el CINV este panorama es relevante, razón por la cual ya están abordando los desafíos de la inclusión y fomentando la igualdad de género. “Como CINV no sólo nos interesa aquello que ocurre en los laboratorios, sino que nos importa generar mayores estándares de integración en todas las áreas, teniendo presencia de hombres y mujeres en igualdad de condiciones. Incluso, frente a un currículum equivalente, estamos privilegiando al de la mujer, generando así una discriminación positiva que también busca dar una mayor visibilidad a las científicas”, explica el Dr. Ramón Latorre, Premio Nacional de Ciencias y director de esta institución. Como Instituto Milenio el CINV se está preocupando muy activamente en darle espacio a nuestros investigadores jóvenes quienes, finalmente, son el futuro de nuestro centro.

Acerca de la Academia Mundial de Ciencias

La Academia Mundial de Ciencias (TWAS), basada en el mérito, fue fundada en 1983 por un grupo de científicos liderados por el físico pakistaní y premio Nobel, Abdus Salam. Su objetivo principal es promover y difundir la capacidad científica y excelencia para la sustentabilidad de los países en vías de desarrollo. Su sede está ubicada en los edificios del Centro Internacional de Física Teórica (ICTP) en Trieste, Italia.

En 1985 fue inaugurada oficialmente con el nombre de Academia de Ciencias del Tercer Mundo, nominación con la que fue conocida hasta 2013. En sus inicios estaba integrada por 42 becarios, 9 de ellos galardonados con el Premio Nobel. Actualmente está integrada por más de 1.200 becarios elegidos en más de 90 países, considerados los investigadores más exitosos del mundo. Del total de sus miembros, 14 han recibido el Premio Nobel en alguna área de las ciencias.

Aproximadamente el 85% de sus integrantes provienen de países en desarrollo y el 15% son científicos e ingenieros de naciones desarrolladas, con investigaciones que han impactado significativamente a América del Sur.

Líneas de investigación de la científica

Actualmente, Karen Castillo está investigando el funcionamiento de una clase de proteínas que residen en la membrana de nuestras células y que, como antenas moleculares, actúan como receptores de la temperatura y el dolor. Son estas proteínas, las que llevan el extraño nombre de “canales receptores de potencial transitorio”, o TRP en la jerga de los expertos. “En ese contexto, mi principal pregunta es dilucidar los mecanismos moleculares que le permiten a estas proteínas informarle a nuestro sistema nervioso cuándo tenemos que retirar la mano de un objeto muy caliente o muy frío. La o las respuesta que podamos obtener a través de estas investigaciones, nos pueden llevar a la confección de fármacos que nos sirvan para paliar el dolor”, señala.

Actualmente, la investigadora se está concentrando en estudiar el comportamiento de dos canales capaces de responder a los cambios de temperatura en distintos rangos. El TRPM8 es conocido como el canal receptor de frío, mientras que el TRPV1 es un canal que se activa con calor. “Estamos estudiando estos canales para que puedan ser usados como blancos terapéuticos en ciertas patologías que tienen que ver con el dolor, incluso con la neuropatía y dolores producidos por cáncer, diabetes y migraña”, finaliza la investigadora.

3) “They appoint chilean female as new member of The World Academy of Science”

Newspaper: Las Últimas Noticias

October 24, 2018

Link: <https://www.lun.com/Pages/NewsDetail.aspx?dt=2018-10-24&PaginaId=14&bodyid=0>

Scope: National

EL DÍA

Miércoles 24 de octubre de 2018 / Las Últimas Noticias

El reconocimiento lo obtuvo la neurocientífica Karen Castillo.

Podrá ir de intercambio a prestigiosas universidades, pero deberá volver al país a aplicar lo aprendido.

La entidad financia y promueve la investigación en países en vías de desarrollo

Nombran a chilena como nueva integrante de la Academia Mundial de Ciencias

CAMILA FIGUEROA

En el selecto grupo de investigadores que conforman la Academia Mundial de Ciencias (<https://bit.ly/2ywpFbz>), con sede en Italia, no reciben postulaciones. Para convertirse en miembro, uno de los integrantes tiene que nominar a alguien, quien posteriormente es evaluado por un consejo.

Karen Castillo (38), investigadora del Instituto Milenio Centro Interdisciplinario de Neurociencias de la Universidad de Valparaíso, fue votada y elegida como la nueva integrante de aquel grupo integrado por 1.222 genios de la ciencia, entre ellos, catorce ganadores del Premio Nobel.

“El objetivo de esta academia es promover el desarrollo científico en países en vías de desarrollo. La fundó a comienzos de la década de los 80, el Nobel de Física Abdus Salam, quien estaba preocupado por la fuga de científicos hacia países desarrollados. La academia, a través de sus redes, nos da cupo para ir a aprender en laboratorios y universidades internacionales. La idea es que uno vuelva a su país de origen para generar avances”, explica la neurocientífica. Agrega que, por mientras, solo es miembro aso-



PHOTOS: PUNOZ

Castillo estudia los sensores de temperatura de la piel.

ciado por cinco años, que pueden prolongarse por otros cinco. Eso porque para ser un integrante estable es necesario contar con una trayectoria de más años.

A Castillo la nominó el Premio Nacional de Ciencias Naturales y miembro de la academia, Ramón Latorre. “La competencia es feroz porque todos quieren postular a alguien. Se abrió un proceso especial para nominar a menores de 40 años. Este año aceptaron a cinco latinoamericanos. Esta academia es muy importante porque la integran miembros de países desarrollados, subdesarrollados y en vías de desarrollo. Todos colaboran para que la ciencia llegue a todos lados”, celebra Latorre, quien además integra la Academia de Ciencias de Estados Unidos.

Latorre cuenta que eligió a Castillo por su creatividad en la investigación. “Estudio los sensores de temperatura que están en la piel. Le avisan al cerebro cuándo quitar la mano de las cosas calientes. Cuando estos sensores fallan, aparece el dolor crónico en enfermedades como el cáncer, neuropatía diabética o migraña. Por eso es importante estudiar por qué ocurre eso. Así encontraremos el medicamento ideal para frenar esa falla de los sensores”, detalla la investigadora.

4) “Biologist tells how he trains the artificial retina that seduced the gringos”

Las Últimas Noticias

Página 2, sección El Día.

29 de julio, 2018

Link: <http://www.lun.com/Pages/NewsDetail.aspx?dt=2018-07-29&PaginaId=2&bodyid=0>

Scope: National

EL DÍA

Domingo 29 de julio de 2018 / Las Últimas Noticias

Tomás Pérez-Acle tiene apoyo de la Fuerza Aérea de USA (USAF) y de Intel

Biólogo cuenta cómo entrena la retina artificial que sedujo a los gringos

Junto al neurocientífico Adrián Palacios, crearon inteligencia artificial que imita la función de esta parte del ojo.

CAMILA FIGUEROA

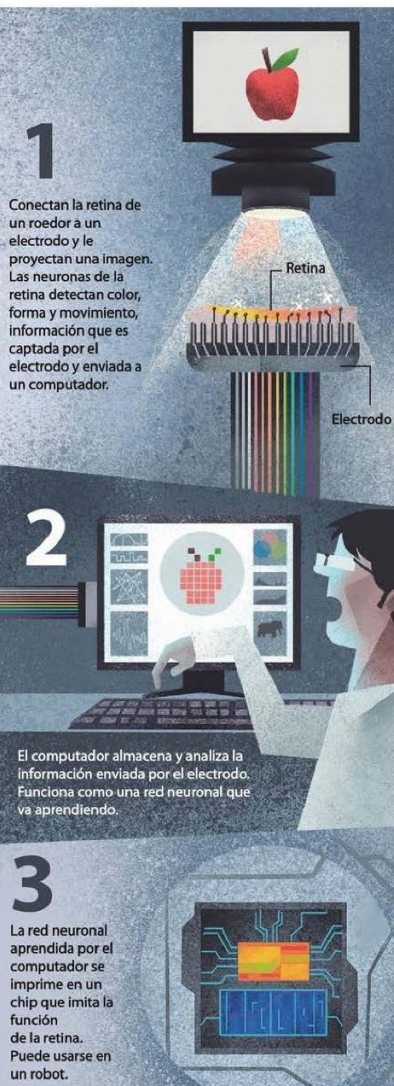
Todo comenzó con el Imperio Galáctico descrito perfectamente por el escritor Asimov en la saga “Fundación”. Tomás Pérez-Acle tenía unos diez años cuando descubrió que tal vez, solo si se topaba con un computador a finales de la década de los 70 en Chile, podría iniciar su camino en el desarrollo de modelos matemáticos para predecir el comportamiento de la sociedad. Tal como lo hacía el personaje de Hari Seldon, quien trabajaba para dilucidar los movimientos de los pobladores del imperio Galáctico.

“Partió como ficción cuando era un niño, pero se transformó en realidad cuando me dediqué a la biología computacional. Ahora, junto al investigador Adrián Palacios, doctor en Neurociencia y experto en retina, estamos trabajando en una retina robótica, financiada por la Oficina de Investigación de la Fuerza Aérea de Estados Unidos (AFOSR) y gracias al apoyo de la empresa tecnológica Intel, que imita el funcionamiento de la retina del roedor Degus”, cuenta el investigador de la Fundación Ciencia para la Vida y del Instituto Milenio Centro Interdisciplinario de Neurociencia de la Universidad de Valparaíso (CINV).

La primera vez que los estadounidenses se fijaron en Pérez-Acle fue luego de que diseñara matemáticamente el comportamiento de los chilenos frente a una invasión zombie. “Publicamos los resultados en una revista científica y bien. Pero después empezó a difundirse en los diarios, hasta que le llegó a la Fuerza Aérea estadounidense. Les gustó la idea y ahora nos están financiando inteligencia artificial”, dice.

Retina artificial

Sin retina no hay visión. Es un tejido que reacciona ante la luz y que manda información vía impulsos nerviosos al cerebro, para que éste la descifre. “Por eso es que la inteligencia artificial tiene que lograr imitar este tejido para ser eficiente. Lo imita, es cierto, pero no con la eficiencia que desearíamos. Imagínate que en milésimas de segundo puedes ver una imagen, no gastas energía en eso, ni



siquiera te lo cuestionas. La inteligencia artificial aspira a eso, a ser eficiente”, explica John Atkinson, director del Centro TI de la Facultad de Ingeniería y Ciencias de la Universidad Adolfo Ibáñez, quien aplaude la retina robótica de su colega.

¿Cómo logra esa eficiencia Pérez-Acle? Con dos áreas de la inteligencia artificial que se llaman redes neuronales y computación neuromórfica. “Las redes neuronales son varios softwares que se comunican entre sí e imitan el funcionamiento del sistema nervioso central. En este caso, los softwares aprenden cómo se comportan las neuronas de la retina del roedor frente a distintos colores, movimientos y formas”, describe.

La retina, explica Pérez-Acle, se encarga de detectar el color, la forma y el movimiento de una imagen. “El tálamo relaciona esos patrones y la corteza cerebral se encarga de darle sentido a la imagen y determina si la imagen es una manzana o no, por ejemplo. Estamos con la primera parte del proceso de imagen que es la retina”.

► **Retina del roedor.** “Sacamos la retina y la ponemos en un electrodo de dos milímetros cuadrados. La mantenemos viva con algunas sustancias. Sobre ella vamos pasando imágenes con un proyector”.

► **Electrodo.** “Cuando la retina detecta la forma, movimiento y color de la imagen, las neuronas se ponen a disparar señales eléctricas al cerebro. Nosotros, en vez de tener un cerebro, las capturamos con un electrodo que las envía a un computador vía cable USB. En el computador hay muchos softwares que hacen de red neuronal”.

► **Red neuronal.** “Nosotros conocemos cómo funciona la retina y esa información se la pasamos al computador. Entonces la red neuronal (softwares que imitan la comunicación que tienen las neuronas de la retina) detecta qué neuronas están emitiendo las señales. Eso varía de acuerdo a la imagen proyectada”.

► **Aprendizaje.** “La red neuronal va aprendiendo. Mientras más imágenes le proyectes, más información aprende. Justo estamos en la etapa de entrenar la red. Le decimos: Acá tienes los datos y esto es lo que tienes que obtener. En un momento la red neuronal artificial va a poder aprender a distinguir cientos de formas, colores y movimientos”.

► **Chip neuromórfico.** “Este es el paso final para crear la retina robótica. Se imprime un chip con todos los patrones más o menos del tamaño de la palma de una mano y se puede incluir en la visión de cualquier aparato que use inteligencia artificial”.



Tomás Pérez-Acle, biólogo computacional.

5) “Young man walked again to pure boldo and kinesiology”

Newspaper: Las Últimas Noticias

August 25, 2018

Link: <http://www.lun.com/Pages/NewsDetail.aspx?dt=2018-08-25&PaginaId=2&bodyid=0>

Scope: National

GANAR UN DEPARTAMENTO CUPÓN COMODÍN
WWW.PROMOCIONLUN.CL

Las Últimas Noticias

\$300 • Regiones I, II, XI, XII y XV: \$500 • Año CXVI • N° 38.925 • Sábado 25 de agosto de 2018

“No hay otro caso como el de Víctor Abusleme (diagnosticado con Disferlinopatía)”, dice el doctor en fisiología Luis Cea



Joven volvió a caminar a puro boldo y kinesiología

¿Quiere borrar un tatuaje? Si es negro o azul es más fácil 16

Farándula sube el rating a late de Kathy Salosny 36

6) “The works of the building of the science in the neighborhood La Matriz starts”

Newspaper: El Mercurio de Valparaíso

September 02, 2018

Link: <http://www.mercuriovalpo.cl/impresas/2018/09/02/full/cuerpo-principal/6/>

Scope: National

EL MERCURIO

DE VALPARAÍSO



LA EMPRESA CONSTRUCTORA TENDRÁ UN PLAZO DE 20 MESES PARA HABILITAR ESTE INMUEBLE.

Partieron las obras del edificio de la ciencia en el barrio La Matriz

VALPARAÍSO. El proyecto impulsado por el CINV contempla una inversión que se empina a los \$ 7 mil 400 millones.

Ya se dio inicio a la construcción del Edificio de la Ciencia en Valparaíso, denominado Juan Ignacio Molina, en homenaje al primer científico del país. La obra, situada a un costado de la Iglesia del barrio La Matriz, es impulsada por el Instituto Milenio, Centro Interdisciplinario de Neurociencia de la Universidad de Valparaíso (CINV) y busca posicionar a la ciudad puerto como un polo de referencia para la neurociencia en Latinoamérica.

El Ministerio de Obras Públicas, a través de su Dirección de Arquitectura, adjudicó la obra a la empresa constructora BROTEC, que tendrá un plazo de 20 meses para habilitar este inmueble, que albergará a más de 150 investigadores chilenos y extranjeros a partir del primer trimestre del año 2020.

INVERSIÓN

Emplazado en el área declarada como Patrimonio de la Humanidad por la Unesco, la ini-

El inmueble ha sufrido diversos desastres naturales e incendios que han afectado sus cimientos desde 1905 a la fecha. Del último de ellos -un incendio el año 2004- sólo se mantiene la fachada del edificio, que será preservada por este proyecto.

ciativa arquitectónica contempla una inversión cercana a los 7 mil 400 millones de pesos. Dichos recursos son aportados por la Universidad de Valparaíso (\$1500 millones), el Ministerio de Obras Públicas (\$1.000 millones), el Gobierno Regional de Valparaíso (\$2.500 millones) y la Subsecretaría de Desarrollo Regional (\$2.400 millones). El edificio llevará el nombre de Juan Ignacio Molina, conocido popularmente

como “Abate Molina”, sacerdote de origen italiano considerado como precursor de la ciencia chilena en los siglos XVIII y XIX, quien residió durante un período en ese mismo lugar. La empresa constructora Brotec -una de las tres firmas licitantes en el proceso-, quien tendrá a cargo el desarrollo del proyecto, tiene más de 50 años de experiencia en edificaciones públicas, y entre sus proyectos más emblemáticos destaca la ruta entre Rodillillo y El Salto en Viña del Mar, las obras civiles del Aeropuerto Matavari en Hanga Roa y el Aeropuerto Pudahuel de Santiago.

ZONA TÍPICA PORTEÑA

Durante cinco siglos, el edificio Severín ha sido testigo privilegiado en hitos de Valparaíso y la vida republicana de Chile desde sus orígenes como templo jesuita en el Siglo XVI, el funcionamiento del retén Santo Domingo de Caballeros a finales del Siglo XIX, lugar donde sesionó el primer Congreso bicameral de Chile y se redactó la Constitución chilena de 1828.

El inmueble ha sufrido diversos desastres naturales e incendios que han afectado sus cimientos desde 1905 a la fecha. Del último de ellos -un incendio el año 2004- sólo se mantiene la fachada del edificio, que será preservada por este proyecto.

Cabe recordar que el informe ICOMOS (entidad técnica asesora de la Unesco), a raíz de su visita el año 2015 con el objetivo de evaluar el estado del patrimonio porteño, menciona que la recuperación de este inmueble contribuirá a reactivar social y económicamente el Barrio Puerto, a través de un polo de desarrollo científico de primer nivel.

Moderno centro de investigación con instrumentos de alta tecnología

Al interior del Edificio de la Ciencia en Valparaíso, impulsado el CINV, funcionará un moderno centro de investigación en neurociencia, con laboratorios de alta tecnología, que albergarán a más de 150 profesionales, entre investigadores, académicos, estudiantes de doctorado y postdoctorado y personal administrativo. La construcción tendrá un total de 4.800 metros cuadrados y cinco niveles, dos de ellos subterráneos. Su recuperación definitiva

va a contemplar un auditorio con capacidad para 200 personas, que recibirá actividades de ciencia, arte y cultura, además de ser un espacio abierto para actividades de carácter educativo y comunitario en el área. Se espera que este Centro reciba cada año, y desde distintas latitudes, la visita tanto de especialistas ligados a la investigación científica como público atraído por las actividades y la programación que tendrá fijada el área de extensión. ^{CS}

7) “Porteños scientists seek therapy for OCD”

Newspaper: El Mercurio de Valparaíso

October 18, 2018

Link: <http://www.mercuriovalpo.cl/impresa/2018/10/18/full/cuerpo-principal/3/>

Scope: National

EL MERCURIO

DE VALPARAÍSO

Científicos porteños buscan terapia para el TOC

VALPARAÍSO. En Chile, 500 mil personas lo padecen, entre ellas, Gabriel Boric.

Científicos del Instituto Milenio Centro Interdisciplinario de Neurociencia de la Universidad de Valparaíso -CINV-, liderados por el Doctor Pablo Moya, están analizando un gen asociado con un neurotransmisor específico llamado EAAT3, el cual aparece alterado en personas diagnosticadas con Trastorno Obsesivo Compulsivo (TOC).

Este tipo de trastorno adquirió notoriedad luego que el diputado Gabriel Boric (MA) reconociera que lo padece y admitiera que está en tratamiento para mantenerlo bajo control.

Los estudios que se hacen en Valparaíso están orientados a la elaboración de una nueva terapia que beneficie al 50% de los pacientes, quienes, actual-

mente no responden a los tratamientos convencionales ya existentes.

“Esta proteína regula la actividad del neurotransmisor glutamato en el cerebro. Lo que nosotros hemos observado es que existen variantes genéticas que la codifican, las cuales están mucho más presentes en las personas con TOC que en la población en general”, explica Pablo Moya.

Precisa que a partir de estos estudios, generaron un modelo transgénico que permite manipular a EAAT3 para ver cuáles son las consecuencias a nivel cerebral. “Descubrimos que cuando este neurotransmisor está sobreexpresado, aumentan los niveles de conductas compulsivas, repetitivas y la ansiedad. Debido a esto es



EL DOCTOR PABLO MOYA LLEVA 12 AÑOS DE INVESTIGACIÓN EN EL TEMA.

que estamos proponiéndolo como un nuevo modelo para el estudio y blanco terapéutico para la patología”, expuso el especialista.

MOLÉCULAS

En ese contexto, el investigador de CINV confirmó que ya han diseñado moléculas que bloquean la actividad de EAAT3. “Ahora queremos ver si es que acaso, bloqueando a esta proteína, podemos revertir el efecto”, comenta.

El Trastorno Obsesivo Compulsivo afecta a un 2 ó 3% de la población mundial. Esto

significa que en Chile son aproximadamente 500 mil los casos existentes. Por lo general, los síntomas aparecen entre los 8 y 18 años. Es un problema crónico, que persiste a lo largo de la vida de los pacientes, aunque hay ciclos de severidad.

Moya, quien también es director alterno del Núcleo N-MIND, agrega que los tratamientos clásicos para el TOC son la terapia conductual y los inhibidores de la recaptura de serotonina. Sin embargo, sólo la mitad de los casos responden favorablemente a estos tratamientos.

8) “Neuroscientist use boldo to treat very rare disease”

Newspaper: Las Últimas Noticias

November 22, 2018

Link: <http://www.lun.com/Pages/NewsDetail.aspx?dt=2018-11-22&PaginaId=27&SupplementId=46&bodyid=0>

Scope: National

27

CIENCIA

JUAN CARLOS SÁEZ DESCUBRIÓ QUE LA BOLDINA FRENA EL DETERIORO EN LA Distrofia MUSCULAR

Neurocientífico utiliza boldo para tratar rarísima enfermedad



L. GARCÍA

Sin querer queriendo

Ramón Latorre

La ciencia es curiosidad pura. Los hallazgos importantes en ciencia no nacen porque el científico quiera innovar en algo o porque quiera descubrir algo que pueda tener una aplicación inmediata. El arte del descubrimiento en ciencia se basa en la más pura curiosidad de entender cómo funcionan los seres vivos, el universo o las moléculas. Ese acto casi épico de hacer ciencia

Por la curiosidad, Sáez llegó a un posible avance terapéutico, sin ser un médico.

parte por hacerse una pregunta, realizar los experimentos y formular una hipótesis. Es esta curiosidad insaciable de los seres humanos la que finalmente produce el GPS o las más diversas drogas que por miles se usan para batallar contra diferentes enfermedades.

Como la ciencia se ha especializado tanto, destaca en el área de la biología a Juan Carlos Sáez. Justamente su investigación con el boldo nació por la curiosidad, quería entender un proceso al nivel molecular. Sáez es el ejemplo de cómo la curiosidad llegó a un posible avance terapéutico. Sin querer queriendo, como decía el Chavo, llegó a algo tan importante como la salud del ser humano. Y eso que no es médico.

CAMILA FIGUEROA

Esta es la historia del boldo, a fin de cuentas. Y la de un paciente, que por iniciativa propia, agarró el estudio de un investigador y decidió poner en práctica la alimentación que tuvieron unos ratones durante un año. Víctor Abusleme tiene un tipo de distrofia muscular llamada distrofina. En el laboratorio demostramos que los ratones enfermos que consumieron boldina (compuesto del boldo), no presentaron deterioro muscular. Este joven tomó agua de boldo durante casi tres años. Antes caminaba con bastones, ahora anda en bicicleta y sube cerros, cuenta el neurocientífico Juan Carlos Sáez, investigador del Instituto Milenio Centro Interdisciplinario de Neurociencias de la Universidad de Valparaíso.

-¿Por qué el boldo es tan potente en la distrofia muscular?
-Hay varios tipos de distrofias musculares. Son enfermedades genéticas que van deteriorando las fibras musculares. Nosotros descubrimos que en las células que componen esas fibras musculares aparecen unos hoyitos llamados hemicanales. Por ahí entra mucho calcio, lo que termina por matar a la célula.

-Ahora entra el boldo, me imagine...

-Exacto. La boldina cierra esos hoyos. La enfermedad no desaparece, porque sigue existiendo la mutación genética. Lo que hace la boldina es frenar la destrucción de las células musculares.

-¿Lo probó solo en ratones?

-Sí. Pero alrededor de 120 personas con distrofia muscular en el mundo están tomando extracto de boldo. Esos pacientes han mejorado su caminata. De todos modos es necesario avanzar con un estudio clínico para evidenciar y demostrar el efecto del boldo en humanos.

-¿En qué está ese estudio en humanos?

-Formamos una empresa y estamos avanzando con inversionistas norteamericanos para hacer estudios preclínicos (en animales). En cinco años más esperamos comenzar en humanos.

A fines del 2019 pensamos publicar un estudio retrospectivo con personas que han ingerido extracto de boldo por su cuenta.

-Una cosa, doctor. El boldo es endémico de Chile y demora en crecer, ¿de dónde sacarán tanto boldo?

-También pensamos en eso. Por eso creamos una molécula sintética que se puede fabricar en toneladas. Estamos en proceso de solicitud de patente.



Juan Carlos Sáez

Un paciente que casi no caminaba se enteró del estudio de Sáez en ratones. Decidió tomar agua de boldo por su cuenta. Ahora anda en bicicleta.